

DEPOSITIONAL STACKING PATTERNS AND CYCLES OF
GARZAN FORMATION IN THE GARZAN-GERMİK OIL FIELD: AN
APPROACH TO CYCLE TO LOG CORRELATION

A THESIS SUBMITTED TO
THE GRADUATE SCHOOL OF NATURAL AND APPLIED SCIENCES
OF
MIDDLE EAST TECHNICAL UNIVERSITY

BY

ZEYNEP ELİF GAZİULUSOY YILDIZEL

IN PARTIAL FULFILMENT OF THE REQUIREMENTS
FOR
THE DEGREE OF DOCTOR OF PHILOSOPHY
IN
GEOLOGICAL ENGINEERING

JUNE 2008

This thesis is dedicated to those,
who work with great effort in order to explore a drop of black gold;
Oil for this Country.

ABSTRACT

DEPOSITIONAL STACKING PATTERNS AND CYCLES OF GARZAN FORMATION IN THE GARZAN-GERMİK OIL FIELD: AN APPROACH TO CYCLE TO LOG CORRELATION

Yıldız, Zeynep Elif Gaziulusoy

Ph. D., Department of Geological Engineering

Supervisor: Prof. Dr. Demir Altın

June 2008, 202 pages

The Garzan Formation is a deepening upward marine carbonate including successions ranging from subtidal to open marine facies deposited in the Maastrichtian. The Garzan Formation is composed of five microfacies types; Miliolid Wackestone (subtidal), Orbitoid Miliolid Wackestone, Rudist Wackestone (backshoal to shoal), Rotalid Miliolid Wackestone (shoal to foreshoal) and Pelagic Foraminiferal Mudstone (foreshoal to open marine).

These five microfacies are stacked in different combinations consisting of five types of depositional cycles. The type A and D cycles the building blocks of transgressive systems tract (retrogradational), whereas type B and C cycles are deposited during highstand systems tract (aggradational). The type E cycle is progradational and also corresponds to the highstand systems tract deposits. The maximum flooding surface is usually located within the type D cycle towards the top of the formation.

Generally, the base of the Garzan Formation deposition starts with highstand systems tract deposits (type E and C cycles) and overlain by transgressive systems tract deposits (type A cycle) in between there is a type 2 sequence boundary. Then deposition continues with highstand systems tract deposits (alternation of type B and C cycles) which are aggradational in character. The top of the Formation is characterized by transgressive systems tract deposits (type D cycle) which usually includes the maximum flooding surface. The second type 2 sequence boundary is located below the type D cycle.

There are four of the stacking patterns observed in the Garzan Formation. The GR values change from relatively high to low API in type D and A cycles, whereas a relative shift from low to high API is observed in type E cycle. The GR in the type B and C cycles does not display any relative change. There is no net movement in the SONIC readings in type A, B, C and E cycles; however there is a relative shifting from low velocity to high velocity in type D cycle.

In Garzan deposition opposing the general patterns, a decrease in GR readings indicates a decrease in energy and relatively deepening. In carbonate depositional systems predicting the depositional environment from the logs should only be accomplished with microfacies control, otherwise the interpretation will be erroneous.

Key Words: Microfacies, Stacking Pattern, Cycle, GR-SONIC Logs, Garzan Formation, Garzan-Germik Oil Field.

ÖZ

GARZAN-GERMİK PETROL SAHASINDA GARZAN FORMASYONU'NUN ÇÖKEL DEVİRLERİ VE YIĞMA MODELLERİ İLE ÇÖKEL DEVİR-LOG KORELASYONUNA YAKLAŞIM

Yıldız, Zeynep Elif Gaziulusoy
Doktora, Jeoloji Mühendisliği Bölümü
Tez Yöneticisi: Prof. Dr. Demir Altın

Haziran 2008, 202 sayfa

Garzan Formasyonu Mestrişiyen zamanında, gel-git altından açık denize kadar olan alanlarda çökelmiş yukarı doğru derinleşen denizel bir karbonat istifidir. Garzan-Germik petrol sahasında bu formasyon beş mikrofasiyese ayrılmıştır. Bunlar: Milolidli Vaketaşı (gel-git altı), Orbitoidli Milolidli Vaketaşı, Rudist Kavkılı Vaketaşı (sıgık gerisi ve sıgık), Rotalidli Milolidli Vaketaşı (sıgık ve sıgık önü) ve Pelajik Foraminiferli Vaketaşıdır (sıgık önü ve açık deniz).

Bu mikrofasiyelerin değişik tipte üst üste yığılmasından beş adet devirsel çökel tipi oluşmuştur. Bunlar: aşmalı düzey birim sisteminde ve fasiyelerin karaya doğru gerilemesi şeklinde çökelen A ve D tipi devirsel çökeller, yüksek düzey birim sisteminde ve fasiyelerin üst üste yığılması karakterinde çökelmiş B ve C tipi devirsel çökeller, ve bu birim sistemine ait denize doğru ilerleyen fasiyes yığılımlarının ürünü olan E tipi devirsel çökellerdir. Maksimum sellenme düzeyi D tipi devirsel çökel içinde ve istifin üst tarafında gözlenmektedir.

Genellikle Garzan istifı yüksek düzey birim sistemi ile başlar ve aşmalı birim sistemi çökelleri ile üzerlenmektedir. Bu çökeller karaya veya denize doğru net fasiyes ilerlemesi olmayan yüksek düzey birim sistemi ile örtülmektedir. İstifin en üst kısmı ikinci bir aşmalı düzey çökelleri ile temsil edilmektedir. Garzan çökeliminde tip 2 özelliğinde iki adet istif dokanağı gözlenmiştir.

Garzan istifinde dört adet yığma modeli gözlenmiştir. A ve D tipi devirsel çökellerinde GR göreceli olarak yüksek değerden düşük değere doğru, E tipi devirsel çökelinde ise bunun tam tersi şeklinde okuma yapmaktadır. B ve C tipi devirsel çökellerde GR değerlerinde bir değişim olmamaktadır. Bununla beraber A, B, C ve E tipi devirsel çökellerde SONIC okumaları bir değişiklik göstermezken, D tipi devirsel çökelde göreceli olarak düşük hızdan yüksek hıza doğru okuma yapmaktadır.

Garzan istifinde genel durumun tersine olarak GR değerleri düşük olduğunda çökel ortamın enerjisinde düşüş ve deniz seviyesi yükselmesi gözlenmiştir. Karbonat çökel ortamlarında direkt olarak loglar vasıtası ile çökel ortamı yorumuna gidilmesi yanlış sonuçlar çıkarılmasına neden olacaktır.

Anahtar Kelimeler: Mikrofasiyes, Yığma Modelleri, Devirsel Çökel, GR-SONIC Logları, Garzan Formasyonu, Garzan-Germik Petrol Sahası,

ACKNOWLEDGEMENTS

I wish to express my sincere gratitude to my supervisor Prof. Dr. Demir Altiner, who supported and guided me in this study. He always encouraged me in doing this study and he believed in me that I can fulfill the requirements of a PhD. study.

I would like to especially thank to my friend and colleague Mr. Mehmet Sünnetçiođlu for his positive attitude and his help for supporting me that I can overcome this work.

I would like to articulate my gratitude to Mrs. Ekmel Uygur, who also supported me and believed in me doing this work. I also wish to thank her for supplying the thin sections and the other material.

I also wish to express my gratitude to TPAO management on behalf of Ahmet Faruk Öner, the Exploration Manager, for guiding me correctly and permitting me to supply the data and related material and to use the data for this study.

Many thanks are due to my family who had given me the ambition to explore and learn knowledge and trained me to work hard for the things I want to achieve in my life.

Special thanks and indebtedness are extended to my dear husband Dr. Ali Yıldızel; who always supported me emotionally. I would like to express my deep appreciation for his unending support and encouragement whole through the times we have.

And finally, many thanks are due to my daughter, Miss. Zeynep Ezgi Yıldızel, who provided her own time to my thesis work. Today she is too young to realize how generous she is to me in sharing her valuable time with my PhD work; but all I can say is, she gives meaning to my life being my daughter.

TABLE OF CONTENTS

ABSTRACT.....	v
ÖZ.....	vii
ACKNOWLEDGEMENTS	ix
TABLE OF CONTENTS.....	x
LIST OF TABLES.....	xv
LIST OF FIGURES	xvi
CHAPTERS	
1. INTRODUCTION.....	1
1.1 Purpose and Scope	1
1.2 Geological Setting of The Study Area.....	3
1.3 Historical Precedence of the Garzan-Germik Oil Fields.....	6
1.4 Methods of Study	11
1.5 Previous Works.....	17
1.6 Terminology and Concept of Logs	26
1.6.1 Terminology and Concept of SONIC Logs.....	26
1.6.2 Terminology and Concept of GR Logs.....	29
1.6.3. Terminology and Concepts of Resistivity Logs.....	35
2. STRATIGRAPHY	37
2.1 General Geology of Southeast Turkey.....	37
2.2 Stratigraphy and the Structural Setting of the Study Area.....	42

2.2.1	Beloka Formation	46
2.2.2	Kıradağ Formation	48
2.2.3	Garzan Formation	50
2.2.4	Germav Formation	53
2.2.4.1	Alt Germav Formation	58
2.2.4.2	Üst Germav Formation	59
2.2.5	Gerçüş Formation	59
2.2.6	Hoya Formation.....	60
2.2.7	Germik Formation	61
3.	MICROFACIES AND CYCLES, AND THEIR STACKING PATTERNS OF GARZAN FORMATION	62
3.1	Microfacies of Garzan Formation in Garzan-Germik oil field.....	63
3.1.1	Miliolid Wackestone	64
3.1.2	Rotalid Miliolid Wackestone	72
3.1.3	Orbitoid Miliolid Wackestone.....	73
3.1.4	Pelagic Foraminiferal Wackestone.....	80
3.1.5	Rudist Wackestone	85
3.2	Cycle Types of Garzan Formation in the Garzan-Germik Oil Field.....	90
3.3	Depositional Environment of Garzan Formation in the Garzan- Germik Oil Field	94
3.4	Stacking Patterns and Sequence Stratigraphy of Garzan Formation in the Garzan-Germik Oil Field	106

3.5	Microfacies of Garzan Formation with in the Studied Wells of Garzan-Germik Oil Field	112
3.5.1	Microfacies and Cycles of the Garzan Formation in Garzan-47	112
3.5.2	Microfacies and Cycles of the Garzan Formation in Germik-21	115
3.5.3	Microfacies and Cycles of the Garzan Formation in G. Germik-1.....	117
3.5.4	Microfacies and Cycles of the Garzan Formation in Garzan-82	119
3.5.5	Microfacies and Cycles of the Garzan Formation in Garzan-23	122
3.5.6	Microfacies and Cycles of the Garzan Formation in Germik-6	124
3.5.7	Microfacies and Cycles of the Garzan Formation in Garzan-43	124
3.5.8	Microfacies and Cycles of the Garzan Formation in Garzan-33	127
3.5.9	Microfacies and Cycles of the Garzan Formation in Garzan-31	127
3.5.10	Microfacies and Cycles of the Garzan Formation in Germik-3	129

4.	CORRELATION OF CYCLES STACKING PATTERNS TO LOG DATA IN THE GARZAN FORMATION.....	132
5.	DISCUSSIONS AND CONCLUSIONS.....	152
5.1	Discussion and Contributions	152
5.2	Results and Conclusions	159
	REFERENCES	163
APPENDICES		
A	THE STRATIGRAPHIC CLOUMN OF THE STUDIED WELLS IN THE GARZAN-GERMIK OIL FIELD	187
A.1	Garzan-23	187
A.2	Garzan-31	188
A.3	Garzan-33	189
A.4	Garzan-43	190
A.5	Garzan-47	191
A.6.	Garzan-82.....	192
A.7	G.Germik-1.....	193
A.8	G.Germik-2.....	194
A.9	Germik-3	195
A.10	Germik-6	196
A.11	Germik-21	197
B.	THE TABLE OF POINT COUNTING OF THIN SECTIONS	198
	CURRICULUM VITAE	201

LIST OF TABLES

TABLES

Table 1. The list and the data availability of the 116 studied wells in Garzan Germik oil field	14
Table B.1. The list of point counting of the thin sections, representing the five microfcaies types of this study.....	198

LIST OF FIGURES

FIGURES

Figure 1. Location map of the study area. The rectangle shows the zoomed area of Southeast Anatolia.....	2
Figure 2. Geological map of the X th Petroleum District of Southeast Türkiye (1/250.000)	4
Figure 3. Structure map of top of the Garzan Formation in Garzan-Germik oil field	7
Figure 4. Completion types of the wells in Garzan oil field.....	9
Figure 5. Completion types of the well in Germik oil field.....	10
Figure 6. The base map of Garzan-Germik oil field and the studied wells are located	12
Figure 7. Photographs of the condition of the cores of Garzan Germik oil field wells	15
Figure 8. The share percentage of topics concerning the Garzan Formation.....	19
Figure 9. The distribution percentage of studies about Garzan Formation according to years.....	20

Figure 10. Facies map of Garzan Formation carbonates according to Salem et. al., (1986).....	22
Figure 11. The sonic log showing a formation's ability to transmit sound waves according to its lithology and rock texture (Rider, 1996).....	28
Figure 12. The sonic log tool showing its positioning, T=transmitter, R=receiver (Thomas,1977 and Purdy, 1982)	30
Figure 13. The typical response of gamma ray log for lithologies. The gamma ray log shows natural radioactivity (Rider, 1996) (He:heavy minerals; g:glauconite; M:mica; F:feldspar).	32
Figure 14. Radioactivity of Ypresian (Eocene) Limestones, Tunisia, related to uranium concentrations. The uranium is associated with early diagenesis, organic matter and phosphatic concentrations (Hassan, 1973).....	33
Figure 15. Facies distribution from the gamma ray log. a) the changes in sandstone grain size are reflected in changes in gamma ray value, b) Graphic representation of the variation of grain size with gamma ray value (Rider, 1996).....	34
Figure 16. The map showing the major structures of Southeast Anatolia and the location of Garzan-Germik oil field (modified from Perinçek, D. et. al., 1987).....	41
Figure 17. Generalized stratigraphic column of Southeast Anatolia (Dinçer, 1991).....	45

Figure 18. Generalized stratigraphic columnar section of the study area formed from the subsurface data of Garzan-Germik oil field	47
Figure 19. Correlation chart of the Campanian to Oligocene formations from the previous studies	49
Figure 20. Average porosity and permeability of Garzan Formations in Garzan oil field (the measured data of the plug porosity and permeability is the courtesy of TPAO).....	54
Figure 21. Average porosity and permeability of Garzan Formation in Germik oil field (the measured data of the plug porosity and permeability is the courtesy of TPAO).....	55
Figure 22. The thickness of Garzan Formation penetrated in the wells of the Garzan oil field	56
Figure 23. The thickness of Garzan Formation penetrated in the wells of the Germik oil field	57
Figure 24. The occurrence percentage of the constituents found in Miliolid Wackestone facies	65
Figure 25. Photomicrograph of Miliolid Wackestone facies from Germik-21 well (X4, core) (m:miliolid, d:disyclina?).	66
Figure 26. Photomicrograph of rudist fragments in Miliolid Wackestone facies from Germik-21 well (X4, core) (r:rudist)	67
Figure 27. Photomicrograph of microspar rarely found in Miliolid Wackestone facies from G. Germik-1.well (X10, cutting).(ms:microspar, v:valvulina).....	69

Figure 28. Photomicrograph of dolomite rhombs formed within the matrix of Miliolid Wackestone facies from Garzan-47 well (X4, cutting) (d:dolomite).....	70
Figure 29:The standart microfacies belts of carbonate depositional environment, a) synopsis of standart faices belts reviewing second order bodies of sediment and standart microfacies associated with each belt (Wilson, 1975), b)The standart facies zones of the modifed Wilson model (Flügel, 2004)	71
Figure 30. The occurence percentage of the constituents found in Rotalid Miliolid Wackestone facies.	74
Figure 31. Photomicrograph of rotalids found together with rudist and orbitoid fragments from G. Germik-1 well (X4, cutting) (o:orbitoid, ro:rotalid, r:rudist)	75
Figure 32. Photomicrograph of other bentic foraminifers found in Rotalid Miliolid Wackestone facies from Garzan-47 well (X4, cutting) (c:cuneolin).....	76
Figure 33. The occurence percentage of the constituents found in Orbitoid Miliolid Wackestone facies.	78
Figure 34. Photomicrograph of Orbitoid Miliolid Wackestone facies from Garzan-31 well (X4, core) (o:orbitoid, r:rudist).	79
Figure 35. The occurence percentage of the constituents found in Pelagic foraminiferal Wackestone facies.	82

Figure 36. Photomicrograph of Pelagic Foraminiferal Wackestone facies with ostracodes from Garzan-23 well (X10, cutting) (p:planktonic foraminifera).....	83
Figure 37. Photomicrograph of Pelagic Foraminiferal Wackestone facies from G. Germik-1 well (X4, cutting) (c:calcisphere?, d:dolomite rhomb).....	84
Figure 38. The occurrence percentage of the constituents found in Rudist Wackestone facies	87
Figure 39. Photomicrograph of Rudist Wackestone to Packstone facies from Garzan-95 well (X4, core) (r:rudist, b:bryozoan?)	88
Figure 40. Photomicrograph of rare miliolid in Rudist Wackestone facies from Germik-6 well (X4, core) (e:echinoid?, o:ostracode,m: miliolid).	89
Figure 41. Cycle types observed in the Garzan Formation in Garzan-Germik oil field.....	91
Figure 42. Paleogeographic facies map of middle – upper Maastrichtian of South East Anatolia (Güven et.al.,1991).....	96
Figure 43. Depositional model of Campanian- Paleocene units in South East Anatolia in District X (based on the data of this study and Yılmaz and Duran et. al., 1997).	97
Figure 44. Paleoecological distribution of Garzan Formation microfossils (Altiner, 1983).	100
Figure 45. Depositional model for Garzan Formation in Garzan-Germik oil field (modified from Altiner, 1983)	102

Figure 46. The depositional geometry of the wells of Garzan-Germik oil field with in the depositional environment. The studied wells are located schematically within the depositional environment. ...	103
Figure 47. Microfacies arrangement of the cycles types in Garzan Formation in Garzan- Germik oil field.....	104
Figure 48. Generalized stacking patterns of Garzan Formation within the Garzan-Germik oil field and its representative GR log responce.	109
Figure 49. The fossil content, cycles and the depositional environment of the Garzan-47 well (for arrows see figure 41)	113
Figure 50. The fossil content, cycles and the depositional environment of the Germik-21 well (for arrows see figure 41) (* means cycles located from log correlation).	116
Figure 51. The fossil content, cycles and the depositional environment of the G.Germik-1 well (for arrows see figure 41).....	118
Figure 52. The fossil content, cycles and the depositional environment of the Garzan-82 well (for arrows see figure 41).	120
Figure 53. The fossil content, cycles and the depositional environment of the Garzan-23 well (for arrows see figure 41).	123
Figure 54. The fossil content, cycles and the depositional environment of the Germik-6 well.	125
Figure 55. The fossil content, cycles and the depositional environment of the Garzan-43 well (for arrows see figure 41).	126

Figure 56. The fossil content, cycles and the depositional environment of the Garzan-33 well. (for arrows see figure 41) (* means cycles located from log correlation).....	128
Figure 57. The fossil content, cycles and the depositional environment of the Garzan-31 well (for arrows see figure 41) (* means cycles located from log correlation).....	130
Figure 58. The fossil content, cycles and the depositional environment of the Germik-3 well.	131
Figure 59. Idealized log trends (Milton and Emery, 1996).....	136
Figure 60. Representation of a maximum flooding surface in well data. (Myers and Milton, 1996).	138
Figure 61. The evidence of presence of sequence boundary (Myers and Milton, 1996).	140
Figure 62. Generalized GR-SONIC-Resistivity log patterns of Garzan Formation in Garzan-Germik oil field.....	144
Figure 63. The GR log correlation between Germik-21, G. Germik-1, G. Germik-2, Garzan-33, Garzan-31 and Garzan-23 in Garzan-Germik oil field from northwest to southeast.	147
Figure 64. The log correlation between G. Germik-1 (GR), Garzan-47 (Resistivity), Garzan-23 (GR) and Garzan-82 (SP) in the Garzan-Germik oil field from northwest to southeast	148

Figure 65. The log correlation between Germik-21 (GR), Garzan-33 (GR), Garzan-43 (Resistivity) and Garzan-82 (SP) in the Garzan- Germik oil field from northwest to southeast.....	150
Figure 66. The SONIC log correlation of Germik-21, G. Germik-1,G. Germik- 2 and Garzan-82 in the Garzan-Germik oil field from northwest to southeast.....	151
Figure 67. Representative GR readings for the environments. This shows that same type of GR readings indicating different environments.....	155

CHAPTER 1

INTRODUCTION

1.1. Purpose and Scope

There are many attempts trying to predict the depositional facies from wire line logs by using neural networks and statistical methods for a long time (Anderberg, 1973; Saggaf and Nebrija, 2000). Geologists use the log shapes to determine sandstone grain size trends and hence depositional facies (Rider, 1990). A universal application of log shape to grain size trend and depositional facies in clastics is wrong (Rider, 1990). On the contrary this study tries to hold a unique place in carbonates by trying to put forward a direct correlation between log response and the facies. The main theme of this research is to find a conclusion for the carbonates on the topic of direct prediction of depositional environment from logs.

In order to be able to state the result, the answers to the statements below are searched for;

-Whether there is a direct correlation between log response and the facies of the Garzan Formation.

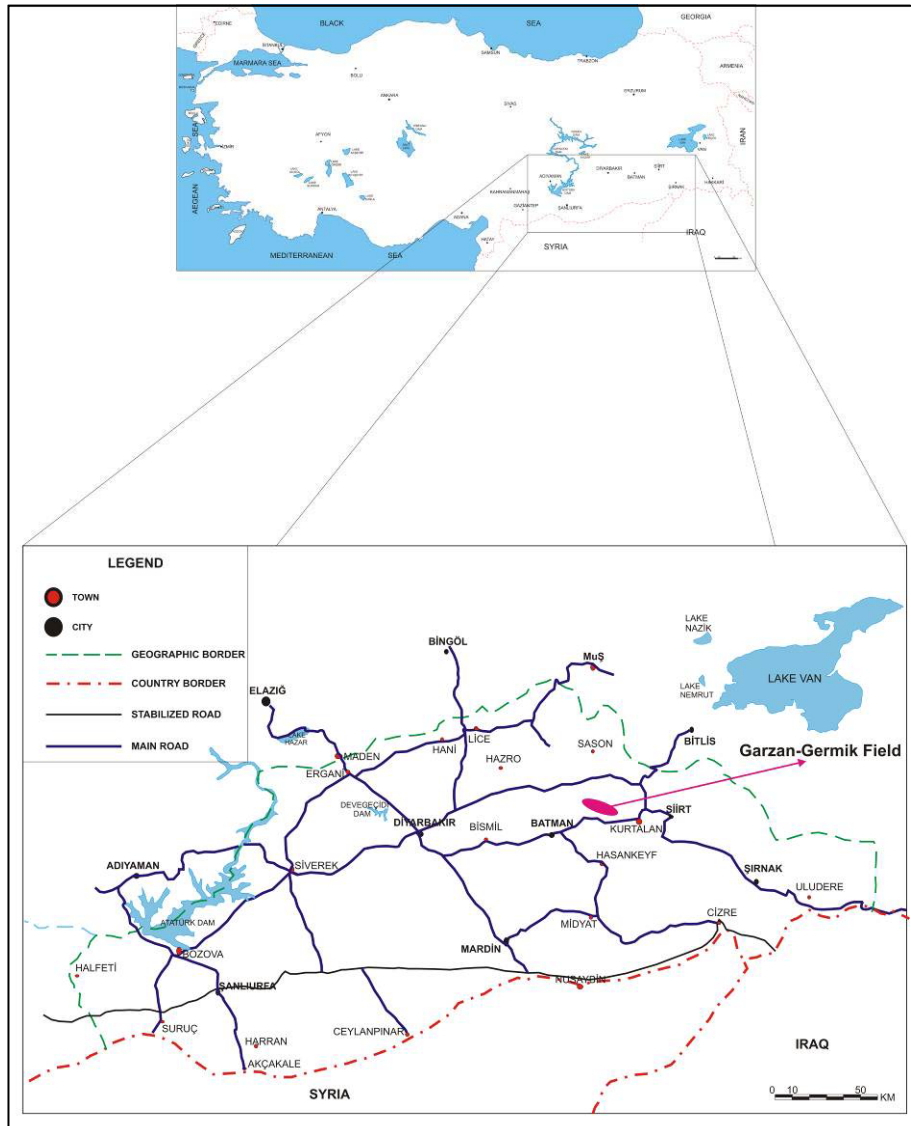


Figure 1: Location map of the study area. The rectangle shows the zoomed area

-If this direct correlation can be used to predict the facies without using the thin sections, so that the method can be applied to anywhere needed.

To achieve the answers to these questions, the microfacies types are described by using Dunham (1962). Microfacies are used to construct the stacking patterns and the cyclicity of the Garzan Formation in the Garzan-Germik oil field. This documentation used to analyze the characteristics of log response and the genetic relation between the microfacies, stacking patterns, cycles and the log; in other words petrophysical parameters of the formation.

1.2. Geological Setting of the Study Area

The study area is located within X. Petroleum District of South East Anatolia. The Garzan - Germik oil fields are located at about 45 km west of Siirt and 120 km to the east of Diyarbakır towns (Figure 1). The fields are located on a surface anticline trending northwest-southeast about 25 km long, which is shaped by Miocene tectonics (Figure 2 and 3). The anticline is bordered by a reverse fault from the southern part which is dipping to northeast (Figure 3). The highest topographic point is towards the east of Garzan field of the structure and the Hoya Formation (Middle – Upper Eocene) is the oldest unit exposed along the crest. Germik (Upper Eocene-Oligocene) and Şelmo Formations (Miocene) outcrop along the flanks (Figure 2). The Germik structure forms a separate topographic high at the northwest

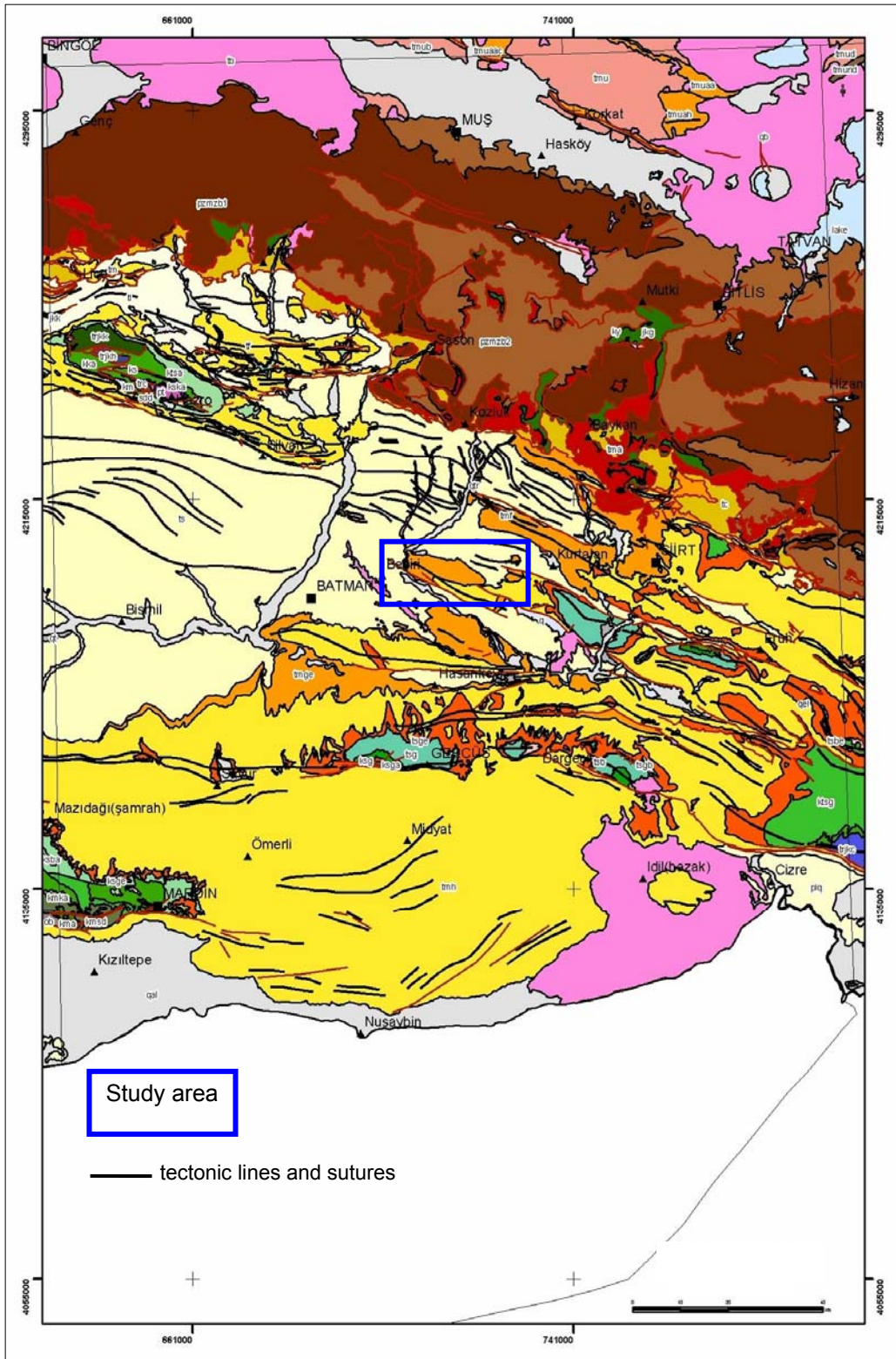


Figure 2: Geological map of the Xth. Petroleum District of Southeast Türkiye (1/250.000) (courtesy of TPAO) (for legend see page 5).

LEGEND	
qal	:Quaternary Aluvium
qb	:Basalt (Quaternary)
plq	:Plioquaternary Aluvium
tb	:Bazalt (Tertiary)
ts	:Şelmo Formation (U. Miocene)
tf	:Fırat Formation (Miocene)
tl	:Lice Formation (Miocene)
tc	:Cüngüş Formation (Eocene)
tmge	:Germik Formation (Eocene- Oligocene)
tmh	:Hoya Formation (Eocene- Oligocene)
tmua	:Aliboca Formation (Eocene)
tmuah	:Ahlat Formation (Eocene)
ktsa	:Antak Formation (Paleocene)
ktsg	:Germav (Maastrichtian-Paleocene)
tsb	: Becirman (Paleocene)
tsbe	:Belveren Formation (Paleocene)
tsg	: Üst Germav (Paleocene)
tsge	:Gercüş Formation (Paleocene)
ksga	:Alt Germav (Maastrichtian)
km	:Mardin Group (Aptian-Santonian)
ks	:Sayındere Formation (Campanian)
kmsd	:Derdere+Sabunsuyu Formations (Albian-Turonian)
kma	:Araban Formation (Aptian)
trjkk	:Koçali Complex (Paleozoic Mesozoic)
kka	:Karadut Complex (Paleozoic Mesozoic)
trjkh	:Hezan Formation (Paleozoic Mesozoic)
pt	:Tanin Group (Permian)
ptg	:Gomaniibrik Formation (Permian)
sdd	:Dadaş Formation (Silurian)
tma	:Maden Complex (Eocene)
jkg	:Guleman Ophiolite (Paleozoic-Mesozoic)
ky	:Yüksekova Complex (Paleozoic-Mesozoic)
pzmzb1	:Paleozoic Mesozoic Shist
pzmzb2	:Paleozoic Mesozoic limestone

Figure 2: Continued.

plunge of the anticline with the Germik Formation at the surface (Figure 3). The anticline is asymmetric, with dips of up to 15° on the northeast flank and as much as 75° at the eastern end of southern flank (Sanlav et. al., 1963). The reverse fault bordering the anticline from south has a vertical throw of 600 m along the central area but decreasing towards the end (Sanlav et. al., 1963) (Figure 3). Other minor faults complicate the structure and a small reverse fault cut the structure which has a lineation of north - northwest from the southern part of Garzan-26 well (Figure 3). A narrow asymmetric syncline parallels the anticline to the southwest of the bordering fault (Figure 3).

1.3. Historical Precedence of the Garzan-Germik Oil Fields

The Garzan – Germik oil fields are located in the ARI/TPO/777 license and 107 wells were drilled on the Garzan structure between 1944 – 1989 years and 23 well were drilled within the Germik structure between the periods of 1957 – 1988 (Figure 3).

Field work concerning the area had begun on the obvious feature at Garzan – Germik in the late 1930s by MTA after the discovery of Raman field. The first well in the Garzan field was spudded on December 1947 penetrating 1511 meters. At the depth of 1937m, 1417m, 1440m and 1466m there were shows of oil and gas. The well was abandoned as a dry hole without being properly tested because of technical reasons. Later in

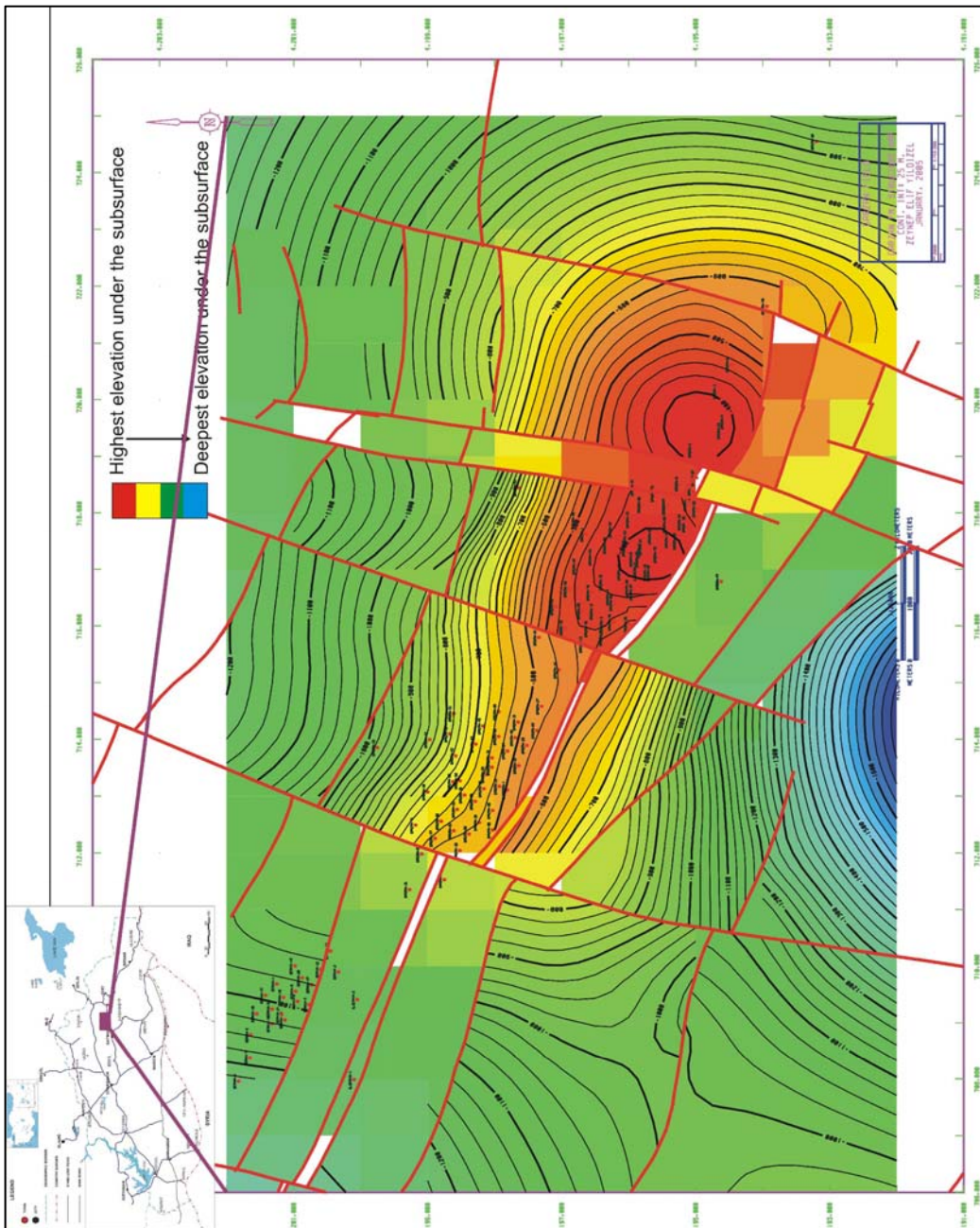


Figure 3: Structure map of top of the Garzan Formation in Garzan-Germik oil field.

November 1950 the Garzan-2 well was spudded and ended up as a discovery well. The second well was drilled down to 1511m. The first well on the Germik structure was spudded on June 1957 on gravity high and completed on February 1958 down deep to 2015 m. The Germik-1 well was a discovery well. In the Garzan field among the 107 wells drilled through the history of the field only 73 of them was ended up as oil well and 14 of them was a dry hole, 6 of them was completed as dry hole with oil show, 5 of them resulted as water well, 2 of them was abandoned for technical reasons and 7 of them was injection well (Figure 4). However within the 23 wells drilled on the Germik field only 2 of them was resulted as discovery well, 3 of them was dry hole, 10 of them was abandoned for technical reasons and 7 of them was water well (Figure 5).

The reservoir is the Maastrichtian Garzan Formation which is the subject of this thesis (Köylüoğlu, 1986; Güven et. al., 1991). The formation is a shallow to open marine carbonate spread out through the X. Petroleum District in Southeast Anatolia. The formation is being the subject of many studies, which is reported in detail in the previous work section, aiming to discover commercial oil trapped in. There are several oil fields producing from the Garzan Formation in the area; however the Garzan Field is the first one discovered commercial oil in the Garzan Formation and the formation is named after this discovery.

Garzan field is operated by TPAO and it was the second field to be discovered in Turkey. Garzan field went on stream in 1956 with an average

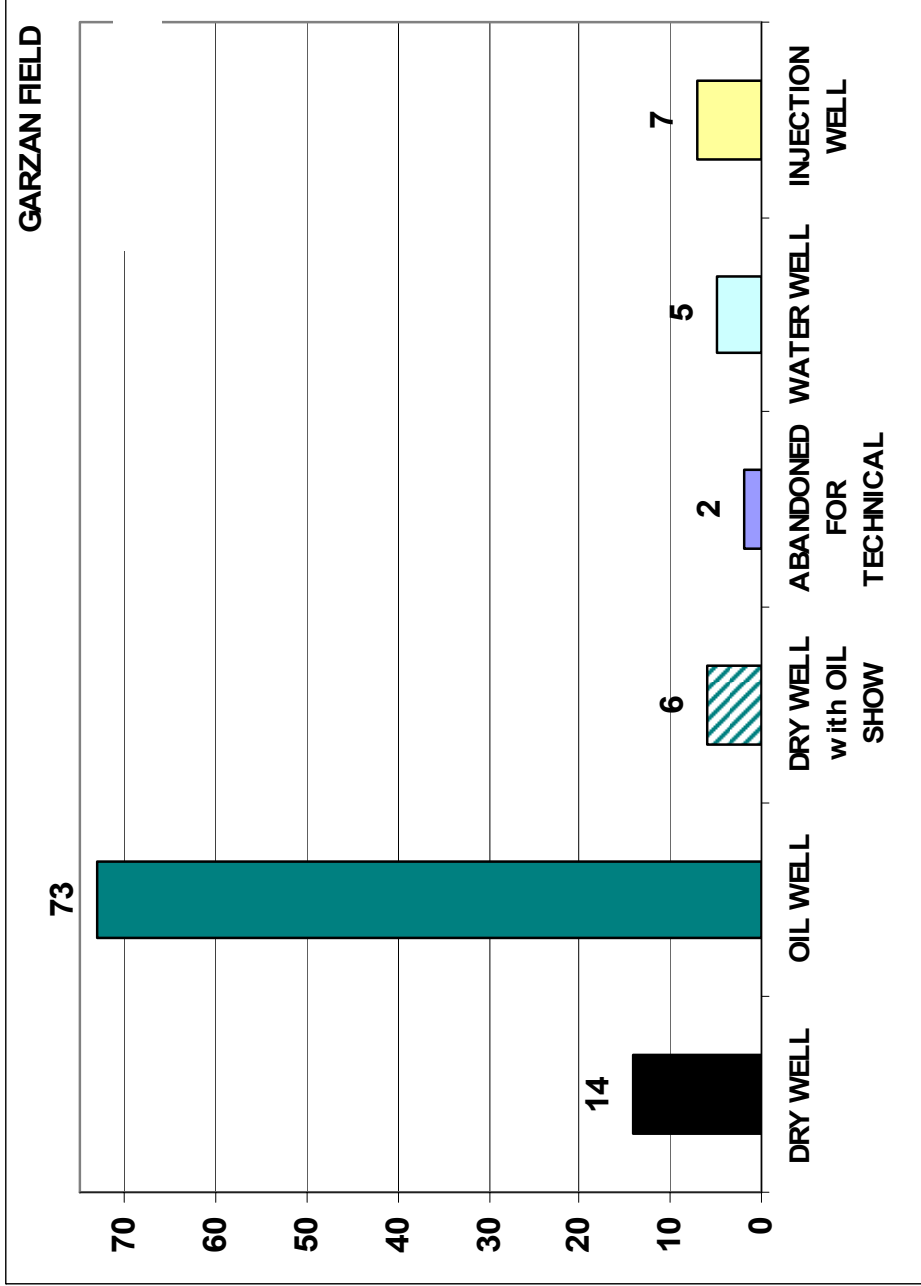


Figure 4: Completion types of the wells in Garzan oil field.

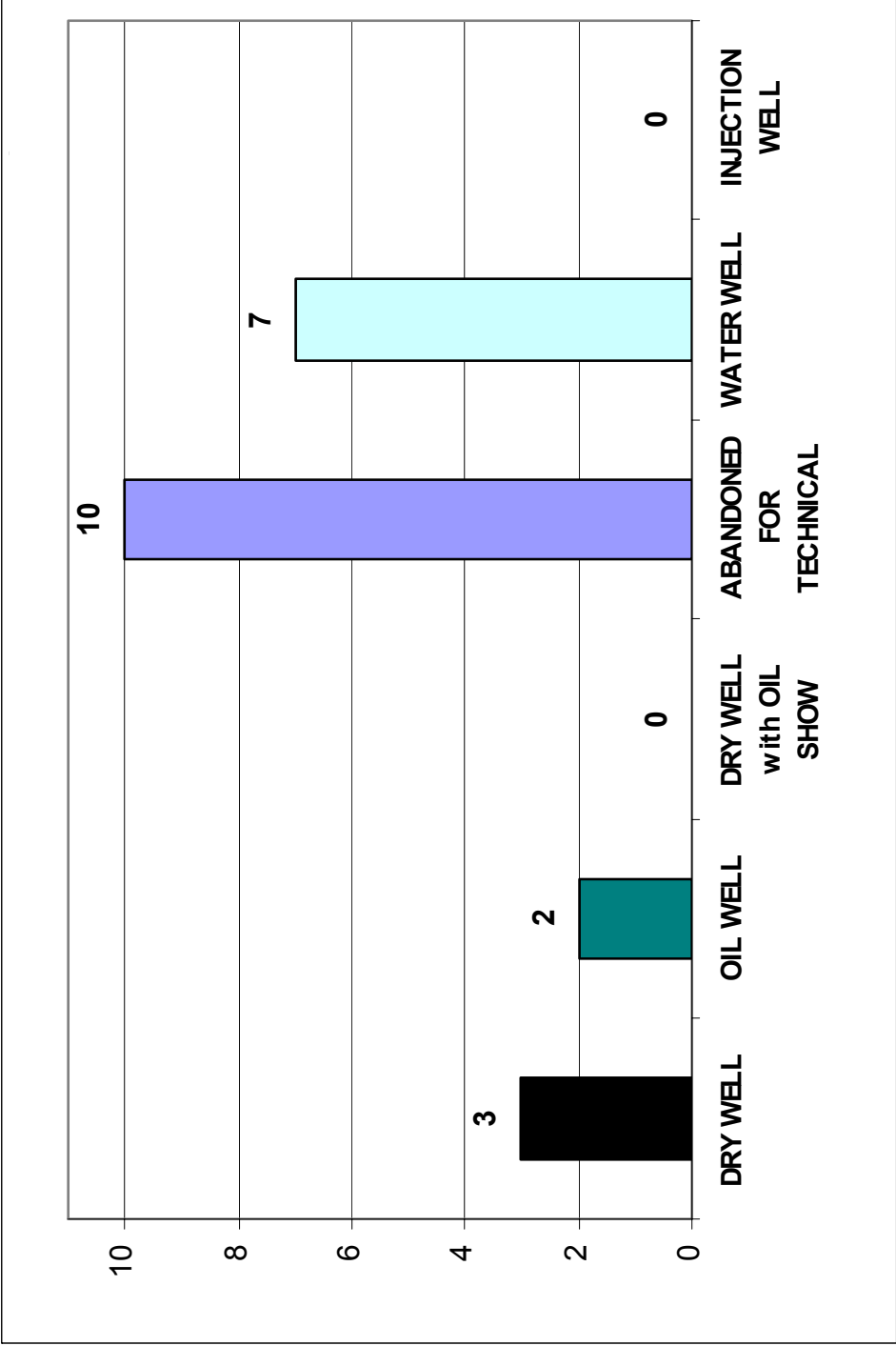


Figure 5: Completion types of the wells in Germik oil field.

production of 1058 BOPD (BOPD: barrels of oil per day) in 1989. The Germik field is also operated by TPAO and went into production in 1973. In 1989 the average production was 293 BOPD. Since the first discovery the Garzan Germik oil field produced a total of 45810823 bbl of oil by the end of April 2008.

1.4. Methods of Study

The study is divided into three main phases. The first one is literature survey, the second one is data gathering and the third one is laboratory work.

Literature survey was carried on the two main bases. One is concerning the Garzan Formation and the second one is concerning the correlation of facies with log response or prediction of facies from log response. During the survey it has been identified that the wire-line logs are used to predict the depositional facies and/or lithology by using statistical methods and neural network. In these studies they are mostly used as combination of logs and derivatives of them. The second part of the survey was about the Garzan Formation. There are many reports concerning the Garzan Formation in the archives of TPAO Exploration Group; however limited numbers of them were published.

The microfacies study of the Garzan Germik oil field started with six wells. These wells are: Garzan-11, Garzan-23, Garzan-31, Garzan-82,

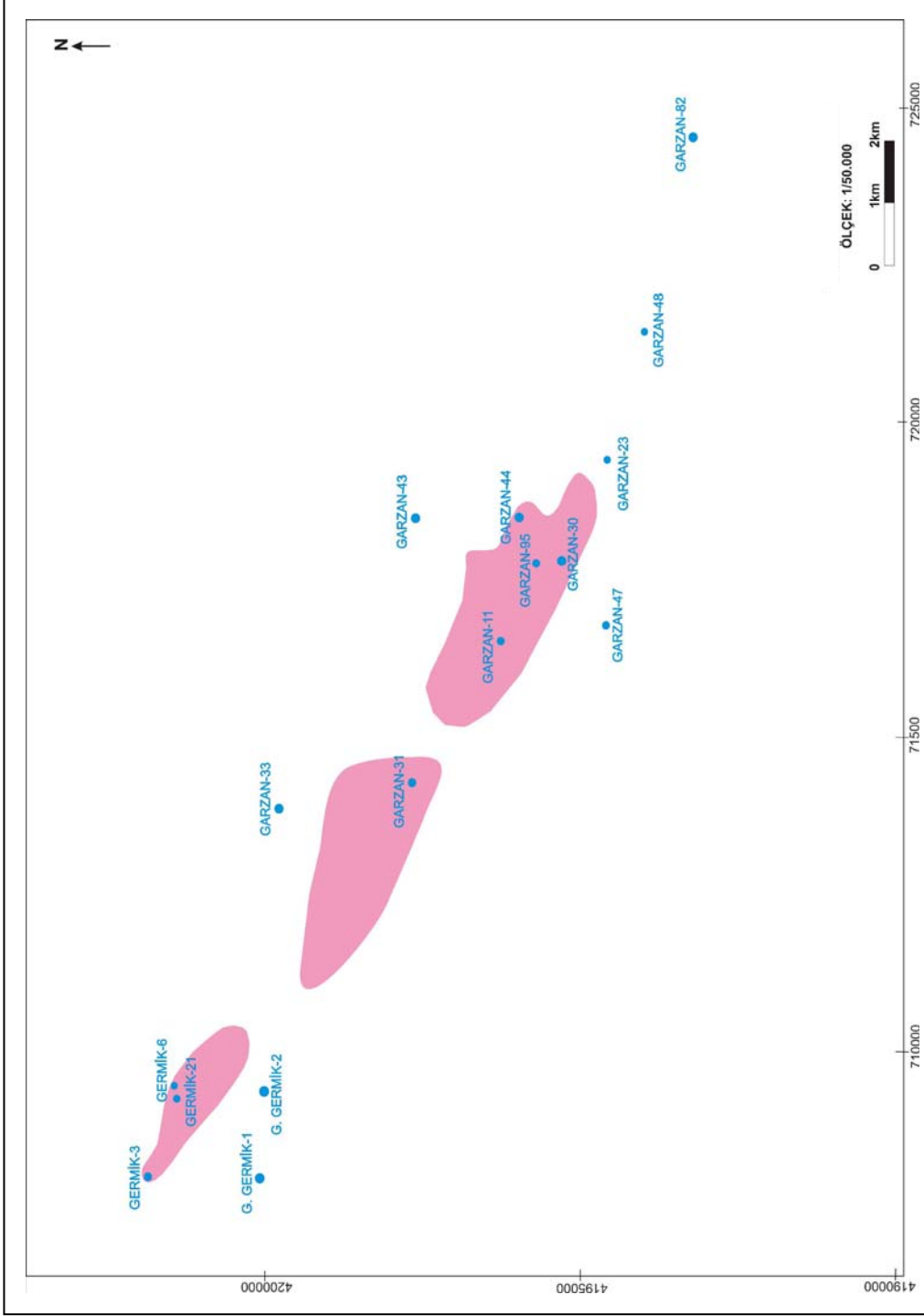


Figure 6: The base map of Garzan-Germik oil field and the studied wells are located.

Garzan-95 and Germik-6 (Figure 6). These wells were selected on the basis of two criteria; the first one is they have full Garzan Formation penetration except Germik-6 and the second important criteria was their core availability observed on papers in the archives of TPAO. The Garzan Formation in these well were fully or near fully cored during the drilling. Considering that these data is not enough for to complete the study, 10 more wells were added to the study. Those wells are Germik-3, Germik-21, G.Germik-1, G. Germik-2, Garzan-33, Garzan-30, Garzan-43, Garzan-44, Garzan-47 and Garzan-48 (Table 1). These wells were also chosen for the criteria written above and also for their nearly recent log suits and the position within the oil field (Figure 6).

There is 244.45 m of core for the Garzan Formation for the wells located in the Garzan-Germik oil fields (Table 1). However among the studied wells; the cores of the wells G.Germik-1, Garzan-11, Garzan-23, Garzan-30, Garzan-33, Garzan-43, Garzan-44, Garzan-48 and Garzan-82 were found in TPAO archives and they are examined and their photos were taken. However; it is seen that most of the cores were not suitable for macro investigation as seen from the pictures of the cores (Figure 7). As these wells are mostly very old and cores were used for many times and they lost their orientation and broken down into small pieces and their reliability were very poor so that the core examination is taken out of the study (Figure 7).

The wells used within the study are listed in the Table 1; Garzan-23, Garzan-31, Garzan-33, Garzan-43, Garzan-47, Garzan-82, Germik-3,

Table 1: The list and the data availability of the 11 studied wells in the Garzan Germik oil field .

WELL NAME	X	Y	TD	DATE	STATUS	GARZAN THICKNESS		GARZAN Fm TOP and BASE	CORE		LOG	NUMBER OF GARZAN THIN
						m			number	meter		
GARZAN -47	4194630	716800	2508	1960	oil show	190		2219-2409	5	14	SP-EL	72
GERMIK-21	4201171	709167	2220	1986	water	173		1920-2093	1	5	GR-SONIC	16
G.GERMIK-1	4200103	707989	2205	1986	water	134		1957-2091	3	25	GR-SONIC	25
GARZAN-82	4193207	724544	1792	1963	oil show	166		1553-1719	2	10	SP-SONIC	51
GARZAN-23	4194610	719420	1694	1957	oil show	63		1461-1524	4	8.4	GR-EL	22
GERMIK-6	4201370	709280	2020	1961	water	90p		1930-2020p	20	81.05	SP-EL	15
GARZAN-11	4196261	716508	1460	1958	oil	73p		1387-1460p	1	4	GR-EL	1
GARZAN-95	4195628	717586	1488	1987	oil	80p		1408-1488p	2	8.5	GR-SONIC	2
GARZAN-43	4197638	718452	1835	1959	water	85		1613-1698	1	4	SP-EL	8
GARZAN-33	4199810	713860	2014	1958	oil show	112		1783-1895	1	6	GR-EL	10
GARZAN-30	4195670	717790	1525	1960	oil	88p		1437-1525	12	49.35	GR-EL	*
GARZAN-44	4195940	718420	1548	1959	dry	113		1416-1529	1	3.07	GR-EL	*
GARZAN-48	4193970	721640	1629	1960	dry	70		1494-1564	2	2.35	GR-EL	*
G.GERMIK-2	4200041	709410	2185	1988	water	114		1969-2083	2	18	GR-SONIC	*
GERMIK-3	4201870	708000	2244	1959	oil	172		1985-2157	9	35.89	SP-EL	9
GARZAN-31	4197690	713310	1753	1958	oil	151		1501-1652	5	23.45	GR-EL	21



Figure 7: Photographs of the condition of the cores of Garzan Germik oil field wells.

Germik-6, Germik-21 and G. Germik-1. The well G.Germik-2 is used for log correlation because the well has a full Garzan Formation penetration but lacks thin section (Table 1). The wells studied in this research were drilled in between the years 1957-1988. Among them 10 of the wells (Garzan-23, Garzan-31, Garzan-33, Garzan-43, Garzan-47, Garzan-82, Germik-3, Germik-21, G. Germik-1 and G. Germik-2) have full Garzan Formation penetration with a thickness range between 63 m to 190 m (Table 1). The wells Germik-6, has only limited penetration in the Garzan Formation (Table 1). The depth of top Garzan Formation in these wells ranges between 1387 m and 2219 m. There are total of 252 thin sections belonging to these wells and the best thin section control belongs to the Garzan-47 with 72 thin sections (Table 1). Germik-21, G. Germik-1, and G. Gremik-2 owns GR-SONIC, Garzan-43 Garzan-47, Germik-3 and Germik-6, owns SP-EL and Garzan-23, Garzan-31 and Garzan-33 owns GR-EL log suits. Garzan-82 is the only well retaining SP-SONIC log suit in this study (Table 1). The wells Garzan-47, Garzan-82, Garzan23 and Garzan-33 are completed as dry hole with oil show, Germik-6, Germik-21, G. Germik-1, G. Germik-2 and Garzan-43 are ended as water well and Garzan-31 and Germik-3 discovered oil (Table 1).

Wells were examined in order to construct the depositional model for the Garzan Formation and their microfacies was classified according to Dunham (1962) classification which is chosen as it briefly explains the energy and the depositional environment.

The structure map was constructed with Landmark graphics programme by using formation tops of 120 wells. Faults were interpreted with the aid of seismic lines which will not be emphasized in this document (Figure 3).

The laboratory work concerning the thin section analysis carried on the transmitted light microscope. Also 10 to 5 representative thin sections for each of the facies were counted by point counting method, in order to give the quantitative ingredients. The average occurrences of the constituents of the facies given in the related chapters, and the detailed documentation of the results are given in Appendix B.

All the data used in this manuscript is used with the permission given by Türkiye Petrolleri A.O. with General Manager authorization number 1158 at 24th October 2003.

1.5. Previous Works

In this section only the previous works about the Garzan Formation and selected literature related to the log to facies and log to lithology correlations are going to be given.

Garzan formation has been the subject of many studies carried since the first discovery had been made in 1956 with the well Garzan-2. The formation takes its name from the Garzan field and firstly defined by Turkish Petroleum Company (1961). However, the formation never crops out and

was named from the drilled well Garzan-47. Before that, some of the foreign petroleum companies named it as the Kiradağ Limestone (Kellog, 1961).

The 33% of the studies is about the stratigraphy, paleontology, sedimentology and petrography of the formation in order to construct the depositional environment and stratigraphic evaluation. The second popular topic is about the hydrocarbon potential of the formation and the reservoir characteristic of the formation both holds the 16% of the whole studies. The seismic evaluation, log evaluation and geochemical analysis cover the 50% of all the studies. The thickness maps of the formation and other topics cover minor percentage of the studies (Figure 8). Among all the studies about Garzan Formation there is only 2% related with the Garzan-Germik oil field.

The distribution of the studies according to the years is that; 59% of the whole is done with in the years 1982-1989 and the 23% with in 1990-1999 and 11% within 1972-1979. There is only one study in the year 1967 and 1961 both occupy 2%, where the studies after the year 2000 covers 5% of the whole (Figure 9).

The Middle –Late Maastrichtian Garzan Formation (Güven et. al., 1991) was being deposited with in the central and northern part of the District X and NW of District XI; at the northern margin of Arabian Platform. The sedimentation of Garzan Formation which consists of shallow marine carbonates is defined by the basinal areas where the north and southwest border of formation grades into time equivalent marl and shale deposits (Güven et. al., 1991). The results of the micropaleontological study carried

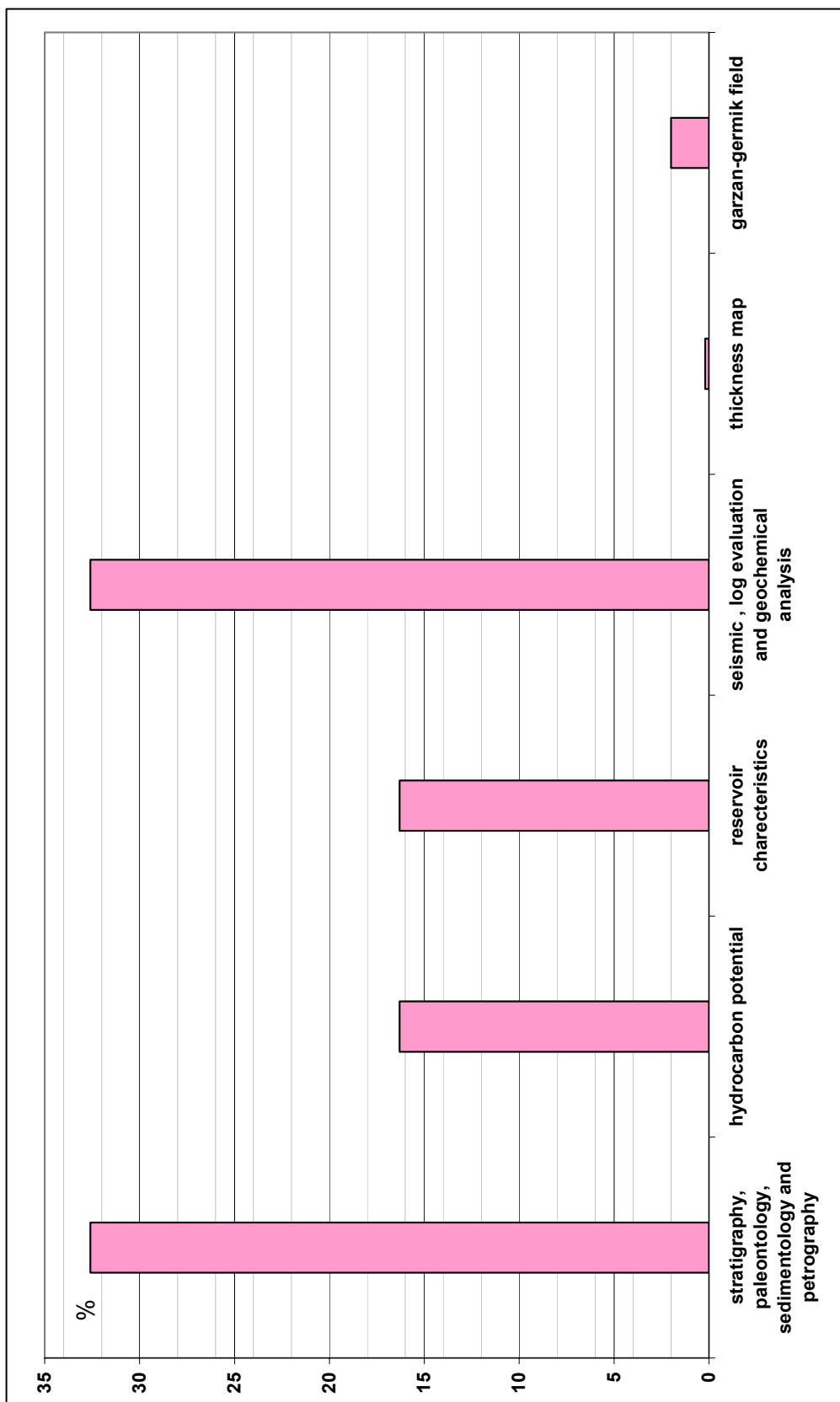


Figure 8: The share percent of topics concerning the Garzan Formation.

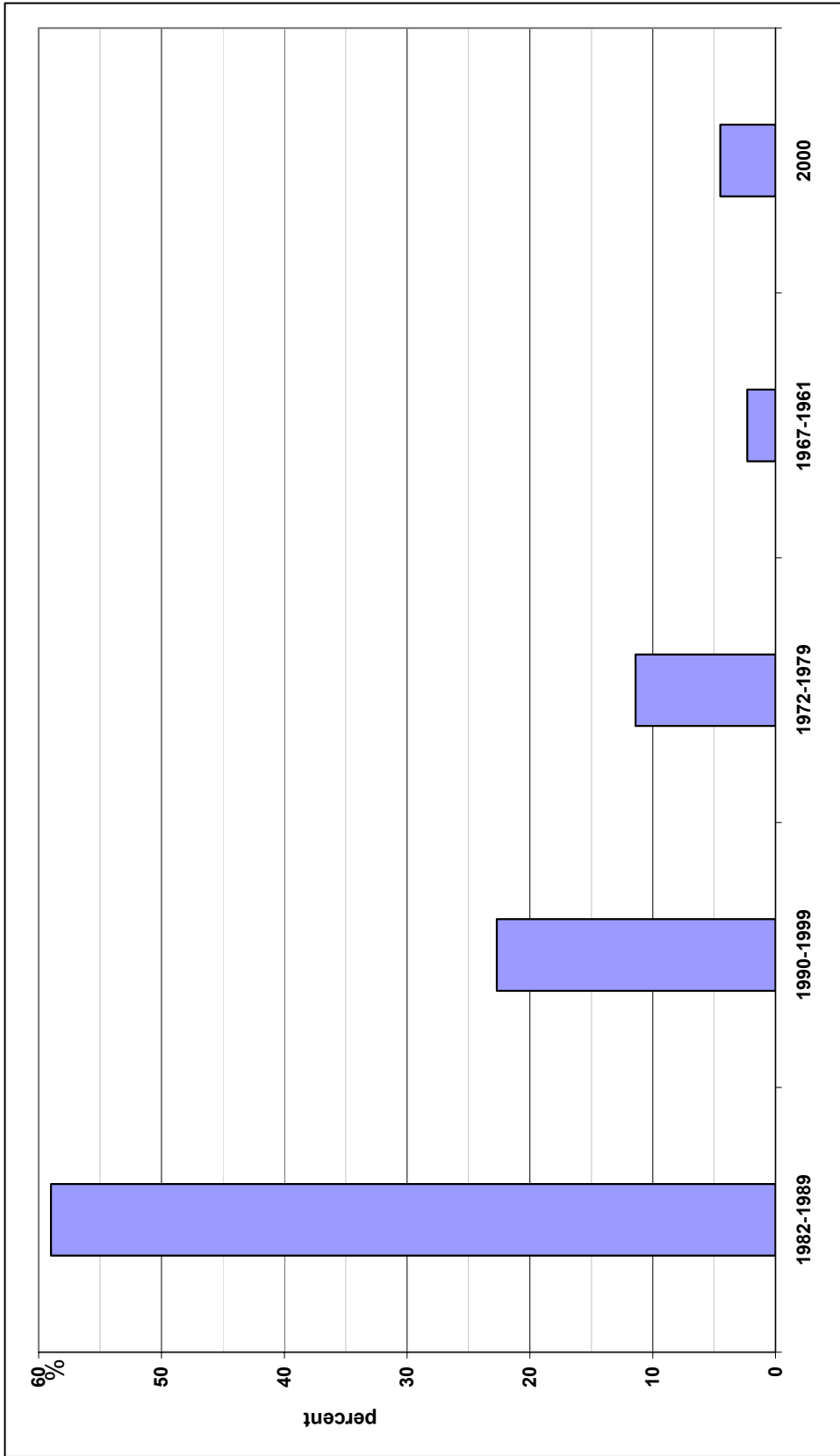


Figure 9: The distribution percent of studies about Garzan Formation according to years.

with in the Raman field revealed that, according to the cuttings taken from 7 wells of the field the age of the formation is Late Maastrichtian (Yöndem et. al., 1985). However, three different biofacies was put forward for the formation within the study of Erenler et. al. in 1992 which showed that the age of the Garzan Formation is Early Maastrichtian (Erenler et. al., 1992).

The first researcher who divided the formation into 3 members is Keskin (1967). He studied seven wells and divided the formation into three members as C-limestone with shale alternation, B-with small foraminiferal spary calcite with pyrite and quartzite and A-biomicrite with ostracode and recrystallization. This division was quiet different than the divisions of Açıkbash et. al. (1981), Erenler et. al. (1992), Araç and Yılmaz (1989), Araç et. al. (1990), Yılmaz (1989), Değirmenli et. al. (1985), Sezgin (1982) and Araç (1982).

Among the studies concerning the Garzan Formation facies the work of Salem et. al. (1986) keeps its place where he informs that the formation starts with low energy micritic sediments grading into reefal and bioclastic intraclastic facies. He defines shallowing upward sequence starting with subtidal environment and grading into intertidal area (Figure 10).

Later Yılmaz and Araç (1990) divided the Garzan Formation into five facies with microfacies analysis by using Dunham (1962) classification. These are planktonic foraminiferal wackestone, small benthonic foraminiferal wackestone, big foraminiferal packstone, mollusk wackestone, intraclastic bioclastic packstone. Eseller (1987) also divided the formation into five microfacies; rudist-miliolid packstone, miliolid wackestone, sulcoperculina

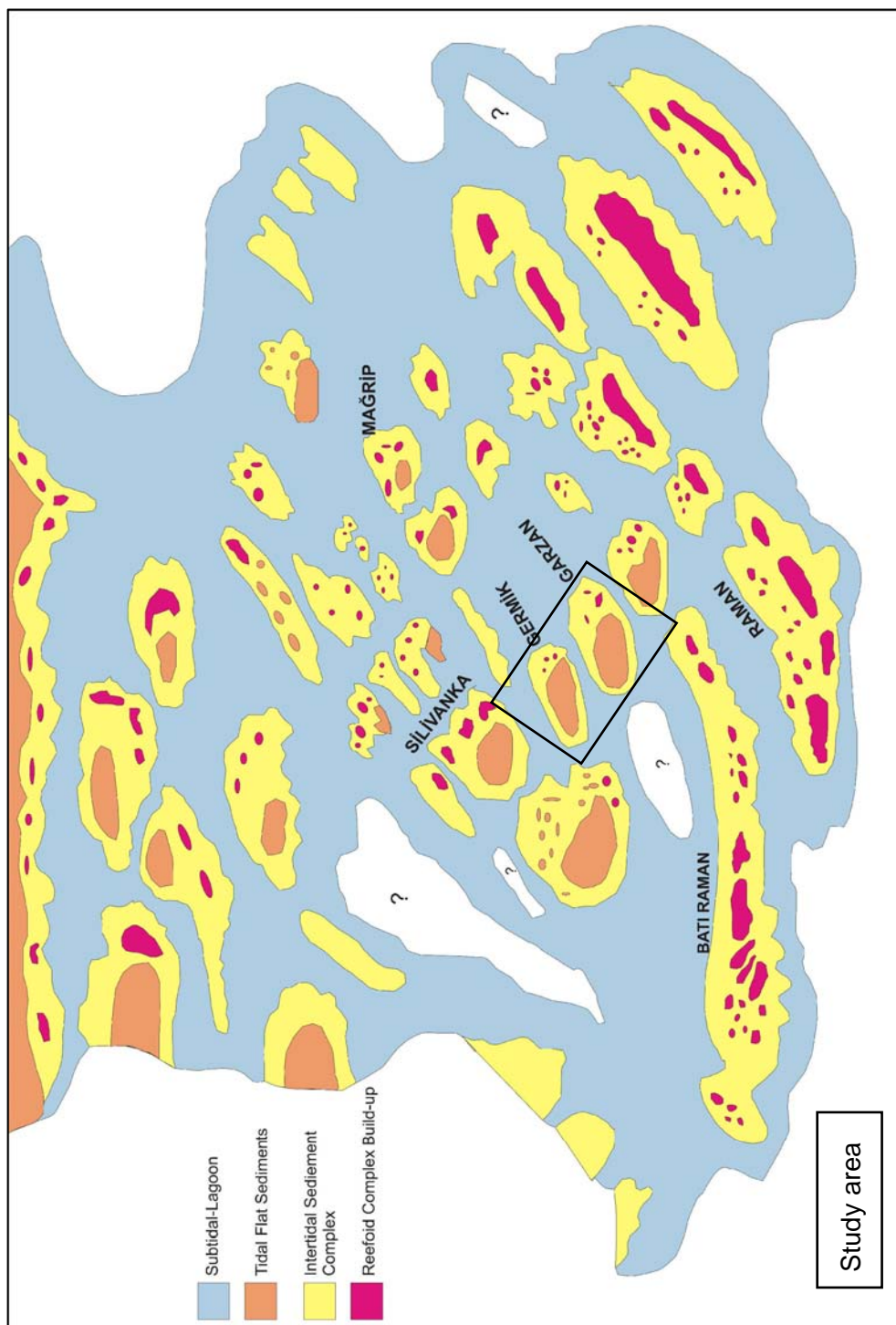


Figure 10: Facies map of Garzan Formation carbonates according to Salem et. al. (1986)

wackestone, pelagic foraminiferal wackestone-mudstone and grainstone.

Before this study (Yılmaz et. al., 1990) Garzan Formation was subdivided into six facies by studying Mağrip oil field (Naz,1986; Naz,1987).In this study the intraclastic bioclastic packstone of Yılmaz et. al. (1990) was classified as planktonic foraminiferal rudist silty packstone and miliolid wackestone was the sixth one which is not present in Yılmaz et. al.,(1990).

Meanwhile; as Garzan Formation is producing oil at some of the fields, the researchers tried to find out its reservoir properties and carried on studies on the topic. It is found that the dolomitic zones in the formation have good reservoir quality (Karandili, 1991) where there is porosity. By studying different oil fields the formation is said to have %6-10 porosity with 45md permeability and 40000-70000ppm salinity (Çoban and Kaya, 1992). However, another study carried showed that the formation salinity is very low (3000-6000ppm) and permeability increases from NW to SE (Namoğlu et. al., 1997). Some of the fields as B. Raman, Mağrip, Oyuktaş, Kurtalan, Silivanka, Beyçayır, Raman, Sezgin was also studied in order to construct the reservoir parameters of the formation and porosity, salinity, pressure gradient, temperature gradient, reservoir thickness maps were constructed and log lithology correlations with tectonic evolution and clay mineralogy affecting the reservoir quality are evaluated in order to set production policy to increase the production (Değirmenli et. al.,1989; Sarı,1986; Pehlivan,1984;

Gürel,1984; Kavukçu,1984; Sarı,1984a; Sarı,1984b; İşbilir,1982; Çubukçu and Ertürk, 1982; Sarı et. al., 1979; Yöndem, et. al.,1985).

Although Garzan Formation is a producing reservoir some of the researchers wondered whether it has enough potential to be a source rock. Today it is believed that carbonates can also be a good source rock. In order to search this, Garzan formation is investigated through the samples of some of the wells (Kıradag-1, Mağrip-8) and it is revealed that it has only source rock potential in Mağrip-17 well and increasing maturity with increasing depth from south to north (İleez and Öztümer; 1982, İztan,1988; İztan, 1989).

In order to reconstruct the structural map of Garzan Formation with in different areas Tekiner (1989), Tekiner (1988), Tosunkara (1984), Üngör (1983), Baştuğ (1972), Baştuğ (1973), Boroğlu, (1983) studied and resulted with seismic maps. The seismic quality within Bada, Bastokan, Mağrip, Kentalan and Kurtalan fields gives permission only for constructing structural maps and it is impossible to see the facies changes in the seismic (Tekiner, 1988).

There have been a limited number of studies carried about the Garzan Formation with in the Garzan-Germik field where the formation takes its name. The evolution of Upper Cretaceous units especially the Garzan Formation was studied with a wide comprehensive work in the Garzan-Germik field. According to this study the fault leaned NW-SE and folds related with Cretaceous tectonics affects the facies distribution of the formation (Özbahçeci and Üngör, 1988).

The reverse faults of Miocene tectonics define the southern border of the field. Garzan Formation shows different facies characteristics and diagenesis within a short distance and owns three different oil-water contacts. This shows a permeability barrier with NW-SE leaning impermeable faults (Özbahçeci and Üngör, 1988). The most productive facies of the formation in the lower block of the field was deposited to northern border of the fault (Coşkun,1978).

As a last word Garzan Formation is productive where NE-SW leaning porosity zones and NW-SE leaning structures are cut across each other (Sanlav,1972). Even after the 50 years of exploration and use of the most advanced technology Garzan exploration is still a challenge.

There are attempts trying to predict the lithology or depositional facies from the wire line logs by using neural networks. Saggaf and Nebrija (2000) used cross plot of the log values of well; neutron porosity, density and deep resistivity. However before them Delfiner (1987) and Bush et. al. (1987) used discriminant factor analysis to correlate the log values to lithology facies. The other researchers give more complete treatments for multi dimensional statistical analysis methods (Anderberg, 1973; Rao, 1973).

Saggaf and Nebrija (2003) also put forward a method based on fuzzy logic inference which can be used to identify the lithological and depositional facies from wire line logs. Although fuzzy logic is sometimes used as a synonym for multivalent logic, its more common use is to describe the logic of fuzzy sets (Zadeh, 1965).

Previously, identifying facies from well logs has been carried out by methods that rely on multivariate statistics and regression, such as principle component analysis (Wolff and Pelissier-Combescure, 1982) and discriminant factor analysis (Bush et. al.,1987; Delfiner et. al.,1987) as well as techniques based on various forms of neural network, such as self organizing maps (Baldwin, et. al., 1990; Zhang et. al.,1999), back propogation feed forwards neural networks (Rogers, et. al., 1992; Kapur, et. al., 1998; Benaouda et. al., 1999) and competitive networks (Saggaf and Nebrija, 2000). Wylie and Wood (2005) used a well log tomography technique that uses the amplitudes of standard well log curves, to map the internal architecture of geologic formations and reservoirs. Aguilera (2004) tried to show that a Pickett plot of interparticle porosity vs. true resistivity should result in a straight line for intervals with a constant rock fabric. This method helps to illustrate the important link between geology, petrophysics and reservoir engineering.

1.6. Terminology and Concept of Logs

1.6.1. Terminology and Concept of SONIC Logs

The sonic log provides a formations interval transit time which is the reciprocal of the velocity. It is a measure of the formation capacity to transmit sound waves which varies by lithology and rock texture and porosity (Rider,

1996). Geologically this capacity varies with lithology and rock texture (Figure 11). Sonic log is used to evaluate porosity and as an aid to seismic interpretation it can be used to give interval velocity profiles. Qualitatively the sonic log is sensitive to subtle textural variations and it can help to identify the lithology.

Sonic values are given in microseconds (μs) per foot. This value is called *interval transit time* (Δt) (Rider, 1996). The most common interval transit times (Δt) fall between $40\mu\text{s}$ - $140\mu\text{s}$; this scale is usually chosen for the log outputs. The velocity is the reciprocal of sonic transit time. The conventional general purpose, sonic tool measure the time it takes for a sound pulse to travel between a transmitter and a receiver, mounted a set distance away along the logging tool. The vertical resolution of the sonic is the span between receivers in which this is frequently two feet (61cm) (Rider, 1996; Thomas, 1997; and Purdy, 1982). The sonic log can be used to calculate porosities and rock texture and there is a simple relationship between velocity and porosity (Wyllie et. al., 1956).

The transit time measured by the tool is the time spent in the solid matrix and the time in fluid: it is called the time average relationship (Wyllie et. al., 1956). The sonic log response is not very diagnostic in lithology, but it is very sensitive to rock texture. The way in which sound travels through a formation is associated with matrix, matrix materials, grain size distribution and shape and cementation (Wyllie et. al., 1956). The natural occurrence of high velocity is most likely to be associated with carbonates, middle velocities

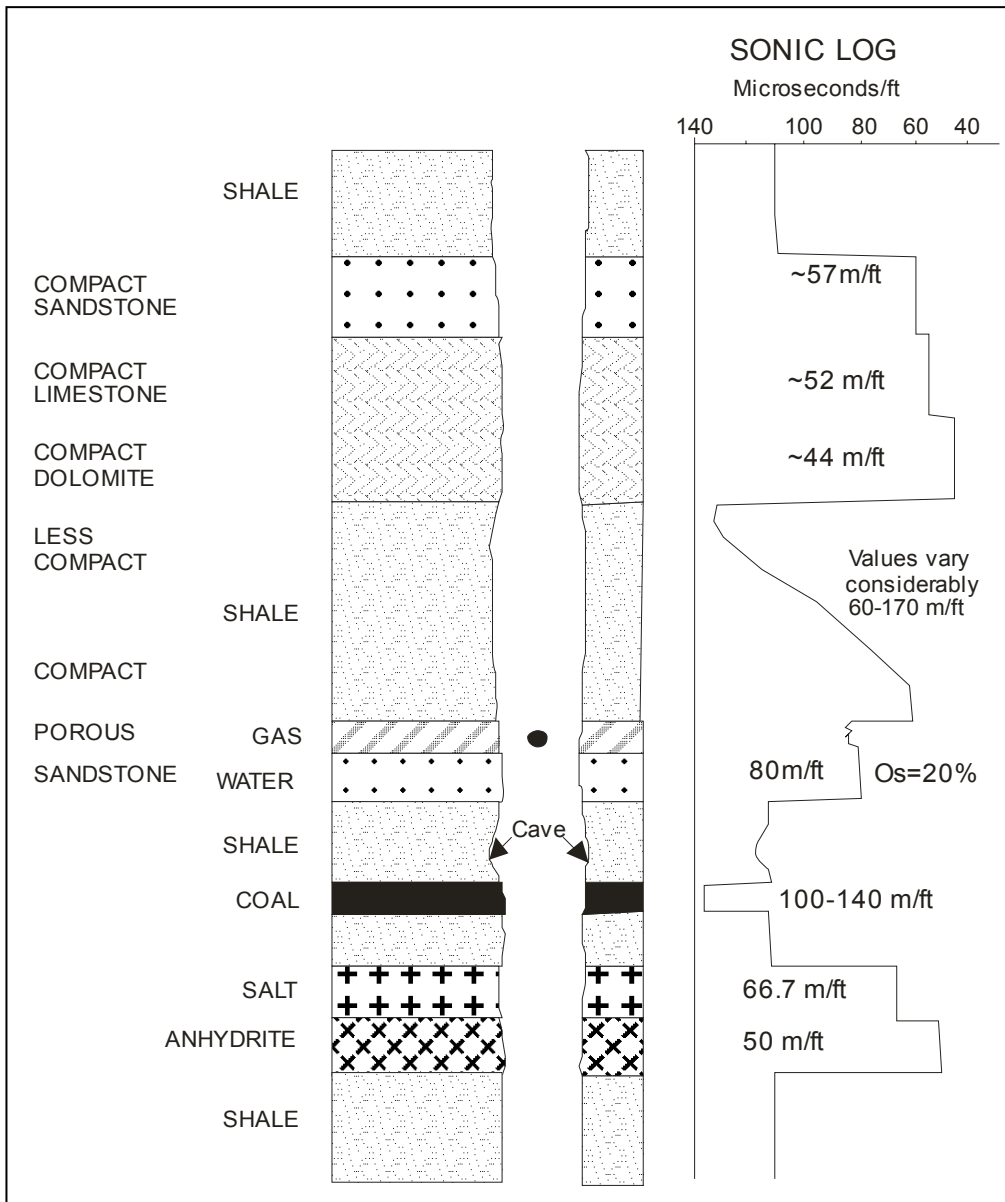


Figure 11: The sonic log showing a formation's ability to transmit sound waves according to its lithology and rock texture (Rider, 1996).

with sands and shales and low velocities with shales (Rider, 1996).

Shales will have a higher transit time (lower velocity) than sandstones of a similar porosity which sometimes allows the sonic log to be used as a grain size indicator (Rider, 1996). High concentration of organic rich condensed sections will result in very long travel times in sonic logs. The log is also affected by post depositional cementation and compaction and by the process of fracturing (Emery and Myers, 1996)

The sensitivity of the sonic to bedding as well as texture at smaller scale is because the detected signals physically travel up and down through the formation (Rider, 1996). Any horizontal feature as bedding must be crossed and it will affect the response. The sonic transit time character of a formation is a very distinctive characteristic and sonic log picks out small variations and indicate a very distinctive stratigraphic interval regardless of depth differences. Sonic log is used for correlation because of its distinctive characteristic and there are many examples in the literature in this concept (Michelson, 1989; Whittaker et. al., 1985) (Figure 12).

1.6.2. Terminology and Concept of GR Logs

The gamma ray log is one of the most useful logs and is run in most of the wells. The radioactivity of the rock measured by GR log tool is generally a direct function of the clay mineral content and this grain size and depositional

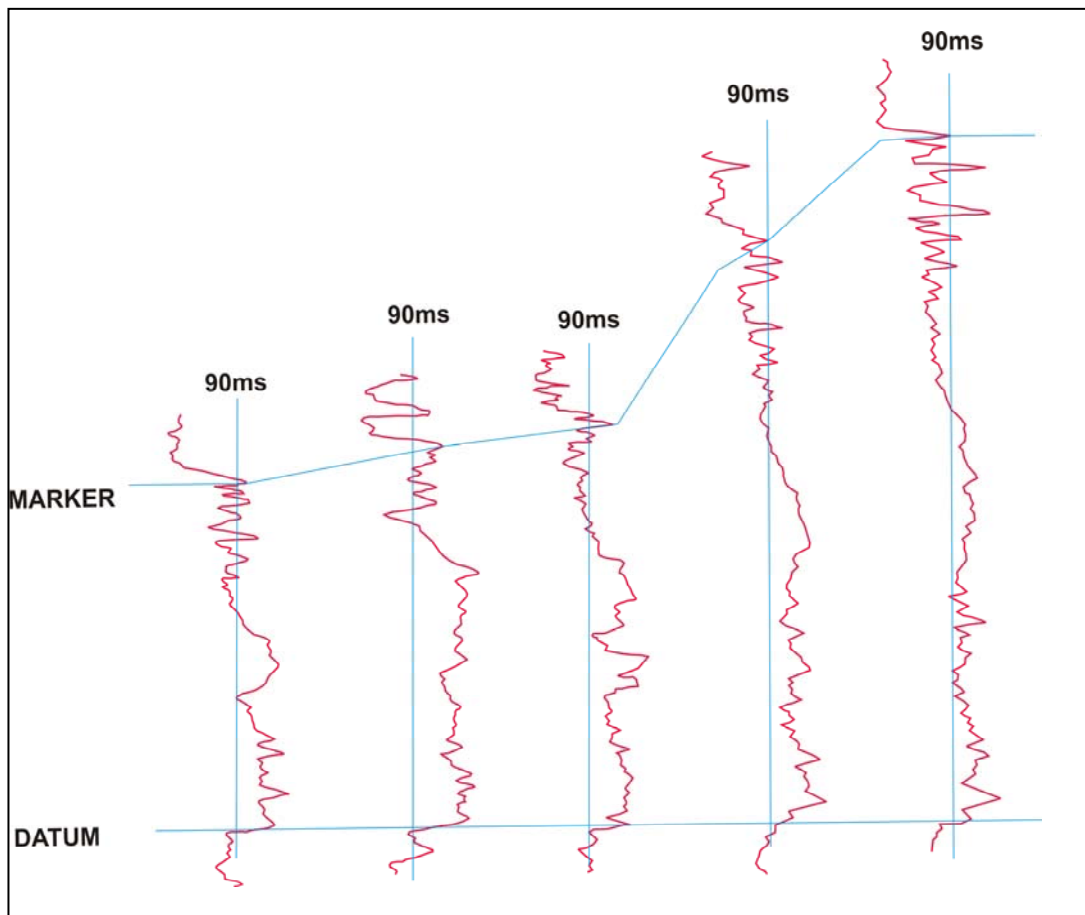


Figure 12: The character of sonic log used for correlation. The log is sensitive to lithological changes as indicated by the logs in this sequence (Rider, 1996).

environment. Gamma ray logs are often used to infer changes in depositional energy, with increasing radioactivity reflecting increasing clay content with decreasing depositional energy (Emery and Myers, 1996).

The GR log is a record of formation's radioactivity. The radiation emanates from naturally occurring uranium, thorium and potassium. The geological significance of radioactivity lies in the distribution of these elements (Rider, 1996). Among the sediments, shales have the strongest radiation.

The GR log can be used to correlate and to suggest facies and sequences and to identify lithology. As a first indicator of lithology the gamma ray log is extremely useful as it suggests where shale may be expected (Figure 13). Carbonates in their pure state are not radioactive and this aids their identification (Figure 13). However, carbonates contain organic matter and this is frequently radioactive due to uranium (Hassan, 1973) (Figure 14). If the carbonates contain shale to some extent then they will show the presence of potassium and thorium.

The GR log is used as a grain size indicator also (Figure 15). The basis for this is the relationship between grain size and shale content. For example coarse grained sand will have very low shale content and will read low gamma ray values due to the low potassium and thorium content. A fine grained sand mat has high shale content and will read high gamma ray values due to high concentration of potassium and thorium. The first look at GR log will lead to understand the shale content of the formation and also the

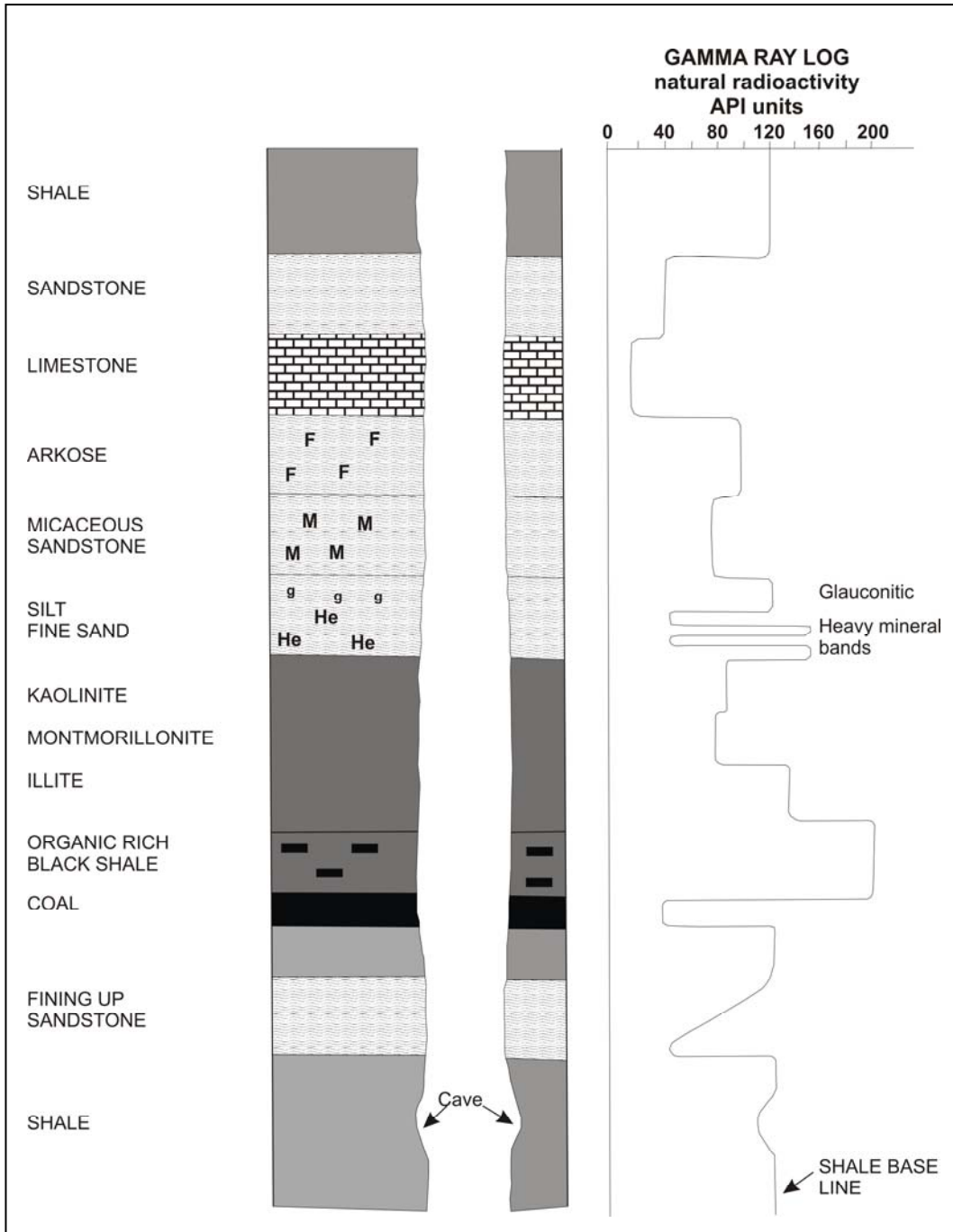


Figure 13: The typical responses of gamma ray log for lithologies. The gamma ray log shows natural radioactivity (Rider, 1996). (He:heavy minerals; g:glaucinite; M:mica; F:feldspar).

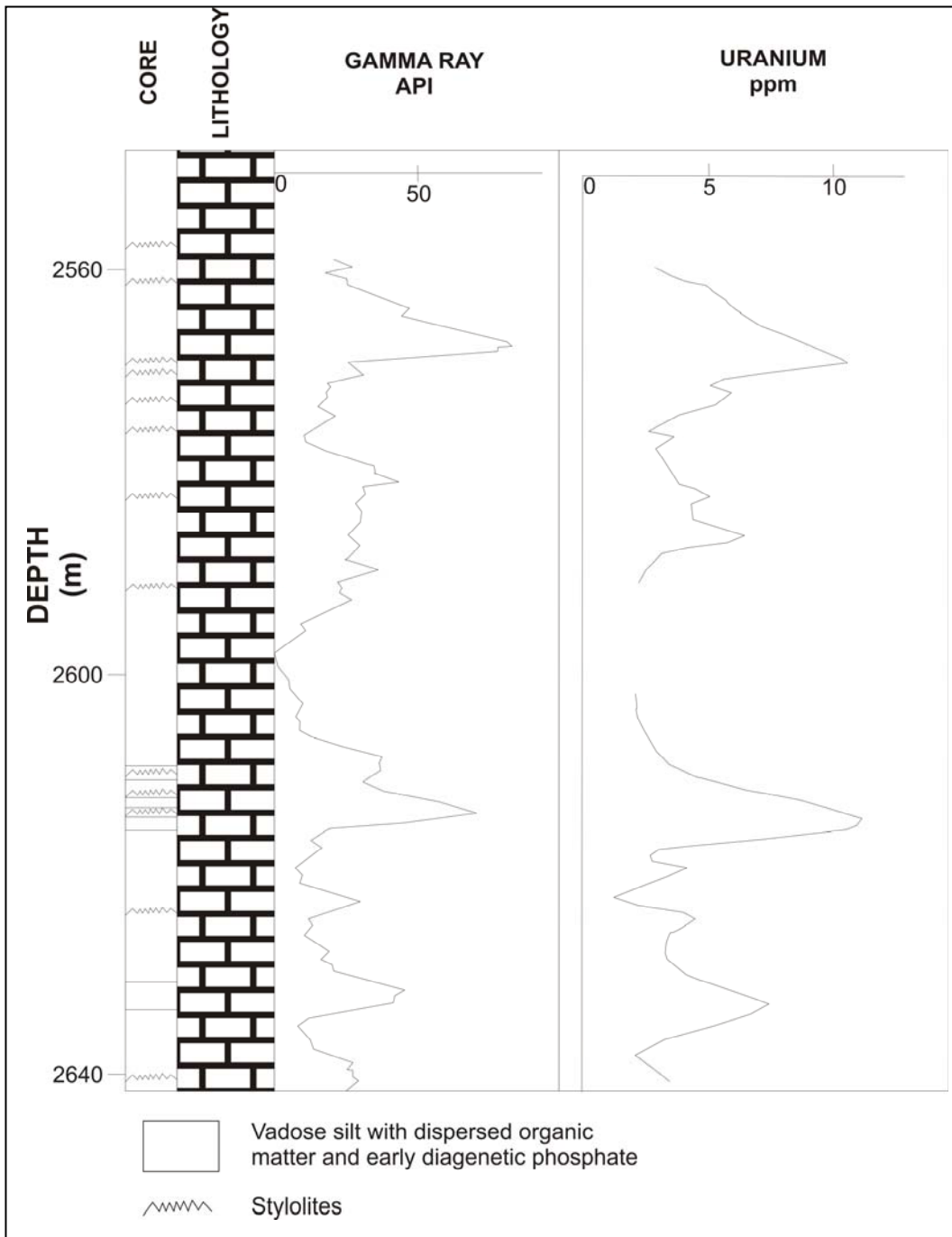


Figure 14: Radioactivity of Ypresian (Eocene) Limestones, Tunisia, related to uranium concentrations. The uranium is associated with early diagenesis, organic matter and phosphatic concentrations (Hassan, 1973).

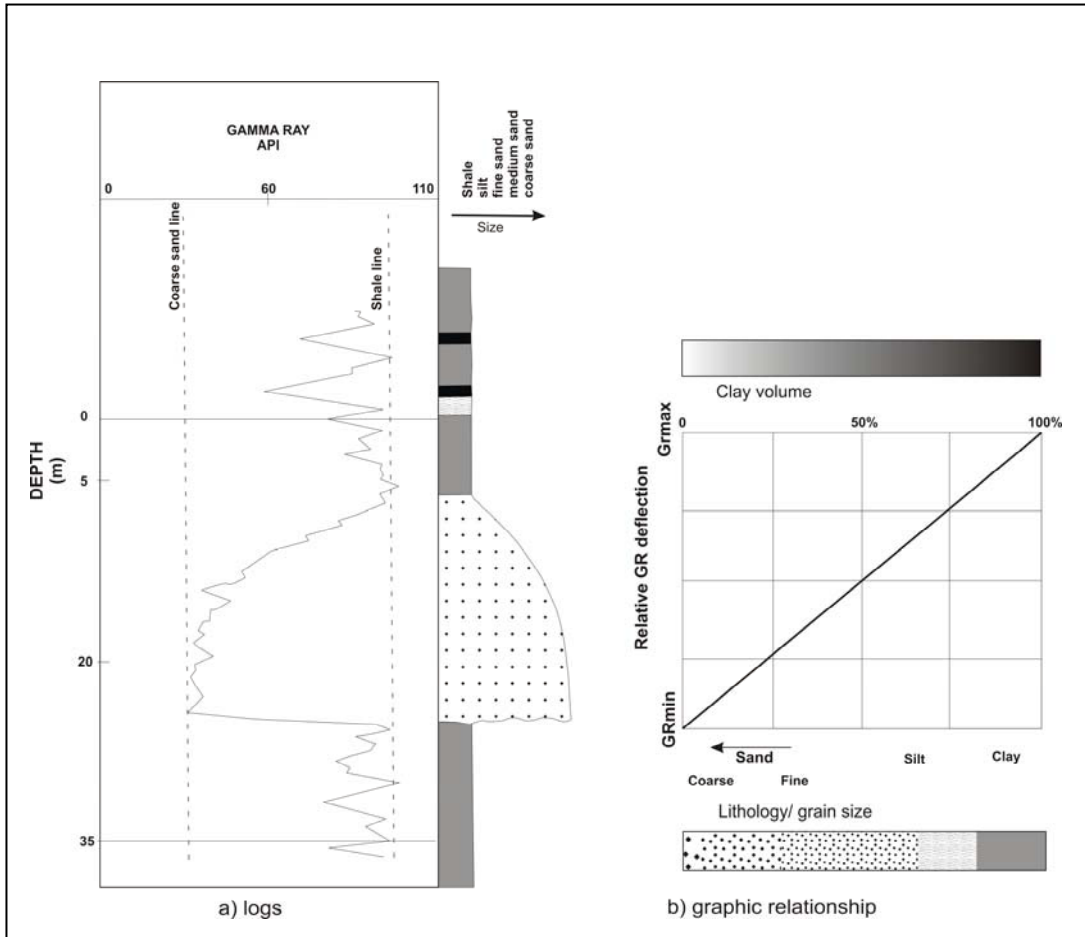


Figure 15: Facies distribution from the gamma ray log. a) The changes in sandstone grain size are reflected in changes in gamma ray value, b) Graphic representation of the variation of grain size with gamma ray value (Rider, 1996).

grain size distribution in the formation (Rider, 1996) (Figure 15). Shapes on gamma ray log can be interpreted as grain size trends and by sedimentological association as facies succession (Rider, 1996; Simon and Brygoo, 1980). A decrease in GR log values will indicate an increase in grain size and an increase in gamma ray value will indicate a smaller grain size. The sedimentological implication of this relationship leads to a direct correlation between facies and log shape. There are many articles on this log shapes and expected facies. The major ones to be mentioned here is Galloway and Hobday (1983), Vail and Warnardth (1990), Van Wagoner et. al., (1990). Log shapes also used as a tool for sequence stratigraphy with variation in log shape indicating facies relationships within parasequences (Van Wagoner et. al., 1990).

1.6.3 Terminology and Concepts of Resistivity Logs

The resistivity of a rock is intimately related to texture. The simplest expression of this is the variation of the resistivity with porosity changes. When the porosity decreases the resistivity increases other things being equal (Rider, 1996). However, resistivity logs cannot be used for a first indicator of lithology. The values depend on many variables, on the contrary in any restricted zone gross characteristics tend to be constant and the resistivity log may be used as a discriminator.

In specific cases however resistivity logs can be used as to indicate a lithology (Rider, 1996). These cases are clearly where certain minerals have distinctive resistivity values; salts, anhydrite, gypsum and coal have usually high diagnostic resistivities (Rider, 1996).

Usually low resistivities may also be indicative. This is the case for mineral concentrations. The effect is noted with pyrite, especially when concentrations are higher than 7% (Rider, 1996). An other example is the chamosite, a hydrated iron mineral with very high densities and low resistivities (Rider, 1996).

The sensitivity of resistivity logs to subtle lithological changes is the basis for their use in correlation. Resistivity logs in facies analysis depends on its ability to register changes in quartz shale mixture (Rider, 1996). Also distinctive shapes, trends or peaks over shale zones are related to subtle compositional changes reflecting original patterns of sedimentation (Rider, 1996). Concerning these resistivity tool can be effectively used as a correlation tool when certain conditions and minerals having certain reactions on the logs are observed.

CHAPTER 2

STRATIGRAPHY

2.1. General Geology of Southeast Turkey

The Southeast Turkey is a hilly plateau with minor relief, cut by the Euphrates and Tigris rivers which flow around the basaltic volcano of Diyarbakır (Righi and Cortesini, 1964). From a geological standpoint, the region was a shelf area during most of the Mesozoic time (Righi and Cortesini, 1964). Southeast Turkey is separated from the Anatolian plateau of central Turkey on the north by the Taurus range, which is considered the eastern extension of Zagros Mountains (Righi and Cortesini, 1964).

The Paleozoic rocks of Southeast Turkey occurred in two major sedimentary cycles; first one in Cambrian to Devonian age and the second Carboniferous to Permian (Righi and Cortesini, 1964). The sedimentary events of this cycle are interpreted as related to a regional transgression overlapping the Arabian Shield around which unstable shelf conditions originated (Righi and Cortesini, 1964). Cambro-Ordovician sediments outcrop in several localities to the southwest of Mardin town near Syrian frontier.

They are exposed in an angular unconformity with the overlying Cretaceous (Temple and Perry, 1962). A sparse fauna of trilobites, brachiopods and graptolites dates the unit (Temple and Perry, 1962). Silurian and Devonian sediments are absent over most of the area. It is likely that Silurian, Devonian and probably Lower Carboniferous sediments were deposited over most of the Southeastern Turkey, but Upper Paleozoic and later periods of uplift and erosion have stripped them away from large areas having only erosional remnants (Temple and Perry, 1962). The Upper Paleozoic section which represents the second sedimentary cycle displays an interfingering of sub continental, lithoral and shallow marine sediments (Righi and Cortesini, 1964).

The Mesozoic section in Southeast Turkey is also separated into two main cycles by a regional unconformity at the base of Cretaceous (Righi and Cortesini, 1964). The first cycle Triassic Jurassic is represented by shallow marine, tidal flat carbonates. The clastic sedimentation characteristic of the Permian and Lower part of Triassic gave way to a long interval of carbonate-evaporate deposition (Temple and Perry, 1962). The second cycle is represented by Mardin Group (Aptian-Santonian) and the formations of Campanian and Maastrichtian. During the Albian, Cenomanian and Turonian shallow shelf conditions prevailed throughout the Southeast Turkey and a blanket of neritic carbonates largely altered to crystalline dolomites and deposited everywhere. During the Campanian time much of the Southeast Turkey was still a shelf area (Temple and Perry, 1962).

Southeast Anatolia was affected by regional marine transgression during the Campanian and the Kastel Basin, a narrow rapidly subsiding foredeep, developed to the south of the Campanian to Early Maastrichtian thrust belt (Ala and Moss, 1979; Sungurlu, 1974). Maastrichtian neritic limestone and marly limestone in the eastern and southern part of the basin were eventually covered by a shale and marl. During the Aptian-Lower Maastrichtian Southeast Anatolia lay on a shelf, characterized by intrashelf basins, along the northern passive margin of the Arabian Plate (Horstink, 1971). The reefoidal buildups and shelfal limestones which developed during Maastrichtian were finally buried in shale and marls. Restricted shallow marine environments were developed as a result of sea level changes throughout the Late Maastrichtian to the Late Eocene. The allocthonous mass is the result of the southward obduction of rock masses which are believed to have originated from uplifted basins. Allocthonous slide mass partly filled the Kastel Formation fore deep (Righi and Cortesini, 1964). Clastics derived from the erosion of these nappes deposited as a thick undifferentiated sequence of Upper Maastrichtian-Lower Eocene red beds and the lower part of this formation grades southward into a varicolored silty shale sequence and extends over part of the basin. These red beds indicate a regression corresponding with a strong tectonic event and characterized by a sharp unconformity along the northern border of the basin and by local sedimentary gaps occurring in a few parts of the basin (Righi and Cortesini, 1964).

The Tertiary section starts with marl and shale lithology and no well defined lithologic break at the K/T boundary in Southeast Turkey. Emergent ophiolitic areas bounding the northern part of the basin were the source of the most of the Paleocene sediments (Temple and Perry, 1962). A regional regression began in Early Eocene time as evidenced by local reefoidal carbonates which are intercalated or overlain by red beds (Righi and Cortesini, 1964). A regional transgression followed the deposition of the red bed sequence and shallow marine carbonates were deposited during the Middle Eocene over all Southeast Turkey (Righi and Cortesini, 1964). The Eocene limestones are overlain by Oligocene evaporates and chalky marls which are indicative of foreland conditions (Righi and Cortesini, 1964). The Oligocene is unconformably overlain by Lower Miocene sediments. The Lower Miocene was a time of shallow marine transgression (Temple and Perry, 1962). The continuation of the uplift and compressional orogeny during Upper Miocene and into the Pliocene resulted in the final retreat of the sea and impressed the present structural framework on the Southeastern Turkey (Temple and Perry, 1962) (Figure 16). The foreland area located far from the orogenic belt was mostly affected by epiorogenic movements and builds tangential stress whose intensity decreased southward (Righi and Cortesini, 1964). The epiorogenic movements probably originated the north-northwest-south-southwest cratonic trend which is predominant in the Mardin and Karababa areas and strong tangential stresses which affected the folded belt.

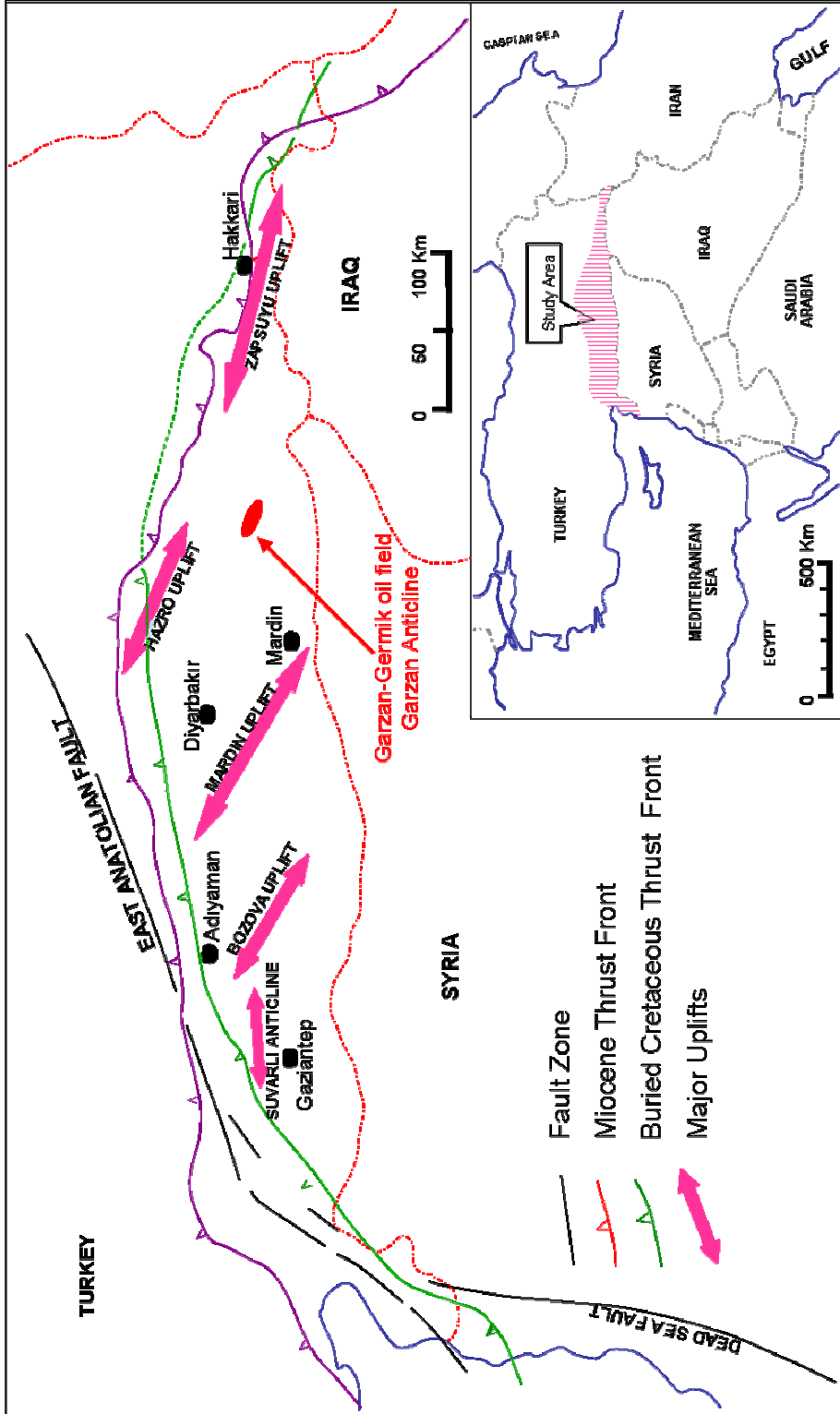


Figure 16: The map showing the major structures of Southeast Anatolia and the location of Garzan-Germik oil field (modified from Perinçek et. al., 1987).

region formed several asymmetrical features parallel with the Taurus mountains (Righi and Cortesni, 1964). Many of the structures in this area seem to have been outlined during the late Mesozoic time and were probably rejuvenated by subsequent structure building movements the strongest of which correspond with the late Tertiary tectonism (Righi and Cortesini, 1964). The Late Miocene interval is marked by continental tectonics in the northern part of Southeast Anatolia.

From the Mid-Early Cretaceous, this shelf area deepened northwards into the southern branch of Neo-Tethys Ocean and ophiolites originating from the Tethyan ocean floor were thrust southwards over the Arabian Shelf in Late Cretaceous (Perinçek and Özkaya, 1981; Şengör and Yılmaz, 1981). The tectonic slices consisting of turbidites and olistostromes of the Karadut Unit, which are time equivalent units to the Mardin Group, were deposited on the continental slope. Ophiolites of the Koçali Complex originate from the Tethyan ocean floor (Şengör and Yılmaz, 1981). Towards the north, closer to the orogenic zone the foreland grades in to the folded belt area where the features are represented by large east-west trending elongate anticlines

2.2. Stratigraphy and the Structural Setting of the Study Area

The study area is located within the Xth Petroleum District of the southeast Turkey. The oldest Mesozoic section penetrated within the study

area is the Aptian period of Cretaceous (Figure 17). This chronostratigraphic unit is represented by the Areban Formation which is composed of a sandstone unit and it is the first product of the Cretaceous cycle in the northern part of the Arabian Plate. The Areban sandstone is overlain by the Albian Sabunsuyu Formation and the Cenomanian-Turonian Derdere Formation (Figure 17). The all three sequences belong to the Mardin Group carbonates. Sabunsuyu is a dolomite unit and the Derdere Formation is highly dolomitized. The Derdere Formation is the major reservoir in the whole Southeast Turkey. Both units constitute the platform type monotonous facies and they are overlain by Karababa Formation during which the environment became deeper and anoxic. The Coniacian- Santonian part of the Cretaceous starts with a member called the Karababa-A which has a high total organic carbon and it is revealed that some of the oil was derived from this member where the overburden and geological past is suitable for generation. The second member of the section is called the Karababa-B member which is characterized by the presence of phosphatic nodules in it. The top of the section is named as the Karababa-C member which is a lagoonal facies having benthic foraminifers and fossils indicating the subtidal environment. This member occasionally acts a reservoir in parts of the Southeast Turkey. On to the Karababa Formation the Campanian aged formations were deposited (Figure 17). Within the district X; the Campanian is represented by the Beloka Formation which consists of shallow water Bada member, being the reservoir and the Dirik member characterized by the facies of deep

marine carbonates. The Maastrichtian overlying the Campanian is represented by sublittoral the Kıradağ Formation and the Garzan Formation (Figure 17). The Garzan Formation is the subject of this thesis and is a shallow water carbonate including tidal to open marine facies. The Alt Germav which is also Maastrichtian in age is a clayey limestone which is relatively deposited in a deep marine environment. The major reservoir in the Garzan-Germik oil field is the Garzan Formation overlain by the Alt Germav Formation. The K/T boundary in the study area is not distinct and the facies gradually passes into deep marine shales named as Üst Germav which is Paleocene in age (Figure 17). Over the Üst Germav, the littoral Gerçüş red beds of Paleocene age were deposited (Figure 17). The sequence continues with the Eocene-Oligocene platform carbonates of the Hoya Formation and ends up with the Germik Evaporites at the same age (Figure 17).

The deformation affecting the foothill belt is known to be late Cretaceous in age. Also the Late Tertiary compression had far reaching effects in the northern part of the region causing reactivation of earlier lines of weakness and particularly development of high angle reverse faulting on east-west trends (Lovelock, 1984).

The Garzan, Raman and Gerçüş anticlines are characterized by a strong relief, generally with a closure of several hundred meters, definite asymmetry and by a slight disharmony (Righi and Cortesini, 1964). Moreover, the steep

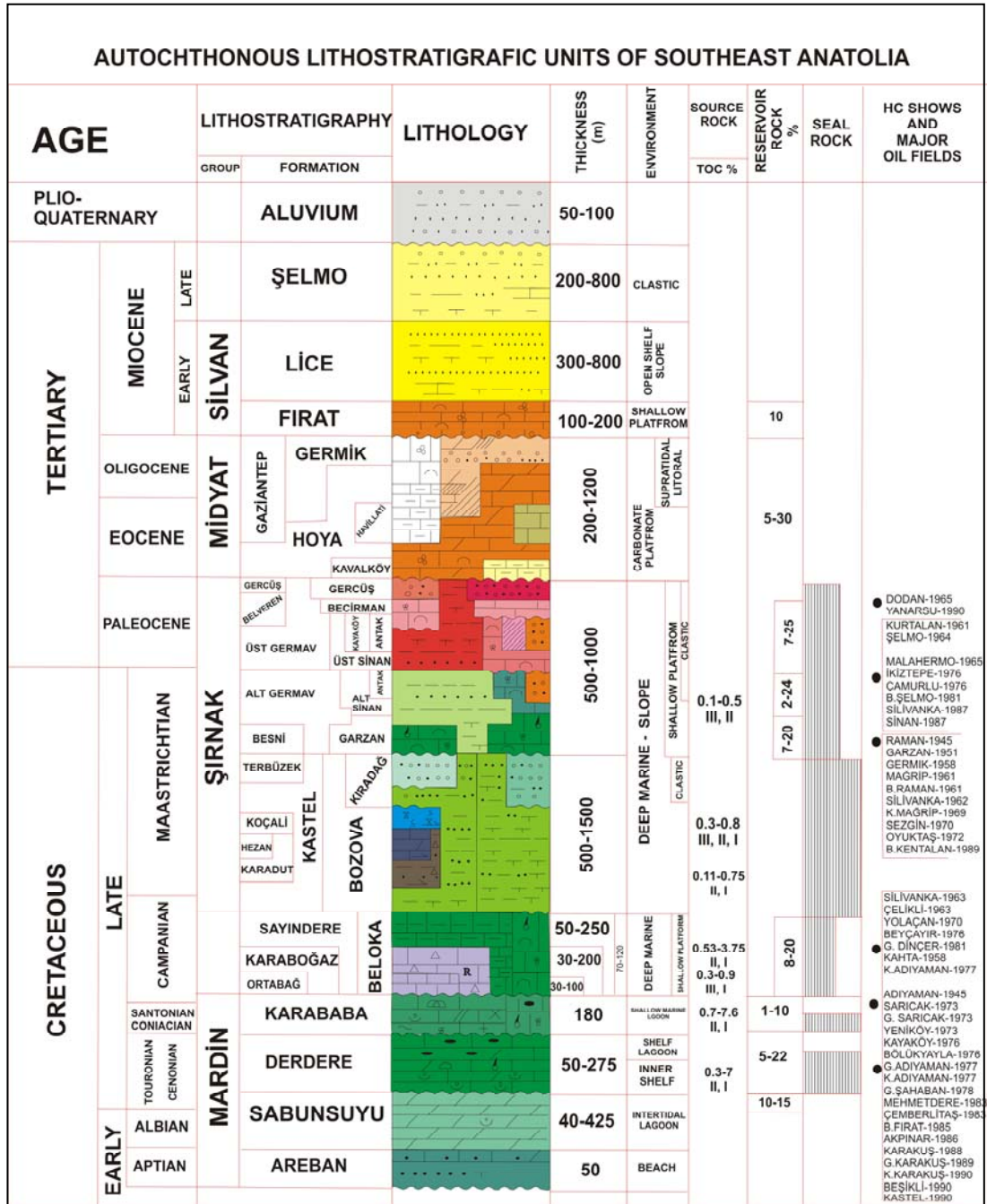


Figure 17: Generalized stratigraphic column of Cretaceous to Recent rock units of Southeast Anatolia (Dinçer, 1991).

southern flank normally are affected by high angle(50-60°) reverse fault indicating at depth Mardin Carbonate section as evidenced by drilling in the Raman and Garzan oil fields (Sanlav et. al., 1963).

The Cretaceous along the study area starts with the Aptian-Santonian Mardin Group carbonates; however the well within the Garzan-Germik oil field rarely penetrates the Mardin Group. So this time period of Cretaceous will not be discussed in this study. Some of the wells in the Garzan-Germik field penetrated the first few meters of Campanian section in Cretaceous and the stratigraphy is going to be explained starting from the Campanian section below (Figure 18).

2.2.1. Beloka Formation

This formation is Campanian in age and most of the wells in this study penetrated the few tens of meters of the formation. The type locality of the formation is at the southern part of Mazıdağ town near Beloka village of Mardin city. The formation belong to the Adiyaman Group and is composed of two members, Dirik and Bada, (Yılmaz and Duran, 1997). The Dirik member consists of clayey, glauconitic limestone at the bottom and Bada member consist of bioclastic limestone towards the top of formation.

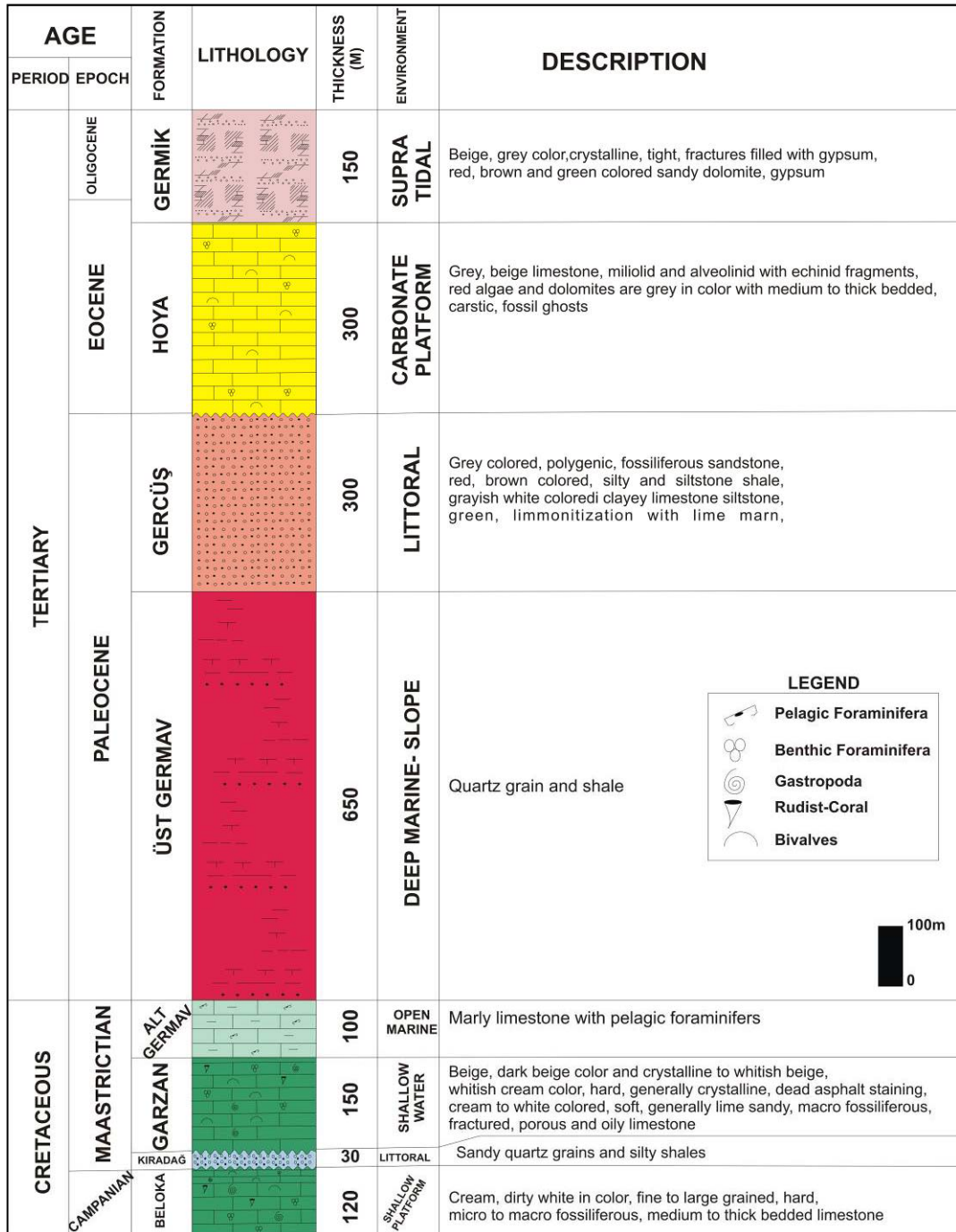


Figure 18: Generalized stratigraphic columnar section of the study area constructed from subsurface data within the wells of the Garzan-Germik oil field.

The formation is firstly defined by Schmidt (1964) as Beloka limestone (Figure 19). Workman (1962) also defined this formation as Raman Formations synonym. The formation is defined as cream, dirty white in color, fine to large grained, hard, micro to macro fossiliferous, and medium to thick bedded limestone (Yılmaz and Duran, 1997). The Beloka Formation unconformably overlies the Mardin Group carbonates and is unconformably overlain by the Kıradağ Formation (Duran and Pekcan, 1980). The Beloka Formation has an aerial extend in subsurface around Batman, Siirt and Mardin cities plus Nusaybin and Cizre towns (Güven et. al., 1991). It has 50-100 m thickness in the District X, however 165 m thickness was reported from the Körkandil area (Perinçek, 1980; Güven et. al., 1991). The age of the formation is Middle to Late Campanian according to fossil content and deposited in shoals of shallow marine, and shelf environment (Güven et. al., 1991; Wagner, et. al., 1984).

2.2.2. Kıradağ Formation

The type locality of the Kıradağ Formation is the Kıradağ village, located 10 m east of Batman city. This formation belongs to the Şırnak Group (Yılmaz and Duran, 1997). It is firstly used as Kıradağ Limestone and the Agro-Kıradağ limestone by Kellog (1961) and Kıradağ Orbitoid reef limestone by Schmidt (1964) corresponding to the Garzan Formation (Figure 19). The

AGE	CRETACEOUS		PALEOCENE	EOCENE	OLIGOCENE
	TERTIARY				
Mason 1930	Greenish Shales		Red Beds		
Schmidt 1935	Calcareous Marn		Lowermost Lmst. + Middlemost Lmst. + Higher Lmst.		
	Cretaceous Shale				
	Cretaceous White Shales				
Maxson 1936	Kemav Formation		Gerçüş Formation	Midyat Limestone	
Schmidt 1961	Akbel Formation		Lower Member	Upper Member	
	Kiradağ Limestone				
Kellog 1961	Gemav Formation		Gerçüş Formation	Midyat Limestone	
	Lower Gemav Formation				
	Upper Gemav Formation				
Workman 1962	Holholik Formation				
	Balman Grp.				
	Garzan Formation				
Schmidt 1964	Kemav Formation		Gerçüş Red Beds Formation	Midyat Limestone / Dolomite	
	Beloka Limestone / Dolomite Fm.				
	Raman Limestone				
	Raman Limestone				
	Kiradağ Limestone				
	Kiradağ Shale				
R. de Righi and Cortesini 1964	Raman Reef		Gerçüş Formation	Midyat Formation	
	Kiradağ Formation				
	Garzan Reef				
	Garzan Limestone				
Kellog 1972	Beloka Formation			Midyat Formation	
	Kiradağ Shale				
	Garzan Limestone				
	Kemav Formation				
Wagner et. al. 1984	Beloka Formation				
Güven et. al. 1991	Beloka Formation		Gerçüş Formation	Hoya Formation	
	Kiradağ Formation				
	Garzan Formation				
	Gemav Formation				
	Üst Gemav Formation				
	Alt Gemav Formation				
	Garzan Formation				
	Kiradağ Formation				
	Beloka Formation				
Yilmaz and Duran 1997	Beloka Formation		Gerçüş Formation	Hoya Formation	
	Kiradağ Formation				
	Garzan Formation				
	Gemav Formation				
	Üst Gemav Formation				
	Alt Gemav Formation				
	Garzan Formation				
	Kiradağ Formation				
	Beloka Formation				
	ADIRYAMAN GROUP				
	ŞIRNAK GROUP				
	MİDYAT GROUP				
This Study	Beloka Formation		Gerçüş Formation	Hoya Formation	
	Kiradağ Formation				
	Garzan Formation				
	Üst Gemav Formation				
	Alt Gemav Formation				
	Garzan Formation				
	Kiradağ Formation				
	Beloka Formation				

Figure 19: Correlation chart of the Campanian to Oligocene formations from the previous studies.

Kıradağ Formation name corresponding to the stratigraphic level as is used is firstly defined by Workman (1962) (Figure 19). The formation is composed of thin laminated sandstone layers with green, brown colored, quartz grains and silty shales (Yılmaz and Duran, 1997). The formation unconformably overlies Campanian Beloka Formation and conformably overlain by Maastrichtian Garzan Formation. The aerial extend of the formation under the subsurface is at around Batman city, towards south and north (Güven et. al., 1991). The thickness of the formation is 50 m, however 125 m thickness was also reported from wells (Eren and Sarı, 1984; Salem et. al., 1986).

The age of the formation is given as Lower-Middle Maastrichtian (Güven et. al., 1991) and the depositional environment is said to be river, flood plain, lagoon and tidal flat area (Duran ve Pekcan, 1980; Salem et. al., 1986).

2.2.3. Garzan Formation

The type locality of the formation is the Garzan oil field at the east of Batman city. The formation is first defined by Kellog (1960) and Halstead (1960) from the wells in the Garzan oil field under subsurface (Figure 19). They have used the Garzan Formation name as is used today and before 1960 the formation is named as “Main Limestone” and “ Massive Limestone” with in the studies. The formation belongs to the Şırnak Group (Yılmaz and

Duran, 1997). It starts with beige, dark beige color and crystalline at the bottom and grades into whitish beige, whitish cream color, hard, generally crystalline, dead asphalt staining, sometimes highly fractured and fractures filled with heavy oil towards top (Yılmaz and Duran, 1997). Towards the upper parts, formation is cream to white colored, soft, generally limesandy, macro fossiliferous, fractured, porous and oily limestones. The Garzan Formation conformably overlies the Kiradağ Formation and is conformably overlain by Maastrichtian Alt Germav Formation (Figure 18). The formation is generally 0-150 m thick and 190 m thickness was reported also. The formation is extended at the subsurface around Mardin, Batman, Siirt cities (Güven et. al., 1991). The thickness reaches to 200-250 m between Batı Raman and Şelmo area. The average thickness for the formation is estimated as 150m from the regional studies (Salem et. al., 1986). The thickness of the formation in the study area in the Garzan oil field ranges in between 20 m to 190 m. This wide range starting from 20 m is due to the wells not penetrating the whole formation in all of the wells (Figure 22). In Germik oil field the thickness of the formation range from 10 m to 150 m and wide range is because of the same reason as in Garzan oil field (Figure 23). The topographic crest and the crest of the reservoir do not correspond, the latter being 150 m closer to the bounding fault (Figure 3). The gross thickness of the pay zone is about 150 m and depth to the reservoir is approximately 400 m from subsea.

The age of formation is Middle Maastrichtian (Köylüoğlu, 1986; Güven et. al., 1991) and deposited with in shallow marine, reef complex and shelf edge (Salem et. al., 1986; Naz, 1986; Eren and Sarı, 1984) (Figure 17).

The major fossil groups observed in Garzan Formation are benthic foraminifers, calcispheres, algs, carophytes, shell fragments and rarely planktonic foraminifers. These benthic foraminifers are Anomalinidae, *Antalya korayi*, *Asterorbis* sp., *Bulimina* sp., *Clypeorbis mamillatus*, *Coskinolina* sp., *Cuneolina* gr. *pavonia*, *Dictyoconella complanata*, *Disyclina schlumbergeri*, Discorbidae, *Gavelinella* sp., *Gaupillaudina* sp., *Gyrodinia* sp., *Lepidoorbitoides socialis*, L. sp., *Loftusia* spp., *Marsonella* sp., Miliolidae, *Omphalacyclus macroporous*, *Orbitoides apiculatus*, *O. medius*, *O. triangularis*, *Pseudoomphalacyclus blumenthali*, *Rotaia* sp., *Scandonea* sp., *Siderolites calcitrapoides*, *Sirtina* spp., *Sulcoperculina* sp., Valvulinidae, Verneulinidae (Çoruh et. al., 1997). The planktonic foraminifers that can be found in the Garzan Formation are; *Archeoglobigerina* sp., *Contusotruncana fornicata*, *Gansserina gansseri*, *Globotruncana bulloides*, *G. linneana*, *G. rosetta*, *G. ventricosa*, *G. spp.*, *Globotruncanella havanensis*, *Globotruncanita angulata*, *G. situarti*, *G. situartiformis*, *Hedbergella* spp., and Heterohelicidae (Çoruh et.al., 1997). In addition to foraminifera red and green algs, bryozoans, shell fragments, echinoids, ostracodes, rudists and coral fragments are the second major constituent of the formation (Çoruh et.al., 1997).

Lateral and vertical variations in grain size and fossil content are related to the original depositional environment and this greatly affected the porosity and permeability of these carbonates (Sanlav et. al., 1963). The available data do not indicate a true reef picture, but thick section with their coarse material and their lateral changes in grain size followed by fauna changes in the same direction from large corals to finer size microfauna suggest reefoid conditions of facies associated with reef (Sanlav et. al., 1963)

When the general porosity and permeability of the Garzan Formation is investigated from the cores, in the Garzan field the average porosity is 10% and average permeability is 10 md (Figure 20). However, in Germik field the average permeability is the same with Garzan field (10 md); but the average porosity is 15% (Figure 21).

.2.2.4. Germav Formation

The type locality of the formation is Germav village which is 40 km east of Gerçüş town of Batman city. The formation belongs to the Şırnak Group (Yılmaz and Duran, 1997). The formation is firstly defined by Maxson (1936) as Kermav Formation (Figure 19). The formation is named as “greenish shales” by Mason (1930), “calcerous marl” by Schmidt (1935). Later Schmidt (1964) used the “Akbel Formation” and changed the rank of

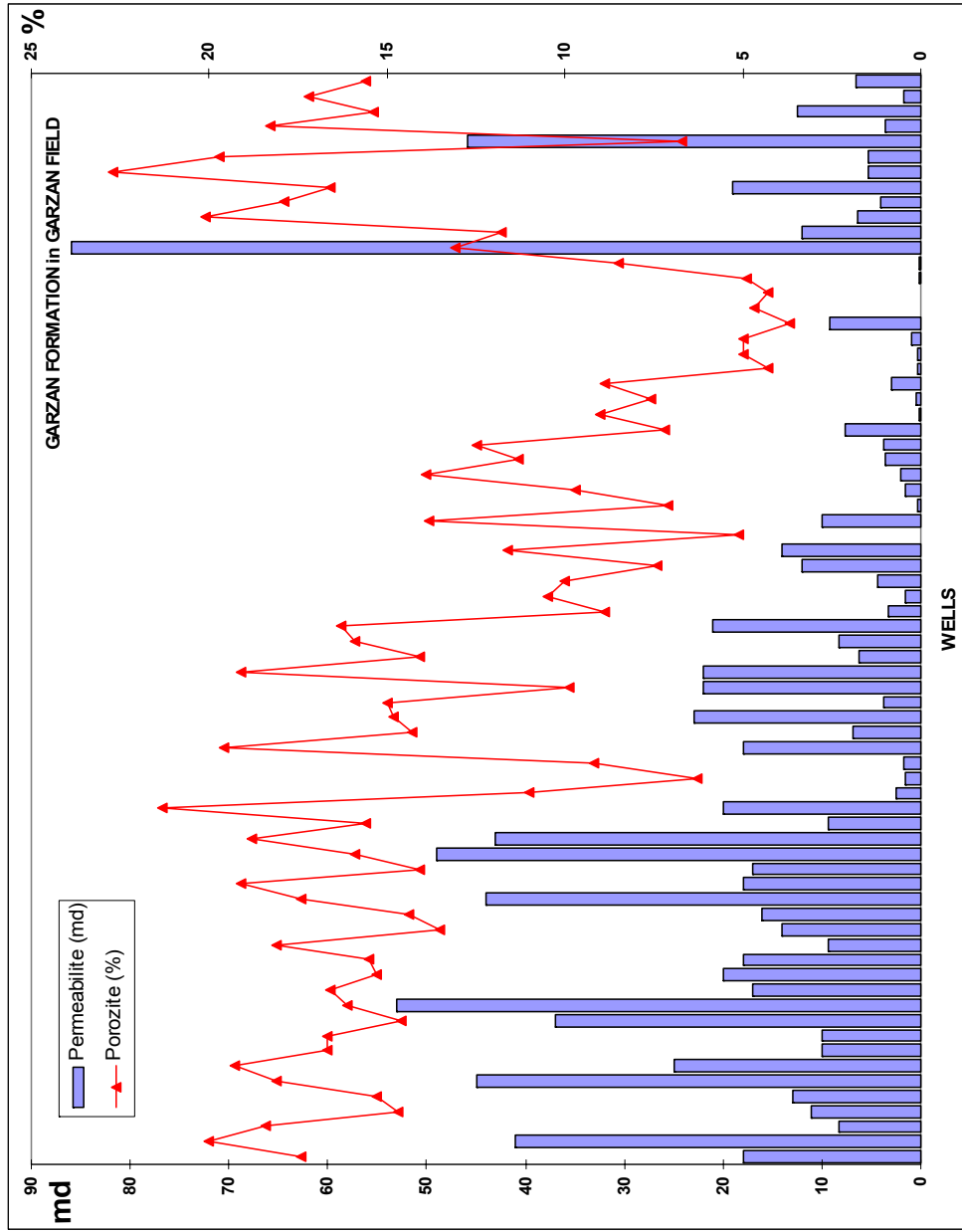


Figure 20: Average porosity and permeability of Garzan Formation in Garzan oil field (the measured data of the plug porosity and permeability is the courtesy of TPAO).

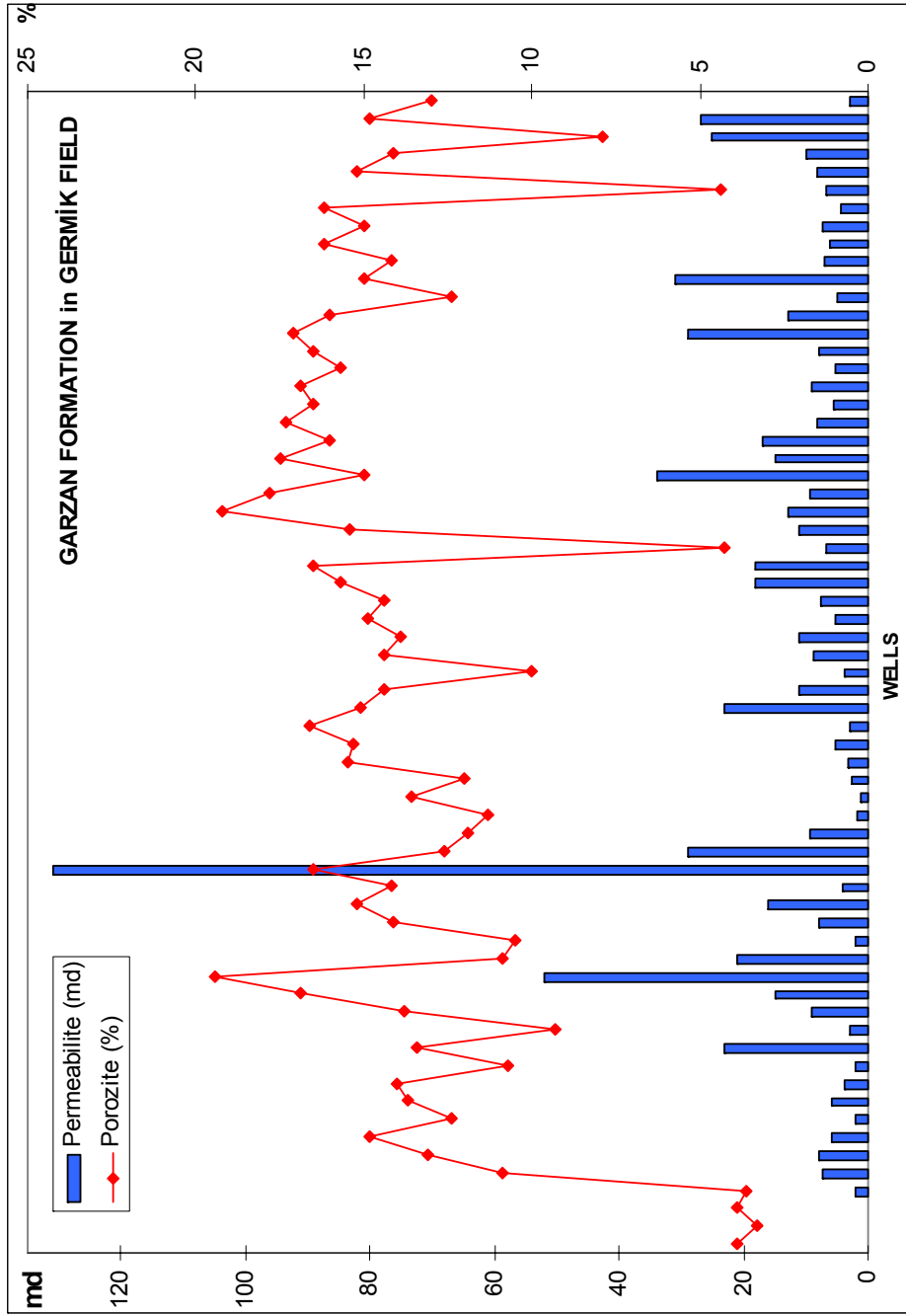


Figure 21: Average porosity and permeability of Garzan Formation in Germnik oil field (the measured data of the plug porosity and permeability is the courtesy of TPAO).

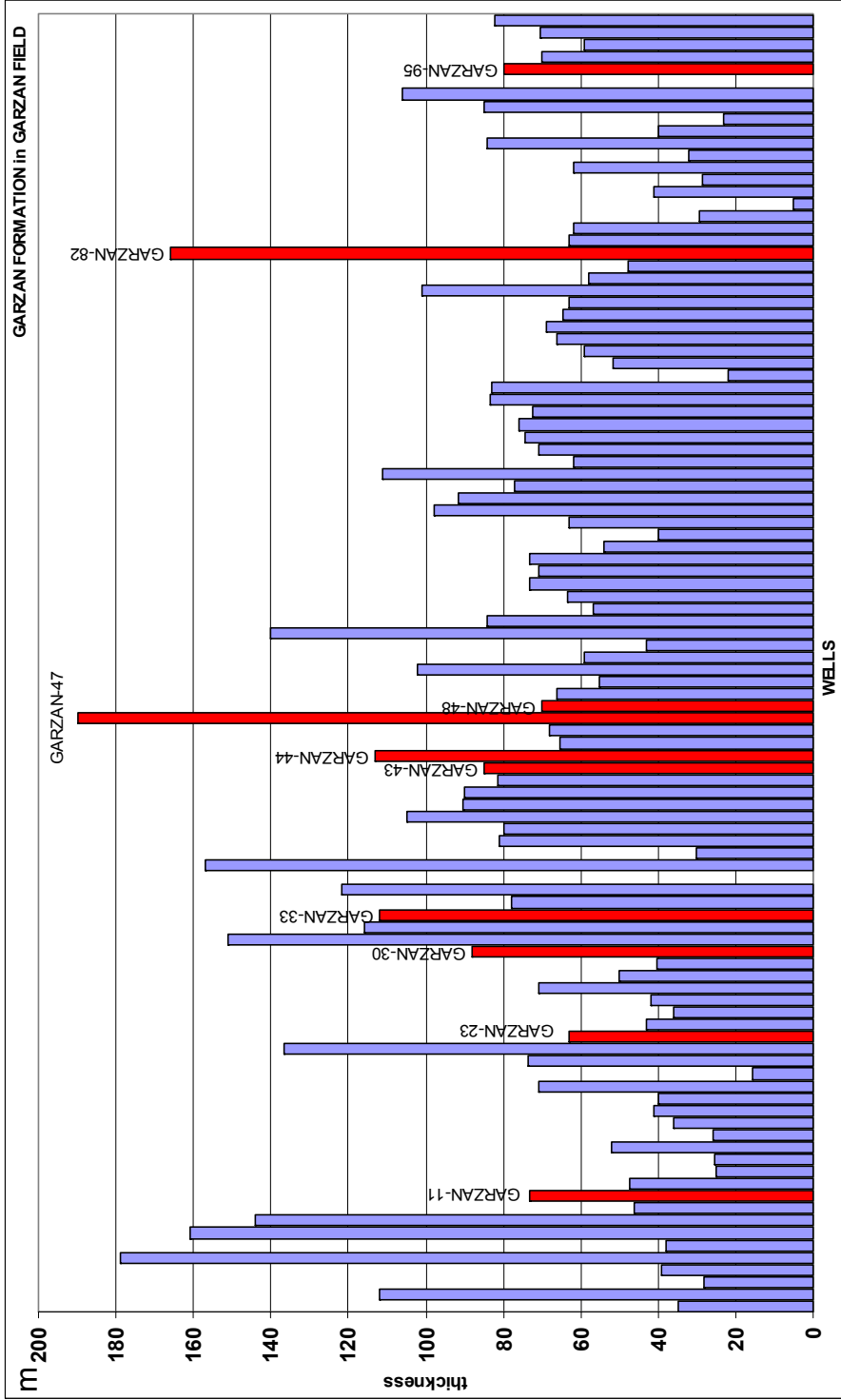


Figure 22: The thickness of Garzan Formation penetrated in the wells of Garzan oil field.

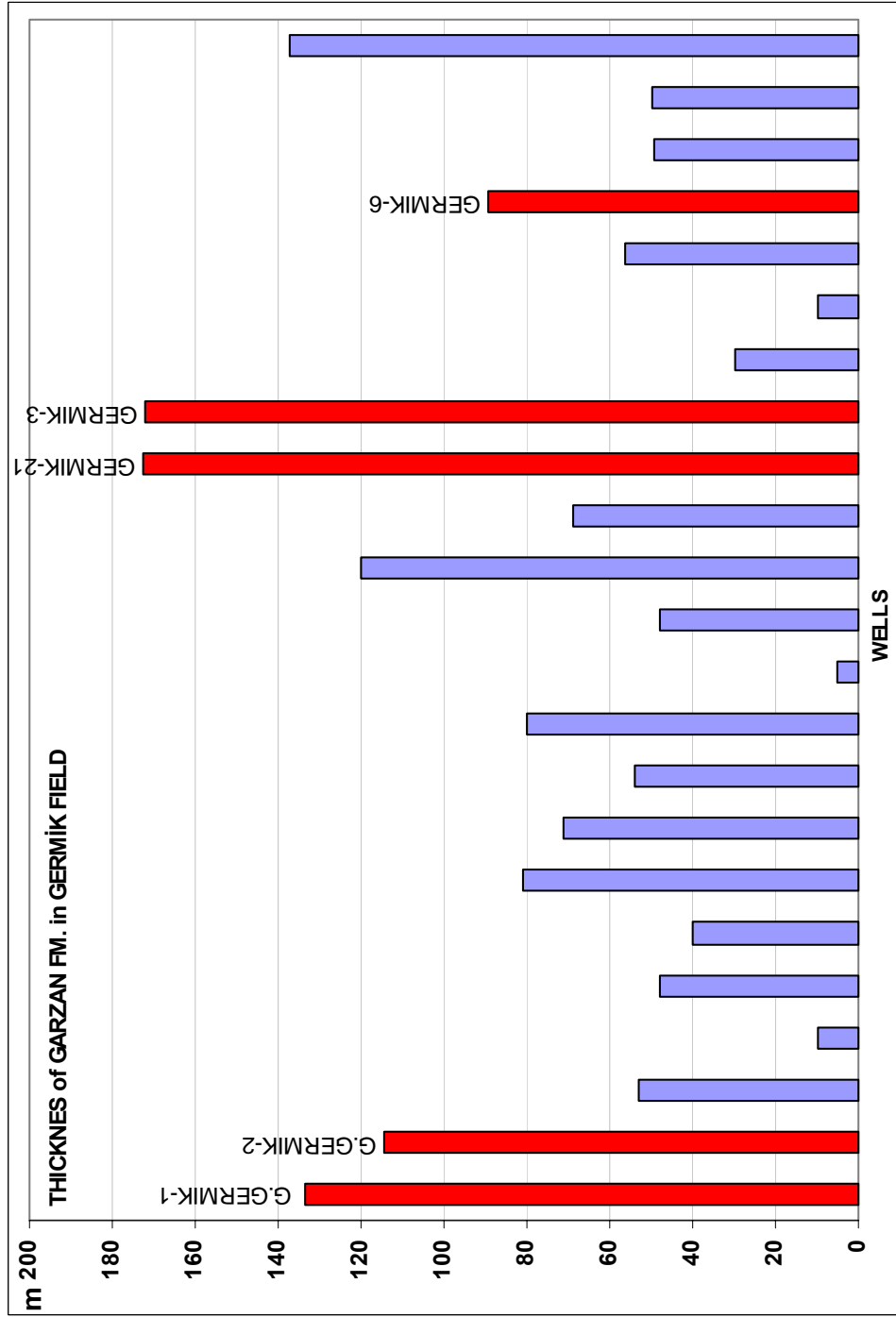


Figure 23: The thickness of Garzan Formation penetrated in the wells of the Germik oil field.

the unit to formation stage. Workman (1962) named the formation as “Holholik Formation”. In 1961 Kellog used the Germav Formation and divided the formation in to two units; Alt Germav Formation and the Üst Germav Formation as is used today and also within this study (Figure 19).

The thickness of the formation is 676 m at the type locality. It is spread all through Southeast Anatolia (Güven et. al., 1991). The formation is used as Germav Formation (Maastrichtian-Paleocene) when it can not be divided lithologically and also by age determination. On the other hand when there is good control of age determination then Alt Germav (Maastrichtian) and Üst Germav (Paleocene) is used in which all of the three are in Formation rank in Şırnak Group (Yılmaz and Duran, 1997).

2.2.4.1. Alt Germav Formation

The formation conformably overlies the Garzan Formation and conformably overlain by the Üst Germav Formation. The formation is marly limestone with pelagic foraminifers and its age is given as Maastrichtian (Dinçer, 1991) (Figure 17). The formation is firstly defined by Schmidh (1935) as “calcerous shales” as lower member of Cretaceous marl. Kellog (1961) used the name Alt Germav Formation as said above (Figure 18). The formation belongs to the Şırnak Group (Yılmaz and Duran, 1997).

2.2.4.2. Üst Germav Formation

The formation conformably overlies the Alt Germav Formation and is conformably overlain by the Gercüş Formation (Figure 18). It is composed of quartz grains and shale and the age of the formation is given as Paleocene (Güven et. al., 1991).. This formation is firstly defined by Schmidt as “white shales” within Cretaceous marls (Figure 19). Kellog (1961) used the Upper Germav Formation for the first time (Figure 19). The formation belongs to the Şırnak Group (Yılmaz and Duran, 1997).

2.2.5. Gercüş Formation

The type locality is the Hermes basin near the Gercüş town. The formation belongs to the Midyat Group (Yılmaz and Duran, 1997). The formation is firstly defined by Maxson (1936) as Gercüş Formation (Figure 19). The formation consists of sandstones (grey colored, polygenic, fossiliferous), shale (red, brown colored, silty and siltstone), siltstones (grayish white colored, clayey, limestone) alternation with marl (green, limonitization with lime), shale (red, brown colored, silty and siltstone) and sandstone (grey colored, polygenic, fossiliferous). Lithologies (Yılmaz and Duran, 1997). The Gercüş Formation conformably overlies the Üst Germav

Formation and is unconformably overlain by Hoya Formation. (Güven et. al., 1991). The age of the formation is Lower Eocene (Duran et. al., 1988) and deposited at lake, lagoon, flood plain, river, alluvial fan (Duran et. al., 1988; Güven et. al., 1991).

2.2.6. Hoya Formation

The type locality of formation is at the Hoya village which is 2 km southwest of Gercüş town of Diyarbakır city. The formation is defined as the member of Midyat Group (Yılmaz and Duran, 1997). It is firstly defined as Midyat Limestone by Maxson (1936) and Kellog (1961) (Figure 19). Schmidt (1964) used “Çuvaldız Formation” for the Gercüş and Midyat together. He divided the formation in to two as Lower Member and Upper Member (Figure 19). The formation starts with limestone and grades into dolomite where limestone is grey, beige in color with 10-100 cm thick bedding, miliolid and alveolinid with echinoid fragments and red algae and dolomites are grey in color with medium to thick bedded and karstic in appearance having fossil ghosts (Yılmaz and Duran, 1997). The formation unconformably overlies Gercüş Formation and is conformably overlain by Germik Formation (Figure 18). The formation is generally 260 m thick and 300 m thicknesses were also reported. The formation extends all through the Southeast Anatolia. The age

of the formation is Early Eocene to Early Oligocene and deposited in shallow epic sea to shallow marine conditions (Duran et. al., 1988 and 1989).

2.2.7. Germik Formation

The type locality is the well located near Kozluk town of Batman. The formation is the member of Midyat Group (Yılmaz and Duran, 1997). The formation is firstly named by Güven et. al. (1991) (Figure 19). It is defined by Perinçek (1978) as Germik Formation in Midyat Group (Figure 19). The formation starts with beige grey color, crystalline, tight, fractures filled with gypsum, lime dolomite intercalation, red brown and green colored sandy dolomite and gypsum alternation (Yılmaz and Duran, 1997). The formation has thickness between 34-465 m (Yılmaz and Duran, 1997). The age of the formation is Middle Eocene and Oligocene and deposited in the evaporitic environment with restricted regressive epic sea (Duran et. al., 1988).

CHAPTER 3

MICROFACIES AND CYCLES, AND THEIR STACKING PATTERNS IN THE GARZAN FORMATION

The three dimensional assemblage of lithofacies is called depositional system (Fisher and McGovan, 1967). The depositional system is composed of system tracts which is a linkage of contemporaneous depositional systems (Brown and Fisher, 1977) The term “microfacies” was suggested by Brown (1943) referring to the criteria appearing in thin sections under the microscope. The microfacies is defined as the total of all the geological and sedimentological criteria which can be classified in thin sections, peels and polished slabs (Flügel, 1978).

This study reconstructs the depositional style systems and stacking patterns by defining microfacies from thin sections. These cycles and stacking patterns are used to correlate the logs. As a result microfacies are genetically related to logs by means of cycles and stacking patterns. Also from this study the depositional environment and the location of the wells in this environment is illustrated.

In order to clarify the microfacies, a spread sheet was prepared for description of microfacies from thin sections. On this classification sheet some of the skeletal and none skeletal grains were identified which are thought to be important for the construction of the depositional environment and analogy of cycles in the Garzan Formation in Garzan-Germik oil field.

3.1. Microfacies of Garzan Formation in Garzan-Germik Oil Field

The thin section analysis under the transmitted light microscope revealed that there are five microfacies types within the Garzan Formation in Garzan-Germik oil field. Those are named as Miliolid Wackestone, Rotalid Miliolid Wackestone, Orbitoid Miliolid Wackestone, Pelagic Foraminiferal Mudstone and Rudist Wackestone according to their fossil content and their location of deposition within the depositional realm of the formation. The occurrence percentage of fossil contents are done by point counting method as mentioned in the first chapter. The major groups counted within the facies are: orbitoids, algs, rudist fragments, miliolids, coral fragments, echinoid fragments, pelecypoda and gastropoda fragments, cuneolins, rotalids, pelagic foraminifera, matrix, ostracode and undifferentiated grains. Valvulina, Minouxia and Moncharmontia and some other benthic foraminifera which are not distinguished separately are counted as other benthic foraminifers. Also pelecypoda and gastropoda are counted together.

3.1.1 Miliolid Wackestone

The majority of this facies is composed from miliolids, cuneolins, other benthic foraminifera and the matrix. The orbitoids, algs, pelecypoda and gastropods, echinoids, rotalids and ostracodes are observed in minor amounts whereas rudist fragments, coral fragments are observed in minor amounts and pelagic foraminifers are not observed in this facies.

Among the thin sections belonging to this facies 10 representative sample were counted. In this 10 thin sections the occurrence abundance of miliolids range between 1%-20%, cuneolins occur about 2%, other benthic foraminifers occurrence range is between 1%-4%, matrix existence range is between 60%-80%, orbitoids occur about 1% mostly as fragments, algs are observed between 1%-3%, pelecypods and gastropods occurrence range is between 1%-5%, echinoid fragments occurrence range is between 1%-6%, rotalids occurrence range is between 1%-3%, ostracodes occurrence range is between 1%-4% in this facies (Appendix B).

In average this facies is composed of 6.48% of miliolids, 2.4% of echinoid fragments, 1.48% of pelecypods and gastropods, 1.04% rotalids, 2.08% of other benthic foraminifers, 1.93% of ostracods, 0.43% of orbitoid fragments, 0.93% of algs and 0.55% of cuneolina (Figure 24, 25, 26). The major constituent of the facies is micrite matrix with 78.73% occurrence (Figure 24). The 3.95% of the fragments are undifferentiated because of micritization, dolomitization or some other processes. Within the facies

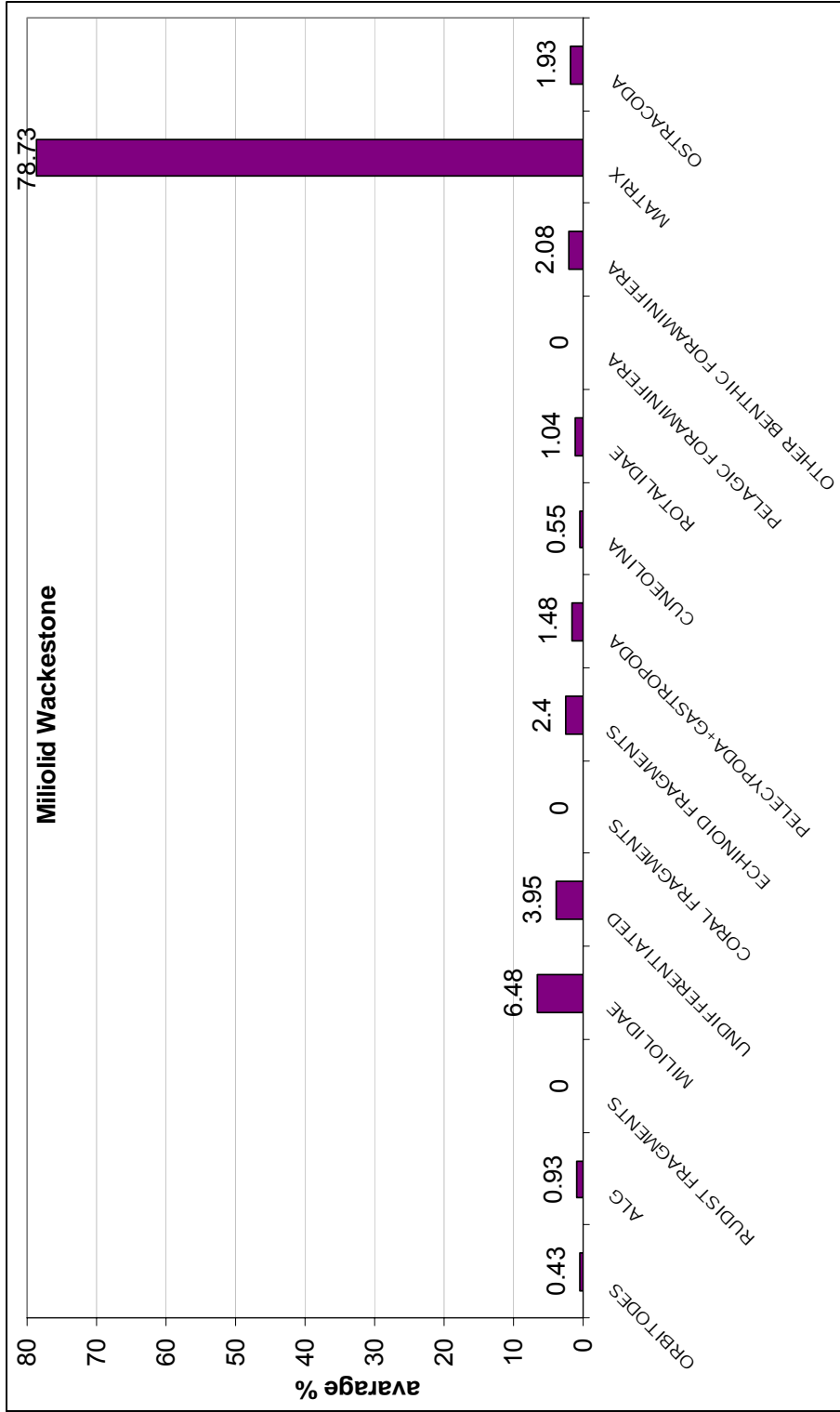


Figure 24: The average occurrence percentage of the constituents found in Miliolid Wackestone facies .

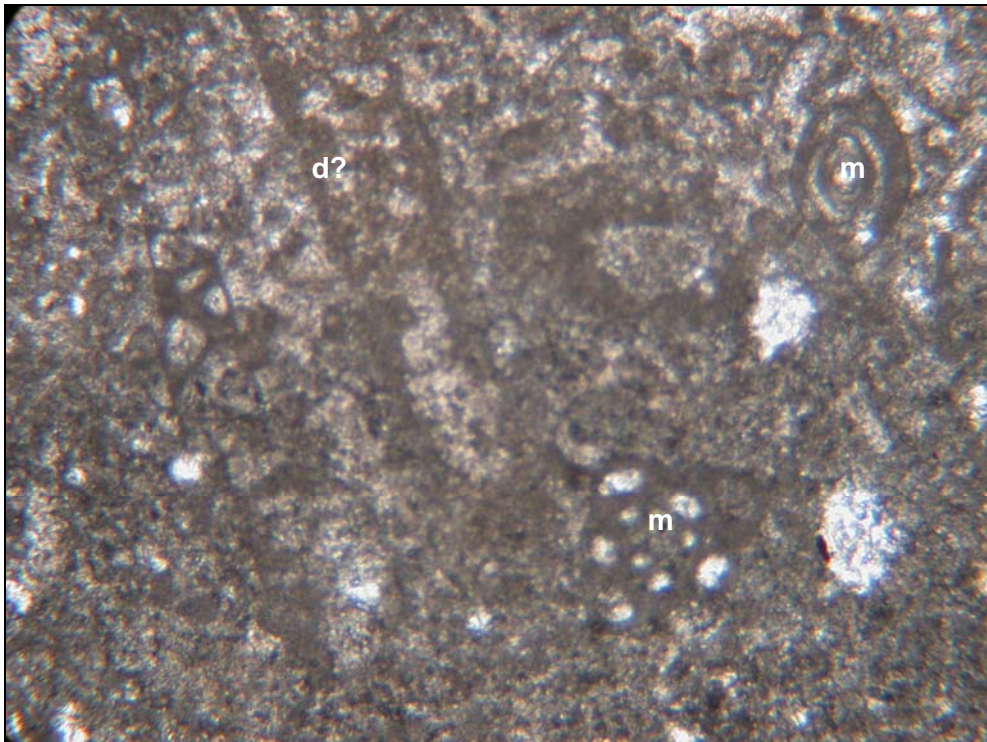


Figure 25: Photomicrograph of Miliolid Wackestone facies from Germik-21 well (X4, core) (m:miliolid, d:disyclina?)

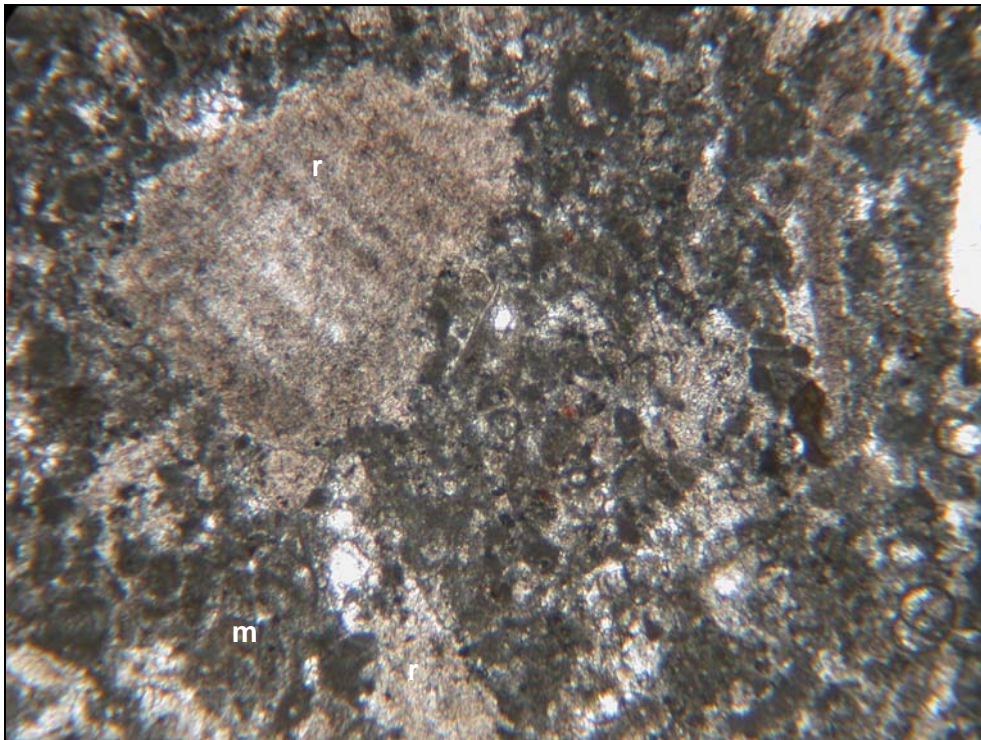


Figure 26: Photomicrograph of rudist fragments in Miliolid Wackestone facies from Germik-21 well (X4, core) (r:rudist, m:miliolid).

rudists fragments are very rare but corals and pelagic foraminifers were absent. The echinoids and orbitoid fragments are found in this subtidal environment because of transportation of the fragments worked by waves. Echinoderms are generally became a major constituent of shallow water benthos during the Cretaceous and also in deep water environments in Late Cretaceous (Flügel, 2004). Miliolid foraminifera are very common in lagoonal environment (Flügel, 2004). So as according to the fossil content and their occurrence abundance in Miliolid Wackestone facies, the facies is deposited within the subtidal environment of the Garzan depositional realm (Figure 45). The matrix is micrite but sometimes microspar can also be observed (Figure 27). During diagenesis some dolomite rhombs formed within the matrix (Figure 28). This facies is a low energy environment facies.

This facies can be correlated with the SMF-7 and 8 of Wilson (1975); which is renamed by Flügel (2004) as FZ-7 and FZ-8; platform interior restricted and open marine (Figure 29). It is called lagoon when protected by sand shoals, islands or reefs of the platform (Flügel, 2004). The typical biota of these shallow water zones are miliolid foraminifera, ostracodes, gastropods, algae with lithofacies lime mudstone, dolomite mudstone, wackestone, grainstone, boundstone, floatstone and packstone (Flügel, 2004).

Eseller (1987) also defined this facies and interpreted as being deposited in a shallow water shelf- lagoon. In this facies the major constituent is the miliolids and rarely mollusk shell fragments. Naz (1987) also defined

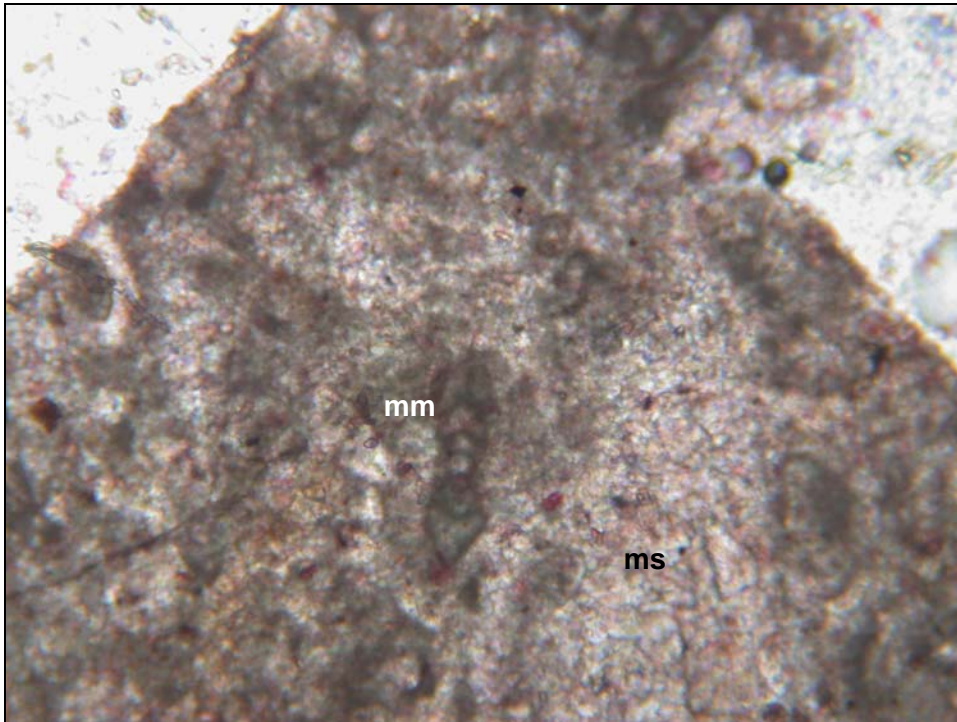


Figure 27: Photomicrograph of microspar rarely found in Miliolid Wackestone facies from G. Germik-1 well (X10, cutting) (ms:microspar, mm:montcharmontia sp.).

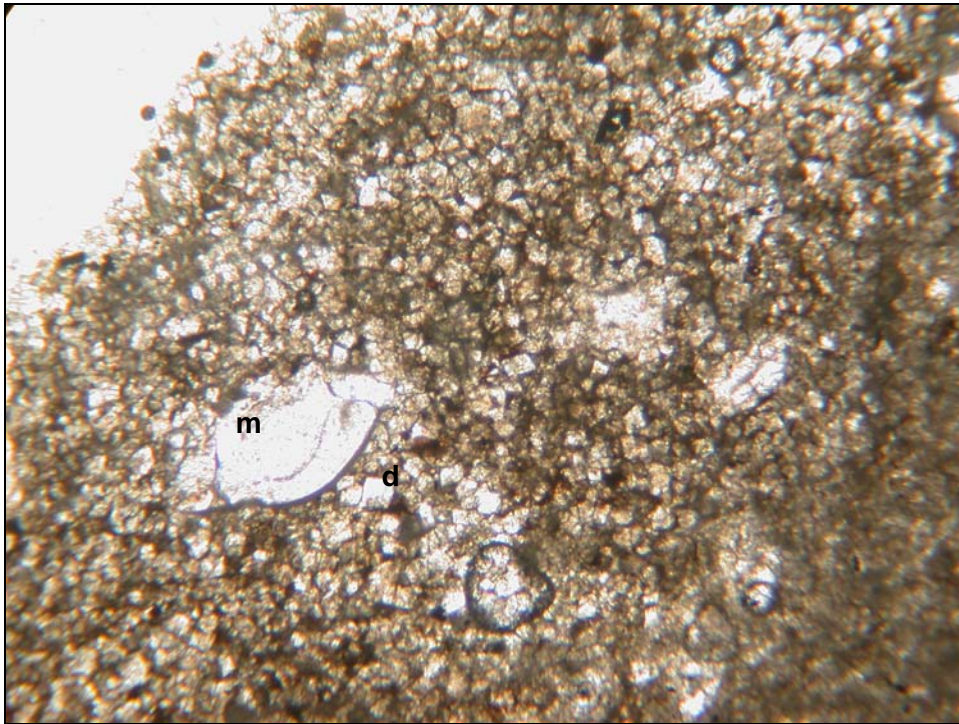


Figure 28: Photomicrograph of dolomite rhombs formed within the matrix of Miliolid Wackestone facies from Garzan-47 well (X4, cutting) (d:dolomite rhomb, m:miliolid).

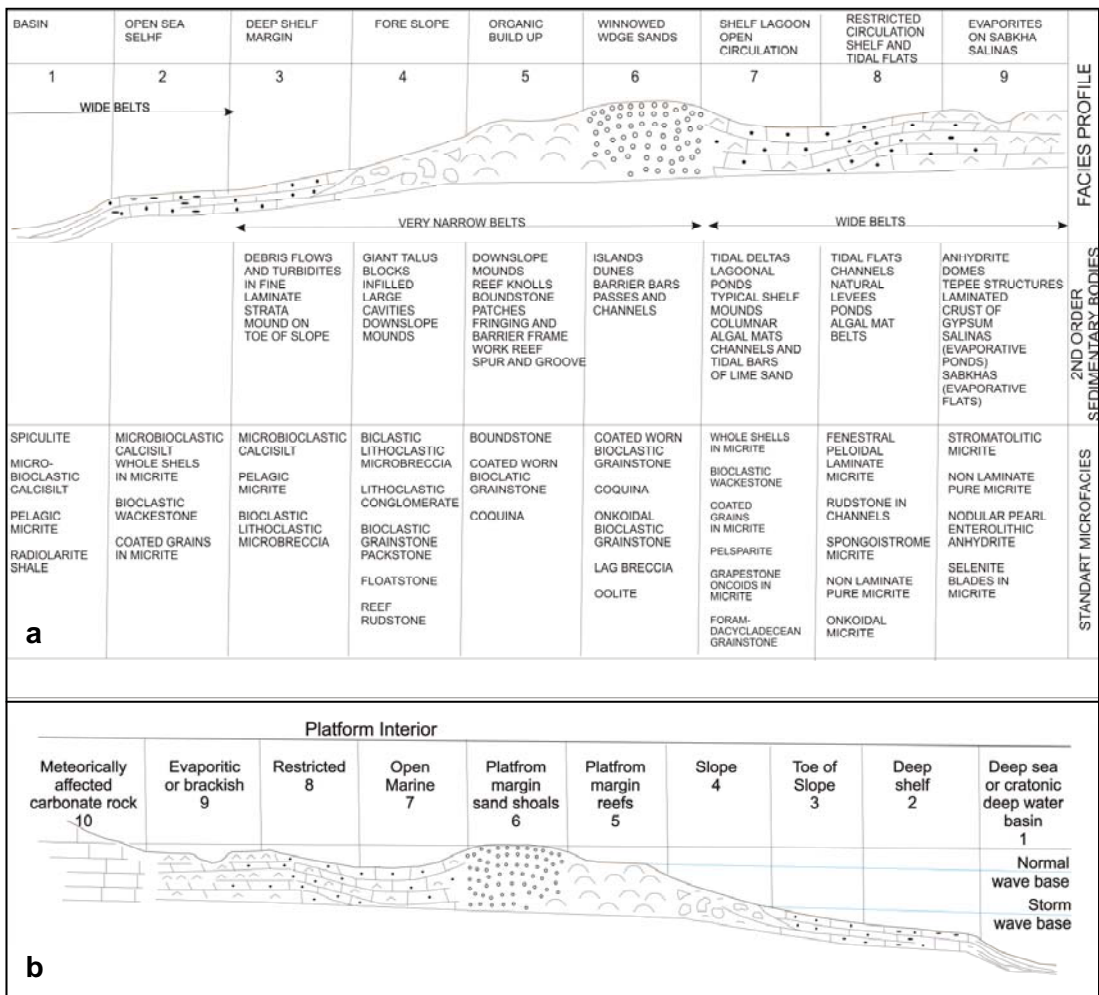


Figure 29: The standard microfacies belts of carbonate depositional environment, a) synopsis of standard facies belts reviewing second order bodies of sediment and standard microfacies associated with each belt (Wilson, 1975), b) The standard facies zones of the modified Wilson model (Flügel, 2004).

this facies within Mağrip oil field and named as lagoon carbonates. Miliolids, arenaceous type of foraminifers such as *Cuneolina* sp, *Discyclina* sp., *Spirocyclus* sp. and *Valvulamina* sp. and Orbitoides are common in this facies (Naz, 1988).

3.1.2 Rotalid Miliolid Wacestone

The majority of the facies is composed of rotalids, miliolids, matrix and orbitoids. The algae, echinoid fragments, rudist fragments, coral fragments, pelecypod and gastropods, cuneolins, other benthic foraminifers and ostracodes are observed in minor amounts. Pelagic foraminifer is rarely observed in few thin sections.

Among the thin sections representing this facies 10 of them were selected and counted. In this facies the fragment abundance are as follows: rudist fragments (2%-4%), miliolids (1%-20%), algae (1%), coral fragments (2%), echinoid fragments (1%-3%), pelecypods and gastropods (1%-6%), cuneolins (1%), rotalids (12%-40%), other benthic foraminifers (2%-5%), matrix (40%-70) and ostracode (1%-5) (Appendix B).

In average this facies is composed of 20.54% rotalids, 10.23% miliolids, 2.38% other benthic foraminifers, 2.91% ostracodes, 1.61% echinoid fragments, 0.52% coral fragments, 0.87% rudist fragments, 2.04% of pelecypoda and gastropoda, 0.46% cuneolina, 0.01% orbitoid fragments and

0.49% algae (Figure 30, 31, 32). The major constituent is the micrite matrix with 57.34% of occurrence (Figure 30). According to the fossil content and their occurrence abundance this facies is deposited within the shoal to foreshoal environment (Figure 45). The facies has more diversity in biota than Miliolid Wackestone facies. The presence of rotalids in high abundance in thin sections makes the facies representative of shoal to fore shoal environment. This division is used to understand the sea level rise as a result of deposition of shoal to foreshoal deposit (Rotalid Miliolid Wackestone) onto shoal to backshoal deposit (Orbitoid Miliolid Wackestone)

This facies coincides with the SMF-4 and 5 of Wilson (1975) and also coincides with the FZ-5 and FZ-6 of Flügel (2004) (Figure 29). The common biota of this facies is described as almost exclusively benthos, frame builders, loose skeletal grains and benthic microfossils such as foraminifera and algae where framestone, baffestone, bindstone, wackestone and floatstone, grainstone and rudstone are commonly observed lithofacies in these environments (Flügel, 2004).

This facies is not observed within the study of Eseller and Naz (1987)

3.1.3 Orbitoid Miliolid Wackestone

The majority of this facies is composed of orbitoides (2%-24%), rudist fragments (20%-36%), echinoid fragments (2%-30%), rotalids (2%-16%) and the matrix (20%-70%). The miliolids (0%-11%), algae (1%), coral fragments

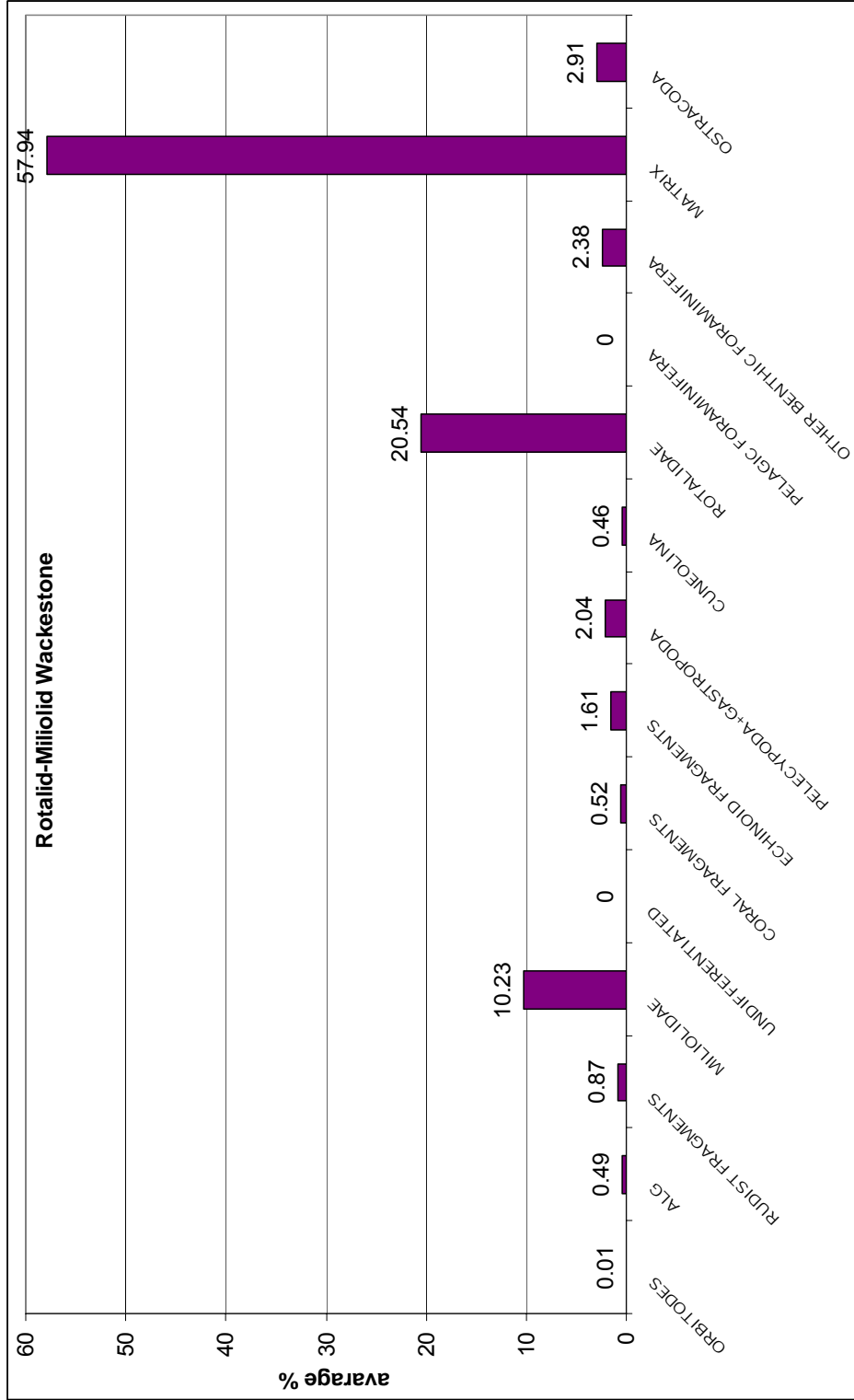


Figure 30: The average occurrence percentage of the constituents found in Rotolid Miliolid Wackestone facies .

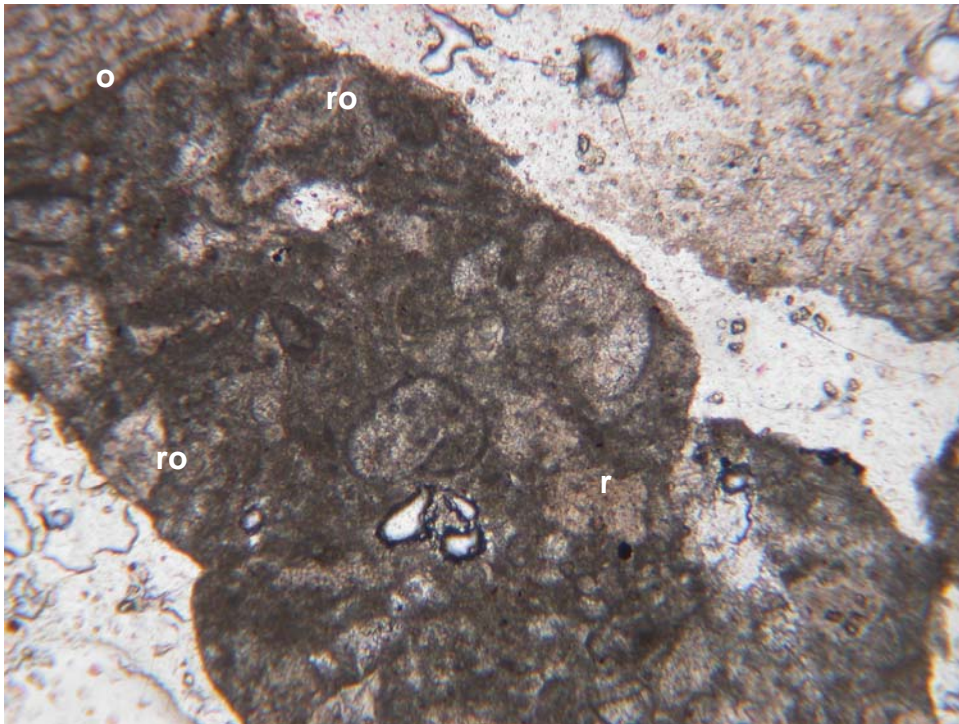


Figure 31: Photomicrograph of rotalids found together with rudist and orbitoid fragments from G. Germik-1 well (X4, cutting), (o: orbitoid, ro: rotalid, r:rudist).

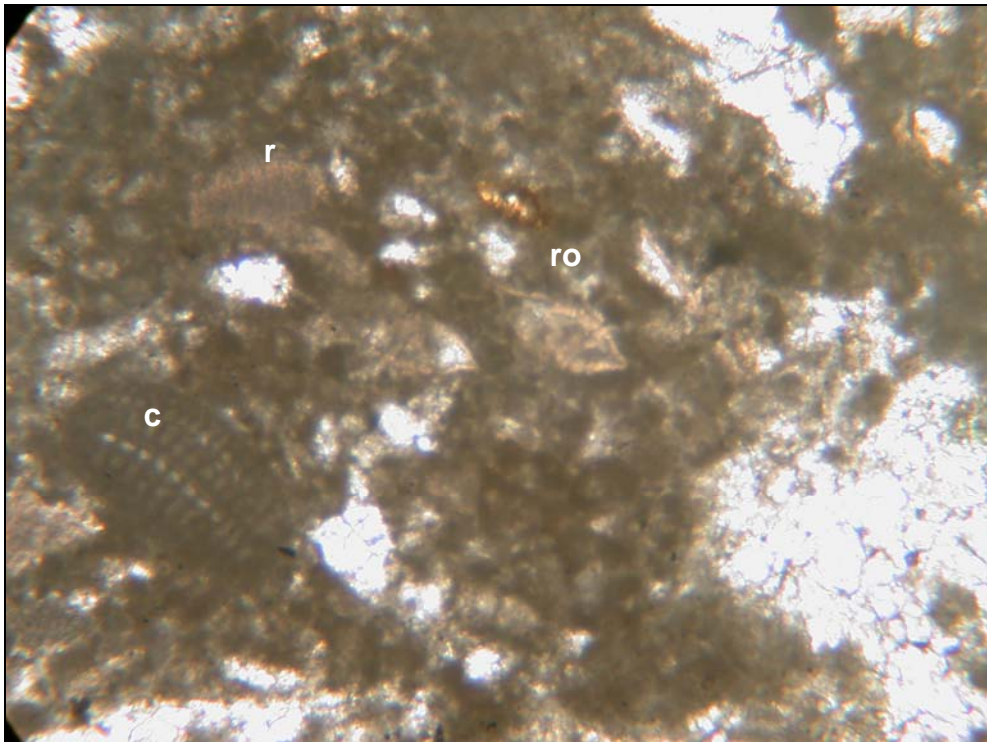


Figure 32: Photomicrograph of other benthic foraminifers found in Rotalid Miliolid Wackestone facies from Garzan-47 well (X4, core) (c:cuneolin, ro: rotalid, r:rudist).

(2%-7%), pelecypods and gastropods (2%-11%), cuneolins (1%), other benthic foraminifers (2%-10%), and ostracodes (2%-6%) occur in minor amounts and pelagic foraminifers are absent in the facies (Appendix B).

Among the thin sections of this facies 8 representative of them were counted. In average this facies is composed of 11.30% of orbitoids, 9.41% of rudist fragments, 2.06% miliolids, 2.99% of pelecypoda and gastropoda, 0.08% cuneolins, 2.20% ostracodes and 2.35% of other benthic foraminifers (Figure 33, 34). The major component of this facies is micrite matrix by 50.43% (Figure 33). According to the fossil content and their occurrence abundance this facies is deposited within the backshoal to shoal environment (Figure 45). This facies is relatively high energy facies however micrite is again the major matrix component. The micrite and microspar is strongly present in the facies explains that the water depth is relatively deeper which is unaffected from washing out. Another interpretation is; the facies deposited during high tide level so that waves are not affective enough to wash out.

This facies resembles to the SMF-5 and 6 of Wilson (1975) and FZ-7 and FZ-6 of Flügel (2004) (Figure 29). The common biota for this facies is large bivalves, gastropods, special type of foraminifera, dacycladacean algae with in grainstone, packstone, lime mudstone, wackestone and floatstone facies (Flügel, 2004). These facies are deposited along the shoals, tidal bars and beaches, within the euphotic zone strongly influenced by tidal currents and towards the shoal parts of lagoons in water depth of few to tens of meters (Flügel, 2004).

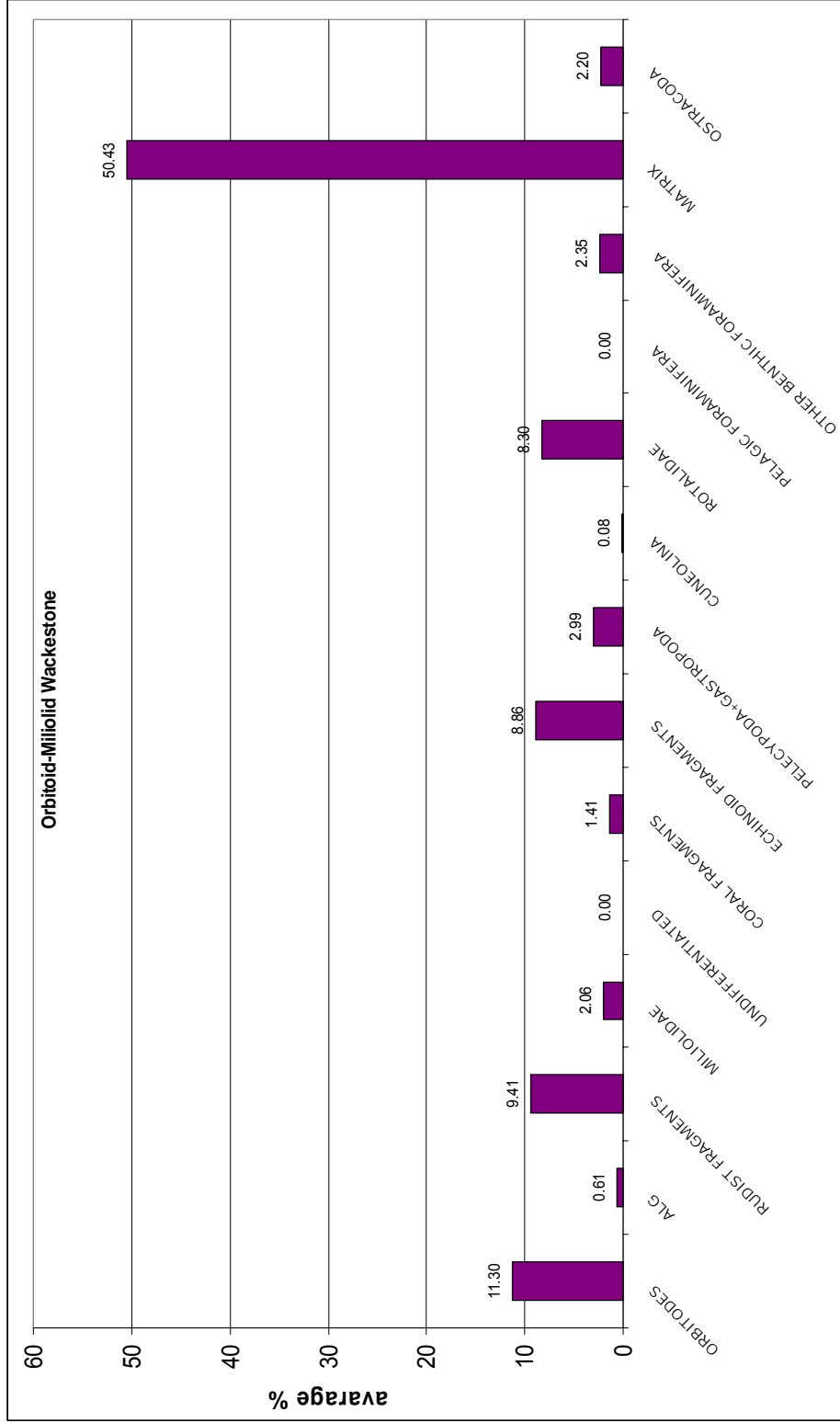


Figure 33: The average occurrence percentage of the constituents found in Orbitoid Miliolid Wackestone facies .

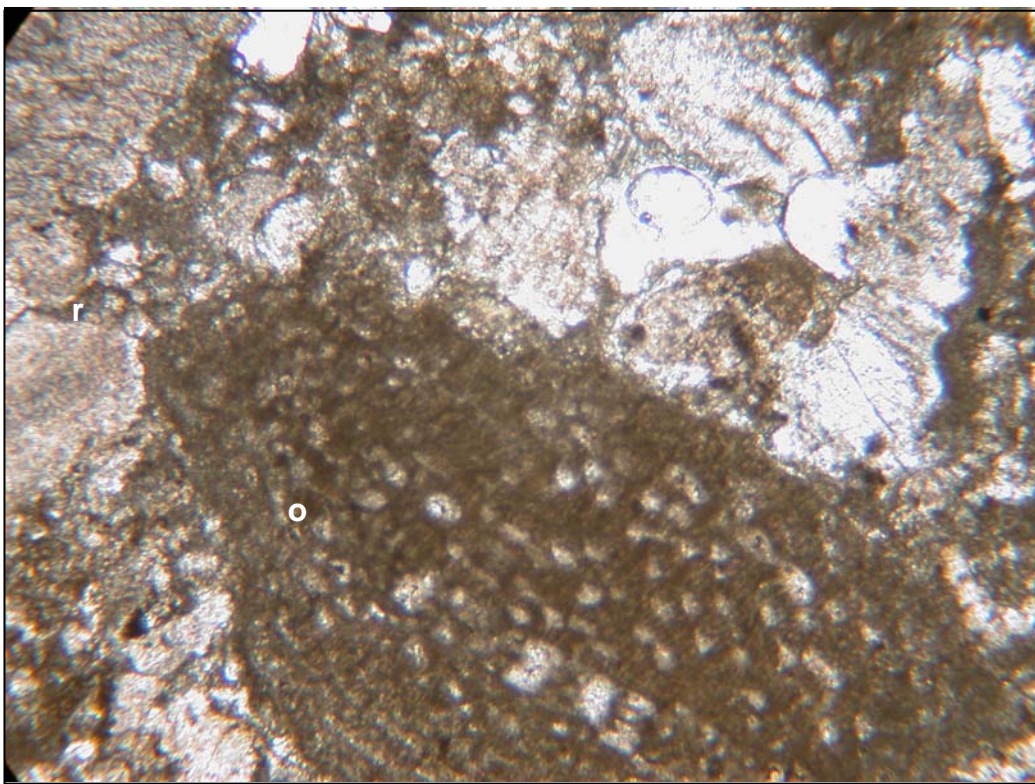


Figure 34: Photomicrograph of Orbitoid Miliolid Wackestone facies from Garzan-31 well (X4, core), (o:orbitoid, r:rudist).

This facies is described as grainstone facies by Eseller (1987). However Eseller (1987) reported the matrix as micrite which conflicts with the grainstone definition. Naz (1987) reported shoal reef complex flank carbonates which might be considered the equivalent of this facies; however, the only common thing in between the Orbitoid-Miliolid Wackestone facies of this study and the shoal reef flank carbonates of Naz (1987) is the orbitoidae and rudist fragments. Keskin (1971) defined the Microfacies B which is composed of packed biomicrites with large foraminifers such as *Orbitoides*, *Omphalacyclus*, *Siderolites* and *Loftusia* and clayey lime mud matrix and the average percent of large benthics in the matrix is given as 18.4%. Miliolids and textulriidae families are common in Microfacies B and *mollusks* are the second important skeletal constituent in the microfacies having an average of 10.4% where echinoderm, corals and ostracodes occur minor in amounts (Keskin, 1971). It is also defined Microfacies C containing the same allochems as Microfacies B, however difference in between the two facies is given as the volumetric average percentage of total allochems is 19.9% in Microfacies C which is less than Microfacies B (Keskin, 1971).

3.1.4 Pelagic Foraminiferal Wackestone

The major components of this facies are pelagic foraminifera (6%-20%) and matrix (70%-90%) where as orbitoids (1%-7%), other benthic

foraminifera and pelecypods and gastropods (1%), and ostracodes (5%) are observed in minor amounts (Appendix B).

Among the thin sections of this facies 6 representative of the whole were counted. In average this facies is composed of 14.77% of pelagic foraminifers, 1.98% of ostracodes, 1.90% of orbitoid fragments and 0.33% of other benthic foraminifers (Figure 35). The 81% of the facies is matrix (Figure 36, 37). This facies is deposited at foreshoal to open marine environment (Figure 45). The facies is usually observed towards the top of the formation. This also implies that the Garzan Formation was deposited during transgressive phase. Although there are small oscillations in sea level, the major trend of eustasy is rising. This might be the reason why we cannot find the most expected high energy environment facies in this Garzan-Germik oil field.

This facies is the equivalent of SMF-4 and 3 of Wilson (1975) and FZ-4 of Flügel (2004) (Figure 29). The setting is upper slope and seaward of the platform margin with mostly redeposited shallow water benthos, some deep water benthos and planktonic foraminifera within the mudstone, allocthonous packstone, grainstone, rudstone and floatstone facies (Flügel, 2004).

Keskin (1971) defined this facies from Garzan Formation as Microfacies A and described the facies as consisting of argillaceous biomicrites with small foraminifers. In this microfacies A, abundant spheroidal forams and pelagic foraminifers with minor amount of mollusk and echinoid shale fragments observed (Keskin, 1971). Eseller (1987) also defined the

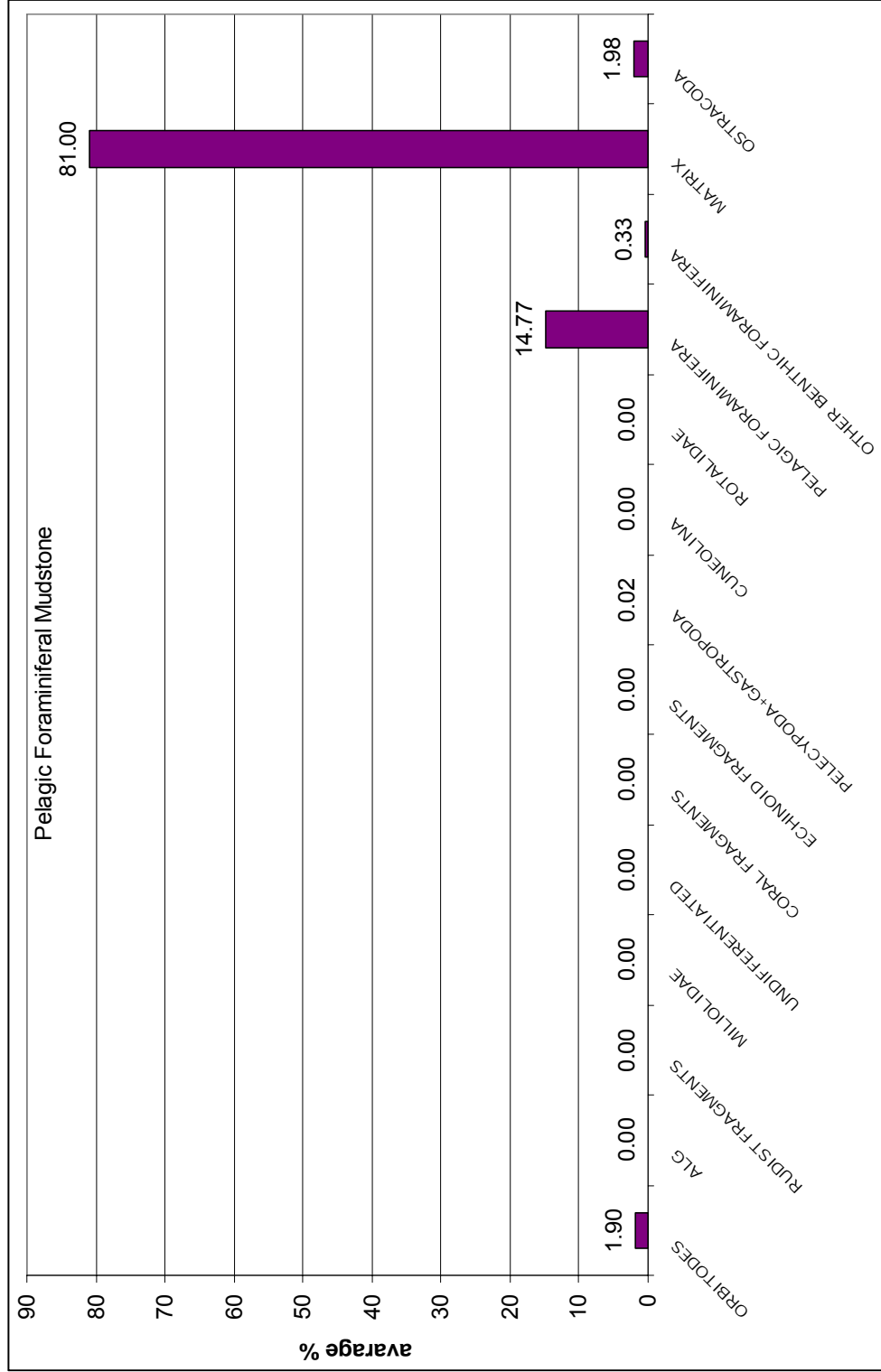


Figure 35: The average occurrence percentage of the constituents found in Pelagic foraminiferal Wackestone

facies .

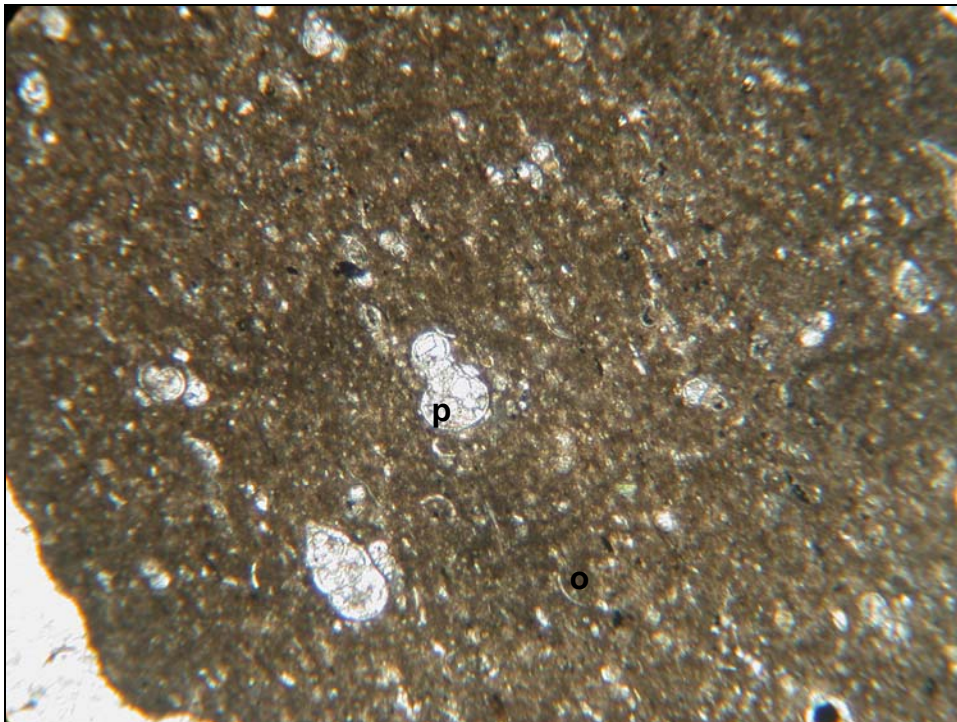


Figure 36: Photomicrograph of Pelagic Foraminiferal Wackestone facies with ostracodes from Garzan-23 well (X10, cutting), (p: planktonic foraminifera; o:ostracode).

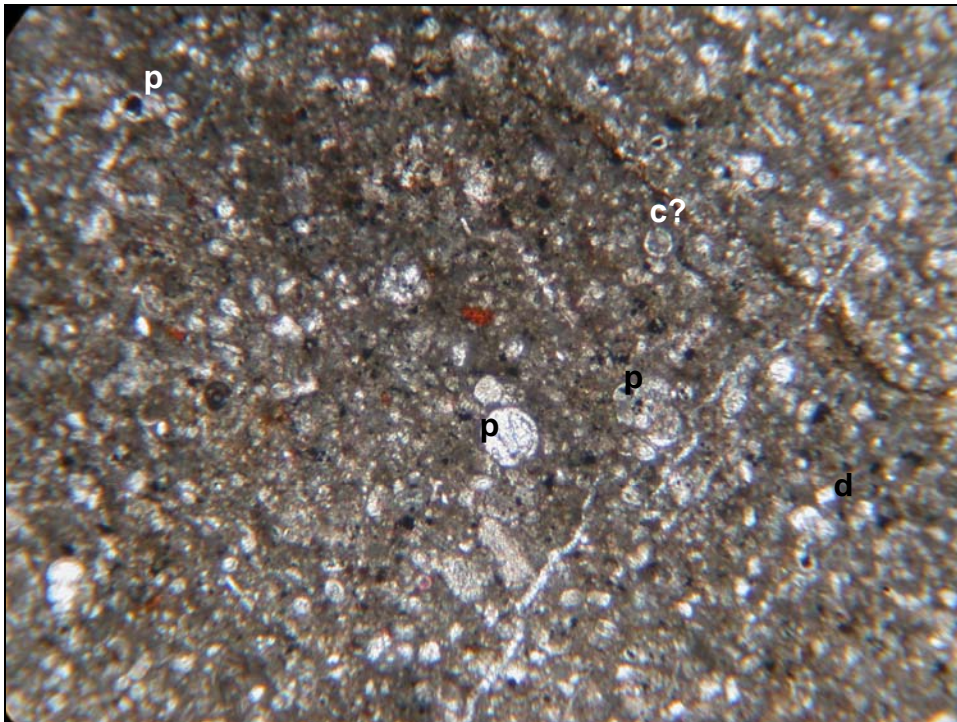


Figure 37: Photomicrograph of Pelagic Foraminiferal Wackestone facies from G. Germik-1 well (X4, cutting) (c:calcisphere ?, d:dolomite rhomb, p: planktonic foraminifera)

same facies as Pelagic Foraminiferal Wackestone-Mudstone and interpreted it to be deposited at open marine. It is observed that calcispheres and rarely echinoid spines are found together with pelagic foraminifers and also reported pyritization in the shells of foraminifera (Eseller, 1987). Naz (1987) defined the same facies as fore reef talus carbonates. Silt sized shell fragments, planktonic foraminifers are the main constituents of this facies (Naz, 1987).

3.1.5 Rudist Wackestone

The majority of components of this facies are rudist fragments (3%-54%), echinoid fragments (3%-15%), pelecypods and gastropods (1%-9%) and the matrix (30%-90%) whereas orbitoids and ostracodes (1%), miliolids (1%-4%), coral fragments (2%), rotalids (1%) and other benthic foraminifera (3%-23%) are observed in minor amounts (Appendix B).

Among the thin sections of this facies 9 representative samples were counted. In average the facies is composed of 27.80% of rudist fragments, 7.44% of echinoid fragments, 4.94% of pelecypoda and gastropoda, 6.23% of other benthic foraminifers, 0.17% of ostracode, 0.32% of rotalids, 0.53% of corals, 0.81% of miliolids and 0.76% of orbitoid fragments (Figure 38, 39 40). The 50.90% of the facies is micrite matrix (Figure 38). This facies is

deposited within the backshoal to shoal environment as same with Orbitoid Miliolid Wackestone facies (Figure 45).

The facies is the representative of SMF-5 and 6 of Wilson (1975) and FZ-7 and FZ-6 of Flügel (2004) (Figure 29). The common biota of these zones are reefs and associated environment, bivalves, gastropods and foraminifers and dacycladecean algae and shallow water benthos within grainstone, packstone, mudstone, wackestone and floatstone facies (Flügel, 2004). The habitat of rudists stretched from protected and open marine parts of platforms of shelf margins where they produce large amount of bioclastic rudist sands (Flügel, 2004).

Keskin (1971) defined this facies as Microfacies D as packed biomicrite indicating that *Mollusks* are predominant skeletal constituents of the facies reaching to a maximum of 71.6% and corals, echinoid fragments and large benthic foraminifers are also present. The facies is defined as rudist miliolid packstone by Eseller (1987). It is implied that the rudist miliolid packstone facies mark the beginning of Garzan transgression including unoriented fragmental rudist debris, large benthic foraminifera together with porcellaneous foraminifera and algae. Naz (1987) defined this facies as back reef carbonates, and the facies was put to the top most of Garzan Formation. Small benthic forams like miliolids, textulariids and mollusk shell fragments are the major constituent of these facies (Naz, 1987).

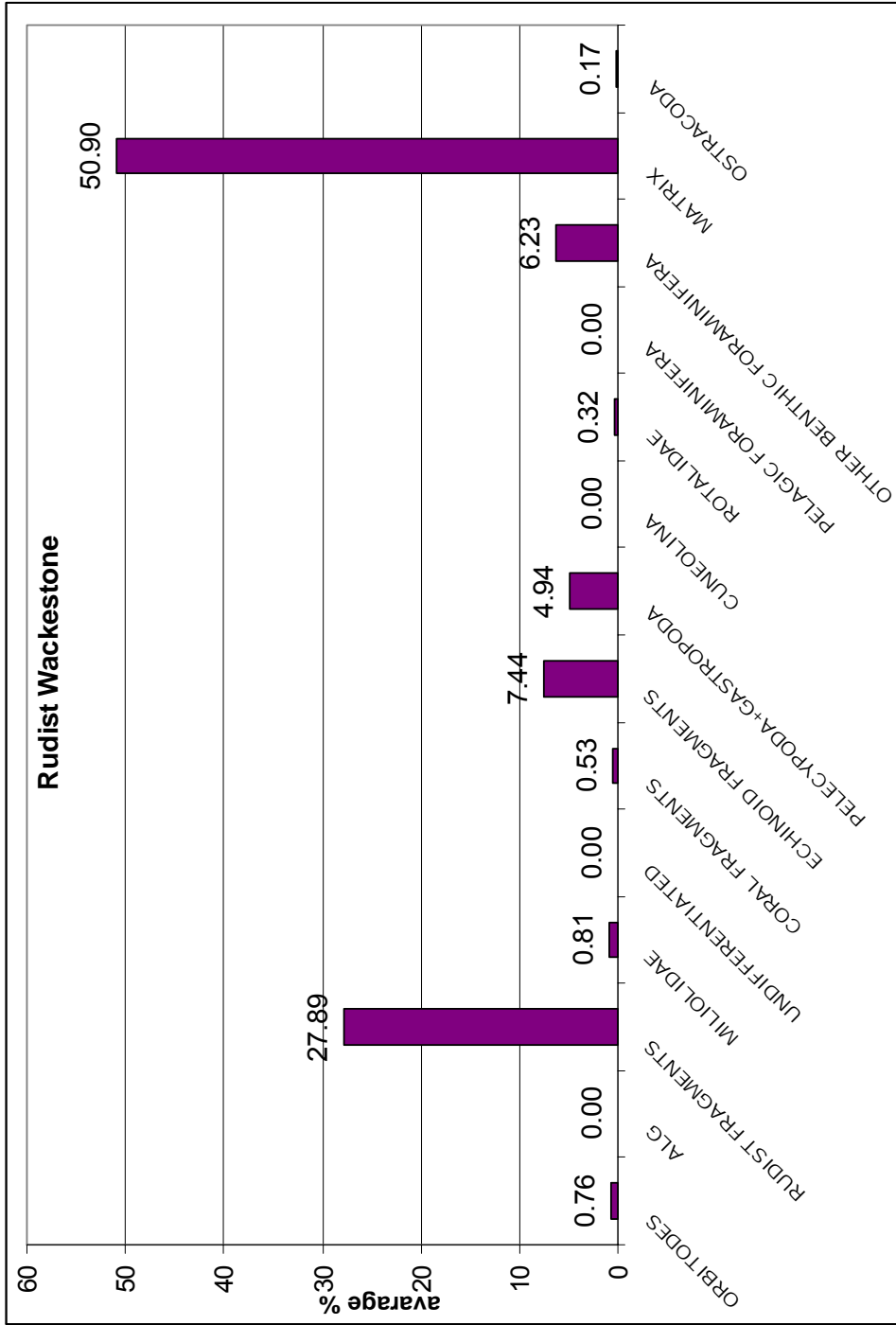


Figure 38: The average occurrence percentage of the constituents found in Rudist Wackestone facies .

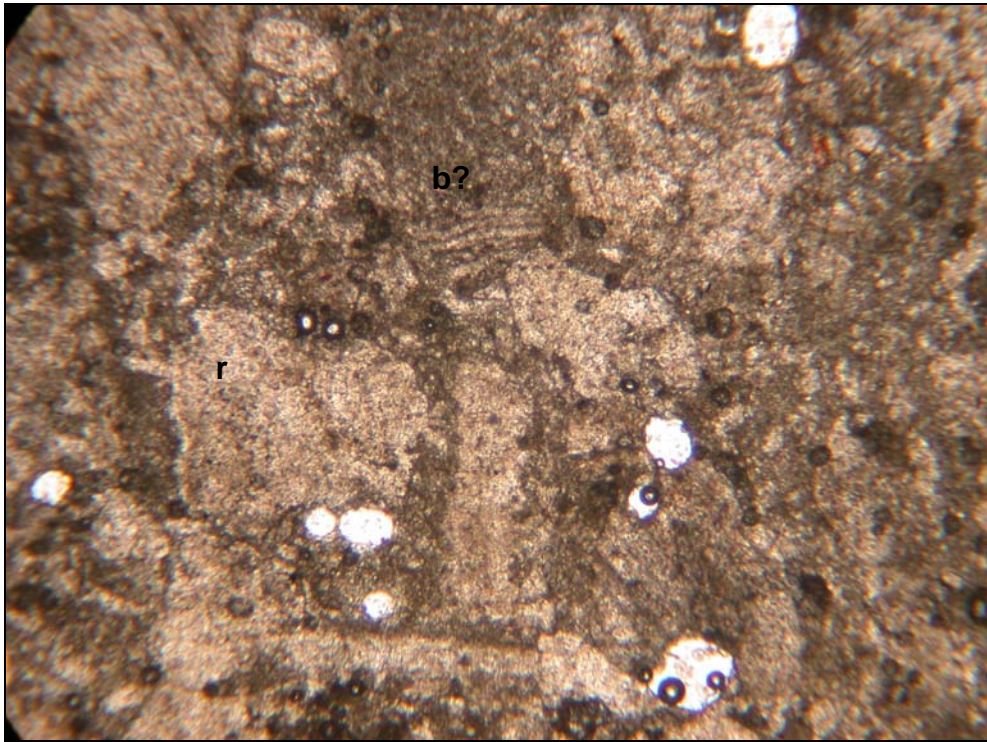


Figure 39: Photomicrograph of Rudist Wackestone facies from Garzan-95 well (X4, core), (r:rudist, b:bryozoan?).

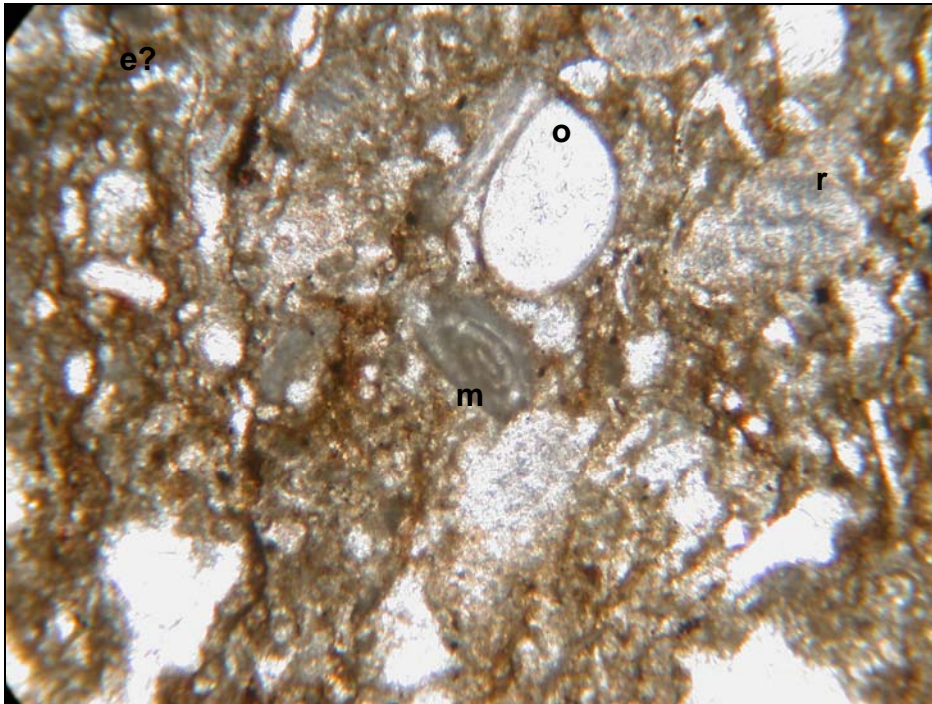


Figure 40: Photomicrograph of rare miliolid in Rudist Wackestone facies from Germik-6 well (X4, core), (e:echinoid?, o:ostracode, m:miliolid) .

3.2 Cycle Types of Garzan Formation in the Garzan-Germik Oil Field

According to the microfacies study there are five microfacies types observed in the Garzan Formation in Garzan- Germik oil field. With the combination of these five microfacies types and their depositional environment there are five cycles observed. Those are named as type A, type B, type C, type D and type E (Figure 41).

The type A cycle starts with Orbitoid Miliolid Wackestone and/ or Rudist Wackestone facies and is overlain by Rotalid Miliolid Wackestone facies and capped by Miliolid Wackestone facies. The cycle starts with backshoal to shoal environment and a relative sea level rise leads the shoal to foreshoal environment deposit on to the backshoal to shoal environment. The subtidal environment is deposited at the top of the cycle. This cycle is a retrogradational type of cycle which is deposited in transgressive systems tract (Figure 41).

The type B cycle starts with Rotalid Miliolid Wackestone and capped by Miliolid Wackestone facies. The environment within the cycle changes from foreshoal to subtidal conditions. This is an aggradational type of cycle deposited in high stand systems tract (Figure 41).

The type C cycle starts with Orbitoid Miliolid Wackestone and/or Rudist Wackestone facies and capped by Miliolid Wackestone facies. The environment changes from backshoal to shoal to subtidal conditions. This is

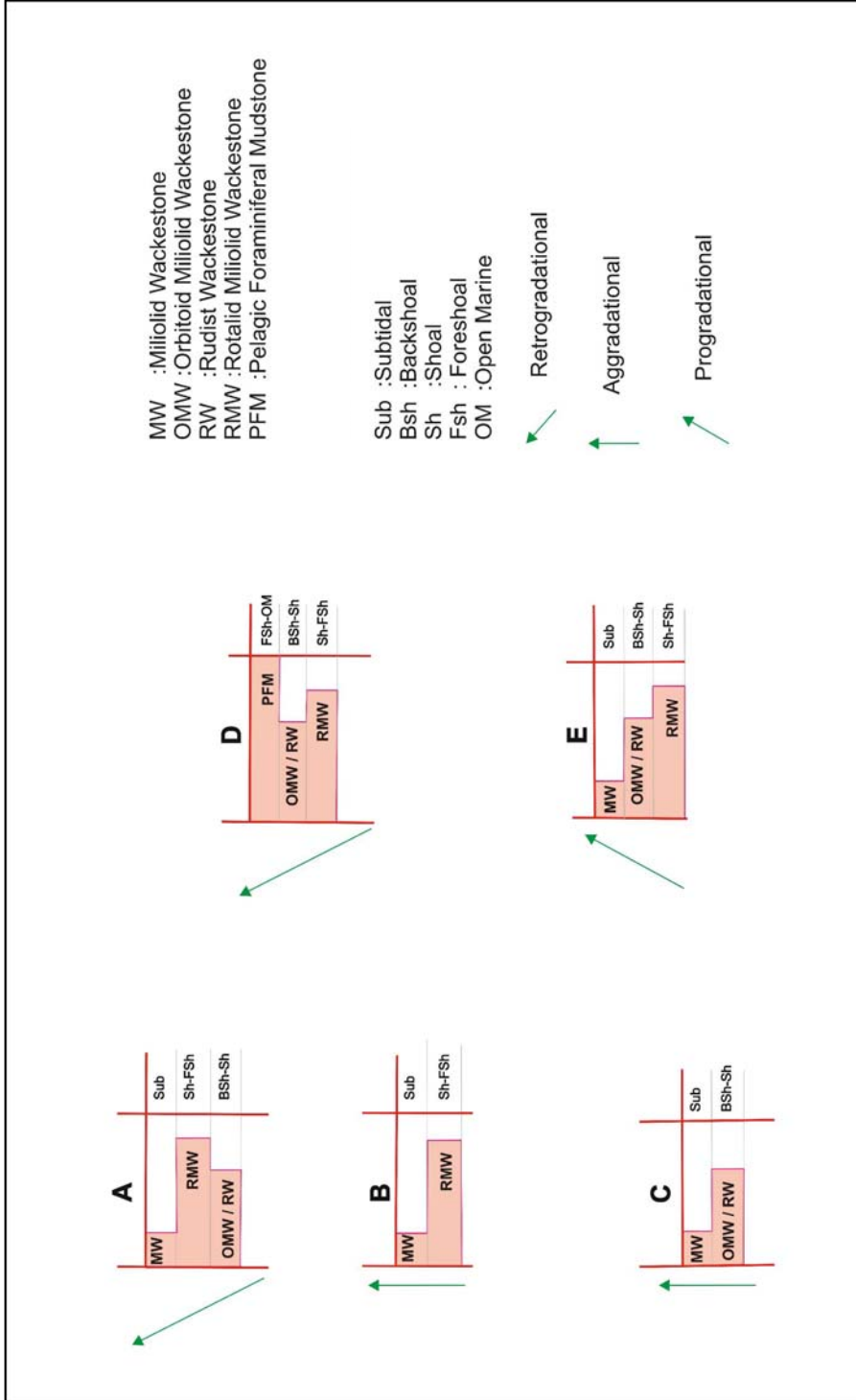


Figure 41: Cycle types observed in Garzan Formation in Garzan-Germik oil field.

an aggradational type of cycle deposited within high stand systems tract (Figure 41).

The type D cycle starts with Rotalid Miliolid Wackestone facies overlain by Orbitoid Miliolid Wackestone and/or Rudist Wackestone facies and capped by Pelagic Foraminiferal Mudstone facies. The environment within the cycle changes from open marine to subtidal. This cycle is a retrogradational type of cycle deposited within transgressive systems tract. The maximum flooding surface is located in or at the top of this cycle.

The type E cycle starts with Rotalid Miliolid Wackestone facies overlain by Orbitoid Miliolid Wackestone and/or Rudist Wackestone facies and capped by Miliolid Wackestone facies. The depositional environment changes from foreshoal to subtidal. This cycle is a progradational type of cycle deposited within the high stand systems tract (Figure 41).

The type A cycle is deposited with in rising sea level and this is the characteristic of the transgressive system tract deposits. Towards the end of the cycle A the amount of sea level rise reaches to a point that, the accommodation space is created by increasing depth of sea level and subtidal environment overlies the shoal to foreshoal environment. The rise in sea level favors the facies of subtidal environment to be deposited over the below lying faices. Also the same conditions stay on for the type D cycle in considering the sea level change. Type D cycle is also a transgressive system tract deposit. The maximum flooding surface is located at about the top of the type D cycle. This cycle is characteristically located at the top of

the Garzan Formation. Type A and D cycles are retrogradational type of cycles. The type B, C and E cycles are deposited within high stand systems tract. The type B cycle is an aggradational type of cycle like type C cycle. The accommodation space kept constant by the combination of rising sea level and deposition so that, there is no relative sea level change in the cycle B and C and there is no net movement of shoreline towards land or basin in these cycles. The cycle E is a progradational type of cycle where the net movement of facies are towards the basinward. The top of the cycles are characterized by subtidal deposits. This is because the sea level rise reaches to a point that the border of subtidal environment is enlarged. This might have been caused a drowning unconformity but the evidence of it such as hardgrounds, phosphate, iron enrichment, or burrowed discontinuities could not be recognized in this study. There is usually a rapid change from shallow water carbonates to deep shelf, slope or basinal deposits (Schlager, 1992). Miocene carbonate platform offshore central Vietnam also show a change from shallow water platform carbonate sedimentation through a drowning sequence of deeper water foraminifera with evidence of marine condensation and glauconite and phosphate (Emery and Myers, 1996). An intermediate version of complete platform drowning is backstepping or retrogradation and drowning will take place when the platform top is flooded with transgressive or high stand systems tract (Emery and Myers, 1996). This is also observed in the wells of this study. Also in the wells Garzan-23 and Garzan-31 the onset from Garzan Formation to Alt Germav formation is described with high

abundance of pelagic foraminifers (condensed section?) associated with glauconite showing slow sedimentation. Also usually the Alt Germav marls overlies faices of the back shoal to shoal environment or overlies the retrogradational type D cycle (Figure 41).

3.3 Depositional Environment of Garzan Formation in the Garzan-Germik Oil Field

The age of the Garzan formation is Middle Maastrichtian (Köylüoğlu, 1986; Güven et. al., 1991) and the depositional environment of the formation is given as shallow water carbonates with reefoidal complex (Eren and Sarı, 1984). Garzan Formation is deposited with in an irregular topography with reefoidal, bioclastic mound and detritic limestones Salem et. al. (1986) described the depositional environment of the formation as tidal flat area with subtidal to intertidal environment present. However, in this study in Garzan Germik oil field it is observed that the Garzan Formation is deposited at subtidal to open marine conditions represented with five microfaices. Intertidal and supratidal environments are not present in this study.

During Early Maastrichtian the southern part of District X was exposed to erosion. The eroded particles filled up the basin by the deposition of Kastel formation. The topography formed at the end of the Early Maastrichtian became underwater by the transgression of Middle- Upper Maastrichtian

forming a shallow water carbonate platform (Güven et. al., 1991). During the same period the deeper parts at the region started to deposit pelagic marl and shale, the deposit of the Alt Germav Formation (Figure 42). Garzan Formation is the first limestone deposit at the study area during the transgression of Middle –Late Maastrichtian. The formation has a wide depositional extend on the platform area of District X. The Garzan Formation was deposited unconformably over the Kiradağ Formation at platform area of the District X and towards the northern part it is deposited over Terbüzek Formation. At the deeper parts of the basin at District X, the Alt Germav is being deposited towards SE during; Middle- Late Maastrichtian (Figure 43). The transgression continued and the marly limestone and pelagic facies of Alt Germav started to transgress over the Garzan Formation. The vertical facies distribution shows that the deposits towards southern and eastern part of the District X were deepening upward towards the top (Figure 43). After the deposition of the Garzan Formation and the lower parts of Alt Germav Formation onto the Garzan Formation, a regressive phase started and marly limestone and pelagic deposits moved towards southeast basinal areas and again shallow water conditions favored the carbonate deposition at the northwest. The Alt Sinan Formation deposited during this regressive period. Towards the end of the Maastrichtian a regional transgression again brought marly limestones and pelagic mudstones to the area. However, this period was very broad and the Alt Germav Formation covered the whole District X and the Southeast Anatolia (courtesy of TPAO) and the Alt Sinan Formation

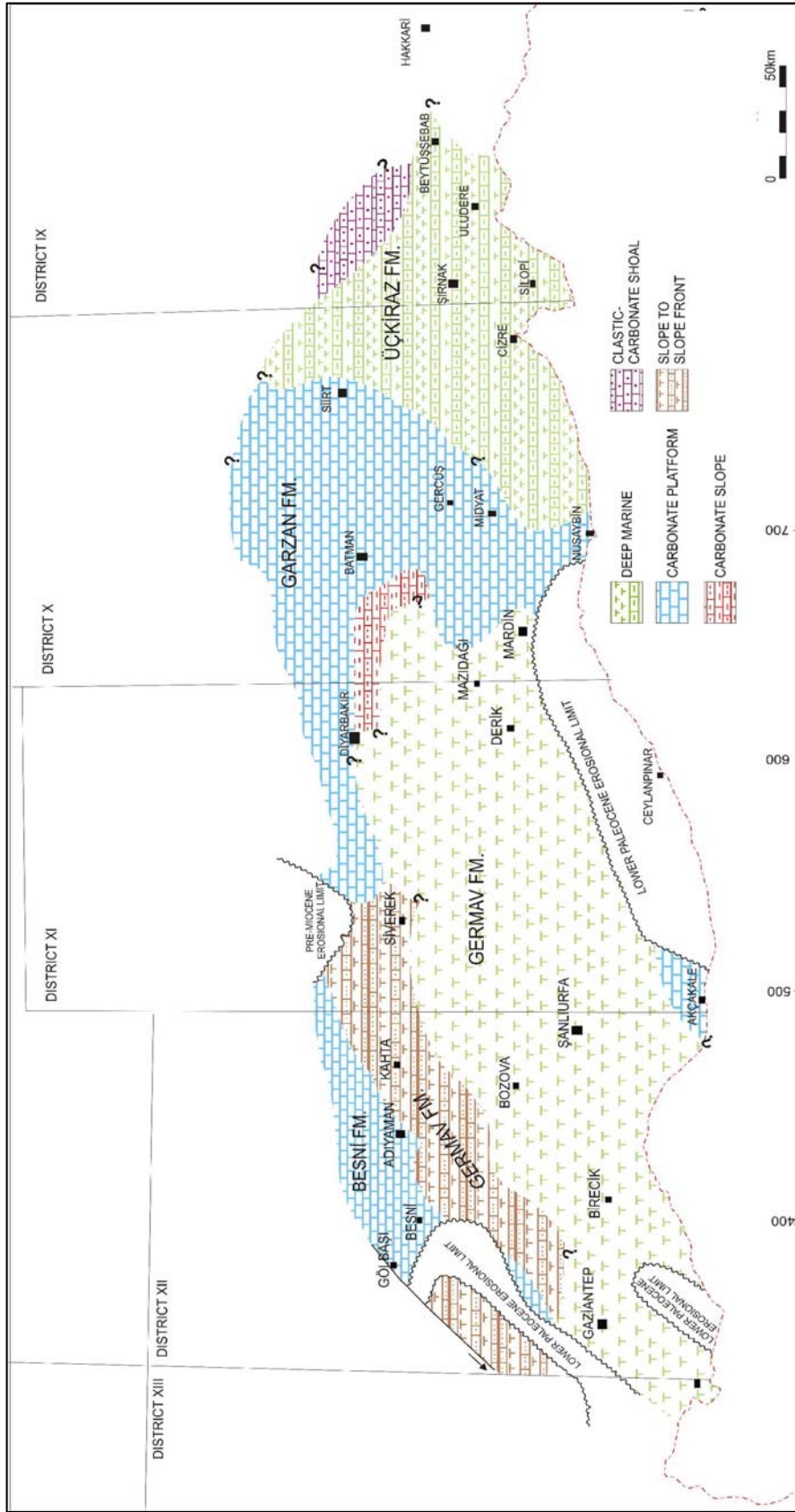


Figure 42: Paleogeographic facies map of Middle – Late Maastrichtian of South East Anatolia (Güven et.al., 1991).

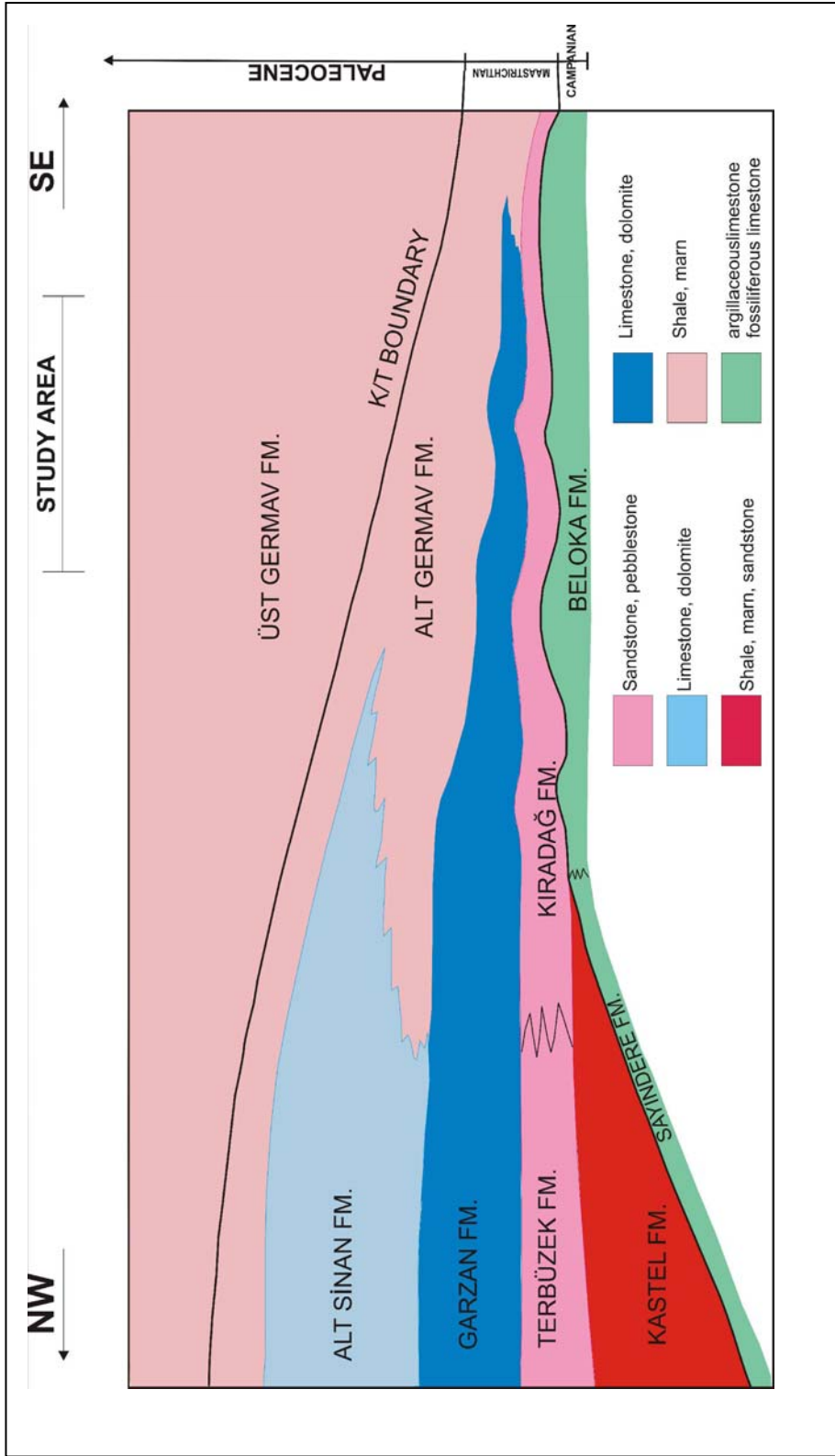


Figure 43: Depositional model of Campanian- Paleocene units in South East Anatolia in District X (based on the data of this study and Yılmaz and Duran, 1997).

and Garzan Formation carbonates became a tongue in the Alt Germav Formation. This was also recognized by Temple and Pery (1962), that they interpreted the Garzan Formation as a lenticular limestone enclosed in shale. The Cretaceous – Tertiary boundary is also represented at the top of the Alt Germav Formation (Figure 43). The Alt Germav Formation deposition drowns the Garzan Formation carbonates. The death of a carbonate platform is caused by different mechanisms, including long and short term sea level fluctuations, tectonic processes, climate and related environment changes (Flügel, 2004). However, succession of shallow marine neritic sediments rapidly passing upward into deep marine deposits is an indication of drowning (Flügel, 2004). This is the same situation with the Alt Germav and the Garzan Formations. In this study area and near around the Garzan Formation never finalizes its deposition towards shallower faices especially characterized by intertidal and supratidal environment. On the contrary, it passes into the Alt Germav marls. Also in few of the thin sections belonging to the base of the Alt Germav Formation lying just above the Garzan Formation, glauconite is observed. As the Garzan Formation boundary is the limit of this study, this drowning unconformity is just mentioned but it is not going to be proofed within this study which is out of the scope of this thesis.

Foraminifers have a world wide distribution in all marine environments from Ordovician to Recent and are increasingly used for environmental interpretation as well as chronostratigraphic correlations (Horowitz and Potter, 1971). Also corals are interpreted as marine animals and were most

abundant in clear shallow carbonate seas where they were major contributors to reef and banks from Ordovician to Recent. Pelecypods are distributed World wide also from Cambrian to Recent and are present in marine and fresh waters where gastropods have the same time duration and present in marine environments (Horowitz and Potter, 1971). Ostracodes are known from Ordovician to Recent in most aquatic environments and echinoderms are exclusively marine usually open marine animals (Horowitz and Potter, 1971). This is because, cuneolins, textulariina and valvulinids are common in lagoonal and shallow inner platform environment where discoidal or lenticular orbitoidacean rotaliid foraminifers indicate Late Cretaceous shelf and shelf slope deposits (Flügel, 2004). The orbitoidacean foraminifera are abundant in Maastrichtian shallow water shelf carbonates in outer platform and upper slope and planktonic foraminifera are abundant in fine grained Cretaceous and Cenozoic carbonate deposits at deep sea bottom of open marine setting (Flügel, 2004). Middle and Late Cretaceous miliolinid are also abundant in inner part of carbonate platforms (De Castro, 1980, 1988).

The depositional model according to fossil groups define the formation from supratidal to slope to basin range with intertidal, subtidal, backshoal, shoal, foreshoal and open marine divisions (Altiner, 1983) (Figure 44). This study used some of the major fossil groups and built the environment accordingly. The major fossil groups used in this study are: planktonic foraminifera, orbitoides, cuneolina, moncharmontia, minouxia, valvulina, rotalidae, miliolidae, rudistacea, pelecypoda, ostracoda, gastropoda, coral,

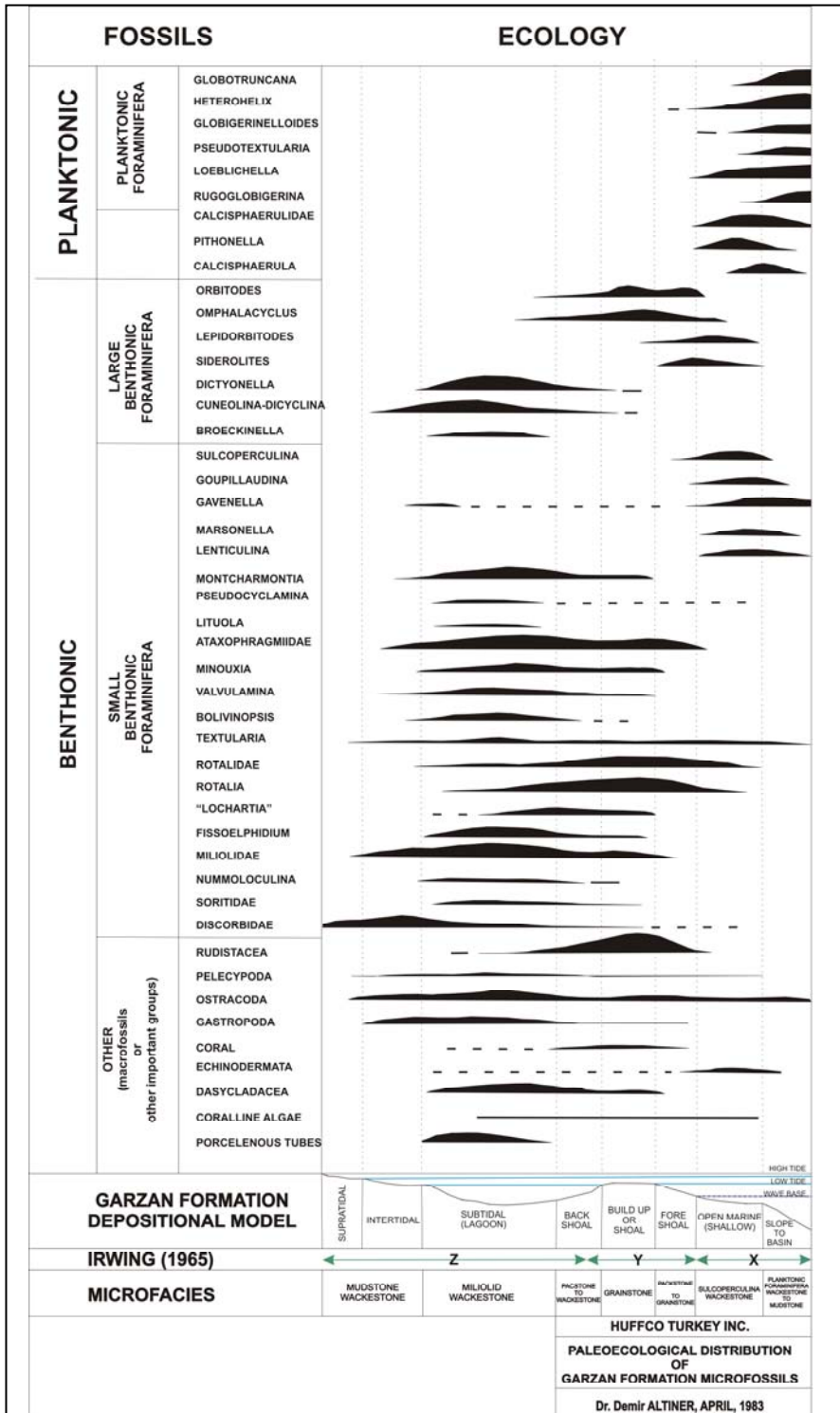


Figure 44: Paleocological distribution of the Garzan Formation microfossils (Altiner, 1983).

echinodermata, dascyladacea (Figure 45). The fossils are used as a tool for environment interpretation. According to these fossil groups and sedimentological observations within the study area, only subtidal, backshoal, shoal, foreshoal and open marine environment are present (Figure 45). The supratidal, intertidal and slope facies are not present in this study.

The deposition of the Garzan Formation is transgressive as said before. The locality of the Garzan- Germik oil fields is at the place where intertidal and supratidal deposits are not present because of geography and topography (Figure 46). The location of the studied wells according to their microfaices are given in figure 46.

The base of the Garzan Formation is represented mostly with Rotalid Miliolid Wackestone and Rudistacea Wackestone facies, at which the energy of the sea was very high at the start of the period (Figure 47). The formation overlies Kıradağ Formation which is sublittoral so high sea level is expected.

Usually porosity is good enough at these levels. When the base of the formation is deposited then environment differentiation occurred and backshoal to shoal environment started to control the deposition of the formation. The formation continues with Orbitoid Miliolid Wackestone and/or Rudist Wackestone facies alternations and capped by Miliolid Wackestone facies. These are the deposits of high stand systems tract and the lower part is characterized by type E cycle and the upper part is characterized by type C cycle (Figure 47). Then again Orbitoid Miliolid Wackestone and /or Rudist

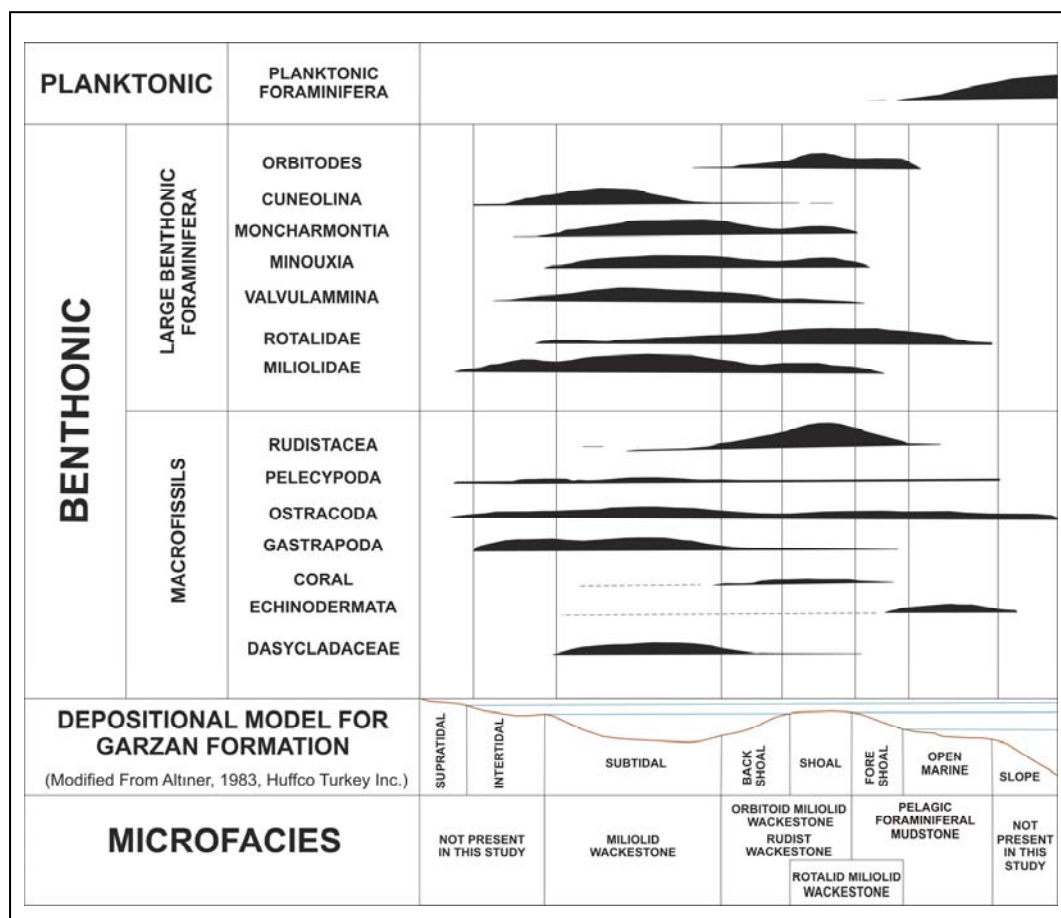


Figure 45: Depositional Model for the Garzan Formation in Garzan–Germik oil field (modified from Altner, 1983).

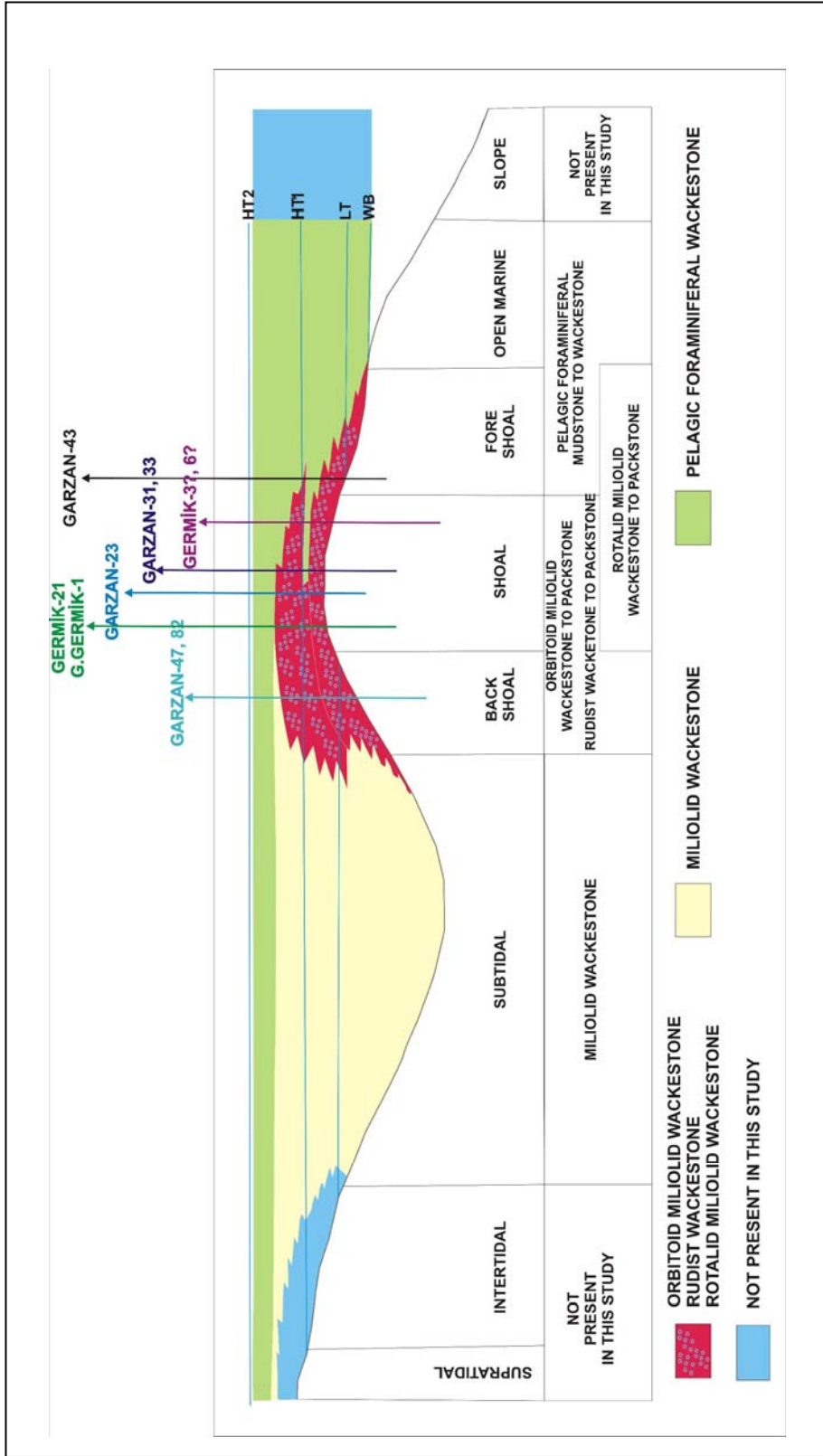


Figure 46: The depositional geometry of the wells of Garzan-Germik oil field with in the depositional environment. The studied wells are located schematically within the depositional environment.

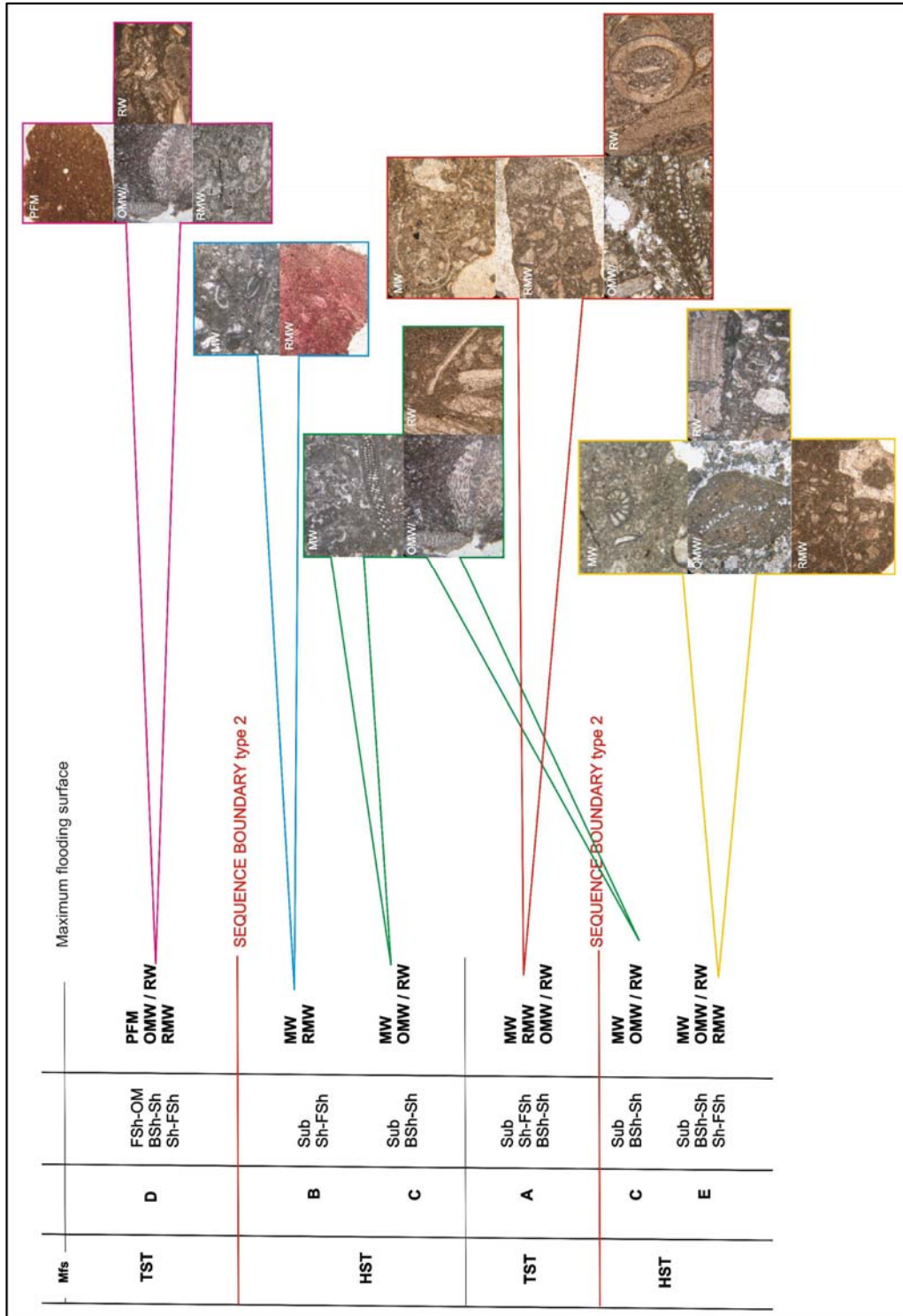


Figure 47: Microfacies arrangement of the cycles types in Garzan Formation in Garzan-Germik oil field.

Wackestone facies is overlain by Rotalid Miliolid Wackestone facies and capped by Miliolid Wackestone facies (Figure 47). This is type A cycle and it is the deposit of transgressive systems tract. Above there is alternation of Rotalid Miliolid Wackestone capped by Miliolid Wackestone and Orbitoid Miliolid Wackestone or Rudist Wackestone capped by Miliolid Wackestone facies. The Orbitoid Miliolid Wackestone and/or Rudist Wackestone facies is capped by Miliolid Wackestone and this type of cycle is named as type C cycle and Rotalid Miliolid Wackestone facies capped by Miliolid Wackestone facies is defined as type B cycle. These are both deposited within the high stand systems tract. Towards the top Rotalid Miliolid Wackestone and Orbitoid Miliolid Wackestone and/or Rudistacea Wackestone facies is overlain by Pelagic Foraminiferal Mudstone facies (Figure 47). Usually this Pelagic Foraminiferal Mudstone facies overlain by maximum flooding surface towards the end of deposition of the formation. This is because regional transgression spilled over the area and started the deposition of the Alt Germav marls. (Figure 47). This facies stacking is type D cycle and it is the deposit of transgressive systems tract. This cycle is the top most cycle of the Garzan Formation deposition and maximum flooding surface is located towards the top of the cycle or at the top of the cycle (Figure 47).

3.4. Stacking Patterns and Sequence Stratigraphy of the Garzan Formation in Garzan-Germik Oil Field

Sequence stratigraphy which had been attracting attention around the World recently is regarded as stratigraphic method from the petroleum geologists point of view that may provide ideas of suitable areas for petroleum exploration on the basis of prediction of sedimentary facies distribution and high resolution global and regional stratigraphic correlations using stratigraphic units defined by their genesis (Mitchum et. al., 1993; Aroto and Tokano, 1995).

The main feature of transgressive systems tract deposits are the large lateral extension of deposits representing carbonate shoals and predominance of open marine types in proximal areas (Bachmann and Kuss, 1998). On carbonate platforms the carbonate production generally reaches its maximum during high stand systems tract (Handford and Loucks, 1993). The major controlling factor for the formation of sedimentary cycles is the changing sea level (Vail et. al.,1977).

The Garzan Formation in Garzan-Germik oil field is deposited from subtidal to open marine environment (Figure 45 and 46). Garzan deposition is a result of sea level rise and it was deepening towards upward. This is because at the base of the Garzan Formation there is Kıradağ Formation which is a sublittoral deposit (Figure 18). Above this formation the Garzan Formation was being deposited as a tongue in the Maastrichtian basin

(Figure 43). It is the time equivalent of the Alt Germav formation and deposited in the shallower parts of this basin. The overall transgressive cycle grades into the Alt Germav Formation which is a deep marine pelagic deposit.

This study revealed that there are five cycle types composed from five microfacies (Figure 41). The cycles deposited on top of each other corresponds to the parasequence sets in the formation. Generally the deposition of Garzan Formation starts with high stand systems tract deposits composed of type C and E cycles (Figure 47). On above there is usually a transgressive systems tract deposits characterized by type A cycle and it is overlain by high stand systems tract deposits composed of alternation of type C and B cycles (Figure 47). The Garzan deposition ends with usually transgressive system tract deposits characterized by type D cycle at the top and a maximum flooding surface within or at the top of the type D cycle (Figure 47). Between the transgressive systems tract and high stand systems tract deposits there is a sequence boundary of type 2. This sequence boundary is generally located at the top of type A cycle and at the base of type D cycle within the wells (Figure 47).

Shallow water deposition occurred during a sea level fall followed by rapidly ascending sea level resulting in deepening upward cycles dominated by deep water facies (Gomez-Perez et. al., 1998). These cycles reflect an increase in accommodation space during the transgressive and highstand system tracts (Gomez-Perez et. al., 1998). The type D cycle is a deepening

upward cycle and maximum flooding surface is usually located within or at the top of the cycle. Gomez-Perez et. al. (1998) stated that the maximum flooding surface would be in the middle parts of the cycle and does not coincide with the cycle boundary. Within this study the type D cycle passes into the marls of the Alt Germav Formation, so that the maximum flooding surface can be at the top of the cycle. Type A cycle is also a deepening upward type of cycle and towards the top of the cycle the accommodation space is being created and high stand systems tract conditions prevailed. Within the type A cycle the sea level rise reached to a point that the Miliolid Wackestone facies is able to deposit over Rotalid Miliolid Wackestone faices of shoal to fore shoal environment. This is to say that the sea level rise favored the subtidal environment deposition over as far as to the shoal to fore shoal environment. Although Garzan formation is a shallow water carbonate the deposition occurred during the ascending sea level and accommodation space is being created within the deposition of formation. The base Garzan deposition starts with high stand system tract deposits usually characterized by type E and overlain by type C cycles (Figure 47 and 48). The GR reading in type E and C cycles changes from low API values towards the higher API values (Figure 48). The examples for this are the wells Germik-21, G. Germik-1, G. Germik-2, Garzan-33, Garzan-31 and Garzan-23. However the base Garzan deposition starts with transgressive system tract deposits in Garzan-47, and Garzan-43. This is because of the geographical location of the wells. Garzan-47 is located towards the south of the reverse fault forming

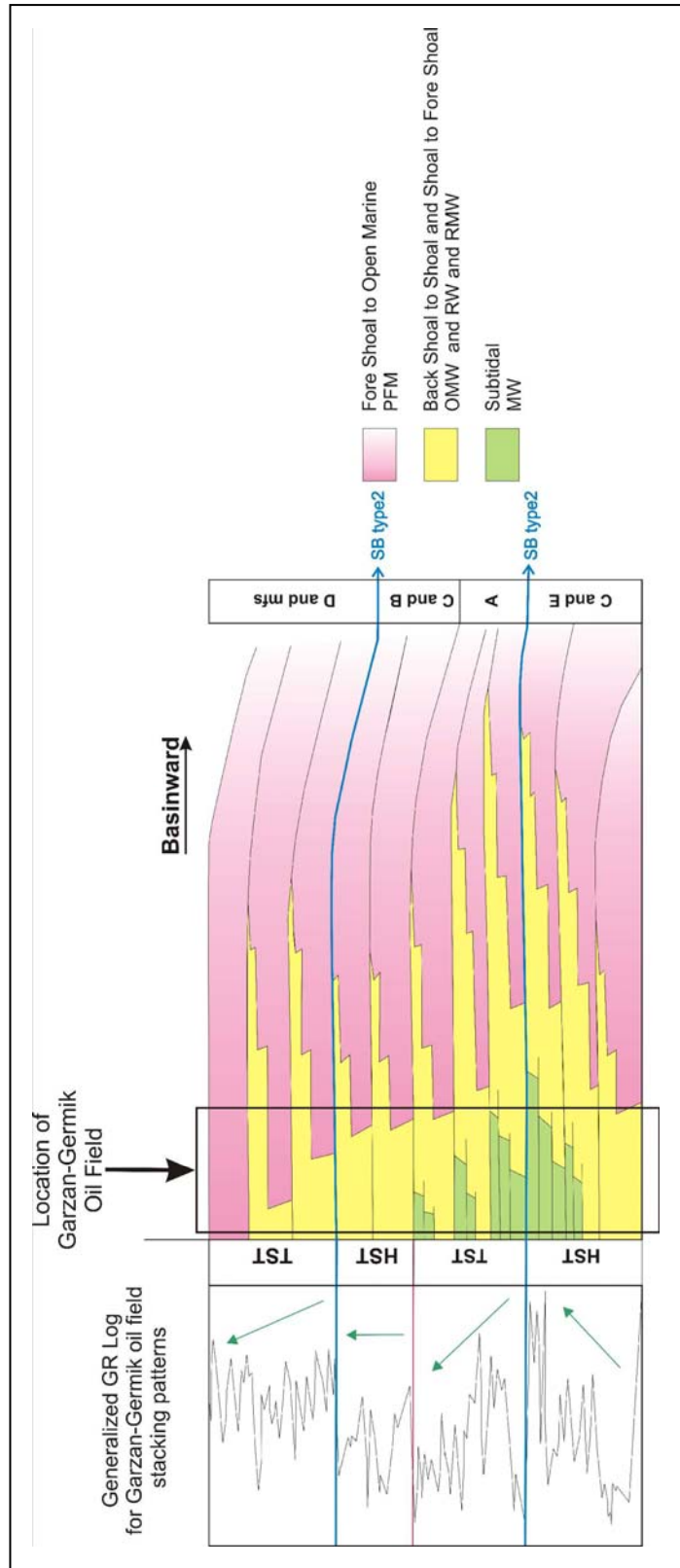


Figure 48: Generalized stacking patterns of the Garzan Formation within the Garzan-Germik oil field and its representative GR log response.

the Garzan anticline and Garzan-43 is located towards the north of the field, at the flank of the structure (Figure 3). The Garzan-82 well is deposited during the base high stand systems tract of Garzan Formation. The whole well is represented with type E and C cycles. The reverse fault bordering the Garzan-Germik oil field from the south was present during the Maastrichtian age and it was controlling the carbonate deposition.

Then above the high stand systems tract deposits type A cycle was being deposited which is a transgressive system tract deposits. The GR readings in this type A cycles changes from relatively high API readings to low API values (Figure 48). This transgressive systems tract was overlain by aggradational type of high stand systems tract deposits. The type C and B cycles are alternating in this high stand systems tract and the GR readings in this system does not show a distinctive pattern, meaning that there is no net movement on the log concerning the high or low API values (Figure 48).

This high stand systems tract and aggradational type of parasequences are observed in the Germik-21, G. Germik-1, G.Germik-2, Garzan-33, and Garzan-31 wells.

Then again the top Garzan deposition is characterized by type D cycle which is a deposit of transgressive systems tract including usually a maximum flooding surface in or at top of the cycle. The GR values changes from relatively high API reading to lower API values (Figure 48). This ends up the Garzan deposition. This transgressive system tract deposits observed well in Germik-21, G. Germik-1, G. Germik-2, Garzan-33, Garzan-31 and

Garzan-23. The well Garzan-43 is completely deposited during the transgressive system tract deposit of type D cycle deposition.

The top Garzan Formation is characterized by transgressive system tract deposits (Figure 48). This results the Alt Germav transgression creating a maximum flooding surface towards the top of the Garzan Formation within the basin and the landward movement of facies observed (Figure 43). The carbonate factory could not keep pace with the rising sea level and bioherms and limestone units became rapidly drowned and covered by argillaceous lime mud deposits (Gomes-Perez et. al., 1998). The same result is observed in this study that the Alt Germav marls drowns the Garzan Formation limestones.

In the theory of sequence stratigraphy between highstand system tract and the above lying lowstand system tract or transgressive system tract there would be a sequence boundary of either type 1 or type 2. In this study sequence boundary is between the type E and C cycles and above lying type A cycles and between the type B and C cycles and above lying type D cycles (Figure 48). This boundary should be type 2 sequence boundary and in this study it is the correlative conformity of the type 2 sequence boundary.

The stacking patterns observed within the wells draws the generalized stacking pattern of Garzan Formation starting with highstand systems tract deposits, overlain by transgressive systems tract deposits and has an aggradational stacking of parasequences of high stand systems tract and ends up with transgressive systems tract deposits (Figure 48). There are two

type 2 sequence boundaries located on top of the two high stand systems tract as the above lying is the transgressive systems tract (Figure 48). The GR of this generalized stacking patterns drawn within the figure 48 also.

3.5 Microfacies and Cycles of Garzan Formation within the Studied Wells of Garzan-Germik Oil Field

3.5.1 Microfacies and cycles of the Garzan Formation in Garzan-47

The Garzan deposition in the well starts with Rudist Wackestone facies (2396 m, 2392 m, 2388 m, 2386 m, 2384 m) at the base over the Kıradağ Formation. Then grades into Rotalid Miliolid Wackestone facies is at 2380 m and the Miliolid Wackestone facies overlies the Rotalid Miliolid Wackestone facies at 2378 m (Figure 49). This stacking is named as type A cycle where the back shoal to shoal deposits are overlain by shoal to fore shoal deposits and capped by subtidal environment (Figure 41). As the location of this well is to the south of the reverse fault bordering the Garzan-Germik anticline the base Garzan starts with this type A cycle which is not common in the Garzan Formation deposition in the study area. On above this type A cycle four type B cycles were deposited (Figure 49). Within this type B cycles Rotalid Miliolid

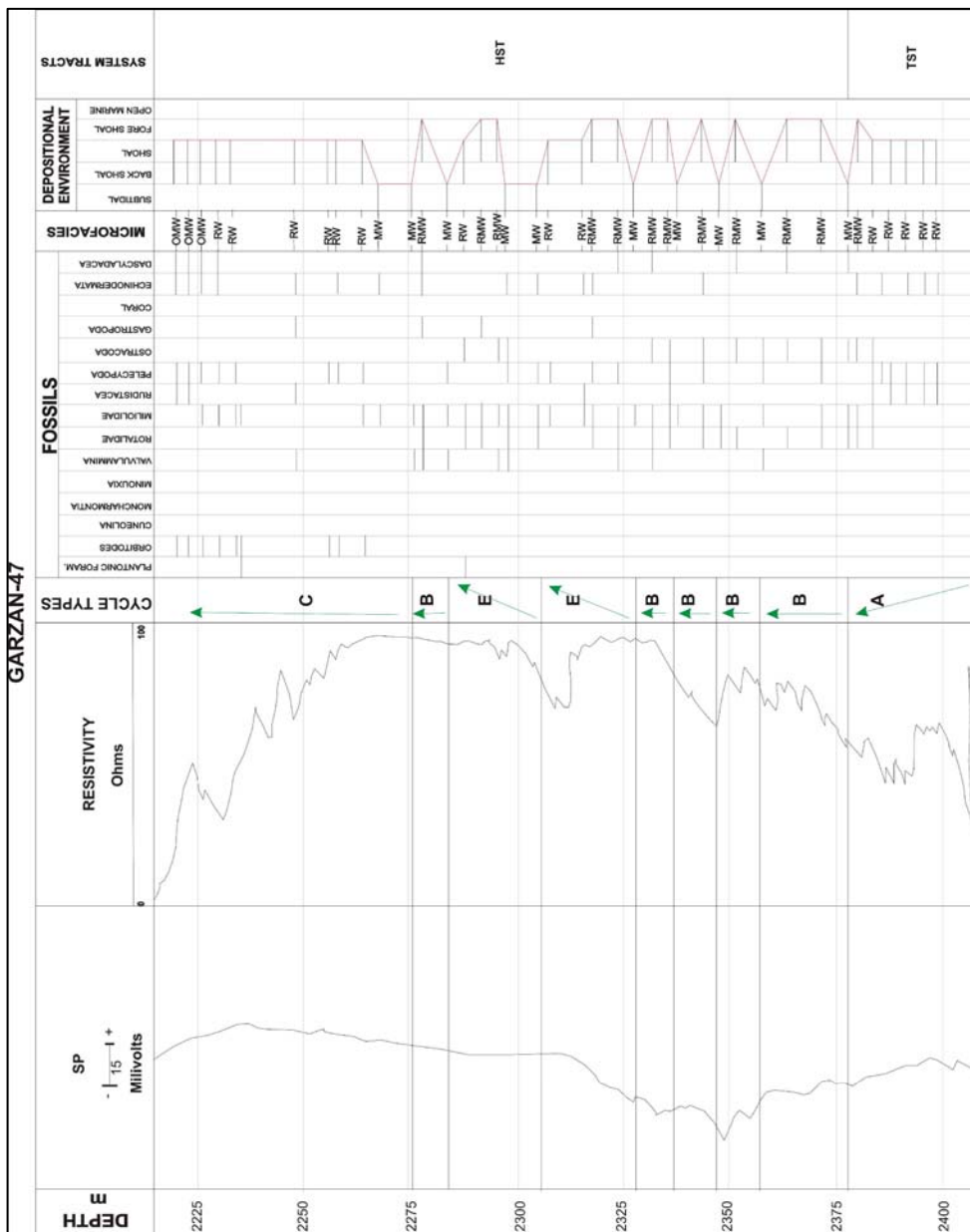


Figure 49: The fossil content, cycles and the depositional environment of the Garzan-47 well (for arrows see figure 41).

Wackestone facies (2372 m, 2364 m, 2352 m, 2344 m, 2336 m, 2332 m) of shoal to fore shoal deposits are capped by Miliolid Wackestone facies (2358 m, 2348 m, 2338 m, 2328 m) of subtidal environment deposits. These type B cycles are aggradational type of cycles deposited in high stand systems tract. Then there are two type E cycles deposited over the type B cycles. The cycles starts with Rotalid Miliolid Wackestone facies (2324 m, 2318 m, 2296 m, 2292 m) of shoal to fore shoal environment and grades into Rudist Wackestone facies (2316 m, 2308 m, 2288 m) of back shoal to shoal environment and capped by Miliolid Wackestone facies (2305 m, 2284 m,) of subtidal environment. The type E cycles are only observed within the high stand systems tract which is located above the transgressive systems tract characterized by type A cycle in Garzan-47 well. This is not common among the other wells. Generally type E cycles are located at the high stand system tract which is at the base Garzan Formation. Then at 2278 m Rotalid Miliolid Wackestone facies is observed and Miliolid Wackestone facies overlies this Rotalid Miliolid Wackestone at 2268 m (Figure 49). This is an aggradational type B cycle represented by shoal to fore shoal environment capped by subtidal environment (Figure 49). The last cycle of the well is type C cycle starting with Rudist Wackestone facies (2264 m, 2258 m, 2256 m, 2248 m, 2240 m, 2234 m) and overlain by Orbitoid Miliolid Wackestone facies (2230 m, 2226 m, 2223 m). Then over Orbitoid Miliolid Wackestone facies at 2219 m. The type C cycle is capped by Miliolid Wackestone facies and the Alt Germav deposition starts.

The aggradational type C cycle which is a deposit of high stand systems tract end the Garzan Formation deposition in this well. This well is an exception to that usually the type D cycle ends up the Garzan Formation deposition. This is due to the location of the well. The Garzan Formation in this well is deposited with in the two sequence boundaries of type 2 of Garzan Formation deposition which are not observed in this well (Figure 48)

3.5.2 Microfacies and Cycles of the Garzan Formation in Germik-21

The Garzan Formation deposition starts with Rotalid Miliolid Wackestone facies (2092 m, 2090 m, 2088 m) overlained by Rudist Wackestone facies (2084 m, 2082 m) and capped by Miliolid Wackestone facies (2080 m). This is a type E cycles. Then this cycle grades into type C cycle starting with Rudist Wackestone facies (2078 m, 2076 m) and capped by Miliolid Wackestone facies (2074 m) (Figure 50). Then above this Orbitoid Miliolid Wackestone facies (2072 m) and Rotalid Miliolid Wackestone facies (2070 m) deposited. The Orbitoid Miliolid Wackestone and Rotalid Miliolid Wackestone faices constitutes the base of type A cycle. At the top of the Garzan Formation in the well there are Orbitoid Miliolid Wackestone facies and Rudist Wackestone facies at 1935 m and 1930 m respectively (Figure 50).

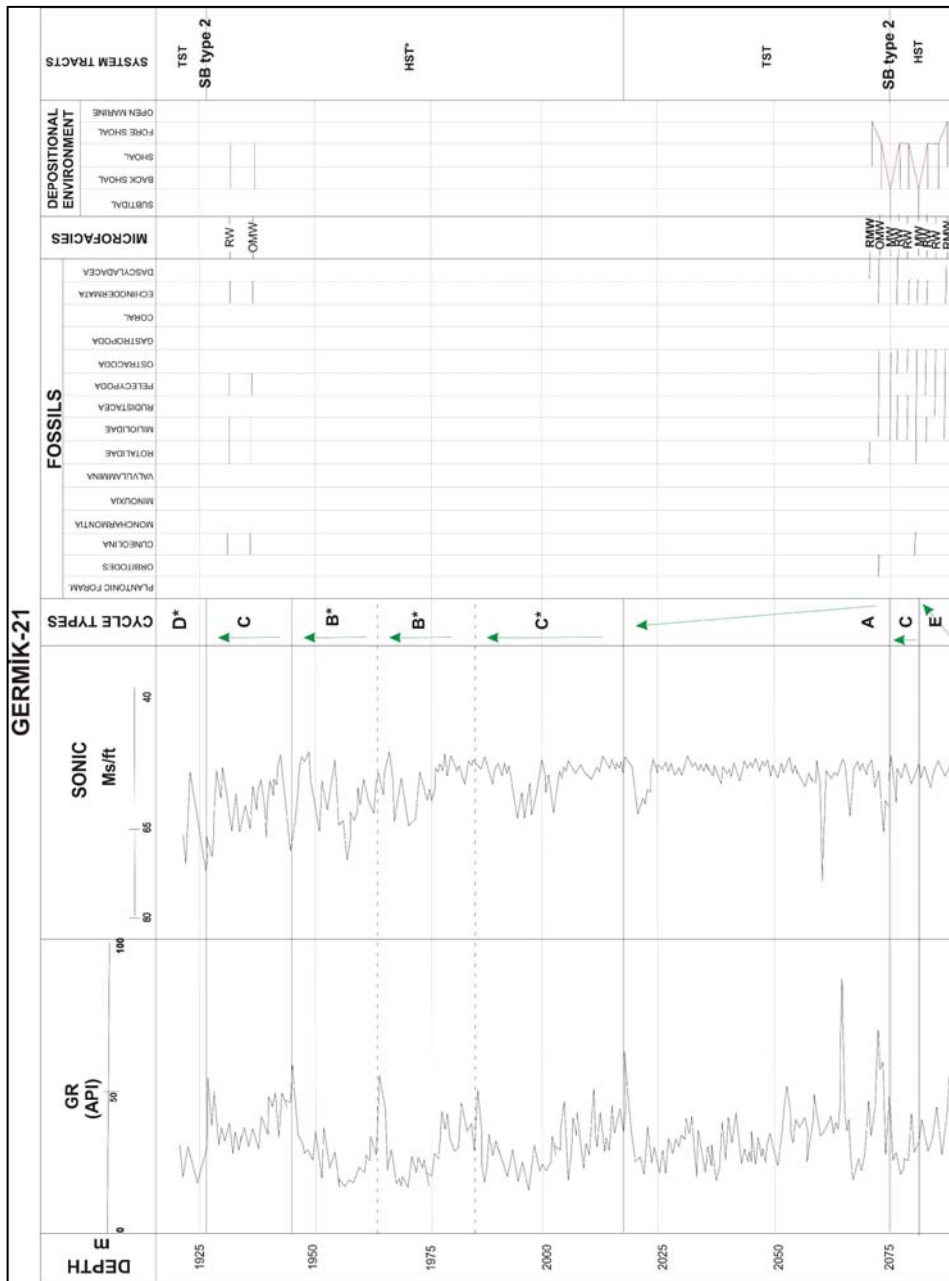


Figure 50: The fossil content, cycles and the depositional environment of the Germik-21 well (for arrows see figure 41) (* means cycles located from log correlation).

3.5.3 Microfacies and Cycles of Garzan Formation in G.Germik-1

The base Garzan Formation deposition starts with type E cycle in which Rotalid Miliolid Wackestone facies (2088 m) is overlain by Rudist Wackestone facies (2086 m, 2084 m) and capped by Miliolid Wackestone facies (2082 m). It is overlain by type C cycle represented by Orbitoid Miliolid Wackestone facies (2076 m) overlain by Miliolid Wackestone facies (2074 m). These cycles are the deposition of high stand systems tract deposits (Figure 51). The next cycle is a type A cycle of transgressive systems tract so that there is a sequence boundary type 2 below type A cycle. The type A cycle is represented by Orbitoid Miliolid Wackestone facies (2072 m, 2068 m) at the base and grades into Rotalid Miliolid Wackestone facies (2064 m, 2060 m) and capped by Miliolid Wackestone facies (2050 m, 2042 m). This type A cycle is overlain by two type C cycles of aggradational type. The first one of these two cycles is characterized by Orbitoid Miliolid Wackestone facies (2030 m) and capped by Miliolid Wackestone facies (2026 m). The second one is characterized by Orbitoid Miliolid Wackestone facies (2018 m, 2014 m, 2010 m, 1986 m) and grades into Rudist Wackestone facies (2004 m, 1994 m, 1990 m) (Figure 51). It is interpreted that in between 1986 m – 1974 m there should be Miliolid Wackestone facies. The above type C cycles there is type D cycle starting with Rotalid Miliolid Wackestone facies (1974 m) and grades into Orbitoid Miliolid Wackestone facies (1932 m) and Pelagic Foraminiferal Mudstone facies (1958 m) caps the cycle and ends the

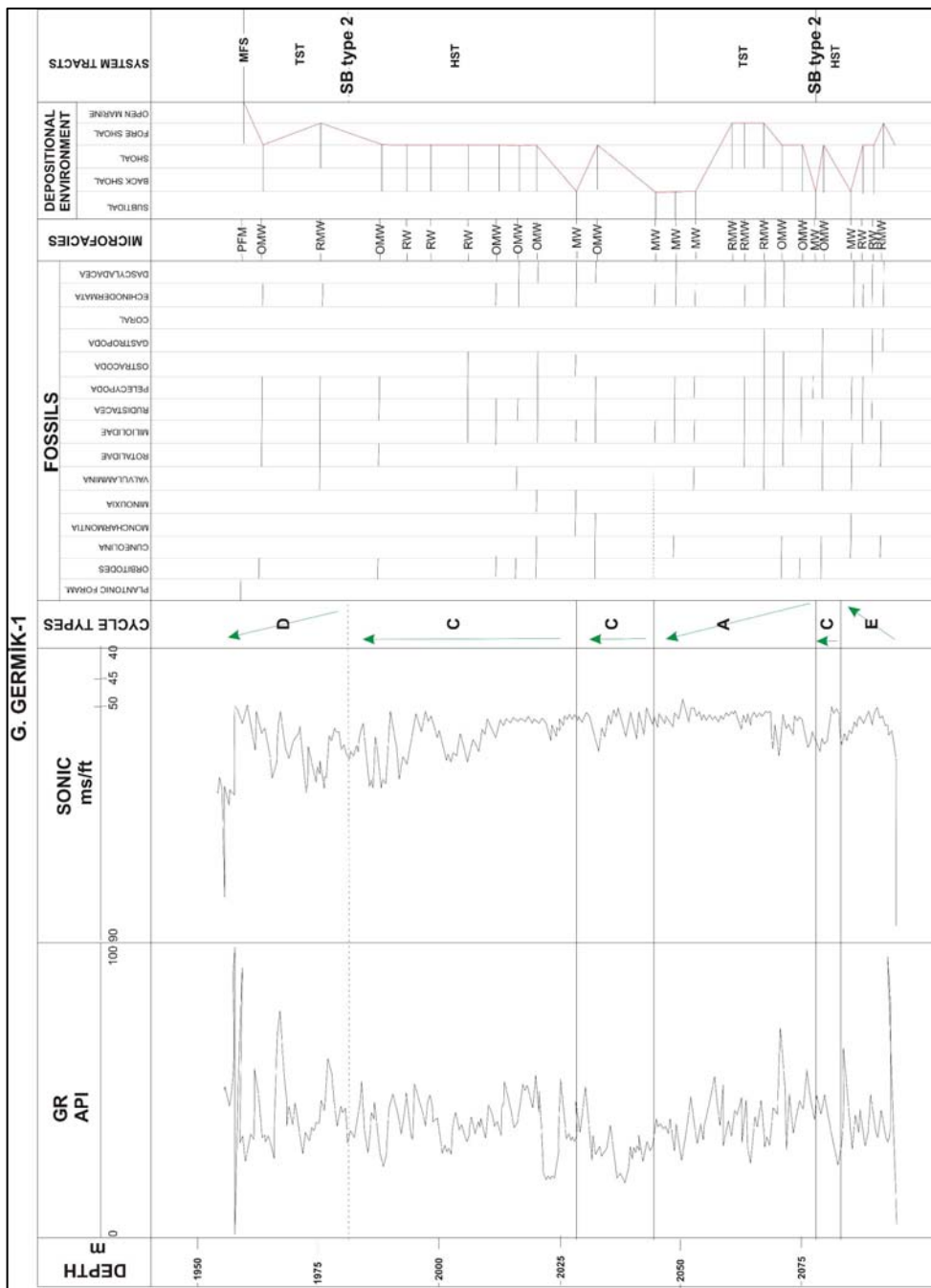


Figure 51: The fossil content, cycles and the depositional environment of the G.Germnik-1 well (for arrows see figure 41).

deposition of Garzan Formation (Figure 51). This Pelagic Foraminiferal Mudstone facies also coincides with the maximum flooding surface. This is because above the Garzan Formation there is the pelagic marls of the Alt Germav Formation. This phase was related to rapidly rising sea levels (Gomez-Perez et. al., 1998). This maximum flooding surface lies within or at the top of the type D cycles. This change is due to the location of the wells within the depositional environment. There is again type 2 sequence boundaries located at the top of high stand systems tract deposits lying below transgressive systems tract deposits (Figure 51).

3.5.4 Microfacies and Cycles of the Garzan Formation in Garzan-82

The base Garzan Formation deposition starts with type C cycle represented by Rudist Wackestone facies (1718 m, 1716 m, 1712 m, 1708 m, 1704 m, 1694 m) and grades into Orbitoid Miliolid Wackestone facies (1700 m) and capped by Miliolid Wackestone facies (1690 m, 1682 m) (Figure 52). The cycle C repeats itself in this well and three of them were stacked on each other in aggradational form representing back shoal to shoal environment (Orbitoid Miliolid Wackestone and / or Rudist Wackestone) capped by subtidal environment (Miliolid Wackestone) (Figure 52). There are two type E cycles deposited over these type C cycles. Both of them are represented by Rotalid Miliolid Wackestone facies of shoal to fore shoal

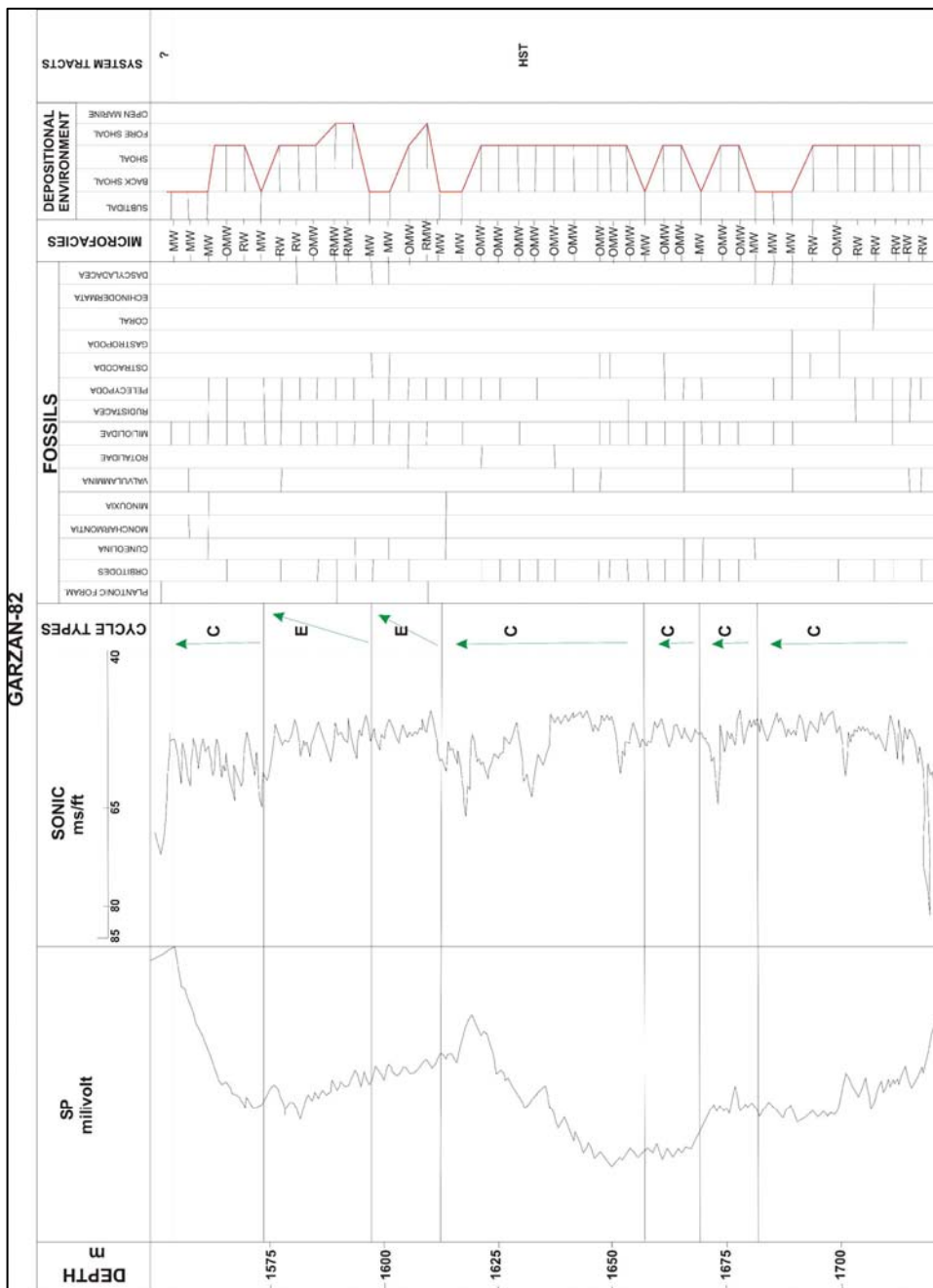


Figure 52: The fossil content, cycles and the depositional environment of the Garzan-82 well (for arrows see figure 41).

environment (1610 m, 1594 m, 1590 m) overlain by back shoal to shoal environment represented by Orbitoid Miliolid Wackestone and Rudist Wackestone facies (1606 m, 1786 m, 1582 m, 1578 m) and capped by Miliolid Wackestone facies (1618 m, 1614 m, 1602 m, 1598 m, 1574 m). The two of the type E cycles are progradational. The top of the Garzan Formation in this well is represented by type C cycle of aggradational type (Figure 52). It is characterized by back shoal to shoal environment deposits (1570 m, 1566 m) and capped by subtidal environment deposits (1562 m – 1554 m).

This well is not characterized by general depositional stacking patterns of the Garzan Formation (Figure 48). This is because of the location of the well in which the conditions prevailed the high stand systems tract deposition during the whole Garzan Formation deposition. The base Garzan Formation starting with type E and C cycles are observed towards the top of this well. This means that up to the first type E cycle the well remained under the aggradational type of conditions and near to the shoal environment. During the deposition of type C cycles below the type E cycles the well could only have a back shoal to shoal environment deposition overlain by subtidal environment. When the sea level rises the subtidal conditions start to control the deposition so that Miliolid Wackestone facies overlies the back shoal to shoal facies. Towards the top of the Garzan Formation in this well type E cycle is overlain by type C cycle, which is usually observed at the base Garzan Formation under the first type 2 sequence boundary. As a result this well is completely deposited during the high stand systems tract (Figure 52).

3.5.5 Microfacies and Cycles of the Garzan Formation in Garzan-23

The base Garzan Formation deposition starts with the type C cycle characterized by Rudist Wackestone facies (1524 m, 1520 m, 1516 m, 1514 m, 1512 m) and Orbitoid Miliolid Wackestone facies (1508 m) of back shoal to shoal environment and capped by Miliolid Wackestone facies (1504 m) of subtidal environment (Figure 53). This is an aggradational type of high stand systems tract deposit. Again Orbitoid Miliolid Wackestone facies (1500 m, 1496 m) overlies this type C cycle. As the GR character is highly correlatable with the ones in G.Germik-1 and G.Germik-2 these two Orbitoid Miliolid Wackestone facies are interpreted as the base of the type A cycle. Towards the upper section Rotalid Miliolid Wackestone facies (1486 m) of shoal to fore shoal is overlain by Orbitoid Miliolid Wackestone facies and Rudist Wackestone facies (1482 m, 1478 m, 1474 m, 1466 m, 1468 m, 1466 m, 1462 m, 1460 m, 1456 m, 1452 m, 1449 m, 1449 m) of back shoal to shoal environment and capped by Pelagic Foraminiferal Mudstone facies (1440 m, 1436 m, 1432 m) (Figure 53). The maximum flooding surface coincides with the Pelagic Foraminiferal Mudstone facies (Figure 53).

This well starts with high stand systems tract deposits characterized by type C cycle and ends up with transgressive systems tract deposits characterized by type A and D cycles. The aggradational high stand systems tract characterized by alternation of type B and C cycles are not observed in this well. Because of this the upper sequence boundary is not observed.

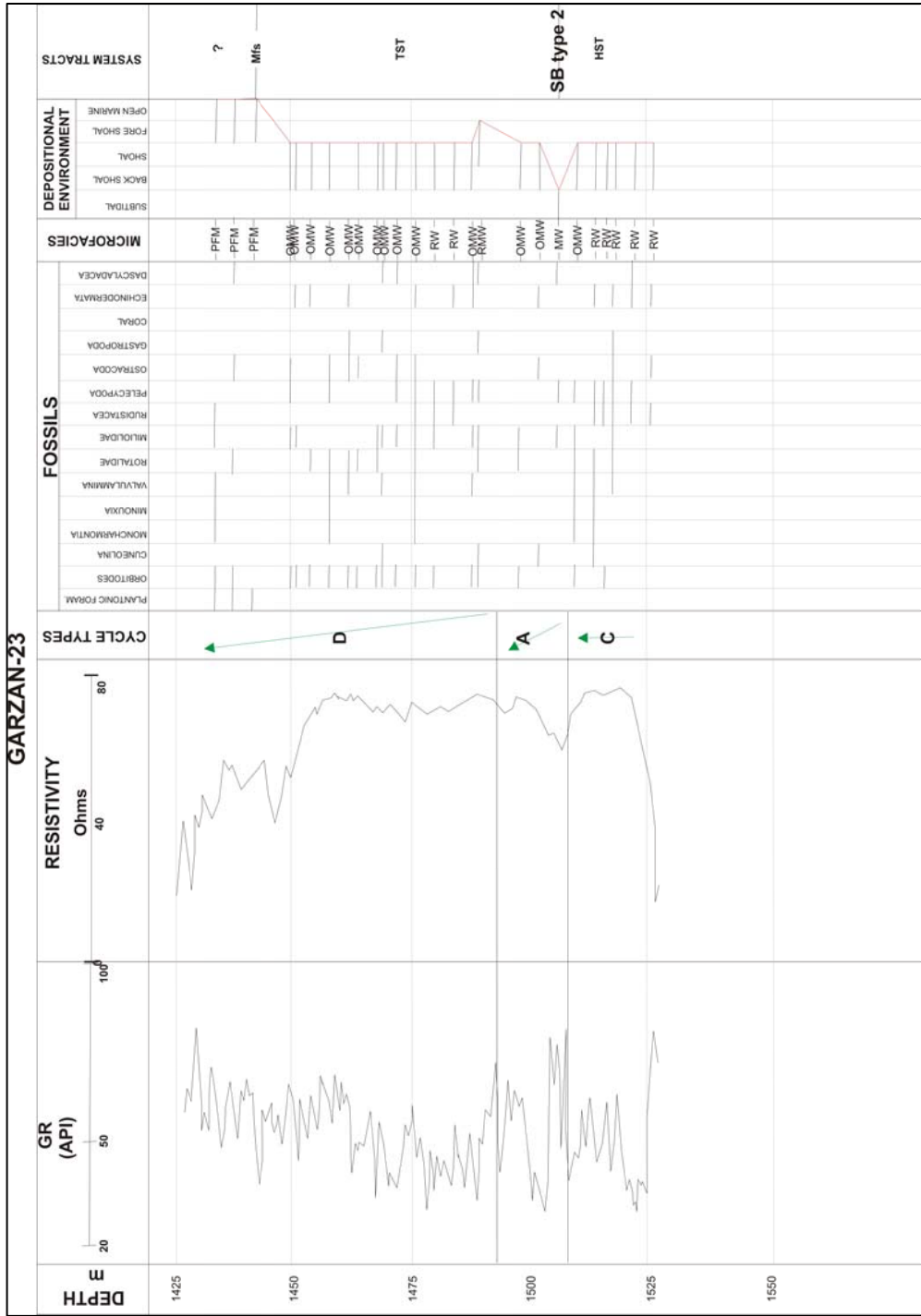


Figure 53: The fossil content, cycles and the depositional environment of the Garzan-23 well (for arrows see figure 41).

3.5.6 Microfacies and Cycles of the Garzan Formation in Germik-6

The microfaices in this starts with Miliolid Wackestone faices (2017 m) and overlain by Rudist Packstone to Grainstone faices (2014 m) and Rudist Wackestone faices of back shoal to shoal (2004 m, 2000 m, 1992 m, 1984 m, 1976 m, 1956 m, 1955 m, 1935 m) (Figure 54). The Orbitoid Miliolid Wackestone faices (1949 m) is observed above Rudist Wackestone faices (Figure 54). This is the well where packstone and grainstone faices is observed (figure 54).

3.5.7 Microfacies and Cycles of the Garzan Formation in Garzan-43

The base of the well starts with Rudist Wackestone faices of back shoal to shoal enviroenmtn at 1696 m. Miliolid Wackestone faices is observed at 1686m and 1682 m deposited in subtidal environment. The Pelagic Foraminiferal Mudstone faices are observed at 1688 m, 1680 m, 1650 m, 1943 m, 1939 m (Figure 55). There are three maximum flooding surface are observed in the well (Figure 55). This well is deposited as type D cycle which is retrogradational during transgressive systems tract. The Garzan Formation in this well is deposited above the upper sequence boundary which is usually located below the type D cycle. This means the area was either dominated

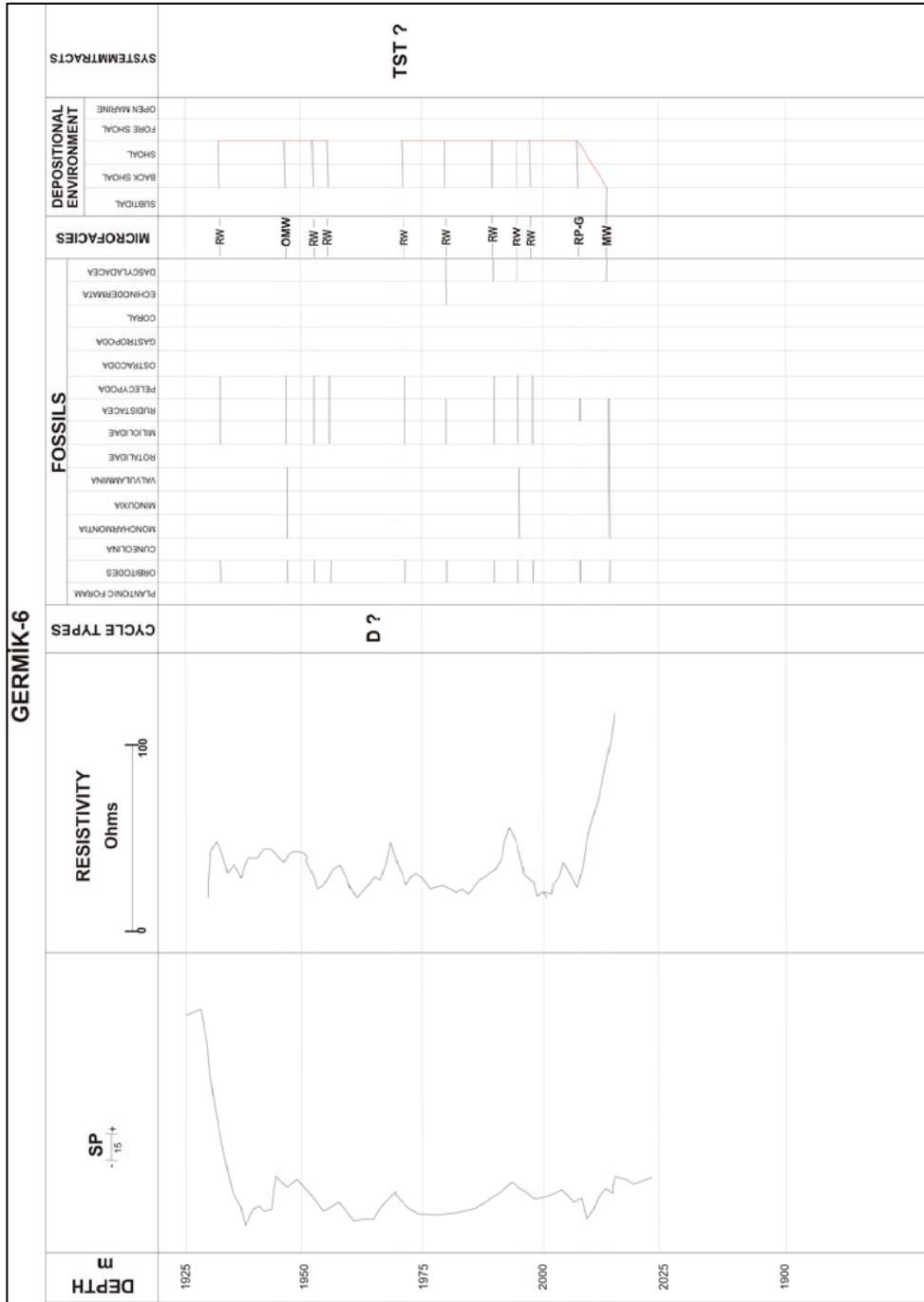


Figure 54: The fossil content, cycles and the depositional environment of the GERMİK-6 well.

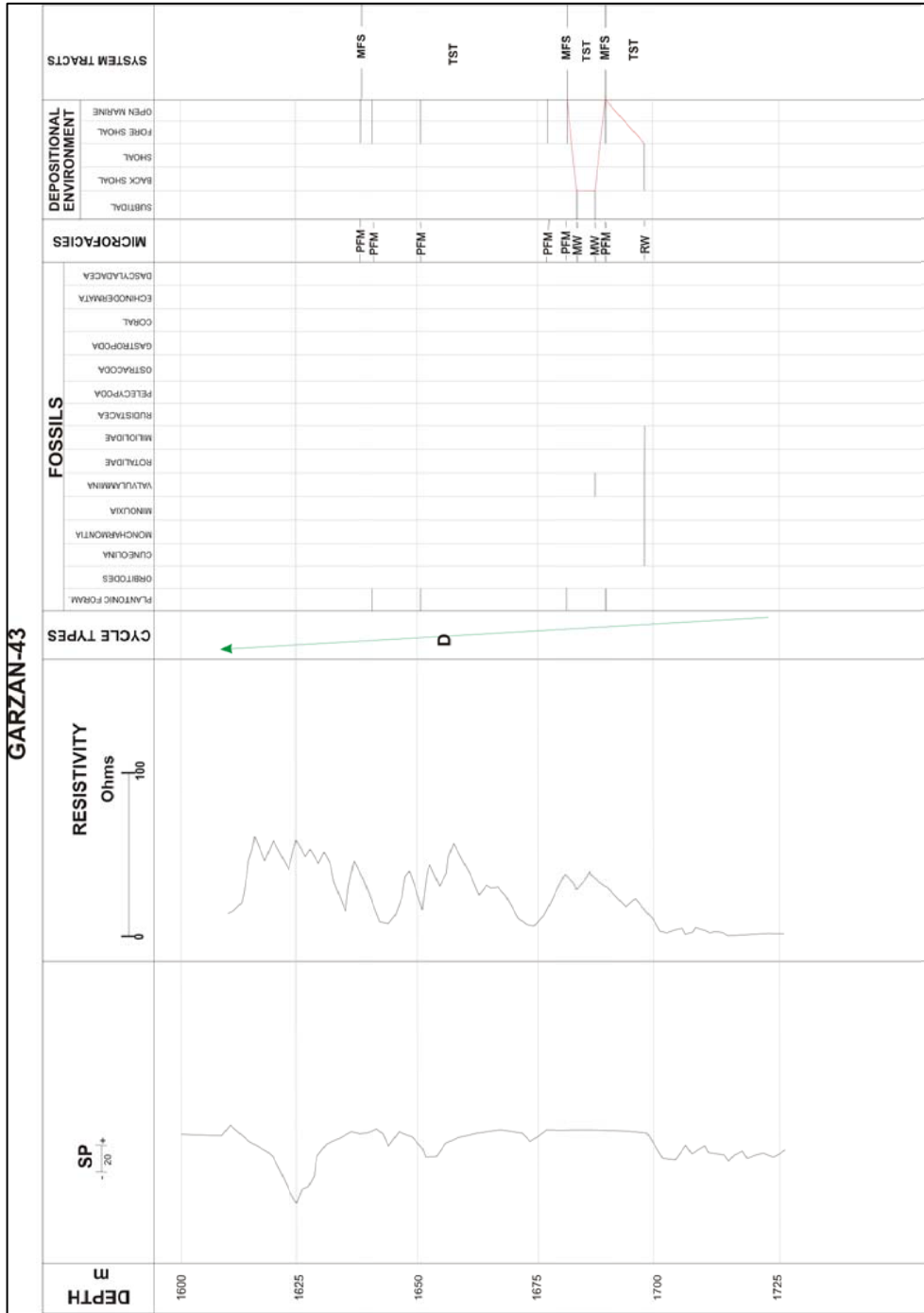


Figure 55: The fossil content, cycles and the depositional environment of the Garzan-43 well (for arrows see figure 41).

by subtidal and open marine environment or could only take deposition during the last transgressive phase during deposition.

3.5.8 Microfacies and Cycles of the Garzan Formation in Garzan-33

The base Garzan Formation deposition starts with Rudist Wackestone facies (1894 m, 1888 m) and Orbitoid Miliolid Wackestone facies (1892 m, 1884 m) of back shoal to shoal environment (Figure 56). The cycle is capped by Miliolid Wackestone facies (1880 m, 1876 m) of subtidal environment. This is an aggradational type C cycle deposited during high stand systems tract. Over type C cycle, Rudist Wackestone facies is observed (1872 m, 1868 m, 1864 m, 1860 m). Rudist Wackestone facies observed here is the beginning of the type A cycle which is a transgressive systems tract deposit (Figure 56). The GR of this level is correlatable with the well G.Germik-1. In between these two cycles, where high stand systems tract is overlain by transgressive systems tract, there is a sequence boundary of type 2.

3.5.9 Microfacies and Cycles of the Garzan Formation in Garzan-31

The well is represented with Orbitoid Miliolid Wackestone facies of back shoal to shoal environment (1634 m, 1632 m, 1606 m, 1544 m, 1540 m, 1506

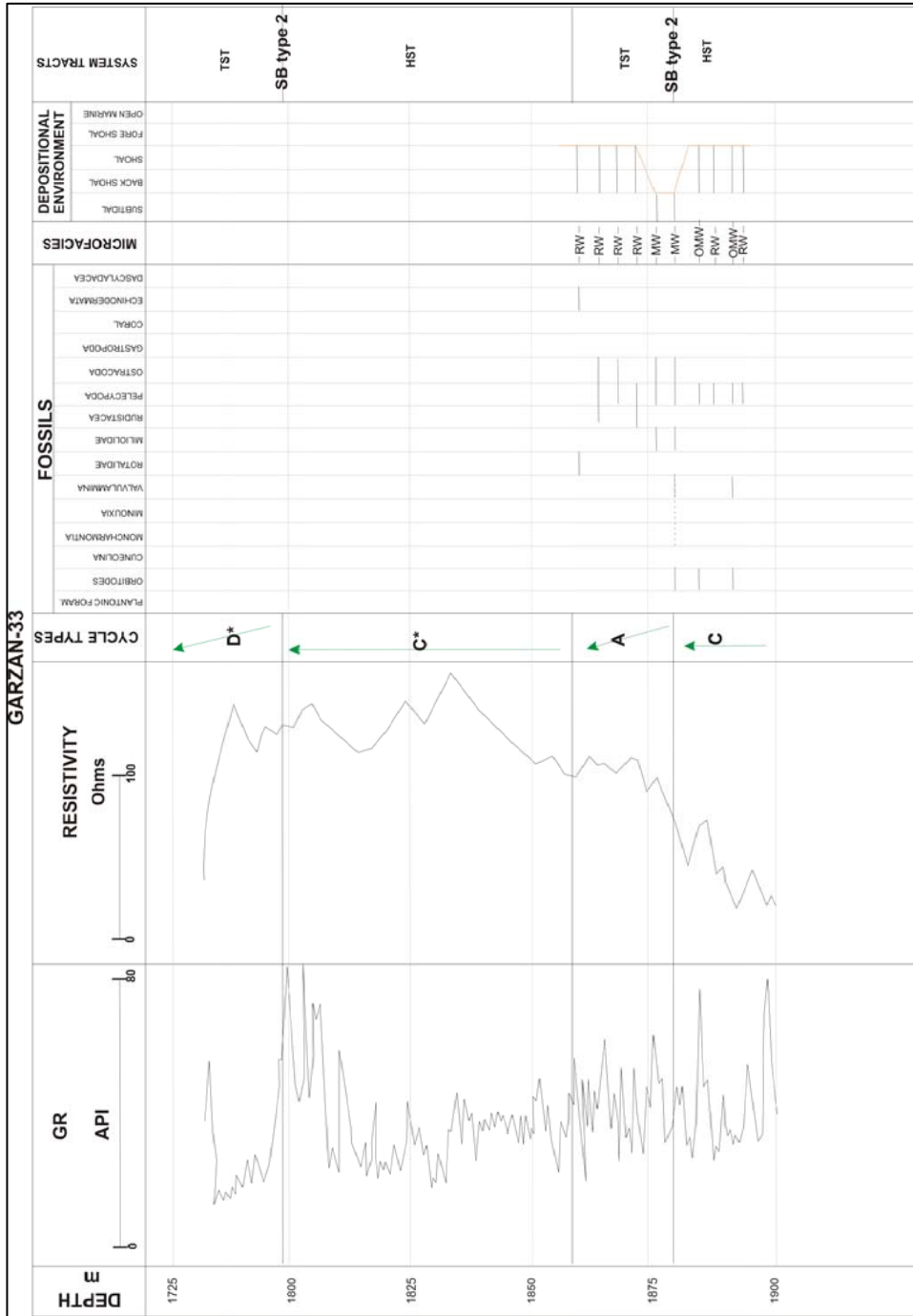


Figure 56: The fossil content, cycles and the depositional environment of the Garzan-33 well (for arrows see figure 41) (* means cycles located from log correlation).

1504 m, 1502 m) and Pelagic Foraminiferal Mudstone facies of fore shoal to open marine environment (1605 m, 1604 m, 1603 m) (Figure 57). The well starts with high stand systems tract overlain by transgressive systems tract deposits. The maximum flooding surface is located within the transgressive systems tract. Garzan-31 well is highly exceptional among the wells in the Garzan-Germik oil field that the maximum flooding surface is located between transgressive systems tract and high stand systems tract (Figure 57). The GR in this well is highly correlatable with G.Germik-2.

3.5.10 Microfacies and Cycles of the Garzan Formation in Germik-3

The well is represented with Orbitoid Miliolid Wackestone facies (2152 m, 2144 m, 2140 m, 1986 m) and Rudist Wackestone facies (1994 m, 1993 m, 1992 m, 1991 m) of back shoal to shoal environment (Figure 58). The Miliolid Wackestone facies of subtidal environment is observed at 1985 m which is located at the top of the Garzan Formation (Figure 58). The Alt Germav marls overlie this subtidal environment deposits. This is because the rising sea level is so effective that the conditions above back shoal to shoal rapidly changes to subtidal conditions and open marine environment. This is also an indication of drowning of Garzan Formation carbonates by Alt Germav marls.

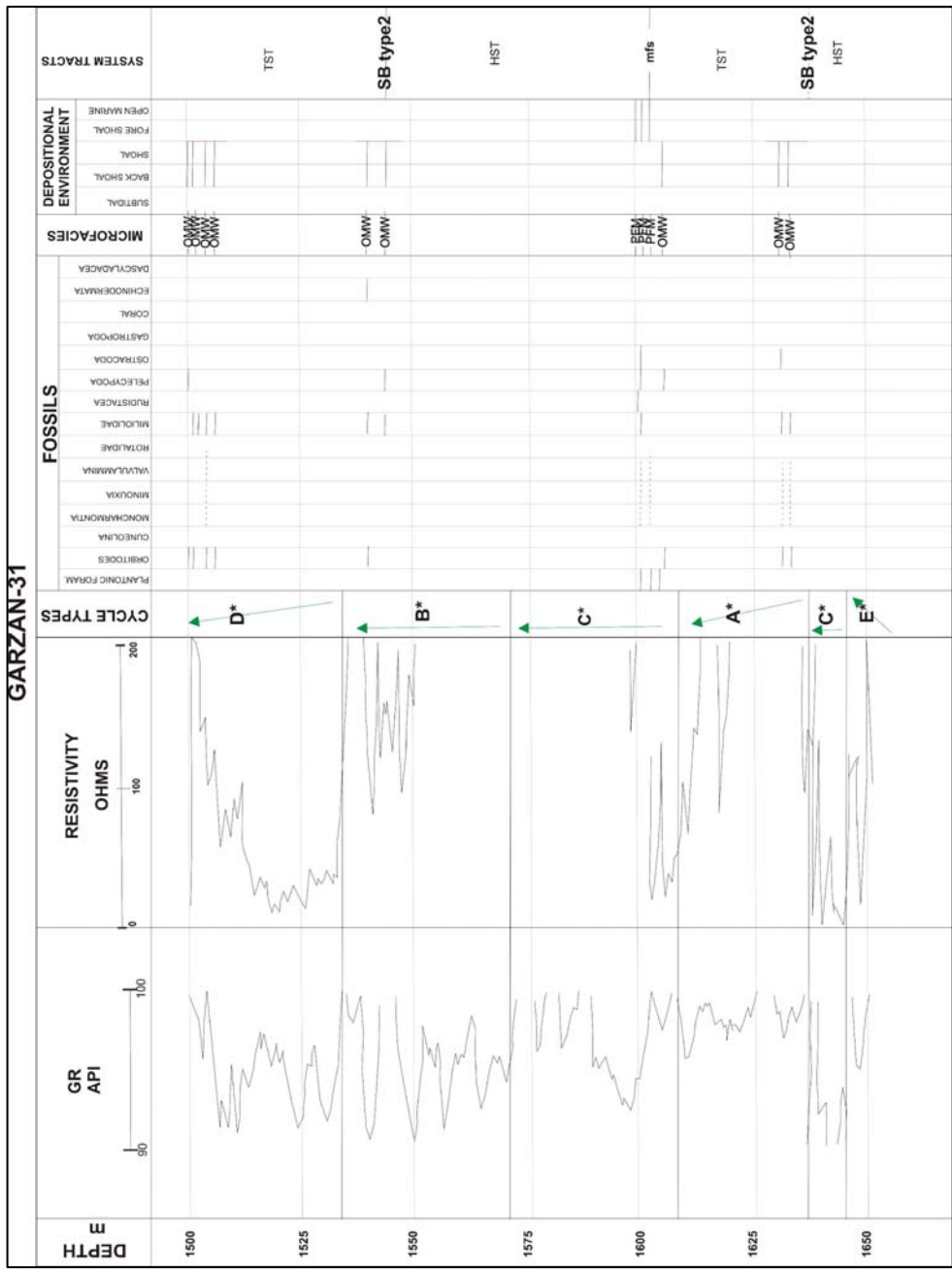


Figure 57: The fossil content, cycles and the depositional environment of the Garzan-31 well (for arrows see figure 41) (* means cycles located from log correlation).

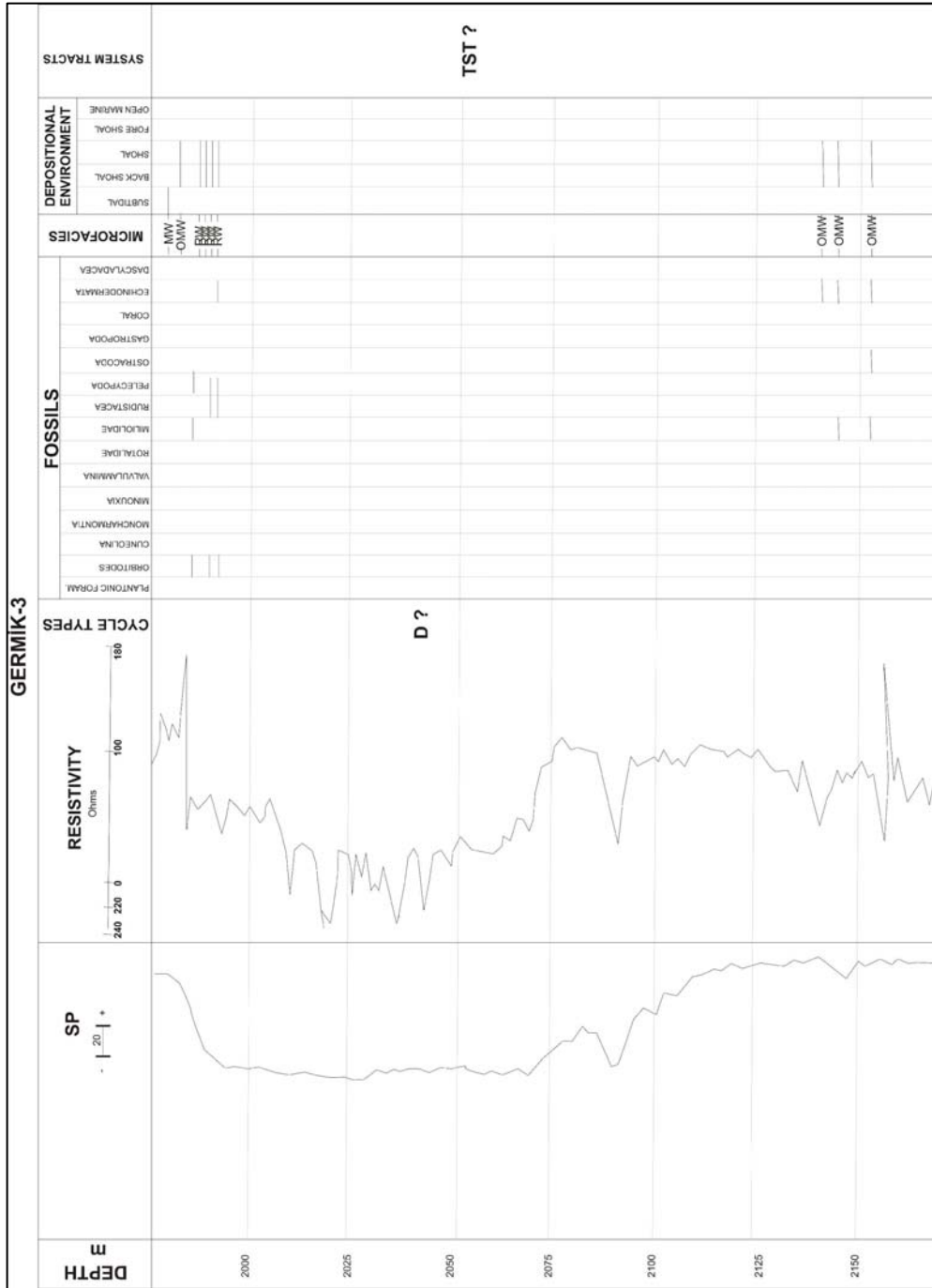


Figure 58: The fossil content, cycles and the depositional environment of the GERMIK-3 well.

CHAPTER 4

CORRELATION OF CYCLES STACKING PATTERNS TO LOG DATA IN THE GARZAN FORMATION

“Carbonates are born not made” James (1992)

“Shallow water carbonates rarely accumulate in a uniform steady fashion”

Shlager (1992)

James (1992) and Shlager (1992) briefly explained carbonates and researchers pain in researching carbonates. Each carbonate is a unique being and like clastics, they cannot be easily uniformitarized and standarized. What ever studied and put forward in a carbonate sequence may not be a model or an example for an other carbonate sequence, even if they are both in the same basin and nearly at the same age. To support this aastrichtian of South East Turkey can be given as an example. During Maastichtian in Southeast Anatolia basin there are nine different lithologies. They are named as Kastel, Bozova, Terbüzek, Kiradağ, Besni, Garzan, Alt Germav, Alt Sinan and Antak Formations (Figure 17). Among them Bozova, Besni, Garzan, Alt

Germav and Alt Sinan are carbonates and each of them represent different depositional geometry and have distinct character. This diversity in the type and facies of the carbonates within the South East Anatolia depends on the environment and geomorphological conditions as expected.

In the subsurface, where data control represents a fraction of a percent of a reservoir volume even in the most densely drilled, logged and cored reservoir, the methodology used to correlate between control points will have an overwhelming influence on the stratigraphic framework and hence all further petrophysical, geostatistical and modeling studies (Kerans and Tinker, 1997). All subsurface geology is largely conceptual and the choice of conceptual models strongly influence the outcome of the stratigraphic interpretation (Kerans and Tinker, 1997).

Sequence stratigraphy places an emphasis on ongoing lithofacies in a time significant context as apposed to a lithostratigraphic context (Kreans and Tinker,1997). The cycles are major building stone of the sequence stratigraphic approach (Mitchum et. al., 1977). In this study cycles and stacking patterns used to make correlations with logs.

This study was carried on thin sections of the drilling cuttings and stacking patterns and cycles were interpreted from them. Although there is lack of core data the system is resolved from these cuttings and emphasis the importance of sampling of cuttings versus core data.

The sequence stratigraphy of outcrop, core and wireline log data was developed in early 1980s with the testing of seismic stratigraphic techniques

against rock data. Converting log properties to lithology does not always provide a unique geological answer. Core data from wells is a good material for sequence stratigraphic analysis, but is rarely acquired in significant quantity (Milton and Emery, 1996). Sequence stratigraphic analysis of wire line log data is neither easy nor unambiguous. Some systems tract boundaries may have a subtle expression on logs and may even be hard to recognize in core and outcrop (Milton and Emery, 1996).

Also fossils have a potential application to sequence stratigraphy. The most useful fossil groups are those which exhibited distinct and rapid morphological change. The useful major fossil groups in sequence stratigraphy depends on depositional environment and the sufficient abundance that their presence is a statistically viable event (Sturrock, 1996). The three most useful groups include; microfossils (foraminifera, ostracods, diatoms, calpionellids, radiolaria, calcereous algae and conodonts), nannofossils (coccoliths and discoasters) and playnomorphs (dinoflagellats, chitinozoa, acritarchs, tasmanitids, pollen and spores) (Sturrock, 1996).

A sequence analysis of a well log suit is concerned with the identification of periods of progradation and retrogradation and the recognition of relative sea level change (Van Wagoner et. al, 1988; Milton and Emery, 1996). This phenomena is carefully done in this study and the progradation, retrogradation and aggradation are tried to be explained by the help of stacking patterns of facies.

In shallow marine settings the cleaning up motif is usually related to an upward transition from shale rich to shale free lithologies owing to an upward increase in depositional energy, upward shallowing and upward coarsening. The dirtying up trends in shallow marine settings often reflects the retreat or abandonment of shoreline shelf system resulting in upward deepening and a decrease in depositional energy. The boxcar trend may represent truncated bases due to a faulting or sharp bases due to falls in relative sea level or other factors. The bow trend is seldom developed in shallow marine setting (Milton and Emery, 1996) (Figure 59). This study revealed that these standard interpretations which are mostly derived from and based on clastic systems are not widely correct for all the carbonate systems. The system in carbonate deposition is unique for each depositional environments and the realm. Since Sarg (1988) introduced the carbonate sequence stratigraphy, many researches were carried on the topic. Each of them comes up with different results for the different carbonates deposited in similar depositional environment.

The transgressive systems tract comprises retrogradational parasequence sets which have an overall deepening upward trend (Armentout et. al., 1991). A fall in relative sea level creates a type 2 or type 1 sequence boundary (Vail et. al., 1977). In this study the Garzan Formation as a whole is a deposit of transgressive systems tract composed of two high stand systems tract and two transgressive systems tract and two type 2 sequence boundaries. There is not any significant fall in relative sea level

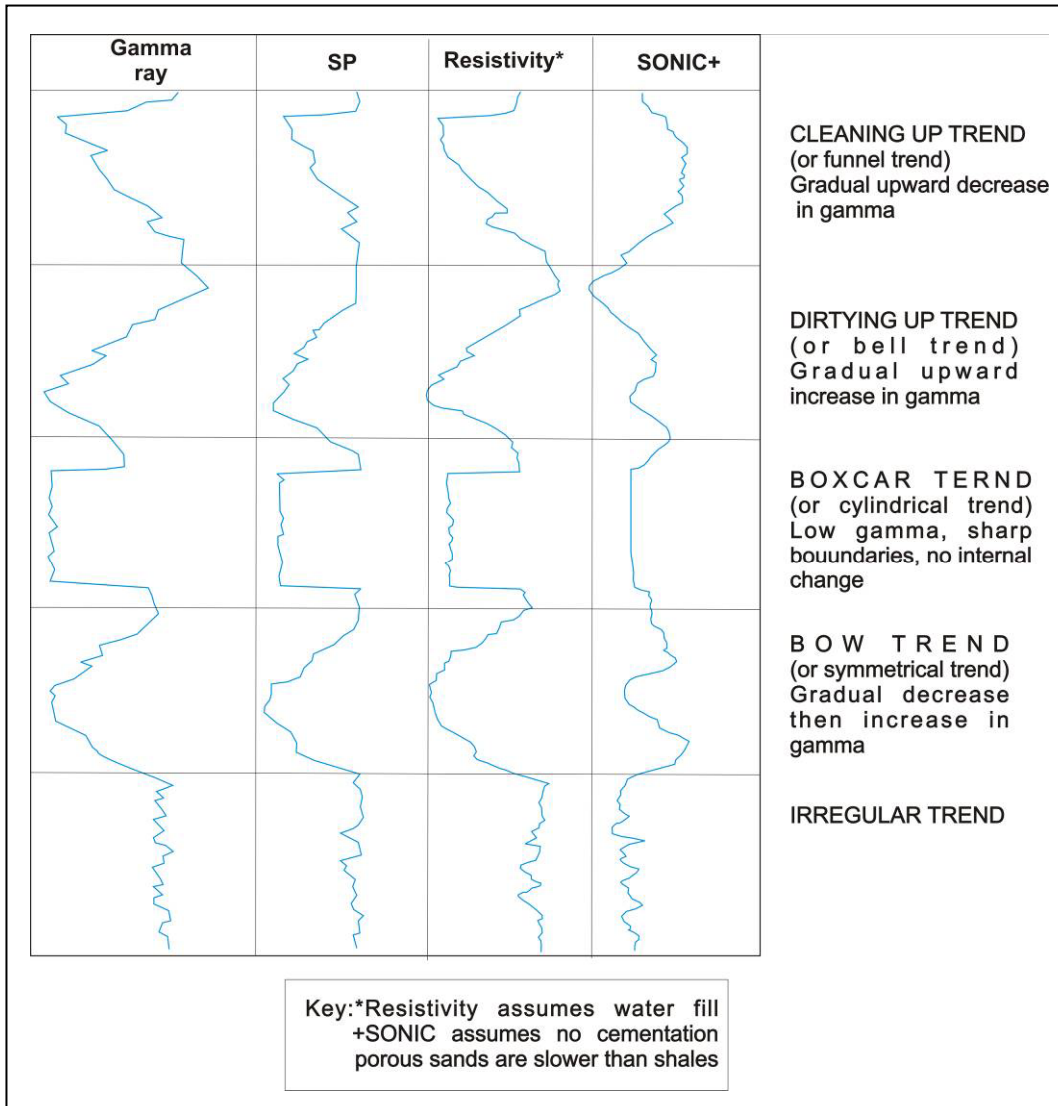


Figure 59: Idealized log trends (Milton and Emery, 1996).

during Garzan Formation deposition: so that an abrupt basinward shift in facies that are shallower and non marine deposits superimpose on deeper marine ones are not observed in this study. Instead there are small oscillations in sea level during Garzan Formation deposition and these two sequence boundaries of type 2 are either 4th or 5th order.

The maximum flooding surface separates the transgressive system tract from highstand system tract and represents the maximum landward extend of marine conditions (Sturrock, 1996). The maximum flooding surface represents the most landward distribution of diverse, open marine, cosmopolitan, often abundant plankton and deep water benthos (Loutit et. al., 1988). In Garzan-23, Garzan-31, Garzan-43 and G. Germik-1 maximum flooding surface are observed. At these levels open marine faices are observed on either subtidal environment characterized by Miliolid Wackestone facies or back shoal to shoal environment characterized by Orbitoid Miliolid Wackestone and / or Rudist Wackestone facies.

Maximum flooding surfaces in well log, core or outcrop data sets are recognized as the boundary between a transgressive unit or retrogradational parasequence set and an overlying regressive unit or progradational parasequence set (Myers and Milton, 1996) (Figure 60). In a proximal direction the maximum flooding surface may be with in an aggradational paraseqeuce set and it passes into a shelf and basinal condensed section in a distal direction. In distal wells the maximum flooding surface clearly overlies a retrogradational parasequence set (Myers and Milton, 1996). In this study

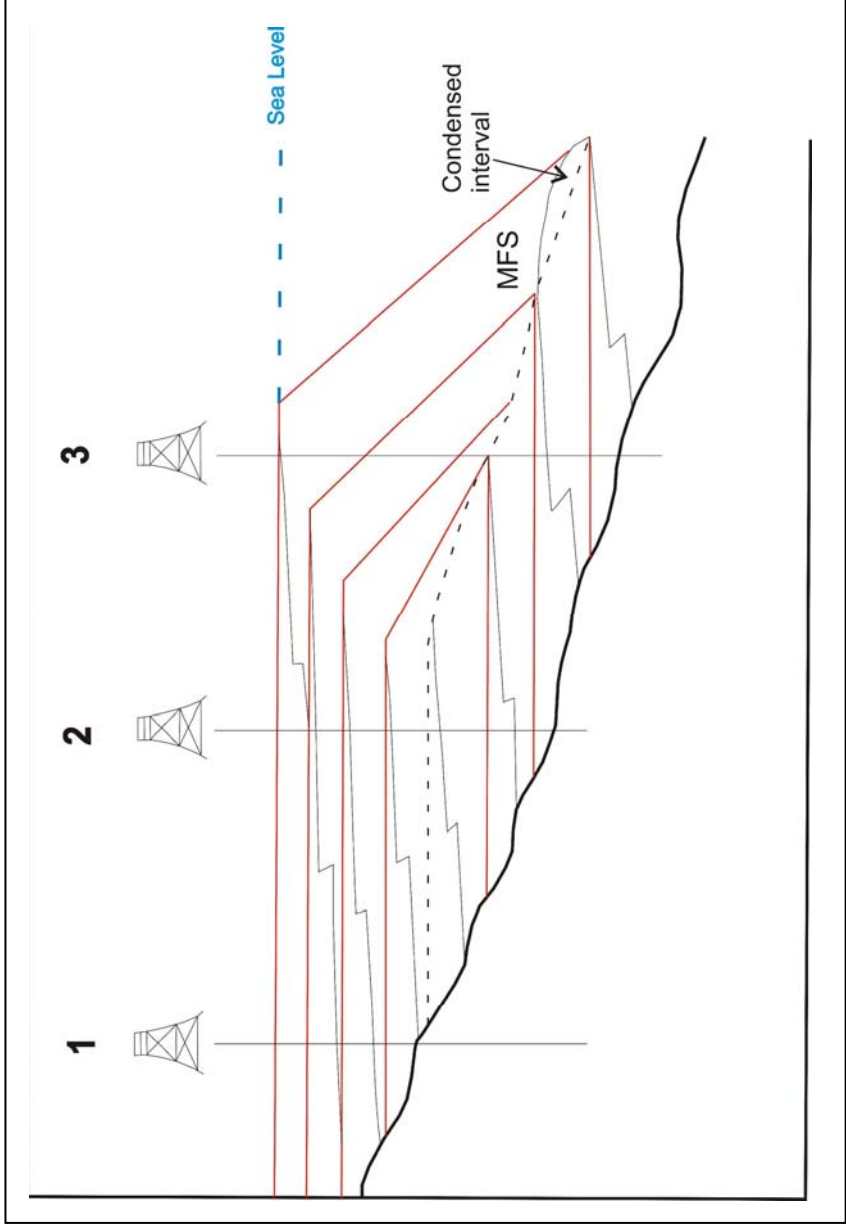


Figure 60: Representation of a maximum flooding surface in well data. (Myers and Milton, 1996)

the maximum flooding surface overlies the retrogradational type A cycle and D cycles in Garzan-23, Garzan-31 and G.Germik-1. Also in Garzan-43 the maximum flooding surface are located within the type D cycle.

Aggrading high stand systems tracts occur when the rate of sediment supply is equal to the amount of accommodation space being created by rising relative sea level (Sturrock, 1996). Progradational highstand systems tract occur when the rate of sediment supply exceeds the amount of accommodation space being created by rising relative sea level (Sturrock, 1996). The type C cycle and B cycles are aggradational deposited during high stand systems tract. They keep up with the sea level rise and sedimentation rate is equal to accommodation space during their deposition. The type E cycle is progradational deposited during high stand systems tract and in that cycle the sediment supply exceeds the sea level rise.

Sedimentological investigations in core and outcrop data within a sequence stratigraphic frame work can improve our knowledge of facies and processes by which the system tracts are deposited. In a core, well log or outcrop data set the downward shift in coastal onlap is rarely evident (Figure 61).

Stacking pattern refers the architecture of a vertical succession of parasequences (Milton and Emery, 1996). There are three types of stacking patterns; progradational, aggradational and retrogradational (Van Wagoner et. al., 1988). In progradational stacking pattern the facies at the top of each parasequence becomes progressively more proximal higher in the

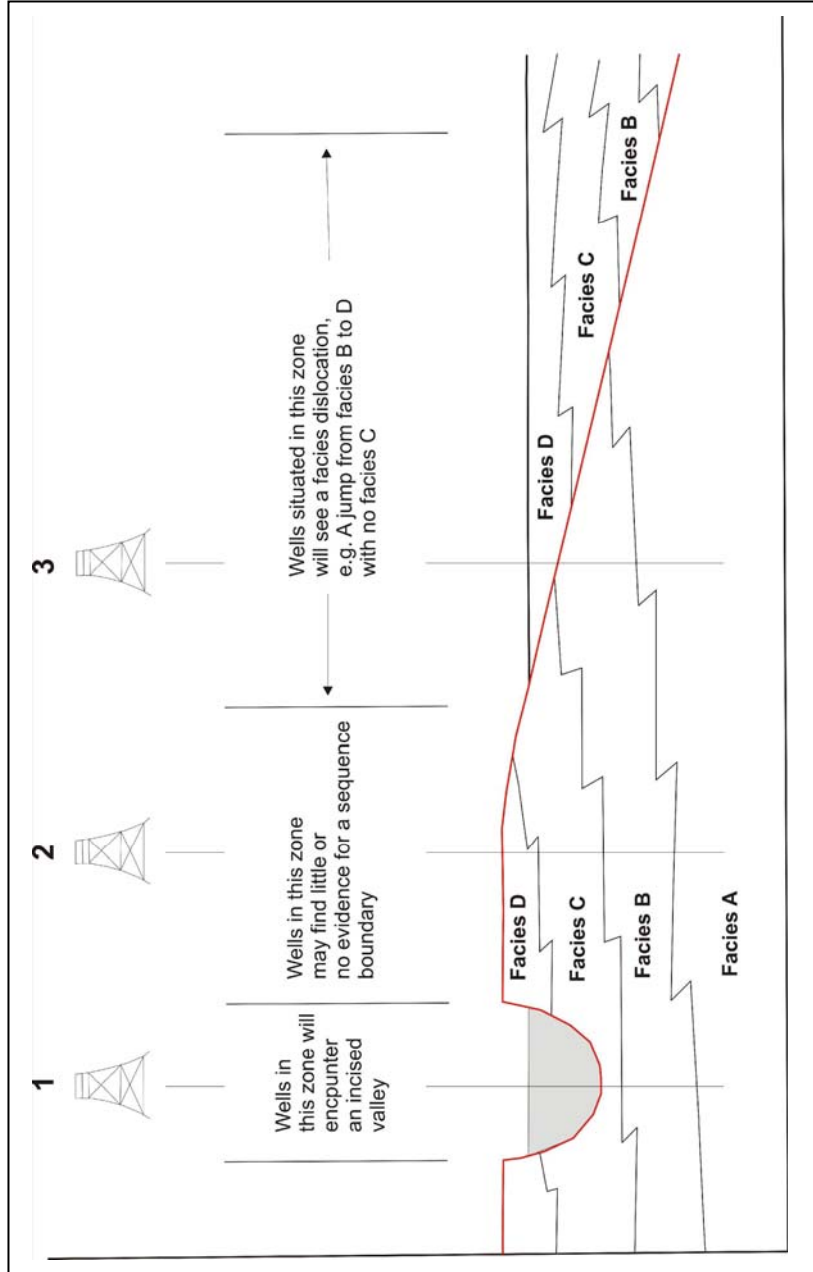


Figure 61: The evidence of presence of sequence boundary (Myers and Milton, 1996).

succession. In a retrogradational stacking, facies become more distal upwards, and in an aggradational stacking the facies at the top of each parasequence is similar (Milton and Emery, 1996) (Figure 60). These stacking patterns can be recognized both in outcrops and in cores (Milton and Emery, 1996). The position of the parasequence with respect to a major stratigraphic surface can help to constrain the systems tract represented by the parasequence architecture. In this study the progradation, aggradational and retrogradational stacking patterns end up with more proximal facies. On the contrary usually type D cycle which is retrogradational, exceptionally, end up with more distal facies.

Geologists usually describe cores and cutting in term of lithology, structure, texture, color, fluid and fossil content. Most of these items can be investigated by log analysts except fossil content and color. Modeling and propagating core descriptions over uncored areas is of prime importance regarding the reservoir understanding of a field. Recognition of sedimentary litho facies is of prime importance when considering the management of uncertainties for geological model of a field (Mathis et. al., 2003). This study aims to use the log response as an indication of a cycles and stacking patterns. The known and described cycles of the Garzan Formation in the Garzan-Germik oil field has a distinctive log character. This distinctive character is gained according to the ingredients of the microfacies, cycles and their stacking patterns.

Identifying lithological and depositional facies is an essential component of petroleum prospecting and reservoir characterization (Saggaf and Nebrija, 2003). Almost every vertical or horizontal well drilled nowadays is logged. Thus identifying facies from wire line logs by correlating their log behavior to that of cored wells becomes a natural way of extending knowledge from cored well, which sparsely cover the field, to logged but uncored wells, which commonly have much more complete coverage of the field (Saggaf and Nebrija, 2003; Dorfman et. al., 1990). This study tries to put a correlation of Garzan Formation facies with log suits of GR, SONIC and Resistivity in wells. These well logs are calibrated with the cycles and their stacking patterns formed from facies studied from drill cuttings (Figure 62).

Geologists have traditionally relied on core data for sedimentological interpretation, but complete coring in all field wells is rare because of high cost, total core recoveries are also rare because of mechanical problems (Dorfman, et. al., 1990). The same problem exists in the Garzan-Germik oil field concerning the Garzan Formation. This problem is solved by studying the thin sections of cuttings.

Cores are rarely available from every well in a reservoir and usually do not cover the entire reservoir interval. Thus the characterization of carbonate textures, fabric, pore types and porosity distribution using well logs in uncored wells provides additional valuable information (Nurmi, et. al., 1990). This study is tired to identify facies from well logs and calibrate these facies by cuttings because of the un available core from the reservoir. The

correlation of electrical imagery with core samples and / or drill cuttings in uncored intervals can help to quantify the porosity fabric and also the geological interpretation of electrical texture and fabrics (Nurmi et. al., 1990).

Log applications solely to identify the composite litho-cyclic nature of the succession require that log sensitivity be greater than the minimum bed thickness (Worthington, 1990).

The generalized GR-SONIC-Resistivity log suit of the Garzan Formation in Garzan-Germik oil field shows four system tracts and two type 2 sequence boundaries (Figure 62). The resistivity logs are used where GR and SONIC are not available. The type E is progradational and the GR values change from relatively low API to high API values. The SONIC does not have any net movement and resistivity changes from high resistant to low resistant values (Figure 62). The type C cycle is an aggradational and there is no net change observed in either GR or SONIC, but resistivity changes from high resistant to low resistant values. Above this type C cycle there is retrogradational type A cycle and GR values in this cycle changes from high to low API values and there is not any net movement in SONIC or resistivity log character. In between type C and A cycle there is a type 2 sequence boundary defined by high API readings in GR and high resistant value in resistivity but SONIC is not affected at this level (Figure 62). Above type A cycle there is alternation of aggradational type C and B cycles in which there is not any net movement in GR, SONIC and resistivity values. The type D cycle which is retrogradational overlies the type C and B cycles alternations.

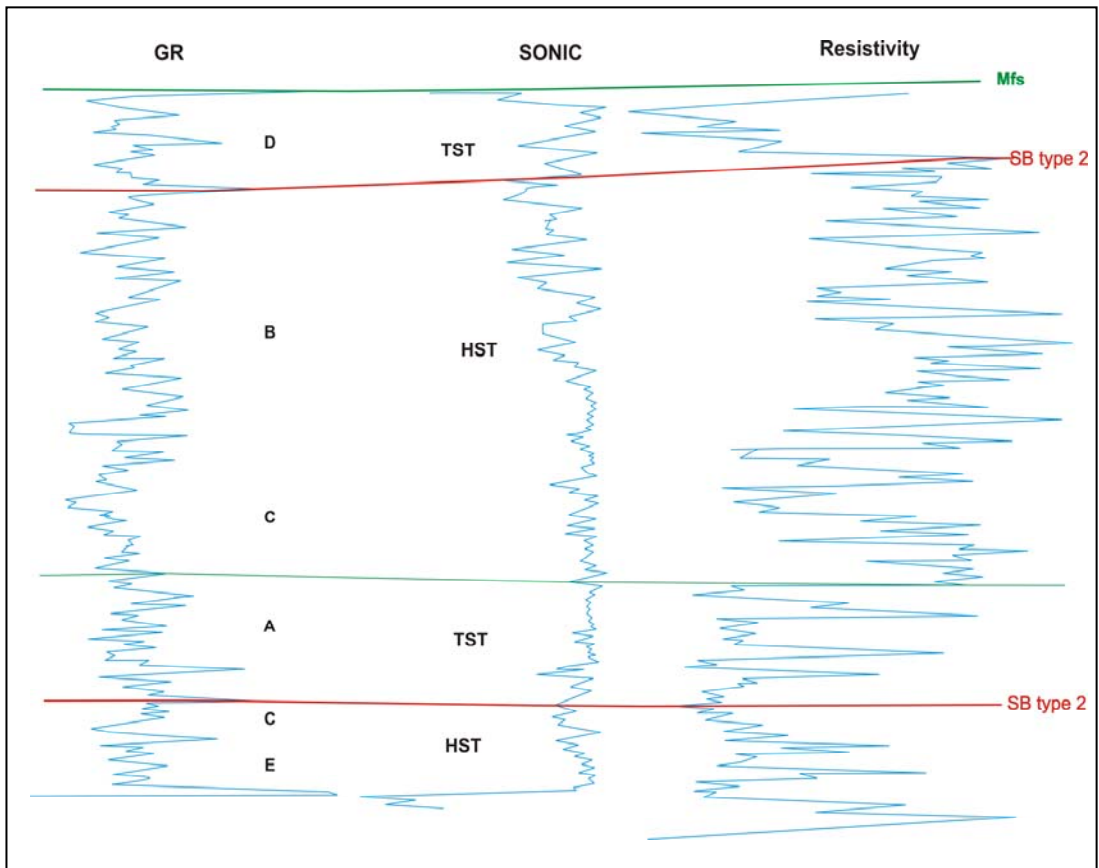


Figure 62: Generalized GR-SONIC-Resistivity log patterns of the Garzan Formation in Garzan-Germik oil field.

Below the type D cycle there is the second sequence boundary of Garzan Formation which is type 2 also. In this type D cycle GR shows net movement from relatively high to low API values and SONIC changes from relatively high velocity to low velocity values and resistivity shows a distinctive shift from high resistant to low resistant values (Figure 62). The upper most of the Garzan Formation is the maximum flooding surface which shifts to high API values in GR and high velocity in SONIC and high resistant values in resistivity (Figure 62). This is to state that the Garzan Formation in Garzan-Germik oil field can be identified into cycles and system tracts by the aid of logs without any facies control (Figure 62).

The different facies within the Garzan Formation are differentiated mainly from the log characters in the previous works (Çoruh et. al., 1997). From the log characters, from bottom to top Garzan Formation is divided in to three members; Zivelikan, Bastokan and Mağrip (Çoruh et. al., 1997). However this differentiation is no longer used today. This study revealed that the log pattern of Garzan Formation in Garzan-Germik oil field can generally be divided into four main parts according to the depositional stacking patterns (Figure 62). The GR correlation from Germik-21, G. Germik-1, G. Germik-2, Garzan-33, Garzan-31 and Garzan-23 revealed that the Garzan-33 and Garzan-31 wells also have stacking patterns of high stand systems tract at the base with type C and E cycles (Figure 63). Then transgressive systems tract deposits overly this high stand system tract deposits and are characterized by type A cycle. This is observed in the G. Germik-1, G.

Germik-2, Germik-21, Garzan-23, Garzan-33, Garzan-31 and Garzan-47 wells (Figure 63, 64 and 65). There is also a type 2 sequence boundary in between these system tracts. Above the type A cycle there is an aggradational type of high stand systems tract deposits also present in the so called wells which is again characterized by alternation of type C and B cycles. This is observed in the G. Germik-1, G. Germik-2, Germik-21, Garzan-23, Garzan-33, Garzan-31 and Garzan-47 wells (Figure 63, 64 and 65). The top Garzan is characterized by type D cycles of transgressive systems tract deposits in G. Germik-1, G. Germik-2, Germik-21, Garzan-23, Garzan-33, Garzan-31 and Garzan-43 wells (Figure 63, 64 and 65). The correlation in the figure 63 is achieved by the cycles to log correlation where thin section data is lacking or not enough such as in Garzan-33, Garzan-31 and G. Germik-2 wells.

The correlation of GR logs of G. Germik-1, Garzan-23 and the Resistivity logs of Garzan-47 and SP log of Garzan-82 revealed that the type 2 sequence boundary exists between the base high stand systems tract and transgressive systems tract deposits as a correlative conformity in Garzan-47 and Garzan-82 wells. This correlative conformity of type 2 sequence boundary is located between Kiradağ and Garzan Formations in Garzan-47 (Figure 64). The correlation from Germik-21, Garzan-33, Garzan-43 and Garzan-82 shows a standart deposition of Garzan Formation between Germik-21 to Garzan-33 (Figure 65). However the whole Garzan Formation in Garzan-43 well is in transgressive systems tract deposits characterized by

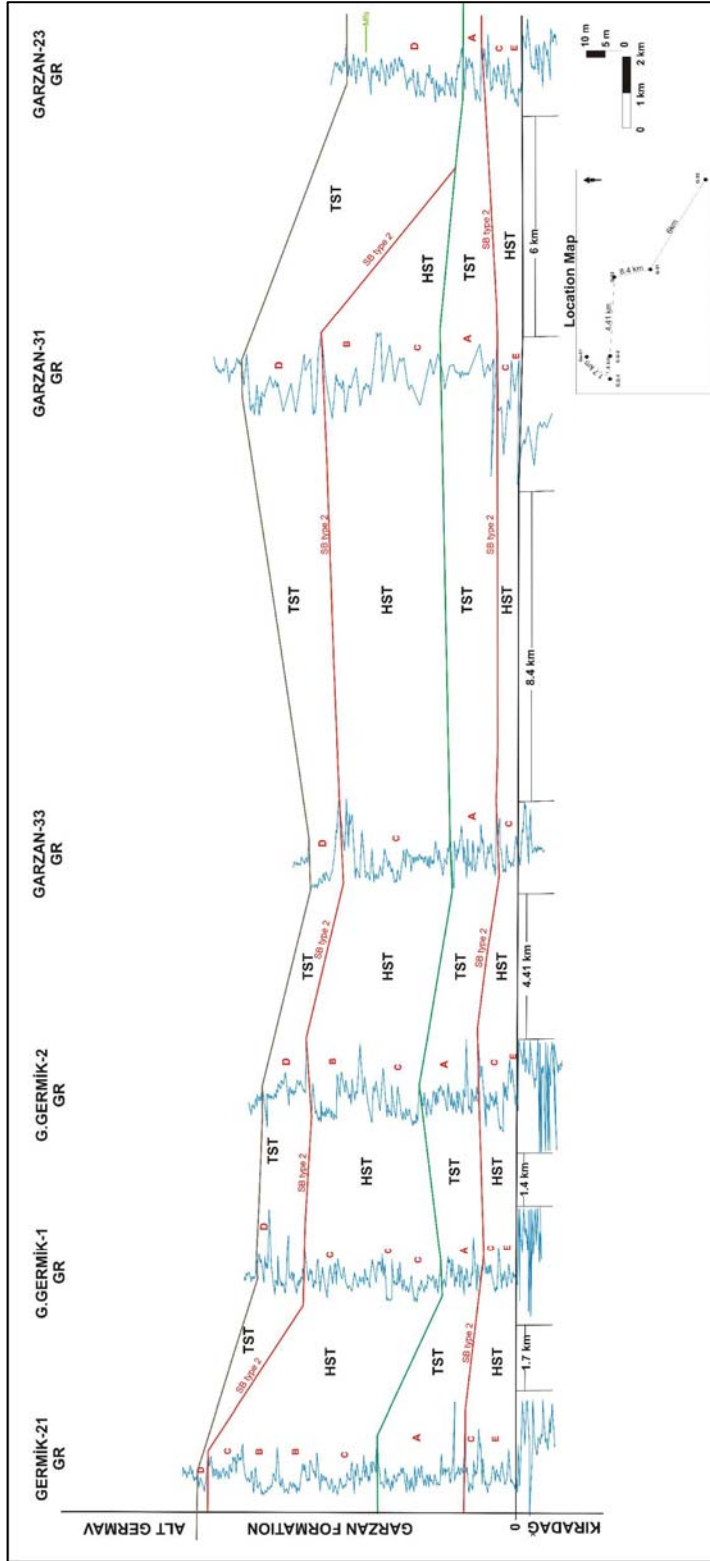


Figure 63: The GR log correlation between Germnik-21, G. Germnik-1, G. Germnik-2, Garzan-33, Garzan-31 and Garzan-23 in the Garzan-Germnik oil field from northwest to southeast.

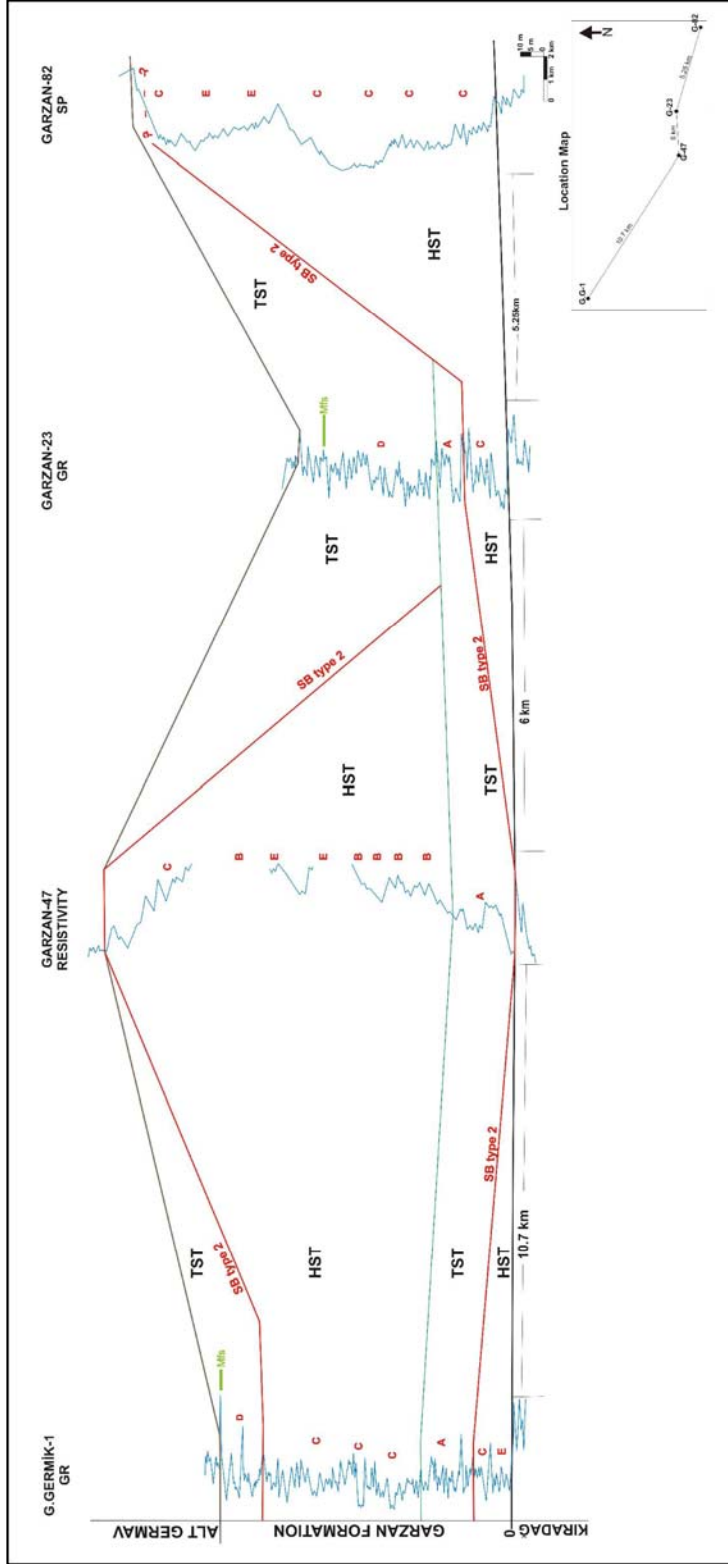


Figure 64: The log correlation between G.Germik-1 (GR), Garzan-47 (Resistivity), Garzan-23 (GR), and Garzan-82 (SP) in the Garzan-Germik oil field from northwest to southeast.

type D cycle. The location of the well in the Garzan-Germik oil field is to the north and did take Garzan Formation sedimentation towards the end period of the Garzan Formation deposition at the last transgressive phase characterized by type D cycle (Figure 65). There are three maximum flooding surfaces in the well. On the contrary Garzan-82 well was in high stand systems tract deposition because of its specific location in the field. The so called location was always at relatively deeper part of the Formations depositional setting. The two type 2 sequence boundary coincides and cut each other at the Garzan-43 well and is located at the onset of Kiradağ to Garzan Formation (Figure 65). The lower sequence boundary is thought to be at the top most of the Garzan-82, but strong evidence for that is not observed (Figure 65).

The correlation of the SONIC log from Germik-21, G. Germik-1, and G.Germik-2 showed the standard depositional stacking patterns of the Garzan Formation (Figure 66). As in GR and also as expected it should be, there are four stacking patterns from base to top as high stand system tract (type C and E cycles), transgressive system tract (type A cycle), high stand system tract (type C and mostly B cycles) and transgressive system tract (type D cycles). There are two sequence boundaries in between high stand system tract and transgressive system tract deposits.

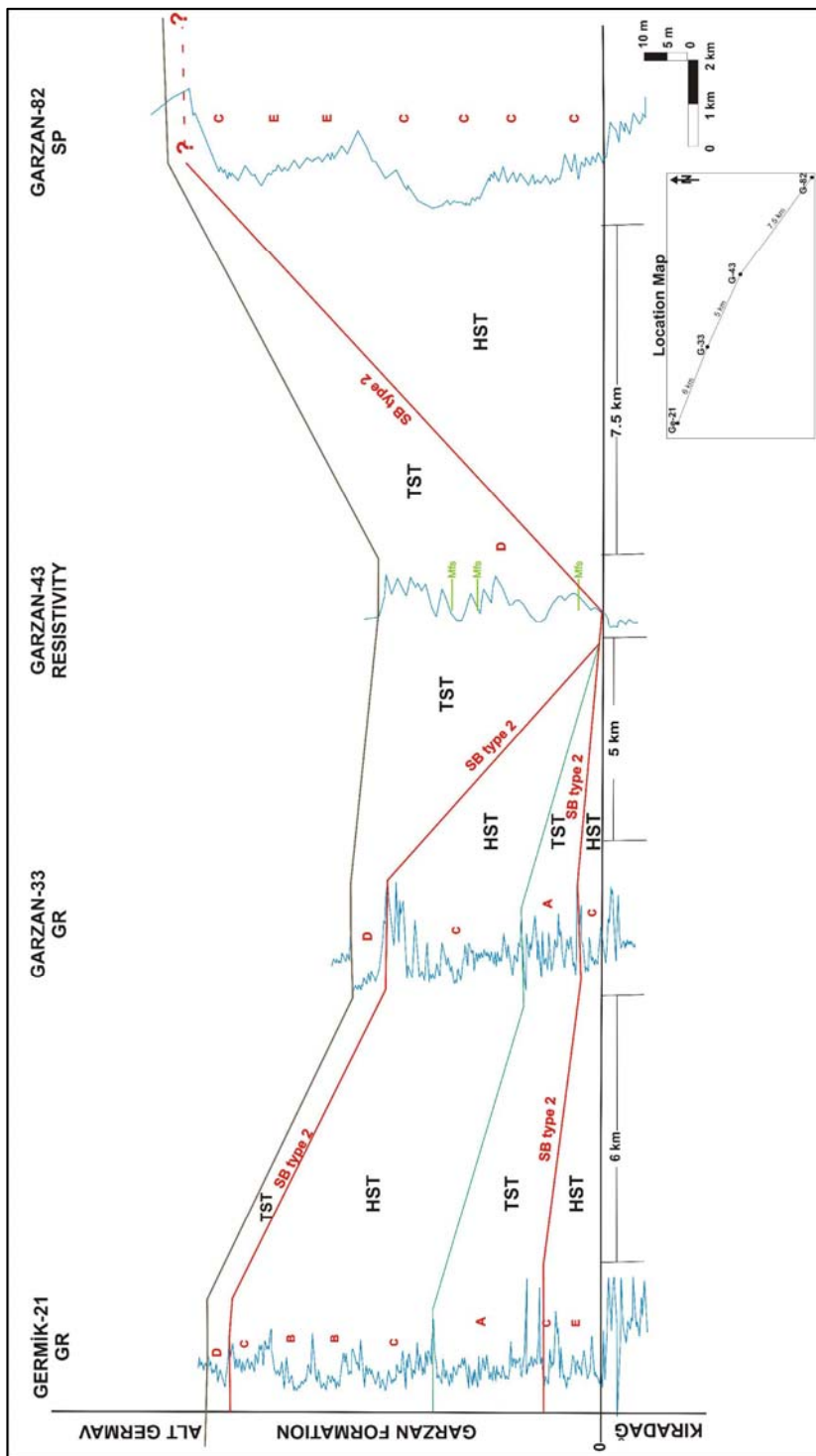


Figure 65: The log correlation from Germik-21 (GR), Garzan-33 (GR), Garzan-43 (Resistivity) and Garzan-82

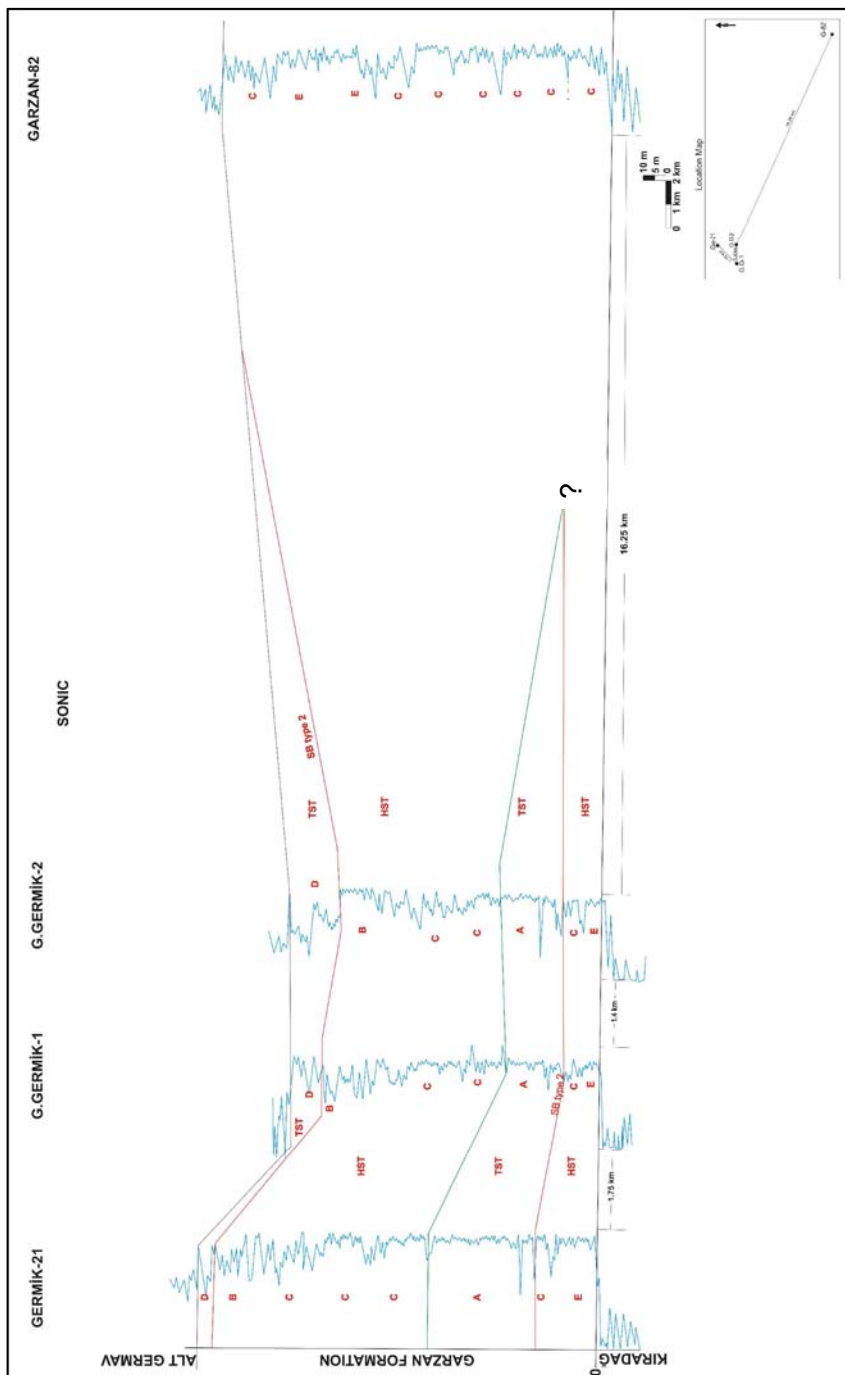


Figure 66: The SONIC log correlation between Germnik-21, G. Germnik-1, G. Germnik-2 and Garzan-82 in the Garzan-Germnik oil field from north-northwest to southeast.

CHAPTER 5

DISCUSSIONS AND CONCLUSIONS

5.1. Discussions and Contributions

The target of this study was to find a direct correlation between log response and the facies of the Garzan Formation. And if this goal was to be achieved the study would have gone further trying to find answer to that if this direct correlation can be used to predict the facies without using the thin sections, so that the method can be applied to anywhere needed concerning the Garzan Formation. The result of the study is achieved and is discussed below.

The high gamma ray reading is interpreted as low energy and smaller grain size and low gamma ray reading means high energy and relatively bigger grain size. According to this, one can interpret that at high gamma ray we are in deeper sea level and in the low gamma ray we are at the relatively shallow water. Also one can add more interpretation to that phrase as when gamma ray reading is decreasing towards up we have a shallowing upward

sequence and the idealized log trend is called “cleaning upward” trend (Figure 59). These are general interpretations, which can be derived from the gamma ray tool. However in this study the result is not exactly as simple as explained above. The Garzan Formation is a carbonate deposited from subtidal to open marine environment so that; in the Garzan Formation in Garzan-Germik oil field those interpretations which are derived automatically from gamma ray reading are not usually the case. In Garzan Formation there are two distinct low energy, relatively deep water carbonate facies; some of them are deposited with in the subtidal (Miliolid Wackestone) and the other one is deposited within the fore shoal to open marine environment (Pelagic Foraminiferal Mudstone) (Figure 45). Also the high energy, relatively shallow water carbonate facies (Orbitoid Miliolid Wackestone, Rudist Wackestone and Rotalid Milolid Wackestone) are deposited with in the shoals and the vicinity (Figure 45). In a theoretical carbonate environment, a cycle representing these environments most frequently will start with subtidal facies and will shallow upward with high energy facies mostly deposited at shoal and the vicinities. In this case the gamma tool will start with high readings representing more micrite and high radioactivity and will grade into low API readings representing more washing out and less radioactivity (Figure 67). This will be a progradational type of parasequence set, which means net basinward movement of the shore line. These types of progradational parasequence sets deposit one over the other then the net observed result will be a regression.

However, one can obtain the same picture explained above by having pelagic deposits such as Pelagic Foraminiferal Mudstone facies of this study overlain by Orbitoid Miliolid Wackestone and / or Rudist Wackestone or Rotalid Miliolid Wackestone representing backshoal, shoal, and foreshoal environment. This sequence of facies again will end up with high GR readings at the base and towards top low GR readings (Figure 67). There is a portion of GR representing a shallowing upward sequence of a carbonate deposit. Within the theory of GR interpretation the energy index is low at the base as the GR is over 70 API in between 0 to 8m depth, which means high content of micrite and clay minerals resulting in high radioactivity due to clay minerals. The depositional environment can be either subtidal or foreshoal to open marine. In order to decide on the environment microfacies analysis is strictly important. If the microfacies observed in this interval is Miliolid Wackestone the environment will be subtidal, and if the microfacies observed in between this interval is Pelagic Foraminiferal Mudstone then the environment considered to be foreshoal to open marine (Figure 67). In between 8 m to 15 m depth interval the GR readings are at 40 API representing relatively high energy environment than the below section. In this case this environment can be backshoal, shoal or foreshoal in which some amount of washing out is expected. As a result of this washing out relatively low radioactivity will be observed as the amount of micrite and/or clay is reduced. The possible facies can be Orbitoid Miliolid Wackestone, Rotalid Miliolid Wackestone and Rudist Wackestone facies (Figure 67).

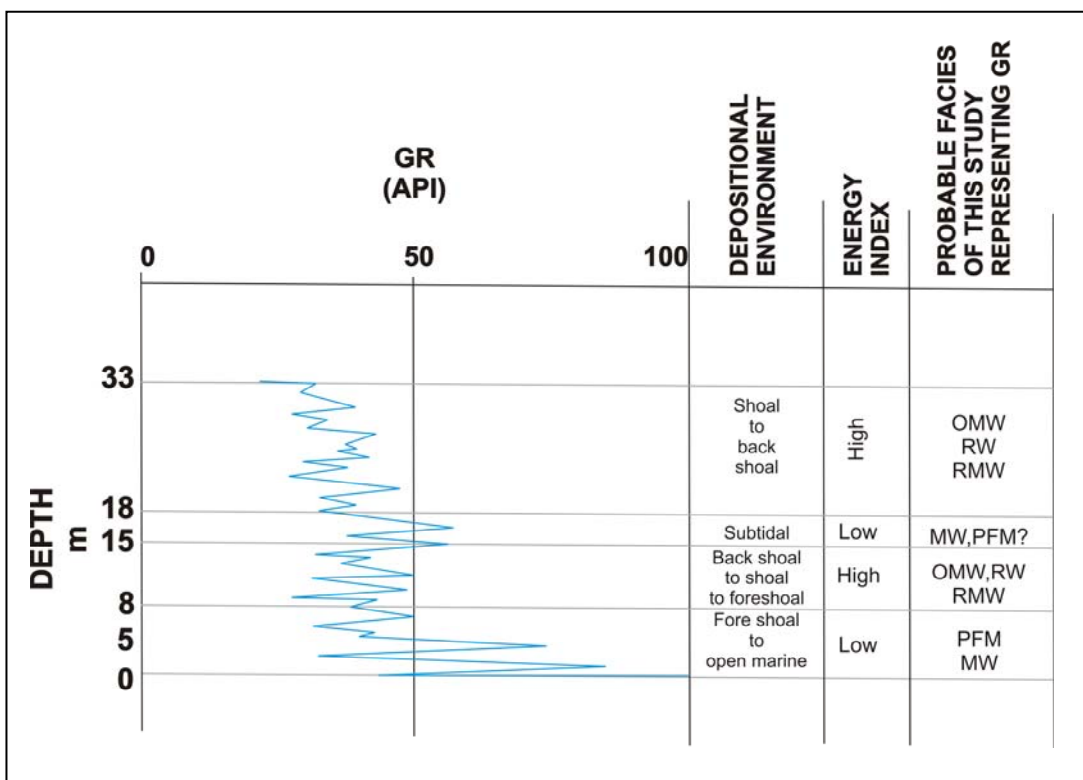


Figure 67: Representative GR readings for the environments. This shows that same type of GR readings indicating different environments.

Above this in between 15 m to 18 m depth interval, the GR reading is at 50 API showing relatively low energy. This may be the result of a smaller deepening which might be represented by subtidal environment. The GR may not reach to high API's because although it is low energy it may not have enough amount of micrite or clay content. From 18 m to 33 m there is again a high energy index and the GR readings are at 30 API. This might be a shoal or backshoal environment (Figure 67).

Nevertheless, this is not the case in this study. In Garzan-Germik oil field the Garzan Formation starts with an increasing trend in GR readings and the base Garzan Formation and it is in high stand system tract deposits of progradational stacking pattern. The top of this progradational stacking pattern is marked by a sequence boundary of type 2 (Vail et. al.,1977). This GR peak coinciding with the type 2 sequence boundary is observed in almost all of the wells (Figure 62). Then the transgressive system tract deposits show a retrogradational type of parasequence set and show a decrease in GR readings. In standart this GR at this transgressive systems tract deposits would shift to higher API values as deeper facies are deposited over shallower facies. A decrease in GR theoretically shows an increase in grain size and indicates a high energy environment. However, in Garzan Formation this indicates a decrease in energy and passing from shoal and vicinity environment to subtidal conditions. The next high stand system tract deposits are aggradational type of parasequence sets and the GR has no net movement towards the either side. This theoretically means that there is no

change in energy index of the environment and grain size of the sediments. However, in Garzan Formation this part is represented by facies deposited at or near shoal complex. They are high energy environment facies and their grain size is greater than the below parasequence set. The top of the formation is represented by a decrease in GR readings (Figure 62). Theoretically this means a grain size and energy increase. However, in Garzan Formation this net movement of the GR is represented by transgressive system tract deposits of retrogradational parasequence sets. The facies representing this environment is usually the fore shoal to open marine facies with very small grain size and high micrite content. There are two highstand and two transgressive phases in the formation separated by two sequence boundaries of type 2 in Garzan deposition.

This phenomena is related with the point where Garzan-Germik oil field stands on the depositional setting of the Garzan Formation. The main reason for this is the transgressive character of the Garzan Formation carbonates on higher order. The point where the Garzan-Germik oil field is deposited stands on subtidal to open marine environment. The geometry of the depositional setting also allows the lower energy facies of wackestone to superimpose on each other. Also the carbonates can retain radioactive minerals (Figure 14).

The correlation of log shape with grain size trend is tenable only under very limited conditions. A universal application of gamma ray log shape to grain size trend and depositional facies is wrong (Rider, 1990). The obvious relation ship is being suggested when low log values indicate a coarse grain

size while high values indicate a fine grain size. This relationship was originally illustrated using the SP by Fans (1969). Later it was extended to include the gamma ray (Serra and Sulpica, 1975; Selley, 1976). The relation to be considered in gamma ray concerns texture, being that between grain size and clay content. There is no doubt that a grain size to clay content correlation exists, but it is by no means that constant relationship required is proposed log shape analysis methodology is to work properly (Rider, 1990).

The stacking patterns of more deeper facies on to shallower ones represents the transgressive phase and the other two high stand systems tract are generally characterized by aggradational type except type E cycle. The cycles are capped by Miliolid Wackestone facies (type A, B, C, and E cycles) and Pelagic Foraminiferal Mudstone facies (type D cycle) because of the rise on sea level is so much that the carbonate production could not keep up and grade into more clay rich facies. In other words subtidal environment enlarges because of rapidly rising sea level. This leads to the domination of muddy cycles in the environment. At the top of the Garzan Formation deposition the rapid rising reached to a maximum level that the open marine conditions start to dominate the deposition. The Alt Germav Formation deposition is a good example for this observable fact.

The deposition of the Garzan Formation is a deepening upward cycle and is deposited during the major transgression of Maastrichtian. If the carbonate factory could not keep pace with the rising sea level and bioherms and limestone units became rapidly drowned and covered by argillaceous

lime mud deposits resulting in deepening upward carbonate sequences (Gomez-Perez et. at., 1998). During high stands, although decelerating rise in sea level led to the establishment of normal marine subtidal conditions (Gomez-Perez et. at., 1998). In rapidly ascending sea level rise in shallow water deposition resulted in deepening upward cycles dominated by the deep water facies. These cycles reflect an increase in accommodation space during the transgressive and high stand systems tract (Gomez-Perez et. at., 1998). During the transgressive systems tract deposition in Garzan Formation the sea level rised so rapidly that Miliolid Wackestone facies of subtidal and Pelagic Foraminiferal Mudstone facies of fore shoal to open marine capes the cycles. Also in high stand systems tract of Garzan Formation in this study the Miliolid Wackestone facies caps the cycles because of increase in accommodation space.

5.2. Results and Conclusions

Considering all the study the results listed below were established:

1. There are five microfacies of Garzan Formation with in Garzan-Germik oil field and they are the representative of five depositional environments. These are; Orbitoid Miliolid Wackestone and Rudist Wackestone of back shoal to shoal , Miliolid Wackestone facies of subtidal, Rotalid Miliolid Wackestone of shoal to fore shoal and

Pelagic Foraminiferal Mudstone of fore shoal to open marine environment.

2. These five microfacies construct five type of cycles named as type A cycle (retrogradational) deposited during transgressive systems tract, type B cycle (aggradational) deposited during high stand systems tract, type C cycle (aggradational) deposited during high stand systems tract, type D cycle (retrogradational) deposited during the upper transgressive systems tract, type E cycle (progradational) deposited during high stand systems tract deposition. there is also the maximum flooding surface located usually at the top of type D cycle which defines the end of the Garzan Formation deposition.
3. These five cycles stack on each other and construct the depositional pattern of the Garzan Formation. The base the Garzan Formation starts with type E and C cycles. Then type A cycle overlies type C cycle and this onset is represented by type 2 sequence boundary as the boundary is between high stand systems tract and transgressive systems tract. Over type A cycle there is an alternation of type B and C cycles and this part of the deposition is an aggradational type of deposition. The top Garzan is defined by type D cycle and maximum flooding surface ends up the Garzan Formation deposition. Below the type D cycle there is the second type 2 sequence boundary as again high stand systems tract deposit are overlain by transgressive systems tract deposit.

4. There are exceptions to the result that the base Garzan Formation is always highstand in character. These are the wells Garzan-47 and Garzan-43. The base Garzan in these wells starts with transgressive system tract deposits and this is because of their geographical location during the Garzan Formation deposition. The Garzan Formation is deposited as highstand character as a whole in Garzan-82.
5. The maximum flooding surfaces are located towards the top of the wells in G. Germik-1, Garzan-23. This is expected as it is the transition from Garzan deposition to Alt Germav deposition. There are 3 maximum flooding surfaces in Garzan-43 well and the whole of the Garzan Formation in the well is represented by type D cycle. The well most probably is located at a relatively deeper part of the basin so that; resulted a deeper facies deposition.
6. The overall Garzan Formation deposition is transgressive and the formation shows deepening upward trend which is deposited during the major transgression of Maastrichtian.
7. The standart GR interpretation is not applicable in most of the carbonates and in the Garzan Formation in Garzan-Germik oil field. In the Garzan Formation deposition a decrease in GR readings indicates a decrease in energy and relatively deepening with domination of deeper facies.. Besides an increase in GR readings indicate an increase in energy and the domination of shallow water

facies. In carbonate depositional environments when GR reading increases in API this should not be interpreted as transgressive cycles without any facies control.

8. The Garzan Formation in Garzan- Germik oil field can be interpreted on the basis of cycles and system tracts without any microfacies control by using the generalized log patterns. This correlation can be carried out whole through the field.
9. The top the Garzan in the well Garzan-23 was given at 1461m. However the thin section study revealed that the top Garzan in this well should be at 1432m.

REFERENCES

Açıkbaş, D., Akgül, A. and Erdoğan, L. T., 1981, Güneydoğu Anadolu'nun hidrokarbon olanakları ve Baykan-Şirvan-Pervari yöresinin jeolojisi, *TPAO Arama Grubu, Rapor no:1543, 347p.*

Aguilera, R.,2004, Integration of geology, petrophysics and reservoir engineering for characterization of carbonate reservoirs through Pickett plots, *American Association of Petroleum Geologists Bulletin, v:88, No:4, p:433-446.*

Ala, M. A. and Moss, B. J., 1979, Comparative petroleum geology of Southeast Turkey and NE Syria, *Journal of Petroleum Geology, v.1, no:4, p.3-27.*

Altiner, D., 1983, Paleoeological distribution of Garzan Formation microfossils, *Huffco Turkey, Inc., Drawing No:481.*

Anderberg, M. R., 1973, Cluster analysis for applications, *New York, Academic Press, 359p.*

Araç, M. ve Yılmaz, E., 1989, X. Bölge Uzunçayır, Habandere-1,3 ve Alıçlı-2 kuyularında Alt Sinan, Garzan Formasyonlarının petrografik incelemesi ve sedimentolojik yorumu, *T.P.A.O. Arama. Grubu Rap. No:2653, 13p.*

Araç, M., 1982, X. Bölge şaryaj önü ve altındaki kuyularda Alt Sinan ve Garzan Formasyonu mikrofasiyes incelemesi, *T.P.A.O. Arama. Grubu Rap. No:268, 48p.*

Araç, M., Erenler, M. ve Yılmaz, Z., 1990, Rıdvan-2 kuyusu Alt Germav, Garzan ve Beloka Formasyonlarının petrografik sedimentolojik ve mikropaleontolojik incelemesi, *T.P.A.O. Arama. Grubu Rap. No:2783, 17p.*

Armentout, J.M., Echols, R.J., and Lee, T.D., 1991, Patterns of foraminiferal abundance and diversity: implications for sequence stratigraphic analysis, in; *Sequence Stratigraphy as an Exploration Tool: Concepts and Practices*, eds; J. M. Armentout and B. F. Perkins, *11th Annual Conference, June 2-5, Texas Gulf Coast Section, Society of Economic Paleontologists and Mineralogists, p.53-58.*

Aroto, H. and Tokano, O., 1995, Significance of sequence stratigraphy in petroleum exploration, *Memoir of Geological Society of Japan, No: 45, p:43-60.*

Bachmann, M. and Kuss, J., 1998, The middle Cretaceous carbonate ramp of northern Sinai: A sequence stratigraphy and facies, Wright, V. P. and Burchette, T.P., in; Carbonate Ramps, *Geological Society of London, Special Publication*, v.149, p.259-280.

Baldwin, J.L., Batenman, M.R. and Wheatly, C.L., 1990, Application of a neural network to the problem of mineral identification from well logs, *The Log Analysts*, v:3, p:279-293.

Baştuğ, C., 1972, X. Bölge Garzan Formasyonu kalınlık haritası ile ilgili ön rapor, *T.P.A.O. Arama. Grubu Rap. No:747*, 3p.

Baştuğ, C., 1973, X. Bölge Garzan Formasyonu bioklastik (Mağrip) üyesi ile ilgili rapor, *T.P.A.O. Arama. Grubu Rap. No:805*, 3p.

Benauda, B., Wadge, G., Whitmarh, R.B., Rothwell, R.G. and MacLead, C., 1999, Inferring the lithology of borehole rocks by applying neural network classifiers to down hole logs- an example from the Ocean Drilling Programme, *Geophysical Journal International*, v:136, p:477-491.

Boroğlu, E., 1983, Silivanak, Mağrip, Oyuktaş ve Garzan arasının jeofizik değerlendirmesi, *T.P.A.O. Arama. Grubu Rap. No:1777*, 21p.

Bush, J. M., Fortney, W. G. And Berry, L. N., 1987, Determination of lithology from well logs by statistical analysis, *Sedimentary Petroleum Engineers Formation Evaluation*, v.2, p.412-418.

Brown, L.F. and Fisher, W. L., 1977, Seismic stratigraphic interpretation of depositional systems: examples from Brazil rift and pull apart basins, eds: C. Payton, *American Association of Petroleum Geologists Memoir 26*, p.213-248.

Brown, J. S., 1943, Suggested use of the word microfacies, *Economical Geology*, v.38, p.325.

Çoban, M. K. ve Kaya, İ. H., 1992, Yemişlik-1,2, Çelikli Sahası arası Üst Sinan, Garzan, Beloka ve Mardin Formasyonlarının rezervuar potansiyelleri, *T.P.A.O. Arama. Grubu Rap. No:3140*, 43p.

Çoruh, T., Yakar, H. and Ediger, V.Ş., 1997, Güneydoğu Anadolu Bölgesi otokton istifin biostratigrafi atlası, *T.P.A.O. Araştırma Merkezi Grubu Başkanlığı, Eğitim Yayınları No:30*, 510s.

Çoşkun, B., 1978, Garzan sahası alt blok petrol imkanları, *T.P.A.O. Arama. Grubu Rap. No:3337*, 3p.

Çubukçu, A. ve Ertürk, O., 1982, X. Bölge sarjay önü ve altındaki Alt Sinan ve Garzan Formasyonları kil minerallerinin incelenmesi, *T.P.A.O. Arama. Grubu Rap. No:1695, 4p.*

Değirmenli, R., Ersoy, R. ve Işık, T., 1989, X. Bölge batı kesiminde Garzan, Alt Sian Formasyonlarının petrol olanakları ve Kastel, Sayındere ve Beloka Formasyonları kalınlık model haritaları, *T.P.A.O. Arama. Grubu Rap. No:2625, 20p.*

Değirmenli, R., Tosunkara, A., Ersoy, R., Işık, T. ve Keskin, E., 1985, Yemişlik, Çelikli sahaları ve yakın civarı Garzan, Beloka Formasyonları yer altı jeolojisi ve hidrokarbon olanakları, *T.P.A.O. Arama. Grubu Rap. No:2125, 280p.*

Delfiner, P., Peyret, O. and Serra, O., 1987, Automatic determination of lithology from well logs, *Sedimentary Petroleum Engineers Formation Evaluation, v.2, p.303-310.*

Dinçer, A., 1991, Güneydoğu Anadolu Otokton Litostratigrafi Birimleri, *Güneydoğu Anadolu Stratigrafi Grubu, TPAO Arama Grubu Rap. No: 2828, ek no:13911.*

Dorfman, M. H., Nevey, J. J. And Coates, G. R., 1990, New techniques in lithofacies determination and permeability prediction in carbonates using well logs, eds; Hurst, A., Lovell, M. A. And Morton, A. C., in; Geological Applications of Wire Line Logs, *Geological Society Special Publication*, v.48, p.113-120.

Dunham, R J., 1962, Classification of carbonate rocks according to depositional texture, in: W.E. Ham, eds: Classification of Carbonate Rocks, A Symposium; *American Association of Petroleum Geologists Memoir 1*, p.108-121.

Duran O., Şemşir, D., Sezgin, İ. ve Perinçek, D., 1989, Güneydoğu Anadolu'da Midyat ve Silvan Gruplarının stratigrafisi, sedimentolojisi ve paleocoğrafyası, paleontolojisi, jeloji tarihi, rezervuar ve diyajenez özellikleri ve olası petrol potansiyeli, *T.P.A.O. Arama. Grubu Rap. No:2563*, 78p.

Duran, O. and Pekcan, İ., 1980, Silivanka-Oyuktaş-Bada-Çelikli, Dodan sahalarındaki Kıradağ ve Beloka (Raman) Formasyonlarının litolojisi ve mikrofasiyes incelemesi, , *T.P.A.O. Araştırma Merkezi Rap. No:349*, 22p.

Duran, O., Şemşir, D., Sezgin, İ. ve Perinçek, D., 1988, Güneydoğu Anadolu'da Midyat ve Silvan Gruplarının stratigrafisi, sedimentolojisi ve petrol potansiyeli, *Türkiye Petrol Jeologları Derneği Bülteni*, v:1, no:2, p.99-126.

Emery, D. and Myers, K.J., 1996, Sequence stratigraphy, *Blackwell Science Ltd., London, 297p.*

Eren, A. A. and Sarı, R., 1984, Güneydoğu Anadolu'da X Bölgenin jeolojik evrimi ve petrol potansiyeli, *TPAO Arama Grubu, Rap. No:1867, 52p.*

Erenler, M., Aköz, Ö., Ertuğ, K., 1992, Tütün-1 kuyusunda kesilen Garzan, Germav ve Üst Sinan Foramsyonlarının paleontolojik incelemesi, *T.P.A.O. Arama. Grubu Rap. No:3052, 16p.*

Eseller, G., 1987, Güneydoğu Türkiye, Garzan Formasyonu Fasiyes Analizi, *Türkiye 7. Petrol Kongresi, p.167-181.*

Fans, L., 1969, Geological applications of well logs, Transactions of the SPWLA, 10th Annual Logging Symposium, Paper AA.

Fisher W. L. and McGovan, J. H., 1967, Depositional systems in the Wilcox Group of Texas and their relationship to occurrence of oil and gas, *Gulf Coast Association of Geological Societies Transactions, v.17, p.213-248.*

Flügel, E., 1978, Microfacies analysis of limestones, *Springer-Verlag, Berlin Heidelberg, 633p.*

Flügel, E., 2004, Microfacies of carbonate rocks, *Springer-Verlag, Berlin, 976p.*

Galloway, W.E. and Hobday, D.K., 1983, Terrigenous clastic depositional systems, Application to petroleum, coal and uranium exploration, *Springer Verlag, New York.*

Gomez-Perez, I., Fernandez-Mendiola, P. A., and Garcia-Mondejar, J., 1998, Constructional dynamics for a Lower Cretaceous carbonate ramp (Corbea Masif, north Iberia), eds; Wright, V. P. and Burchette, T.P., in; Carbonate Ramps, *Geological Society of London, Special Publication, v.149, p.229-252.*

Gürel, M., 1984, Oyuktaş sahası Garzan Formasyonu rezervuar jeolojisi değerlendirme raporu, *T.P.A.O. Arama. Grubu Rap. No:1910, 6p.*

Güven, A., Dinçer, A., Tuna, M. E., Çoruh, T., 1991, Güneydoğu Anadolu Kampaniyen – Paleosen otokton istifin stratigrafisi, *T.P.A.O. Arama. Grubu Rap. No: 2828, 133p.*

Halstead, P. H.,1960, Interim report on the geology of Hilva-Siverek area: Petroleum District VI, Southeast Turkey (AMOSEAS Report), *Petrol İşleri Genel Müdürlüğü Teknik Arşivi, Kutu No:322, Rapor no:6 20p.*

Handford, C. R. and Loucks, R. G., 1993, .carbonate depositional sequences and system tracts- reponses of carbonate platforms to relative sea level changes, eds; Loucks, R. G. and Sarg, J. F, in; Carbonate Sequence Stratigraphy, Recent Events and Applications, *American Association of Petroleum Geologists, Memior 57, p.3-41.*

Hassan, M., 1973, Radioelemensts and diagenesis in shale and carbonate sediments, *SAID 2nd Annual Symposium Transactions, paper.8, p.1-7.*

Hortstink, F., 1971, The Late Cretaceous and Tertiary geological evolution of eastern Turkey, *Proceedings of the 1st Petroleum Congress, p.25-41.*

Horowitz, A.S. and Potter, P. E., 1971, Introductory petrography of fossils, *Springer-Verlag, NewYork, 302p.*

İleez, H. İ. ve Öztümer, E., 1982, Petrol aramalarında petrol sahası sularının jeokimyasal değerlendirmesi ve Garzan Germik sahalarına uygulaması, *T.P.A.O. Arama. Grubu Rap. No:1711, 14p.*

İşbilir, M., 1982, Raman üretim sahasının log verileri ışığında Garzan Formasyonu hidrokarbon olanaklarının araştırılması ve varılan sonuç, *T.P.A.O. Arama. Grubu Rap. No:1728, 13p.*

İztan, H., 1988, Mağrip-18 kuyusunda Garzan, Kıradağ ve Beloka Formasyonları jeokimyasal değerlendirmesi, *T.P.A.O. Arama. Grubu Rap. No:2440, 13p.*

İztan, H., 1989, X. Bölge Garzan Formasyonu jeokimyasal değerlendirmesi, *T.P.A.O. Arama. Grubu Rap. No:2608, 17p.*

James, N.P., 1992, Sedimentology and sequence stratigraphy of reefs and carbonate platforms, *American Association of Petroleum Geologists Continuing Education Course Notes series 34, 71p.*

Kapur, L., Lake, L., Sepehrnoori, K., Herrick, D. and Kalkonery, C., 1998, Facies prediction from core and log data using artificial neural network technology, *Transactions of the 39th Society of Professional Well Log Analysts Annual Symposium, 11p.*

Karandili, Ö., 1991, Papur kuyuları ile çevrili alanda Alt Sinan ve Garzan Formasyonunun petrografik ve rezervuar özellikleri değerlendirmesi, *T.P.A.O. Arama. Grubu Rap. No:2860, 18p..*

Kavukçu, E., 1984, Kurtalan sahası Garzan Formasyonu rezervuar ve üretim jeolojisi değerlendirme raporu, *T.P.A.O. Arama Grubu Rap. No:1869*, 20p.

Kellog, H. E., 1960, Stratigraphic report, Bitlis-Siirt area, Petroleum District V, Southeast Turkey (AMOSEAS Report), *Petrol İşleri Genel Müdürlüğü Teknik Arşivi, Kutu No:150, Rapor No:5*, 52p.

Kellog, H. E., 1961, Regional Stratigraphy and petroleum possibilities of Southeast Turkey (American Overseas Petroleum Report), *Petrol İşleri Genel Müdürlüğü Teknik Arşivi, Kutu No:201, Rapor no:1*, 29p.

Kerans, C. and Tinker, S.W., 1997, Sequence stratigraphy and characterization of carbonate reservoirs, *Society to Economic Petroleum Geologists and Minerologists Short Course Notes No:40*, 130p.

Keskin, C., 1967, Çelikli sahası karbonatlarının mikrofasiyes ve diyajenez incelemesi ön raporu, *T.P.A.O. Arama Grubu Rapor No:422*, 9p.

Keskin, C., 1971, Sedimentary microfacies of the Cretaceous carbonate rock sequence in District V and their importance in stratigraphic correlations, eds: C. Keskin and F. Demirmen, *First Petroleum Congress of Turkey, Proceedings*, p.73-80.

Köylüođlu, M., 1986, Güneydođu Anadolu otokton birimlerin kronostratigrafisi, mikrofasiyes ve mikrofosilleri, *T.P.A.O. Arařtırma Merkezi, Eđitim Yayınları No:9, 53s.*

Loutit, T.S., Hardenbol, J., Vail, P.R. and Baum, G.R., 1988, Condensed sections: the key to age determination and correlation of continental margin sequences, in; *Sea Level Changes – An Integrated Approach*, eds; C.K. Wilgus, B. S. Hastings, C.G. Kendall, H.W. Posamentier, C.A. Ross and J.C. Van Wagoner, *Society to Economic Petroleum Geologists and Minerologists Special Publication No.42, p.183-213.*

Lovelock, P. E. R., 1984, A review of the tectonics of the Northern Middle East Region, *Shell International Petroleum Maatschappij B. V., Exploration and Production Report, 18p.*

Mason, S.L., 1930, Geology of prospective oil territory of Republic of Turkey, *American Association of Petroleum Geologists Bulletin, v:14, No:6, p:687-707.*

Mathis, B., Leduc, J.P. and Vodenabeele, T., 2003, From geologists eyes to synthetic core description: Geological log modeling using well log data, *American Association of Petroleum Geologists Annual Convention, Salt Lake City, Utah, May 11-14,2003.*

Maxson, J. H., 1936, Geology and petroleum possibilities of the Hermis dome, *MTA Derleme No:680, 80p.*

Michelson, O., 1989, Revision of the Jurassic lithostratigraphy of the Danish subbasin, *Geological Society of Denmark, series A, v:24, p:1-21.*

Milton, N.J. and Emery, D., 1996, Outcrop and well data, in; Sequence Stratigraphy, eds; D. Emery and K. Myers, *Blackwell Scientific Ltd. London, p61-79.*

Mitchum, R. M. And Vail, P.R. and Thompson, S., 1977, Seismic stratigraphy and global changes of sea level Part 2: the depositional sequence as a basic unit for stratigraphic analysis, in: Seismic stratigraphy applications to hydrocarbon exploration, eds: C. Payton, *American Association of Petroleum Geologists Memoir 26, p.53-63.*

Mitchum, R.M., Sangree, J.R., Vail, P.R. and Warnardt, W.W.,1993, Recognizing sequences and system tracts from well logs, seismic data and biostratigraphy: Exxamples from the Late Cenozoic of the Gulf of Mexico, in: Siliciclastic Sequence Stratigraphy Recent Developments and Applications, eds: Weimer, P. and Posementier, H.W., *American Association of Petroleum Geologists Memoir 58, p:163-197.*

Myers, K. J. and Milton, N.J., 1996, Concepts and principles of sequence stratigraphy, in; Sequence Stratigraphy, eds; D. Emery and K. Myers, *Blackwell Scientific Ltd. London*, p.11-41.

Namođlu, C., Öncü, H., Aydın, M. ve Can, H., 1997, Dođu Silivanka ve civarı Garzan, Beloka Formasyonları petrol olanakları, *T.P.A.O. Arama. Grubu Rap. No:3803*, 44p.

Naz, H., 1986, X. Bölge Mađrip petrol sahasında maastriyen yaşlı Garzan Formasyonu sedimentolojik, diyajenetik ve rezervuar özellikleri, *T.P.A.O. Arama. Grubu Rap. No:2323*, 35p.

Naz, H., 1987, Mađrip petrol sahasında Garzan Formasyonu'nun sedimentolojik modeli, *Türkiye 7. Petrol Kongresi Jeoloji Bildirileri*, p.182-191.

Nurmi, R., Chararo, M., Waterhouse, M. and Park, R., 1990, Heterogeneties in carbonate reservoirs: detection adn analysis using borehole electrical imagery, eds; Hurst, A., Lovell, M. A. and Morton, A. C., in; Geological Applications of Wireline Logs, *Geological Society Special Publication*, v.48, p.95-113.

Özbahçeci, H. ve Üngör, A., 1988, Garzan-Germik sahalarında Üst Kretase birimlerinin değerlendirilmesi, *T.P.A.O. Arama. Grubu Rap. No:2419*, 11p.

Özdemir, O., 1967, Garzan, Kıradağ Formasyonları sınıflandırması, *T.P.A.O. Arama. Grubu Rap. No:387*, 2p.

Pehlivan, M., 1984, Mağrip sahası Garzan Formasyonu rezervuar jeolojisi değerlendirilmesi, *T.P.A.O. Arama. Grubu Rap. No:2017*, 15p.

Perinçek, D, and Özkaya, I., 1981, Arabistan Levhası kuzeyi kenrainın tektonik evrimi, *Yerbilimleri Dergisi*, v. 8, p.91-101.

Perinçek, D., Günay, Y. And Kozlu, H., 1987, Doğu ve Güneydoğu Anadolu Bölgesindeki yanal atımlı faylar ile ilgili gözlemler, *T.P.A.O. Arama Rap No: 2285*, 47p.

Perinçek, D., 1978, V-VI-IX Bölge (Güneydoğu Anadolu otokton-allokon birimler) jeoloji sembolleri, *T.P.A.O. Arama Grubu Rap. No:657*, 26p.

Perinçek, D., 1980, IX Bölge Hakkari, Yüksekova, Çukurca, Beytüşşebap, Uludere, Pervari dolayının jeolojisi, *T.P.A.O. Arama. Grubu Rap. No:1481*, 80p.

Purdy, C.C., 1982, Enhancement of long spaced sonic transit time data, *SPWLA 23rd Annual Symposium Transactions, Paper V, p:114.*

Rao, C. R., 1973, Linear statistical interference and its applications, *New York, John Wiley and Sons, 625p.*

Rider, M. H., 1996, The geological interpretation of well logs, *Whittles Publishing, 280p.*

Rider, M. H., 1990, Gamma-ray log shape used as a facies indicator: critical analysis of an oversimplified methodology, eds; Hurst, A., Lovell, M. A. and Morton, A. C., in; Geological Applications of Wireline Logs, *Geological Society Special Publication, v.48, p.27-37.*

Rigo de Righi M., and Cortesini, A., 1964, Gravity tectonics in foothills structure belt of Southeast Türkiye, *Associations of Petroleum Geologists Bulletin, v.48, no:12, p.1911-1937.*

Rogers, S.J., Fang, J.H., Karr, C.L. and Stanley, D.A., 1992, Determination of lithology from well logs using a neural network, *Association of Petroleum Geologists Bulletin, v.76, p.731-739.*

Saggaf, M. and Nebrija, Ed. L., 2000, Estimation of lithologies and depositional facies from wire line logs, *American Association of Petroleum Geologists Bulletin*, v.84, no:10, p.1633-1646.

Saggaf, M. and Nebrija, Ed. L., 2003, A fuzzy logic approach for estimation of facies from wire line logs, *Association of Petroleum Geologists Bulletin*, v.84, no:7, p.1223-1240.

Salem, R.; Eren, A., Özbahçeci, H., Araç, M., Öncü, H., İşbilir, M., Üngör, A., Yılmaz, Z., ve Yılmaz, E., 1986, Geologic and hydrocarbon evaluation of Maastrichtian sediments in central district X. Southeast Turkey, *T.P.A.O. Merkezi Rapor no:1009*, 53p.

Sanlav, F., 1972, Exploration for the Garzan limestone Formation petroleum district V., *T.P.A.O. Arama. Grubu Rap. No:750*, 8p.

Sanlav, F., Tolgay, M. and Genca, M., 1963, Geology, geophysics and production history of the Garzan-Germik oil fields, Southeast Turkey, 6th *World Petroleum Congress, Section 1, paper 35*.

Sarg, J. F., 1988, Carbonate sequence stratigraphy, in sea level changes,; An integrated approach, eds: C. K. Wilkus, B. S. Hastings, *Society*

of Economic Paleontologists and Mineralogists, Special Publication, no.42, p.155-181.

Sarı, R., 1984a, Silivanka-Oyuktaş, Mağrip, Garzan arasındaki bölgede Garzan Formasyonu için loglardan yapılan korelasyonlar ve neticeleri, *T.P.A.O. Arama. Grubu Rap. No:1964, 9p.*

Sarı, R., 1984b, Silivanka ve Beyçayır sahalarında Beloka ve Garzan formasyonlarının incelenmesi ve petrol olanakları, *T.P.A.O. Arama Grubu Rap. No:1991, 29p.*

Sarı, R., 1986, X. Bölge Garzan Formasyonu fasiyesi üzerine ön inceleme, *T.P.A.O. Arama. Grubu Rap. No:2156, 9p.*

Sarı, R., Yoğurtçuoğlu, A. ve Yücesoy, A., 1979, Sezgin sahası ve yöresinde Garzan Formasyonu log uygulamaları, *T.P.A.O. Arama. Grubu Rap. No:1461, 7p.*

Schlager, W., 1992, Sedimentology and sequence stratigraphy of reefs and carbonate platforms, *American Association of Petroleum Geologists Continuing Education Course Notes series 34, 71p.*

Schmidt, G. C., 1964, Proposed rock unit nomenclature Petroleum District V, Southeast Turkey (allocthonous terrain) (Mobil Exploration Mediterranean Inc.), *Petrol İşleri Genel Müdürlüğü Teknik Arşivi, Arşiv No:3955/1*.

Schmidt, G.C., 1935, Türkiye'nin grubu cenubi şarkisinde üst Kalker ve Tersiyer'in paleontoloji ve stratigrafisi hakkında rapor, *MTA Derleme No:230, 91s*.

Şengör, A.M.C. and Yılmaz, Y., 1981, Tethyan evolution of Turkey: a plate tectonic approach, *Tetonophysics, v.75, p.181-241*.

Selley, R. C., 1976, Subsurface environmental analysis of North Sea sediments, *Bulletin of the American Association Petroleum Geologists, v.60, p.184-195*.

Serra, O. and Sulpice, L., 1975, Sedimentological analysis of shale sand series from well logs, *Transactions of the SPWLA, 16th Annual Logging Symposium, paper w*.

Sezgin, İ., 1982, X. Bölge sürüklenim örtüleri altında ve önündeki Garzan, Alt Sinan Formasyonları biostratigrafisi ve ortamsal yorumu, *T.P.A.O. Arama. Grubu Rap. No:1694, 14p*.

Simon-Brygoo, C., 1980, Analyse- qualitative des diagraphies, Essai de méthodes d'interprétation, *Thèse Université Bordeaux, No.1557 (unpublished)*.

Sturrock, S.J., 1996, Biostratigraphy, in; Sequence Stratigraphy, eds; D. Emery and K. Myers, *Blackwell Scientific Ltd. London, p.89-107*.

Sungurlu, O., 1974, VI. Bölge kuzeyinin jeolojisi ve petrol imkanları; in: Okay, A. and Deltöz eds., *Türkiye İkinci Petrol Kongresi Tebliğler, p.85-107*.

Tekiner, Y., 1988, Bada, Bastokan, Mağrip, Kentalan ve Kurtalan sahalarının Garzan üstü sismik değerlendirme özet raporu, *T.P.A.O. Arama. Grubu Rap. No:2412, 6p*.

Tekiner, Y., 1989, Garzan üstü 1/25.000 lik L46-c₁, M46-a, M46-b paftaları ve Alt Sinan üstü, Üst Sinan üstü L46-c paftası ve Silivanka sahası ve civarı sismik değerlendirme özet raporu, *T.P.A.O. Arama. Grubu Rap. No:2560, 10p*.

Temple, P. G. And Perry, L. J., 1962, Geology and oil occurrence of Southeast Türkiye, v.46, no:9, p.1596-1612.

Thomas, D.H., 1977, Seismic applications of SONIC logs, *SPWLA 5th European Symposium transactions, Paris, Paper 7, p:1-24.*

Tosunkara, A., 1984, Şelmo, Malahermo ve kuzey sahaları, Alt Sinan ve Garzan Formasyonları yeraltı jeoloji çalışması ve hidrokarbon olanakları, *T.P.A.O. Arama. Grubu Rap. No:1911, 218p.*

Turkish Petroleum Company, 1961, Mağrip- first of three TPAO discoveries in 1961, *Petroleum Administration Bulletin, no.11, p.55-57.*

Üngör, A.,1983, Garzan, Mağrip, Kurtalan sahaları ve civarının Garzan Formasyonu üstü yapıkontur haritası, *T.P.A.O. Arama. Gr. Rap. No:1835, 7p.*

Vail, P. R., Mitchum, R. M. and Thompson, S., 1977, Seismic stratigraphy and global changes of sea level, Part 4: Global cycles of relative changes of sea level in Seismic stratigraphy, applications to hydrocarbon exploration, eds: C. Payton, *American Association Petroleum Geologists Memoir 26, p.83-97.*

Vail, P. R. and Warnardth, W.W., 1990, Well log seismic sequence stratigraphy; an integrated tool for the 90's. *G.C.S. Society to Economic Petroleum Geologists and Minerologists Foundation, 11th Annual Res Conference, Programmes and Abstracts, p.379-389.*

Van Wagoner, J.C., Posementier, H.W., Mitchum, R. M., Vail, P.R., Sarg, J. F., Loutit, T.S. and Hardenbol, J., 1988, An overview of the fundamentals of sequence stratigraphy and key definitions, in; Sea level changes: an integrated approach, eds; Wilgus, C.K., Hastings, B.S., Kendall, C.G.C., Posementier, H.W., Ross, C.A. and Van Wagoner, J.C., *Society of Economic Paleontologists and Mineralogists Special Publication No:42*, p.39-45.

Van Wagoner, J.C. Mitchum, R. M., Campion, K. M. and Rahmanian, V. D., 1990, Siliciclastic sequence stratigraphy in well logs, cores and outcrops, *American Association Petroleum Geologists, Methods in Exploration Series, No:7*, 55p.

Wagner, C., Biçer, Z., İşbilir, M., Başkurt, T. ve Baysal, E., 1984, Reservoir distribution in the Beloka carbonates of the Nusaybin-Cizre area, Southeast Turkey, A joint sedimentary geological, petrophysical, seismic pilot study, *TPAO Arama Grubu, Rap. No:1997*, 16p.

Whitlaker, A., Holliday, D.W. and Penn, I.E., 1985, Geophysical logs in British stratigraphy, *Geological Society of London, Special report, v:18*, p:1-74.

Wolff, M. and Combescure, J.P., 1982, Faciolog: automatic electrofacies determinations, *Society of Professional Well Log Analysts annual Logging Symposium, Paper FF*, p:6-9.

Workman, L. E., 1962, Subsurface geology of the Batman region, *TPAO Arama Grubu Rap. No:262/1, 29p.*

Wilson, J. L., 1975, Carbonate facies in geologic history, *Springer-Verlag, New York, Heidelberg, Berlin,471p.*

Worthington, P. F., 1990, Sediment cyclicity from wire line logs, eds; Hurst, A., Lovell, M. A. and Morton, A. C., in; Geological Applications of Wireline Logs, *Geological Society Special Publication, v.48, p.123-132..*

Wylie, A. S. Jr. and Wood, J.R., 2005, Well log tomography and 3D imaging of core and log curve amplitudes in a Niagaran reef, Belle River Mills field, St. Clair County, Michigan, United States, *Associations of Petroleum Geologists Bulletin, v.89, No:42, p:409-433.*

Wyllie, M. R. S., Gregory, A. R. And Gardener, L. W., 1956, Elastic wave velocities in heterogeneous and porous media, *Geophysics, v.21, no:1, p.41-70.*

Yılmaz, E. and Duran, O., 1997, Güneydoğu Anadolu Bölgesi otokton ve allohton birimlerin stratigrafi adlama sözlüğü "Lexicon", *T.P.A.O. Araştırma Merkezi Grubu Başkanlığı, Eğitim Yayınları No:31, 460s.*

Yılmaz, E., ve Araç, M., 1990, X. Bölge Sezgin sahası ve Yalınkavak-1, Yavuz-1 kuyuşarında Alt Germav, Garzan ve Kıradağ Formasyonlarının petrografik incelemesi ve sedimentolojik yorumu, *T.P.A.O. Arama .Grubu Rap. No:2761, 20p.*

Yılmaz, Z., 1989, X. Bölge Batı Kentalan-3 kuyusu Garzan Formasyonu özelliklerinin sedimentolojik ve petrografik incelemesi, *T.P.A.O. Arama. Grubu Rap. No:2621, 26p.*

Yöndem, F., Aydın, M., Türker, M. ve Kalyoncu, G., 1985, Raman sahası Garzan Formasyonu yeraltı jeolojisi çalışması ve hidrokarbon olanakları, *T.P.A.O. Arama. Grubu Rap. No:666, 18p.*

Zadeh, L. A., 1965, Fuzzy sets, *Information and Control, v:8, p:338-353.*

Zhang, Y., Salish, H.A. and McPherson, J.G., 1999, application of neural networks to indentify lithofacies from well logs, *Exploration Geophysics, v:30, p:45-49.*

APPENDIX A

THE STRATIGRAPHIC CLOUMN OF THE STUDIED WELLS IN THE GARZAN-GERMİK OIL FIELD

A.1 Garzan-23

X :4194610
Y :719420
GL:1032m
KB:1035m

SPUD DATE :18-05-1957
COMPLETION:18-09-1957
TD :1694m
COMP.TYPE :oil show

AGE	FORMATION	LITHOLOGY	DEPTH m	THICKNESS m	CORE	DESCRIPTION
EOCENE - OLIGOCENE	HOYA		255	252		Limestone: greyish, thin bedded pelagic foraminiferal shell fragments, benthic foraminifers, echinit, chrinoid Dolomite: greyish, medium-thick bedded, karstic
			608	353		Shale: red Marl: greyish white thin laminated Conglomerate: greenish grey, polygenic
PALEOCENE	ÜST GERMAV		1274	666		Shale: green, brownish pink, grey, laminated Sandstone: greenish grey, fossiliferous Marl: cream
			1461	187		Marl: cream
MAASTRICTIAN	ALT GERMAV		1461	187		Marl: cream
	GARZAN		1524	63		Limestone: white, clayey, oil shows, pelagic foraminiferal
	KIRADAG		1561	37		Limestone: cream, white, oil shows, fossiliferous, glauconite
CAMPANIAN	BELOKA		1561	37		Sandstone: brown, green, greenish white, conglomerates
SANTONIAN TOURONIAN	MARDIN		1632	71		Limestone: dirty white to cream, middle - thick bedded, cherts, glauconite, rarely clayey, fossiliferous
			62p	1694		Limestone: white, dolomitic

TD:1694m



A.2 Garzan-31

X :4197690
Y :713310
GL:883m
KB:887m

SPUD DATE :25-04-1958
COMPLETION:06-09-1958
TD :1753m
COMP.TYPE :oil

AGE	FORMATION	LITHOLOGY	DEPTH m	THICKNESS m	CORE	DESCRIPTION
EOCENE - OLIGOCENE	HOYA		351	351		Limestone: greyish, thin bedded pelagic foraminiferal shell fragments, benthic foraminifers, echinit, chrinoid
			355			Dolomite: greyish, medium-thick bedded, karstic
PALEOCENE	GERCÜŞ		660	305		Shale: red
						Marl: greyish white thin laminated
PALEOCENE	ÜST GERMAV		1274	708		Conglomerate: greenish grey, polygenic
						Shale: green, brownish pink, grey, laminated
MAASTRICTIAN	ALT GERMAV		1501	133		Sandstone: greenish grey, fossiliferous
						Marl: cream
MAASTRICTIAN	GARZAN		1501	151	1501-1506	Marl: cream
			1652			Limestone: white, clayey, oil shows, pelagic foraminiferal
CAMPANIAN	BELOKA		1700	40	1539.5-1544.5 1568.2-1573.9 1601.55-1606 1632.5-1634.5	Limestone: cream, white, oil shows, fossiliferous, glauconite
			1740			Limestone: dirty white to cream, middle - thick bedded, cherts, glauconite, rarely clayey, fossiliferous
	MARDIN		1740	40		Limestone: white, dolomitic

TD:753m



A.3 Garzan-33

X :4199810
Y :713860
GL:800m
KB:803m

SPUD DATE :01-10-1958
COMPLETION:31-12-1958
TD :2014m
COMP.TYPE :oil show

AGE	FORMATION	LITHOLOGY	DEPTH m	THICKNESS m	CORE	DESCRIPTION
EOCENE - OLIGOCENE	GERMIK		398	395		Gypsum: white Dolomite: beige, grey , poor porosity Shale: red, brown, beige, sandy, dolomitic, calcerous
	HOYA		600	202		Limestone: greyish, thin bedded, pelagic foraminiferal, shell fragments, benthic foraminiferal, echinoid, chrinoid Dolomite: greyish, middle - thick bedded, kastic
PALEOCENE	GERCÜŞ		948	348		Shale: red Marn: greyish white thin laminated Conglomerate: greenish grey, polygenic
	ÜST GERMAV		1632	684		Shale: green, brownish pink, grey, laminated Sandstone: greenish grey, fossiliferous Marl: cream
MAASTRICTIAN	ALT GERMAV		1783	151		Marl: cream
	GARZAN		1895	112	1 1784 2 1790 3 1794 1808-1813	Limestone: white, clayey, oil shows, pelagic foraminiferal
	KIRADAG		1950	55		Limestone: cream, white, oil shows, fossiliferous, glauconite
	BELOKA		1990	40		Sandstone: brown, green, greenish white, conglomerates Shale and quartz
	MARDIN		24p			Limestone: dirty white to cream, middle - thick bedded, cherts, glauconite, rarely clayey, fossiliferous Limestone: white, dolomitic

TD:2014m



A.4 Garzan-43

X :4197638
Y :718452
GL:830m
KB:833m

SPUD DATE :29-07-1959
COMPLETION:25-10-1959
TD :1835m
COMP.TYPE :water

AGE	FORMATION	LITHOLOGY	DEPTH m	THICKNESS m	CORE	DESCRIPTION
EOCENE - OLIGOCENE	HOYA		410	407		Limestone: greyish, thin bedded pelagic foraminiferal shell fragments, benthic foraminifers, echinoid, chrinoid
						Dolomite: greyish, medium-thick bedded, karstic
PALEOCENE	GERCÜŞ		748	338		Shale: red colored Marl: greyish white thin laminated Conglomerate: greenish grey, polygenic
	ÜST GERMAV		1440	692		Shale: green, brownish pink, grey, laminated Sandstone: greenish grey, fossiliferous Marl: cream
MAASTRICTIAN	ALT GERMAV		1613	173		Marl: cream Limestone: white, clayey, oil shows, pelagic foraminiferal
	GARZAN		1698	85	1 1639 1643	Limestone: cream, white, oil shows, fossiliferous, glauconite
	KIRADAG		1754	56	2 1761 1766 1771	Sandstone: brown, green, greenish white, conglomerates
	CAMPANIAN	BELOKA		81p	3	Limestone: dirty white to cream, middle - thick bedded, cherts, glauconite, rarely clayey, fossiliferous

TD:1835m



A.5 Garzan-47

X :4194630
Y :716800
GL:676m
KB:680m

SPUD DATE :02-05-1960
COMPLETION:13-08-1960
TD :1792m
COMP.TYPE :oil show

AGE	FORMATION	LITHOLOGY	DEPTH m	THICKNESS m	CORE	DESCRIPTION
EOCENE - OLIGOCENE	GERMIK		804	800		Gypsum: white Dolomite: beige, grey, poor porosity Shale: red, brown, beige, sandy, dolomitic, calcereous
	HOYA		1144	340		Limestone: greyish, thin bedded pelagic foraminiferal shell fragments, benthic foraminifers, echinoid, chrinoid Dolomite: greyish, medium-thick bedded, karstic
PALEOCENE	GERCÜŞ		1424	280		Shale: red Conglomerate: greenish grey, polygenic Marl: greyish white thin laminated
	ÜST GERMAV		2098	674	1 1633.4 1635.4 2 1716.7 1718.7	Shale: green, brownish pink, grey, laminated Sandstone: greenish grey, fossiliferous Marl: cream
MAASTRICTIAN	ALT GERMAV		2219	121	3-4-5-6-7 2220-2234.6	Marl: cream Limestone: white, clayey, oil shows, pelagic foraminiferal
	GARZAN		2409	190	8 2409-2411 9 2446-2448	Limestone: cream, white, oil shows, fossiliferous, glauconite
	KIRADAG		2442	33		Sandstone - Shale: brown, green, conglomerates, quartz
CAMPANIAN	BELOKA		2498	56		Limestone: dirty white to cream, cherts, glauconite, fossiliferous
	MARDIN		2498	156		Limestone: white, dolomitic

TD:2508m



A.6 Garzan-82

X :4193207
Y :724544
GL:618.8m
KB:620.36m

SPUD DATE :18-08-1963
COMPLETION:08-10-1963
TD :1792m
COMP.TYPE :oil show

AGE	FORMATION	LITHOLOGY	DEPTH m	THICKNESS m	CORE	DESCRIPTION
EOCENE - OLIGOCENE	HOYA			433		Limestone: greyish, thin bedded pelagic foraminiferal shell fragments, benthic foraminifers, echinoid, chrinoid Dolomite: greyish, medium-thick bedded, karstic
				436		
PALEOCENE	GERCÜŞ		724	288		Shale: red Marl: greyish white thin laminated Conglomerate: greenish grey, polygenic
	ÜST GERMAV		1394	670		Shale: green, brownish pink, grey, laminated Sandstone: greenish grey, fossiliferous Marl: cream
MAASTRICTIAN	ALT GERMAV		1553	159		Marl: cream Limestone: white, clayey, oil shows, pelagic foraminiferal
	GARZAN		1719	166	1 1588 2 1594 1598	Limestone: cream, white, oil shows, fossiliferous, glauconite
	KIRADAG		1747	28		Sandstone - Shale: brown, green, conglomerates, quartz
CAMPANIAN	BELOKA		1747	45p		Limestone: dirty white to cream, cherts, glauconite, fossiliferous

TD:1792m

A.7 G.Germik-1

X :4200103
Y :707989
GL:739.65m
KB:743.21m

SPUD DATE :21-06-1986
COMPLETION:06-08-1986
TD :2205m
COMP.TYPE :water

AGE	FORMATION	LITHOLOGY	DEPTH m	THICKNESS m	CORE	DESCRIPTION
EOCENE - OLIGOCENE	GERMIK		516	512		Gypsum: white Dolomite: beige, grey, poor porosity Shale: red, brown, beige, sandy, dolomitic, calcareous
	HOYA		870	354		Limestone: greyish, thin bedded, pelagic foraminiferal, shell fragments, benthic foraminiferal, echinoid, chrinoid Dolomite: greyish, middle - thick bedded, kastic
PALEOCENE	GERCÜŞ		1210	340		Shale: red Marl: greyish white thin laminated Conglomerate: greenish grey, polygenic
	ÜST GERMAV		1720	510		Shale: green, brownish pink, grey, laminated Sandstone: greenish grey, fossiliferous Marl: cream
MAASTRICTIAN	ALT GERMAV		1957	237		Marl: cream Limestone: white, clayey, oil shows, pelagic foraminiferal
	GARZAN		2091	134	1 1965 1973.5	Limestone: cream, white, oil shows, fossiliferous, glauconite
	KIRADAG		2151	60	2 2136 2145 2157	Sandstone: brown, green, greenish white, conglomerates Shale and quartz
	BELOKA			54p	3 2165	Limestone: dirty white to cream, middle - thick bedded, cherts, glauconite, rarely clayey, fossiliferous

TD:2205m

A.8 G. Germik-2

X :4200041
Y :709410
GL:804m
KB:807m

SPUD DATE :10-08-1988
COMPLETION:04-10-1988
TD :2185m
COMP.TYPE :water

AGE	FORMATION	LITHOLOGY	DEPTH m	THICKNESS m	CORE	DESCRIPTION
EOCENE - OLIGOCENE	GERMIK		494	491		Gypsum: white Dolomite: beige, grey, poor porosity Shale: red, brown, beige, sandy, dolomitic, calcerous
			775			281
PALEOCENE	GERCÜŞ		1160	385		Shale: red Marl: greyish white thin laminated Conglomerate: greenish grey, polygenic
			1700			540
MAASTRICTIAN	ALT GERMAV		1969	269	1	Marl: cream Limestone: white, clayey, oil shows, pelagic foraminiferal
			2083			114
	GARZAN		2146	63		Sandstone: brown, green, greenish white, conglomerates Shale and quartz
			2185			39p
CAMPANIAN	BELOKA					


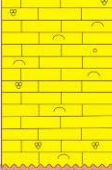
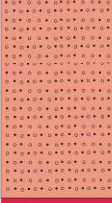




TD:2185m



A.9 Germik-3

X :4201870
Y :708000
GL:732m
KB:736m

SPUD DATE :08-11-1959
COMPLETION:21-03-1960
TD :2244m
COMP.TYPE :oil

AGE	FORMATION	LITHOLOGY	DEPTH m	THICKNESS m	CORE	DESCRIPTION
EOCENE - OLIGOCENE	GERMIK		524	520		Gypsum: white Dolomite: beige, grey, poor porosity Shale: red, brown, beige, sandy, dolomitic, calcerous
	HOYA		824	300		Limestone: greyish, thin bedded, pleagic foraminiferal, shell fragments, benthic foraminiferal, echinoid, chrinoid Dolomite: greyish colored, middle - thick bedded, kastic
PALEOCENE	GERCÜŞ		1182	358		Shale: red colored Marl: greyish white thin laminated Conglomerate: greenish grey, polygenic
	ÜST GERMAV		1884	702		Shale: green, brownish pink, grey, laminated Sandstone: greenish grey, fossiliferous Marl: cream
MAASTRICTIAN	ALT GERMAV		1985	101		Marl: cream Limestone: white, clayey, oil shows, pelagic foraminiferal
	GARZAN		2157	172	1-7 8 1985 2017 2033-2037	Limestone: cream, white, oil shows, fossiliferous, glauconite
	KIRADAG		2220	63	24p	Sandstone: brown, green, greenish white, conglomerates Shale and quartz Limestone: dirty white to cream, middle - thick bedded, cherts, glauconite, rarely clayey, fossiliferous


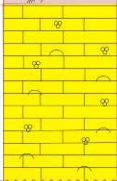




TD:2244m



A.10 Germik-6

X :4201370
Y :709280
GL:822m
KB:825m

SPUD DATE :01-01-1961
COMPLETION:08-05-1961
TD :2020m
COMP.TYPE :water

AGE	FORMATION	LITHOLOGY	DEPTH m	THICKNESS m	CORE	DESCRIPTION
EOCENE - OLIGOCENE	GERMİK		512	509		Gypsum: white Dolomite: beige, grey, poor porosity Shale: red, brown, beige, sandy, dolomitic, calcerous
	HOYA		806	294		Limestone: greyish, thin bedded, pelagic foraminiferal, shell fragments, benthic foraminiferal, echinoid, chrinoid Dolomite: greyish, middle - thick bedded, kastic
PALEOCENE	GERCÜŞ		1098	292		Shale: red Marl: greyish white thin laminated Conglomerate: greenish grey, polygenic
	ÜST GERMAV		1834	736		Shale: green, brownish pink, grey, laminated Sandstone: greenish grey, fossiliferous Marl: cream
MAASTRICTIAN	ALT GERMAV		1930	96		Marl: cream
	GARZAN		1930	90p	1-20 1934 2008	Limestone: white, clayey, oil shows, pelagic foraminiferal Limestone: cream, white, oil shows, fossiliferous, glauconite

TD:2020m



A.11 Germik-21

X :4201171
Y :709167
GL:823.64m
KB:827.06m

SPUD DATE :15-07-1986
COMPLETION:24-09-1986
TD :2220m
COMP.TYPE :water

AGE	FORMATION	LITHOLOGY	DEPTH m	THICKNESS m	CORE	DESCRIPTION
EOCENE - OLIGOCENE	GERMIK		476	472		Gypsum: white Dolomite: beige, grey, poor porosity Shale: red, brown, beige, sandy, dolomitic, calcerous
	HOYA		808	332		Limestone: greyish, thin bedded, pleagic foraminiferal, shell fragments, benthic foraminiferal, echinoid, chrinoid Dolomite: greyish, middle - thick bedded, kastic
PALEOCENE	GERCÜŞ		1119	311		Shale: red Marl: greyish white thin laminated Conglomerate: greenish grey, polygenic
	ÜST GERMAV		1827	708		Shale: green, brownish pink, grey, laminated Sandstone: greenish grey, fossiliferous Marl: cream Marl: cream
MAASTRICTIAN	ALT GERMAV		1920	93	1 1930 1935	Limestone: white, clayey, oil shows, pelagic foraminiferal
	GARZAN		2093	173		Limestone: cream, white, oil shows, fossiliferous, glauconite
	KIRADAG		2192	99		Sandstone: brown, green, greenish white, conglomerates Shale and quartz
CAMPANIAN	BELOKA		2192	28p		Limestone: dirty white to cream, middle - thick bedded, cherts, glauconite, rarely clayey, fossiliferous

TD:2220m



APPENDIX B

THE TABLE OF POINT COUNTING OF THIN SECTIONS

Table B.1. The list of point counting of the thin sections, representative of the five microfaeces types of this study.

FACIES	WELL NAME	DEPTH	TYPE	THIN SECTION NO	ORBITOIDES	ALG	RUDIST FRAGMENTS	MILIOLIDAE	UNDIFFERENTIATED
RW	GERMIK-6	1957.1-1961.8	CORE	211465	0.8	0	2.9	0.3	0
	GERMIK-6	1973-1976.15	CORE	211466	0.1	0	10.7	0.7	0
	GERMIK-6	2000.6-2004.1	CORE	211468	0.8	0	18.7	0.7	0
	GERMIK-6	1954.5-1955.5	CORE	168684	0.6	0	15.5	3.9	0
	GERMIK-6	1955.5-1957.1	CORE	168685	1.3	0	24.2	1.7	0
	GERMIK-6	1952.15-1984.15	CORE	168686	0.5	0	44	0	0
	GERMIK-6	1992-1997	CORE	168688	0.7	0	53.1	0	0
	GERMIK-6	1997.2-2000.6	CORE	168689	0.7	0	50.3	0	0
	GERMIK-6	2010.5-2016.5	CORE	168692	1.3	0	31.6	0	0
	GERMIK-6	1558	CUT	186763/18	1	0	0	2	4.5
MW	GARZAN-82	1552	CUT	186763/19	0.3	1.4	0	3.7	13.3
	GARZAN-82	1686	CUT	186763/50	0.3	1.3	0	0.8	2.2
	GARZAN-82	1690	CUT	186763/51	0	1	0	0.7	3
	GARZAN-82	1682	CUT	186763/49	0	0	0	1.8	8
	GARZAN-47	2328	CUT	8241	0.3	1.1	0	11	4.3
	GARZAN-47	2338	CUT	8242	0.2	0.6	0	8.8	2
	GARZAN-47	2348	CUT	8243	1.2	0.2	0	19.4	1.8
	GARZAN-47	2358	CUT	8244	0.9	1.3	0	8.9	0
	GARZAN-47	2378	CUT	8246	0.1	2.4	0	7.7	0.4
	GARZAN-47	2288	CUT	8237	0	0	2.6	16.4	0
RMW	GARZAN-47	2318	CUT	8240	0.1	0.5	3.5	21.8	0
	GARZAN-47	2324	CUT	186762/22	0	0	0	18.8	0
	GARZAN-47	2332	CUT	186762/23	0	0.3	0	9.1	0
	GARZAN-47	2336	CUT	186762/24	0	2	2.6	9.8	0
	GARZAN-47	2344	CUT	186762/25	0	0.3	0	7.6	0
	GARZAN-47	2352	CUT	186762/26	0	0.3	0	11	0
	GARZAN-47	2354	CUT	186762/27	0	0.8	0	0.6	0
	GARZAN-47	2372	CUT	186762/28	0	0.7	0	6.4	0
	GARZAN-47	2380	CUT	186762/29	0	0	0	0.8	0
	GARZAN-31	1501.14-1506.76	CORE	42464	6.1	0	36.2	4.1	0
OMW	GARZAN-31	1539.5-1544.5	CORE	42475	0.9	0	20.5	11	0
	GARZAN-31	1632.5-1634.5	CORE	42482	1.6	0	18.6	0.8	0
	GARZAN-23	1449	CUT	48275	23.8	0	0	0	0
	GARZAN-23	1452	CUT	48277	19	0	0	0	0
	GARZAN-23	1456	CUT	48278	16.9	1.9	0	0	0
	GARZAN-23	1460	CUT	48279	10.8	3	0	0.6	0
	GARZAN-23	1462	CUT	48280	11.3	0	0	0	0
	GARZAN-43	1650-1652	CORE	398	0	0	0	0	0
	GARZAN-43	1688-1690	CUT	394	0	0	0	0	0
	GARZAN-43	1682	CUT	205669/1	1.2	0	0	0	0
PFM	GARZAN-43	1601.55-1606.2	CORE	42477	0.1	0	0	0	0
	GARZAN-43	1601.55-1606.3	CORE	42478	3.1	0	0	0	0
	GARZAN-43	1601.55-1606.3	CORE	42479	7	0	0	0	0
	GARZAN-43	1601.55-1606.3	CORE	42479	0	0	0	0	0

Table B.1. Continued.

FACIES	WELL NAME	DEPTH	TYPE	THIN SECTION NO	CORAL FRAGMENTS	ECHINOID FRAGMENTS	PELECYPODA+GA STROPODA	CUNEOQLINA
RW	GERMIK-6	1957.1-1961.8	CORE	211465	0	2.5	0.5	0
	GERMIK-6	1973-1976.15	CORE	211466	0	7.6	4.2	0
	GERMIK-6	2000.6-2004.1	CORE	211468	0	9.7	2.1	0
	GERMIK-6	1954.5-1955.5	CORE	168684	0	5.1	3.3	0
	GERMIK-6	1955.5-1957.1	CORE	168685	0.3	5.1	8	0
	GERMIK-6	1982.15-1984.15	CORE	168686	1.5	6.7	3.2	0
	GERMIK-6	1982-1997	CORE	168688	0.6	4.4	6.9	0
	GERMIK-6	1997.2-2000.6	CORE	168691	1.4	12	7.6	0
	GERMIK-6	2010.5-2016.5	CORE	168692	1	14.9	8.7	0
	IMW	GARZAN-32	1558	CUT	186763/18	0	1.5	0
GARZAN-32		1562	CUT	186763/19	0	1.4	0.2	0.3
GARZAN-32		1686	CUT	186763/50	0	1.9	1.2	0.1
GARZAN-32		1690	CUT	186763/51	0	2.7	0.9	0.2
GARZAN-32		1692	CUT	186763/49	0	6.4	1.4	0
GARZAN-47		2328	CUT	8241	0	2.4	0.4	0.6
GARZAN-47		2338	CUT	8242	0	2.7	2.7	1.5
GARZAN-47		2348	CUT	8243	0	2.3	2.2	0.3
GARZAN-47		2358	CUT	8244	0	2.1	4.6	1.1
GARZAN-47		2378	CUT	8246	0	0.6	1.2	1.4
RMW	GARZAN-47	2288	CUT	8237	1.9	1.3	4.2	0.5
	GARZAN-47	2318	CUT	8240	1.7	1.3	5.4	1.2
	GARZAN-47	2324	CUT	186762/22	0	0.5	0.2	0.2
	GARZAN-47	2332	CUT	186762/23	0	0.9	0.1	0.3
	GARZAN-47	2336	CUT	186762/24	1.6	0.7	6.7	0.5
	GARZAN-47	2344	CUT	186762/25	0	3.3	1.4	0
	GARZAN-47	2352	CUT	186762/26	0	1.5	0.1	1.4
	GARZAN-47	2364	CUT	186762/27	0	3.9	1.2	0
	GARZAN-47	2372	CUT	186762/28	0	1.6	0.3	0.5
	GARZAN-47	2380	CUT	186762/29	0	1.1	0.8	0
OMW	Garzan-31	1501.14-1506.76	CORE	42464	7.3	29.3	2.3	0
	Garzan-31	1538.5-1544.5	CORE	42475	1.4	11.7	11.2	0.5
	Garzan-31	1632.5-1634.5	CORE	42482	2.6	19	4.3	0
	Garzan-23	1449	CUT	48275	0	0.2	0.2	0
	Garzan-23	1452	CUT	48277	0	4.5	0.3	0
	Garzan-23	1456	CUT	48278	0	1.7	0.8	0
	Garzan-23	1460	CUT	48279	0	2	3.2	0.1
	Garzan-23	1462	CUT	48280	0	2.5	1.6	0
PFM	GARZAN-43	1650-1652	CORE	386	0	0	0	0
	GARZAN-43	1688-1690	CUT	394	0	0	0	0
	GARZAN-43	1692	CUT	205669/1	0	0	0	0
	GARZAN-43	1601.55-1606.2	CORE	42477	0	0	0	0
	GARZAN-43	1601.55-1606.3	CORE	42478	0	0	0	0
GARZAN-43	1601.55-1606.3	CORE	42479	0	0	0.1	0	

Table B.1. Continued.

FACIES	WELL NAME	DEPTH	TYPE	THIN SECTION NO	ROTALIDAE	PELAGIC FORAMINIFERA	OTHER BENTHIC FORAMINIFERA	MATRIX	OSTRACODA
RW	GERMIK-6	1957.1-1961.8	CORE	211465	0	0	3	90	0
	GERMIK-6	1973-1976.15	CORE	211466	0	0	22	54.7	0
	GERMIK-6	2000.6-2004.1	CORE	211468	0	0	22.8	45.1	0.1
	GERMIK-6	1954.5-1955.5	CORE	186884	0	0	3.8	67.8	0
	GERMIK-6	1955.5-1957.1	CORE	186885	0	0	1.7	58.7	0
	GERMIK-6	1982.15-1984.15	CORE	186886	0.1	0	0.4	43.5	0.1
	GERMIK-6	1992-1997	CORE	186888	1.3	0	0.1	32.9	0
	GERMIK-6	1997.2-2000.6	CORE	186891	0	0	1.3	26.7	0
	GERMIK-6	2010.5-2016.5	CORE	186892	1.5	0	1	38.7	1.3
	GERMIK-6	1558	CUT	186763/18	1.5	0	0	87	2.5
MW	GARZAN-82	1562	CUT	186763/19	0.3	0	3.5	71.9	3.7
	GARZAN-82	1686	CUT	186763/50	0.8	0	0.1	89.4	1.9
	GARZAN-82	1690	CUT	186763/51	0.9	0	1.1	88.6	0.9
	GARZAN-82	1682	CUT	186763/49	0.4	0	1.5	80.1	0.4
	GARZAN-47	2328	CUT	8241	1.4	0	1.8	76	0.7
	GARZAN-47	2338	CUT	8242	0.2	0	2.2	78	1.1
	GARZAN-47	2348	CUT	8243	1.2	0	2.4	67	2
	GARZAN-47	2358	CUT	8244	1	0	4	75	1.1
	GARZAN-47	2378	CUT	8246	2.7	0	4.2	74.3	5
	GARZAN-47	2288	CUT	8237	19	0	2.3	48.6	3.2
RMW	GARZAN-47	2318	CUT	8240	14.9	0	2.1	46.4	1.1
	GARZAN-47	2324	CUT	186762/22	19.5	0	2	57.9	0.9
	GARZAN-47	2332	CUT	186762/23	36.7	0	1.5	50.1	1
	GARZAN-47	2336	CUT	186762/24	12.4	0	2.3	59.4	2
	GARZAN-47	2344	CUT	186762/25	18	0	1.4	66.1	1.9
	GARZAN-47	2352	CUT	186762/26	21.6	0	4.7	55.8	3.6
	GARZAN-47	2364	CUT	186762/27	19.7	0	2.9	66.6	4.3
	GARZAN-47	2372	CUT	186762/28	24.7	0	1.8	58.5	5.5
	GARZAN-47	2380	CUT	186762/29	18.9	0	2.8	70	5.6
	GARZAN-31	1501.14-1506.76	CORE	42464	0	0	1.3	12.3	1.1
OMW	Garzan-31	1539.5-1544.5	CORE	42475	1.6	0	9.7	30.3	1.2
	Garzan-31	1632.5-1634.5	CORE	42482	3.4	0	0.6	48	1.1
	Garzan-23	1449	CUT	48275	7.7	0	4.5	57.5	6.1
	Garzan-23	1452	CUT	48277	12.6	0	0	63.6	0
	Garzan-23	1456	CUT	48278	15	0	1.9	58.6	3.2
	Garzan-23	1460	CUT	48279	10	0	0.8	67.9	1.6
	Garzan-23	1462	CUT	48280	16.1	0	0	65.2	3.3
	GARZAN-43	1650-1652	CORE	386	0	11.4	0	88.6	0
	GARZAN-43	1688-1690	CUT	394	0	5.5	0	94.5	0
	GARZAN-43	1682	CUT	205669/1	0	12.4	0.4	86	0
PFM	GARZAN-43	1601.55-1606.2	CORE	42477	0	17.5	0	80.4	2
	GARZAN-43	1601.55-1606.3	CORE	42478	0	21.7	0.7	70.1	4.4
	GARZAN-43	1601.55-1606.3	CORE	42479	0	20.1	0.9	66.4	5.5
	GARZAN-43	1601.55-1606.3	CORE	42479	0	20.1	0.9	66.4	5.5

CURRICULUM VITAE

PERSONAL INFORMATION

Surname : Yildizel
Name : Zeynep Elif Gaziulusoy
Date and Place of Birth : 19th January 1973, İstanbul
Marital Status : Married, 1 daughter
Nationality : T.C.
Phone : + 90 312 2072368
: + 90 533 6856420
Fax : + 90 312 2869049
Email : zyildizel@tpao.gov.tr

EDUCATION

Degree	Institution	Year of Graduation
MS	METU Geological Engineering	1999
BS	METU Geological Engineering	1995
High School	TED Ankara College	1990

WORK EXPERIENCE

Year	Place	Enrollment
2002-Present	Türkiye Petrolleri A.O.	Project Manager
1996-2002	Türkiye Petrolleri A.O.	Project Geologist
June-October 1994	N.V. Turkse Shell	Summer Student
June- August 1992	N.V. Turkse Shell	Summer Student

PUBLICATIONS

1. D. Altiner, N. Özgül, Ö. Yılmaz, M. Bayazitođlu, N. Akçar, **Z. E. Gaziulusoy**, 1998, Effects of cyclic,eustatic and tectonic events on the Upper Jurassic-Lower Cretaceous cyclic carbonate sequences in the Western Taurus, *TÜBİTAK. (proj. no: YDABÇAG-163)*.
2. D.Altiner, İ.Ö. Yılmaz, N. Akçar, M. Beyazitođlu, **Z. E. Gaziulusoy**, 1999, High-resolution sequence stratigraphic correlation in the UpperJurassic (Kimmeridgian)- Upper Cretaceous (Cenomanian) peritidal carbonate deposits (Western Taurides, Turkey). *Geological Journal, v.34, No:1-2 p.139-158*
3. **Z.E. Gaziulusoy** and Ş. V. Ediger, 1998, Comparison of the Turkish oil fields with the giants of the World, *12th International Petroleum Congress and Exhibition of Turkey Proceedings*.

MASTER OF SCIENCE:

Z. E. Gaziulusoy, 1999, A Sequence Stratigraphical Approach From Microfacies Analysis to the Aptian-Albian Peritidal Carbonates of Polat Limestone (Seydişehir).

BACH ELOR OF SCIENCE:

Z. E. Gaziulusoy, 1995, Petrography and Geochemistry of Ađaçören Gabbros.

ORGANIZATION

Technical Secretary, 13th International Petroleum Congress and Exhibition of Turkey,